

HYDRODYNAMICS AND JUVENILE SALMON MOVEMENT BEHAVIOR AT
LOWER GRANITE DAM: DECODING THE RELATIONSHIP USING 3-D
SPACE-TIME (CEL AGENT IBM) SIMULATION

A Dissertation

Presented to the Faculty of the Graduate School

of Cornell University

in Partial Fulfillment of the Requirements for the Degree of

Doctor of Philosophy

by

Richard Andrew Goodwin

January 2004

© September 3, 2003 Richard Andrew Goodwin

HYDRODYNAMICS AND JUVENILE SALMON MOVEMENT BEHAVIOR AT
LOWER GRANITE DAM: DECODING THE RELATIONSHIP USING 3-D
SPACE-TIME (CEL AGENT IBM) SIMULATION

Richard Andrew Goodwin, Ph.D.

Cornell University 2004

Downstream passage of outmigrating juvenile salmon (migrants) at hydropower dams on the Columbia and Snake Rivers has, generally, not been entirely successful. To date, research in the region has generated considerable, but often inconclusive, results as to the factors influencing observed migrant guidance and passage. This dissertation synthesizes existing fisheries and sensory biology literature together with fundamentals of fluid mechanics and river hydrogeomorphology to develop a theoretically rigorous hypothesis of observed migrant movement behavior at Lower Granite Dam on the Snake River, Washington USA (chapter 1). The hypothesis, the Strain-Velocity-Pressure (SVP) Hypothesis, is supported by existing 3-D acoustic-tag telemetry data, multi-beam hydroacoustic passage data, 3-D computational fluid dynamics (CFD) modeling, and 3-D spatially-explicit, time-varying virtual fish simulation that outputs model results in similar form to data collected by field instrumentation.

The virtual fish model, a coupled Eulerian-Lagrangian agent- and individual-based model (CEL Agent IBM), is a simple, yet theoretically- and computationally-robust, means for simulating individual fish movement behavior. The CEL Agent IBM framework (chapter 2) is based on well-established principles in computer science, foraging theory, and CFD modeling. Virtual fish behavioral rules are biological tractable and mechanistic (i.e., rule-based) in nature. Therefore, one can “plug-and-play” a rule-based hypothesis of fish movement behavior for objective evaluation. In addition, coefficients can be further calibrated or validated in

laboratory experiments and rule structures emerging from back-casting simulation analyses are amendable to forecast simulation.

The CEL Agent IBM for migrants at Lower Granite Dam, i.e., the Numerical Fish Surrogate (NFS), is developed from four independent CFD model and biological data sets from year 2000 studies. The NFS was then 'blindly' validated using seven independent CFD modeled flow conditions from year 2002 studies, i.e., with no prior knowledge of 2002 biological results. NFS predictions from the 'blind' validation runs were first compared to 2002 biological data by an independent entity. The NFS and embodied SVP Hypothesis capture 80% ($r^2 = 0.80$) of the observed variation in 2000 and 2002 migrant passage and 85% ($r^2 = 0.85$) of the observed variation in dawn, dusk, and nighttime passage, i.e., when migrant visual acuity is limited.

BIOGRAPHICAL SKETCH

Richard Andrew Goodwin obtained an undergraduate degree in Civil Engineering, summa cum laude, from Virginia Tech in 1996. In August 1996, Dr. Goodwin started graduate work at Cornell University, and in May 1998 began an internship with the Water Quality and Contaminant Modeling Branch at the U.S. Army Engineer Engineering Research and Development Center Waterways Experiment Station in Vicksburg, MS. In February 2000, Dr. Goodwin completed the degree requirements for a Masters of Science in Environmental Systems Engineering from Cornell University.

ACKNOWLEDGMENTS

I want to thank my advisor, Pete Loucks, and the other Cornell faculty on my Special Committee, Mark Bain and Doug Haith, for allowing me to pursue a unique opportunity to conduct environmental research with the U.S. Army Engineer Engineering Research and Development Center (USAE ERDC). I want to thank Patty Apgar and Ron Watkins for helping me navigate Graduate School policies and administrative details so that the unique research opportunity I had with USAE ERDC remained feasible. I want to thank John Nestler for providing me with the vision and resources I needed to be successful at USAE ERDC. I want to thank Lynn Reese and Mark Lindgren of the U.S. Army Engineer District Walla Walla for taking the risk and providing me with the funding needed to develop a computer-based 3-D virtual fish simulation model. Finally, I want to thank my wife, Wendy Goodwin, for providing me with critical support that has allowed me to devote so much time and energy to wrap up my Ph.D. and the necessary research.

TABLE OF CONTENTS

Biographical Sketch.....	iii
Acknowledgments.....	iv
Table of Contents.....	v
List of Figures.....	vii
List of Tables.....	xii
<u>Chapter 1</u>	
Abstract.....	1
Introduction.....	2
Prior Research.....	4
Hydraulic Strain.....	5
Fish Mechanosensory System.....	7
Lateral Line – Canal Neuromasts.....	8
Lateral Line – Superficial Neuromasts.....	9
Inner Ear – Otolith Organ.....	9
Self-induced Stimulation.....	10
Swim Bladder.....	11
Resultant Capability.....	12
River Hydrogeomorphology.....	15
Strain-Velocity-Pressure (SVP) Hypothesis.....	18
Field Data Analysis.....	26
Site Description.....	26
Biological Data.....	29
Flow-field Data.....	31
Analysis of Integrated 3-D Data.....	31
Graphical Analysis.....	31
Vector Analysis.....	34
Shortcomings in Statistical Approaches.....	39
Plug-and-Play Simulation.....	42
Evaluating the SVP Hypothesis.....	44
Movement Patterns.....	45
Fish Passage.....	49
Discussion.....	51
Utility of SVP Hypothesis.....	51
Discrepancies.....	54
Improving the SVP Hypothesis.....	56
Conclusion.....	56
References.....	58
<u>Chapter 2</u>	
Abstract.....	73
Introduction.....	74

Modeling Approaches	76
Physical Approaches.....	76
Empirical Approaches	77
Intermediate Approach	78
Virtual Sampling	82
Formulating a CEL Agent IBM	82
Potential Stimuli	84
Behavioral Rules.....	85
Selection of Agents.....	87
Events.....	89
Numerically Defining Behavior.....	94
Selecting Behavior.....	97
Behavior Implementation	101
Computational Sensory Environment.....	102
Movement in Computational Space.....	106
Behavior Calibration.....	111
Lower Granite Dam Application	112
Objective	114
Virtual Fish Release Locations	117
Results	118
Movement Patterns.....	118
Fish Passage	121
Residence Times.....	124
Speed Distributions.	126
Sensitivity Analysis	128
Discussion	129
Reasons for Discrepancies.....	133
Model Utility	134
Virtual System Concept.....	134
Scale Issues	135
Archiving Knowledge.....	136
Future Improvements	137
CFD Modeling.....	137
CEL Agent IBM Improvements.....	137
Conclusion.....	139
References	140
Appendix A	157
References	192
Appendix B	193
Hydrodynamics and CFD Modeling – The Basics.....	193
Turbulence.....	195
References	199

LIST OF FIGURES

Chapter 1

Figure 1.1	Simplified illustration of hydraulic rate-of-strain in a river	6
Figure 1.2	Diagram of the canal lateral line system	8
Figure 1.3	Velocity vector patterns of wall-bounded flow in a simplified river cross-section.....	16
Figure 1.4	Wall-bounded and free-shear flow pattern locations in the forebay of Lower Granite Dam.....	17
Figure 1.5	Relationship between strain, velocity, and pressure to the fish mechanosensory system of fishes, turbulence and hydraulics, river hydrogeomorphology, and mathematical behavior	25
Figure 1.6	Lower Granite Dam structural configurations for 2000 and 2002 studies	27
Figure 1.7	Representative milling-path and direct-path individual migrant acoustic-tag telemetry tracks for case DH8	32
Figure 1.8	Integrating 3-D acoustic-tag trajectory and 3-D CFD modeled data	35
Figure 1.9	Circular histograms for 2000 studies of nighttime acoustic-tag migrant xy-plane swimming orientations with respect to the direction of flow at the first ping in each ping-to-ping trajectory, partitioned by the level of strain	37
Figure 1.10	Utility of mechanistic, rule-based model analysis.....	41
Figure 1.11	Numerical Fish Surrogate (NFS) analysis protocol.....	44
Figure 1.12	Flowchart of Strain-Velocity-Pressure (SVP) Hypothesis	45
Figure 1.13	Plan, 3-D, and side views of the movement patterns of five virtual fish for case DH8	46
Figure 1.14	Comparison of the movements of five neutrally-buoyant passive particles and the movement patterns of selected, representative acoustic-tagged migrants for case DH8	47
Figure 1.15	Resultant 3-D velocity magnitude and hydraulic strain for case DH8 flow conditions.....	48
Figure 1.16	Comparison of multi-beam hydroacoustic (i.e., run-at-large) and virtual fish passage estimates at Lower Granite Dam	50
Figure 1.17	Resultant 3-D velocity magnitude and hydraulic strain for case A2 flow conditions.....	52

Chapter 2

Figure 2.1	Relationship between agents, events, and behaviors in a CEL Agent IBM	88
Figure 2.2	Agents, events, and behaviors used in the Numerical Fish Surrogate (NFS) application at Lower Granite Dam	88

Figure 2.3	Flowchart of event evaluations, order of primary computations, and a time-series output of resultant agent utility values for a simulated virtual fish (case DH8)	91
Figure 2.4	Agent utility values for a simulated virtual fish (case DH8)	100
Figure 2.5	Two-dimensional view of a virtual fish computational sensory ovoid	103
Figure 2.6	Eulerian discretization of the Lower Granite Dam forebay and conceptual illustration of the Lagrangian perspective uniquely oriented in time and space to describe movement	107
Figure 2.7	Comparison of a multi-block, near-orthogonal structured grid in original Cartesian space and then, conceptually, in contravariant space	110
Figure 2.8	Bookkeeping virtual fish movement in contravariant space	111
Figure 2.9	Integrated modules of the Numerical Fish Surrogate	113
Figure 2.10	Lower Granite Dam structural configurations for 2000 and 2002 studies	115
Figure 2.11	Approximate virtual fish release locations for both 2000 and 2002 analyses	118
Figure 2.12	Plan, 3-D, and side views of the movement patterns of five virtual fish for case DH8	119
Figure 2.13	Comparison of the movements of five neutrally-buoyant passive particles and the movement patterns of selected, representative acoustic-tagged migrants for case DH8	120
Figure 2.14	Comparison of multi-beam hydroacoustic (i.e., run-at-large) and virtual fish passage estimates at Lower Granite Dam	122
Figure 2.15	Detected forebay residence times of acoustic-tagged migrants, divided into milling- and direct-path classifications	125
Figure 2.16	Forebay residence times of 400 virtual fish	126
Figure 2.17	Volitional swimming speed distributions of nighttime acoustic-tagged migrant and 100 virtual fish for case DH8	127
Figure 2.18	Sensitivity analyses of different virtual fish release locations on passage estimates for cases SH4, SL2, and A2	130
Figure 2.19	The virtual system concept	135
 <u>Appendix A</u>		
Figure A.1	Fish passage estimates for double gate SBC configuration at Lower Granite Dam in 2000	157
Figure A.2	Fish passage estimates for single gate SBC configuration at Lower Granite Dam in 2000	158
Figure A.3	Hydroacoustic and virtual fish passage estimates, CFD modeled flow rates, and sensitivity analyses of release locations (grouped by route type) for case DH8 in 2000	159

Figure A.4	Hydroacoustic and virtual fish passage estimates, CFD modeled flow rates, and sensitivity analyses of release locations (grouped by route type) for case DL5 in 2000.....	160
Figure A.5	Hydroacoustic and virtual fish passage estimates, CFD modeled flow rates, and sensitivity analyses of release locations (grouped by route type) for case SH4 in 2000.....	161
Figure A.6	Hydroacoustic and virtual fish passage estimates, CFD modeled flow rates, and sensitivity analyses of release locations (grouped by route type) for case SL2 in 2000	162
Figure A.7	Hydroacoustic and virtual fish passage estimates, CFD modeled and measured flow rates, and sensitivity analyses of release locations (grouped by route type) for case A2 in 2002.....	163
Figure A.8	Hydroacoustic and virtual fish passage estimates, CFD modeled and measured flow rates, and sensitivity analyses of release locations (grouped by route type) for case B2 in 2002.....	164
Figure A.9	Hydroacoustic and virtual fish passage estimates, CFD modeled and measured flow rates, and sensitivity analyses of release locations (grouped by route type) for case C2 in 2002.....	165
Figure A.10	Hydroacoustic and virtual fish passage estimates, CFD modeled and measured flow rates, and sensitivity analyses of release locations (grouped by route type) for case D2 in 2002.....	166
Figure A.11	Hydroacoustic and virtual fish passage estimates, CFD modeled and measured flow rates, and sensitivity analyses of release locations (grouped by route type) for case E2 in 2002	167
Figure A.12	Hydroacoustic and virtual fish passage estimates, CFD modeled and measured flow rates, and sensitivity analyses of release locations (grouped by route type) for case F2 in 2002	168
Figure A.13	Hydroacoustic and virtual fish passage estimates, CFD modeled and measured flow rates, and sensitivity analyses of release locations (grouped by route type) for case G2 in 2002.....	169
Figure A.14	Hydroacoustic and virtual fish passage estimates and CFD modeled flow rates (for each individual route) for case DH8 in 2000.....	170
Figure A.15	Hydroacoustic and virtual fish passage estimates and CFD modeled flow rates (for each individual route) for case DL5 in 2000	171

Figure A.16	Hydroacoustic and virtual fish passage estimates and CFD modeled flow rates (for each individual route) for case SH4 in 2000	172
Figure A.17	Hydroacoustic and virtual fish passage estimates and CFD modeled flow rates (for each individual route) for case SL2 in 2000	173
Figure A.18	Hydroacoustic and virtual fish passage estimates and CFD modeled and measured flow rates (for each individual route) for case A2 in 2002	174
Figure A.19	Hydroacoustic and virtual fish passage estimates and CFD modeled and measured flow rates (for each individual route) for case B2 in 2002	175
Figure A.20	Hydroacoustic and virtual fish passage estimates and CFD modeled and measured flow rates (for each individual route) for case C2 in 2002	176
Figure A.21	Hydroacoustic and virtual fish passage estimates and CFD modeled and measured flow rates (for each individual route) for case D2 in 2002	177
Figure A.22	Hydroacoustic and virtual fish passage estimates and CFD modeled and measured flow rates (for each individual route) for case E2 in 2002.....	178
Figure A.23	Hydroacoustic and virtual fish passage estimates and CFD modeled and measured flow rates (for each individual route) for case F2 in 2002.....	179
Figure A.24	Hydroacoustic and virtual fish passage estimates and CFD modeled and measured flow rates (for each individual route) for case G2 in 2002	180
Figure A.25	Sensitivity analyses of fish passage (through each individual route) for different release locations of virtual fish for case DH8 in 2000.....	181
Figure A.26	Sensitivity analyses of fish passage (through each individual route) for different release locations of virtual fish for case DL5 in 2000	182
Figure A.27	Sensitivity analyses of fish passage (through each individual route) for different release locations of virtual fish for case SH4 in 2000	183
Figure A.28	Sensitivity analyses of fish passage (through each individual route) for different release locations of virtual fish for case SL2 in 2000	184
Figure A.29	Sensitivity analyses of fish passage (through each individual route) for different release locations of virtual fish for case A2 in 2002.....	185
Figure A.30	Sensitivity analyses of fish passage (through each individual route) for different release locations of virtual fish for case B2 in 2002.....	186

Figure A.31	Sensitivity analyses of fish passage (through each individual route) for different release locations of virtual fish for case C2 in 2002.....	187
Figure A.32	Sensitivity analyses of fish passage (through each individual route) for different release locations of virtual fish for case D2 in 2002.....	188
Figure A.33	Sensitivity analyses of fish passage (through each individual route) for different release locations of virtual fish for case E2 in 2002.....	189
Figure A.34	Sensitivity analyses of fish passage (through each individual route) for different release locations of virtual fish for case F2 in 2002.....	190
Figure A.35	Sensitivity analyses of fish passage (through each individual route) for different release locations of virtual fish for case G2 in 2002.....	191

Appendix B

Figure B.1	Equations of fluid motion for laminar flow	193
Figure B.2	Conceptual view of turbulent flow	196
Figure B.3	Equations of fluid motion for turbulent flow	197
Figure B.4	Mathematical treatment for resolving the turbulence “closure” problem using K-ε turbulence modeling.....	198

LIST OF TABLES

Chapter 1

Table 1.1	General Schedule of Project Operation at Lower Granite Dam during Year 2000 Evaluation	28
Table 1.2	Hydraulic Scenarios Evaluated at Lower Granite Dam in 2000 and 2002	30

Chapter 2

Table 2.1	Intrinsic Utility and Memory Coefficient Values in Numerical Fish Surrogate	99
Table 2.2	Hydraulic Scenarios Evaluated at Lower Granite Dam in 2000 and 2002	116
Table 2.3	Random Number Seed Sensitivity Analysis for Case DH8	132

Hydrodynamics and Juvenile Salmon: Hypothesis Explaining Patterns of Forebay Movement Related to Surface Bypass at Lower Granite Dam

Abstract

Downstream passage of outmigrating juvenile salmon (migrants) at hydropower dams on the Columbia and Snake Rivers has, generally, not been entirely successful. To date, research in the region has generated considerable, but often inconclusive, results as to the factors influencing observed fish guidance and passage. The inherent mathematical complexity of fluid flows in rivers, especially turbulence, and the random and synergistic characteristics of animal behavior complicate research efforts. In this paper, we synthesize existing fisheries and sensory biology literature together with fundamentals of fluid mechanics and river hydrogeomorphology to develop a mathematically- and theoretically-rigorous hypothesis of migrant behavior at Lower Granite Dam on the Snake River, Washington, USA. The hypothesis, the Strain-Velocity-Pressure (SVP) Hypothesis, is supported by existing 3-D acoustic-tag data, computational fluid dynamics (CFD) modeling, and new 3-D spatially-explicit, time-varying “plug-and-play” virtual fish simulation that outputs virtual fish data in the same form as field collected data. Using “plug-and-play” simulation, the SVP Hypothesis explains 80% of variation in migrant passage ($r^2 = 0.80$) as observed by existing multi-beam hydroacoustic data. The SVP Hypothesis explains 85% of observed variation in dawn, dusk, and nighttime passage ($r^2 = 0.85$) when migrant visual acuity is limited. The SVP Hypothesis was developed from literature and calibrated using data from 2000 studies at Lower Granite Dam. The implemented SVP Hypothesis then ‘blindly’ validated on data collected in 2002, i.e., with no prior knowledge of 2002 biological results, at a different hydraulically-based bypass structure. “Plug-and-play”

simulation provides a new, innovative means for objectively interpreting the observed patterns of fish movement as well as a means for objectively implementing hypotheses of fish movement behavior to support engineering decisions.

Introduction

Passage of downstream-migrating juvenile salmon (migrants) around dams in the Pacific Northwest has been difficult to manage and has, generally, not been entirely successful (Coutant and Whitney, 2000). At the same time, relatively consistent patterns have been observed in forebays of several Columbia and Snake River dams and used in an attempt to improve bypass methods. Migrants, for instance, tend to be surface-oriented (Johnson, 1996). At Lower Granite Dam, for instance, 92% of smolts were observed in the upper 11 meters of the water column (Coutant and Whitney, 2000), and at The Dalles Dam powerhouse Steig and Johnson (1986) found 90% of tracked spring smolts were within 7.5 m of the water surface during the day and 70% at night. Coutant and Whitney (2000) suggest that migrants descend towards the turbine intakes for passage through the dam, especially at night, but generally do not descend to the lower two-thirds of the water column in dam forebays, and only enter deep turbines as a last resort when no other passage route is available. Summer migrants tend to be distributed about 2-5 m deeper than spring migrants, but are still surface-oriented (Johnson et al., 1987).

These and other findings led researchers to focus on surface-oriented bypass systems, which would attract migrants into collectors and then pass them into sluices or conduits for passage around the dam. In general, it was determined that surface-oriented routes are safer than routes through more deeply submerged outlets or through turbines (Popper and Carlson, 1998). Migrants passing through turbines are exposed to extreme pressure changes and mechanical injuries (Bickford and Skalski,

2000; Budy et al., 2002). Initial Surface Bypass Collector (SBC) designs and operations focused on finding an optimum entrance plume velocity that would entice migrants into the collector. However, after more than five years of research and mixed performance of SBCs, it has become increasingly apparent that understanding migrant responses to conditions close (< 10 m) to collector entrances is critical to improving SBC performance (Johnson et al., 2000a).

The poor performance of SBCs most commonly results from uncertainty about the characteristics of the intake plume necessary to attract migrants to the vicinity of the collector and entice them to enter. Although some guidelines have been developed, the response of fish to flow remains poorly understood (Popper and Carlson, 1998). With no apparent velocity criterion having been established, attention is gradually shifting to other flow attributes as the responsible stimuli for observed migrant movements and SBC performance. We introduce the hydraulic rate-of-strain as a hydrodynamic constituent that works in juxtaposition with velocity magnitude and hydrostatic pressure in a manner that explains a majority of observed 3-D migrant behavior approaching and passing Lower Granite Dam in 2000 and 2002 with respect to two different bypass structures. The Strain-Velocity-Pressure (SVP) Hypothesis is developed from a synthesis of fisheries and sensory biology literature integrated with fundamentals of fluid mechanics, including turbulence, and concepts in river hydrogeomorphology. The SVP Hypothesis is then substantiated using existing 3-D acoustic-tag data collected at Lower Granite, 3-D computational fluid dynamics (CFD) modeling, and a new form of 3-D spatially-explicit, time-varying “plug-and-play” virtual fish simulation (chapter 2) that outputs virtual fish data in the same form as field collected data. The SVP Hypothesis is developed from a synthesis of literature and data collected in 2000. The hypothesis then ‘blindly’ validated using CFD modeled flow data from 2002 studies and “plug-and-

play” simulation, i.e., with no prior knowledge of 2002 biological results, which were collected with respect to a different hydraulically-based fish bypass structure at Lower Granite Dam.

Prior Research

Recently, water acceleration has become an attribute of increasing interest, although research into its influence on migrants is relatively scant. Haro et al. (1998) studied the response of Atlantic salmon (*Salmo saler*) to accelerating flow fields and results suggest that migrants may be reluctant to enter bypass collectors because of unnatural transition conditions of accelerating water velocity. Haro et al. (1998) suggest expanding the flow transition zone, which they found to result in greater numbers of fish passing as well as fish passing in larger groups. Also suggested are entrances that would allow schools of fish to pass together since Atlantic salmon studied often tried to maintain group cohesion in accelerating flow fields. Other studies on acceleration pointed out by Haro et al. (1998) include Travade and Larinier (1992), who recommend using uniform, low-turbulence water accelerations at bypass entrances. Brett and Alderdice (1958) found that uniform acceleration of water velocities and minimal visual and turbulence cues at bypass entrances improved bypass efficiency. Ruggles and Ryan (1964) also found the transition of water velocity influenced efficiency.

Another flow attribute of increasing interest is turbulence and its various constituents. Coutant (1998, 2001a) introduced the idea that turbulence could serve as a guide to migrants in hydropower forebays. Coutant (1998, 2001a), however, also states that neither the biology of salmonid outmigration nor the potential for inducing conditions is well enough known to help with bypass design improvements. Recent research efforts by Crowder and Diplas (2002), Hotchkiss (2002), and Smith

(2003) have attempted to decipher the relevant hydrodynamic and turbulence constituents using laboratory and in-situ analyses. To date, however, considerable uncertainty remains as to the appropriate turbulence constituents and the transportability of scaling and applying highlighted constituents at other locations. In short, the lack of theoretically robust turbulence quantities relevant to fish is limiting the ability to distill information from various studies on how turbulence may influence the behavior of migrants (Johnson et al., 2000a).

Hydraulic Strain

Tennekes and Lumley (1972) indicate that turbulent flows may be generally viewed as shear flows since shearing flows are precursors to turbulent flows. In fluid environments, shear is a subcomponent of the hydraulic rate-of-strain. The hydraulic rate-of-strain, or strain, is commonly referred to as a spatial velocity gradient, spatial acceleration, or convective acceleration. In essence, strain is a quantity measuring the degree of twisting, stretching, compression, and other forms of deformation on an element of water. Mathematically, there are three component (Cartesian) directions in 3-D space (x, y, and z). Subsequently, there are three component velocities, one in each direction: u, v, and w. Consequently, there are nine variables in (components to) the calculation of total strain in water (Figure 1.1):

$$\frac{\partial u}{\partial x}, \frac{\partial u}{\partial y}, \frac{\partial u}{\partial z}, \frac{\partial v}{\partial x}, \frac{\partial v}{\partial y}, \frac{\partial v}{\partial z}, \frac{\partial w}{\partial x}, \frac{\partial w}{\partial y}, \frac{\partial w}{\partial z}$$

If these components were to act individually and independently on a 3-D element (cube) of water, three would result in elongation or compression of the cube:

$$\frac{\partial u}{\partial x}, \frac{\partial v}{\partial y}, \frac{\partial w}{\partial z}$$

The remaining six components would result in angular deformation of the cube.

These later six components (of strain) are commonly referred to as the hydraulic rates-of-shearing strain, rate-of-shear, or shear:

$$\frac{\partial u}{\partial y}, \frac{\partial u}{\partial z}, \frac{\partial v}{\partial x}, \frac{\partial v}{\partial z}, \frac{\partial w}{\partial x}, \frac{\partial w}{\partial y}$$

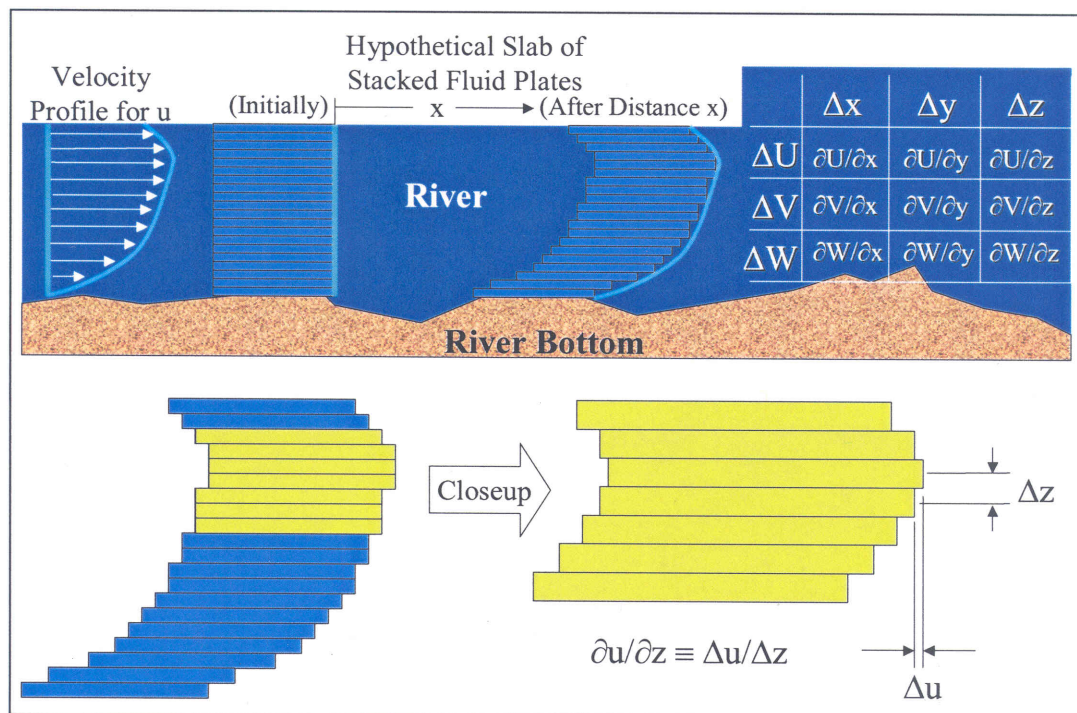


Figure 1.1. Simplified illustration of one of the nine hydraulic rate-of-strain components, i.e., $\partial u/\partial z$, in a river. Total strain is the sum of the absolute values of all nine components of strain.

Hydraulic strain is a mathematical principal that links the observations of Coutant (1998, 2001a), Haro et al. (1998), Travade and Larinier (1992), Ruggles and Ryan (1964), and Brett and Alderdice (1958). In other words, strain mathematically relates to accelerating water velocity, turbulence, and the potential for turbulence. Furthermore, strain is one of the primary flow attributes detected by the mechanosensory system of fishes, which has been implicated in fish exploratory, orientation (rheotaxis), prey detection, station holding, spawning, and schooling behaviors (Coombs and Montgomery, 1999; Coombs et al., 2001; Kanter and Coombs, 2003).

Fish Mechanosensory System

The sensory system used by fish to sense hydrodynamics is often referred to as the mechanosensory system and it is composed of two subsystems: the lateral line and the inner ear. The lateral line is divided into two modalities: superficial neuromasts on the skin surface and canal neuromasts in fluid-filled canals just below the skin surface with pores connecting the canal to the surface (Montgomery et al., 1995). Both superficial and canal neuromasts are distributed spatially on the head and body of the fish. Neuromasts are apical ciliary bundles of mechanoreceptive hair cells that are usually embedded in a gelatinous cupula that is viscously coupled to surrounding water motions. A lateral line system that responds to the relative motion between the individual and the surrounding water is found in all fishes and in larval and permanently aquatic amphibians (Coombs et al., 2001). An inner ear consisting of acceleration-sensitive otolithic organs is present in all fishes (Braun and Coombs, 2000).

Lateral Line - Canal Neuromasts

The bundles of hair cell cilia that make up the canal neuromasts block the subcutaneous canal between pore openings that link water in the canal to the surface (Figure 1.2). Neuromasts are subject to flows within the canal caused by pressure differences between pore openings on the skin surface (Montgomery et al., 1995; Kalmijn, 1989). At the system level, the lateral line canal system usually functions as an acceleration detector because the velocity of the water in the subcutaneous canals is more nearly proportional to the first full derivative of the velocity of the water outside the boundary layer (Kalmijn, 1989). This has led some (e.g., Hudspeth, 1989) to characterize the hair cell arrays of the subcutaneous canal as strain sensors or “biological” strain gages.

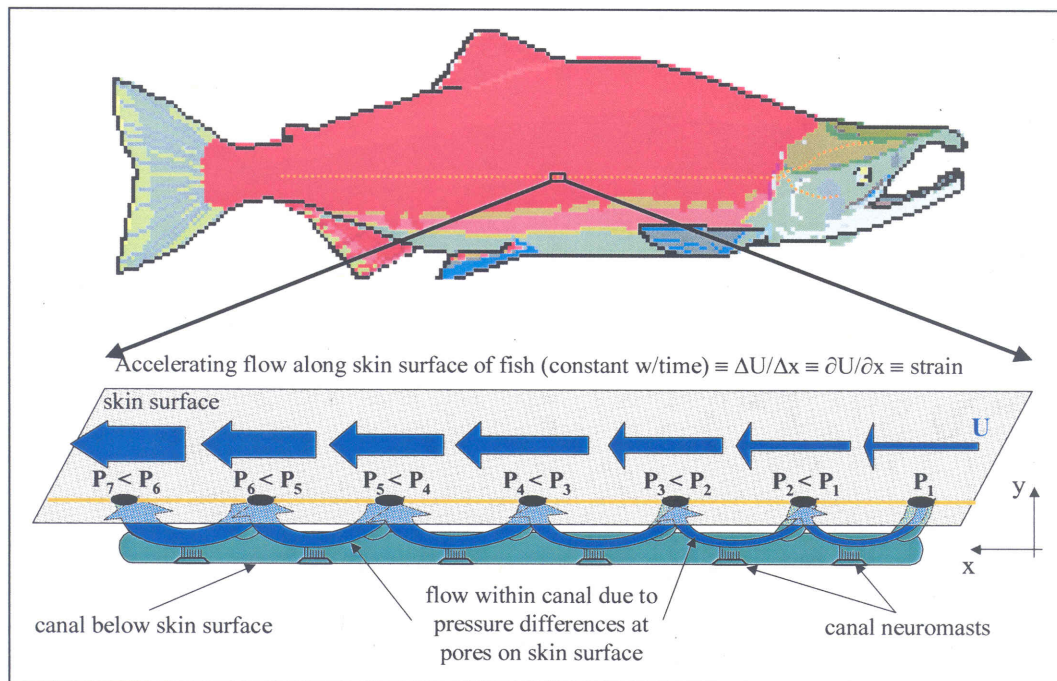


Figure 1.2. Diagram of the canal lateral line system. Adult salmon pictured.

Lateral Line - Superficial Neuromasts

Superficial neuromasts are spatially distributed on the skin surface over the head and body of a fish, giving it access to information on the instantaneous relative velocities over their body as well as a second source of information on flow gradients or areas of current shear (Montgomery et al., 2000). Although the otolith organ of the inner ear can detect accelerations due to unsteady flows and turbulence, rheotaxis has traditionally been thought of as a function of sensory information on movement relative to some external reference (Montgomery et al., 2000). However, superficial neuromasts have the appropriate anatomical distribution and physiological properties to signal the strength and direction of flow (Montgomery et al., 1997). These properties contribute to the detection of regional differences in flow over parts of the body and provide the integration of information needed to decode flow direction (Voigt et al., 2000). While orientation to current requires a fixed external reference in the absence of vision, intermittent or continuous contact with substrate can provide a tactile reference frame against which current can be detected. In addition, superficial neuromasts have a preferred axis of sensitivity, or directional tuning, which would provide the fish with an ability to detect current strength and direction at various positions on the body, thus enabling the fish to detect flow gradients or areas of current shear along its body (Montgomery et al., 2000).

Inner Ear – Otolith Organ

The inner ear is made up of otolithic endorgans that are greater in density than the fish and, thus, lag behind motions of the fish. This provides the fish with a perception of the three-dimensional motions of its body (Braun and Coombs, 2000), a perception of gravity (Paxton, 2000), and a perception of sound (Fay and Edds-

Walton, 2000). Hair cells of the inner ear, upon which the otolith organs sit, are inherently directional receivers and transduce the motion of the very dense otoliths relative to the surrounding tissue providing information on whole body acceleration of the fish and, with regard to imposed flows, information on the acceleration of the water averaged over the volume of the fish (Kalmijn, 1989). Otolith organs are unaffected by nonuniformity of the flow along the length of the lateral line sensory arrays (Kalmijn, 1989), are capable of picking up flow attributes not detected by, or that are beyond the reach of, the lateral line (Kalmijn, 1989), and typically respond to moving objects at greater distances where the higher-order moments detected by the lateral line are negligibly weak (Kalmijn, 1989). With regard to hydrodynamics, otolith organs of the inner ear detect accelerations due to unsteady flow features (Montgomery et al., 2000).

Self-induced Stimulation

Mechanics of the fish mechanosensory system bring up the inevitable question of whether the most significant 'source' a fish encounters is its own movement. The dominance of canal organs in fish that swim continuously suggests that superficial neuromasts are likely compromised by self-induced flow and that a greater proportion of canal neuromasts may dampen, or lessen, the sensitivity of the overall lateral line system to self-imposed low-frequency noise. While self-imposed movement may camouflage, at least to some degree, the hydrodynamic image of the local flow field acquired by the lateral line system (Montgomery et al., 1995), strategies that can potentially overcome this include sit-and-wait, move-stop, and slow glide movements (Montgomery et al., 1995).

Swim Bladder

Some fish, including salmonids, have a fourth sensory modality: the swim bladder. Salmonids have a swim bladder that is sensitive to hydrostatic pressure (Coutant, 2001b), adjusts in volume, and contributes to maintaining near-neutral buoyancy (Lucas and Baras, 2000). Salmonids can adjust the number of moles of gas in their swim bladder, but only relatively slowly. The Ideal Gas Law, $PV=nRT$ ($R = \text{constant}$), stipulates that for a constant number of moles of gas within the bladder, n , in an environment of relatively constant temperature, T , the volume of the bladder, V , expands and contracts due to pressure, P . Outside the near-field influence of hydropower turbines, hydrostatic pressure is generally the dominant pressure constituent. Hydrostatic pressure, furthermore, is directly proportional to depth. This suggests that salmonids could be expected to mitigate their depth at a rate equivalent to that at which they can adjust the number of moles of gas in their bladder. To descend to increasing depths while maintaining a near constant bladder size, salmonids must maintain, approximately, the same number of moles of gas in their bladder, which involves gulping air at the water surface. This is a relatively counter-productive process and may explain the observation by Coutant and Whitney (2000) that surface-oriented migrants, generally, do not descend to the lower two-thirds of the water column in dam forebays.

The sensitivity of migrants to hydrostatic pressure is frequently observed at gatewell slots (Coutant, 2001b). The behavior with respect to gatewells involves migrants entrained with the flow of the turbine being taken into the turbine's deep intake. This results in abnormal increases in hydrostatic pressure from the perspective of the migrant (Coutant, 2001b). Migrants then attempt to resist the change in hydrostatic pressure by swimming upwards (Johnson et al., 2000b) and often tend to stay close to the ceiling of the intake in an attempt to return to the

surface (Coutant, 2001b). As migrants reach the gatewell slot, the repulsion from abnormal increases in hydrostatic pressure causes many migrants to then swim up (rise) into the gatewell where they can frequently return to near-atmospheric pressures (Coutant, 2001b). Coutant (2001b) points out that Skorobogatov et al. (1993) even used the response of fish to hydrostatic pressure to design a new type of passive fish separator.

Swim bladders may also enhance the sensitivity of the canal lateral line to hydrodynamic stimuli in some fishes. Whereas the lateral line system is sensitive to local incompressible flow (near-field stimuli), it is generally not sensitive to pressure waves, i.e., sound (far-field stimuli). For the canal lateral line to be sensitive to pressure waves, a swim bladder must bring the near-field component of the stimulus to the canal, i.e., water movement must be caused to happen in the canals. Various suggestions have been proposed as to how such a connection might exist (Webb and Smith, 2000).

Resultant Capability

The lateral line is a spatially distributed system allowing the fish to detect water movements produced by both biotic and abiotic forces, as long as there is relative movement between the fish and the surrounding water (Kanter and Coombs, 2003). The lateral line is a hydrodynamic detector attending to the local flow field in the vicinity of the source where fluid accelerations are nonuniform and vary in strength and direction (Kalmijn, 1989). Farther from the hydrodynamic source, fluid accelerations and other moments of the flow field due to the disturbance are more nearly uniform giving little differential information for the lateral line to detect. The degree to which fish can “image” their surroundings in a hydrodynamic environment

depends on fish size, orientation to the disturbance source, and size of the disturbance source.

Research on the lateral line of mottled sculpin, *Cottus bairdi*, (Coombs et al., 2000) found that responses to laterally-located sources were better than to frontal sources, indicating information is better acquired from laterally-oriented sources than from frontally-oriented sources. This may be explained by the greater spatial coverage of the lateral line system on the side of the fish compared with the head of the fish, i.e., length as opposed to width of the fish. The operating range of the lateral-line system is, thus, considered to be a function of fish length (Coombs, 1999). The longer the fish, the further away a given source can be detected (Denton and Gray, 1983, 1988, 1989; Kalmijn, 1988, 1989; Coombs, 1996, 1999). With respect to prey items, the operating range of the lateral line system falls within one to two body lengths (Coombs, 1999). However, the distance range or 'active space' of the lateral line system is likely dependent on a number of factors including the size of the disturbance source (Coombs, 1999). Popper and Carlson (1998) indicate that studies by Suckling and Suckling (1964) and Anderson and Enger (1968) found water particle movement of less than 0.5 μm can stimulate nerve response. Popper and Carlson (1998) also indicate that Schwartz (1974) found net water currents relative to fish motion as low as 0.025 mm/s caused sufficient displacement for hair cell nerves to fire. It is plausible, therefore, to suggest that disturbances generated by large natural or structural features, e.g., river bottom or the dam superstructure, produce signals available to the lateral line sensory system over much larger distances than those generated by spatially punctuate sources, e.g., individual prey.

Evidence for many stream fishes indicates they are familiar with their surroundings over substantial distances and are able to find good habitat quickly (Railsback et al., 1999). With respect to the lateral line, the superficial system serves

behaviors dependent on large-scale stimuli, such as abiotic currents, and the canal-based system serves behaviors needing to locate spatially punctuate sources (Coombs et al., 2001). Indeed, the lateral line system can be used to detect inanimate and stationary objects by detecting distortions in the flow field as the fish passes by (Montgomery et al., 1995). Braun and Coombs (2000) suggest that both behavioral experiments (Dijkgraaf, 1963) and theoretical treatments (Kalmijn, 1988; 1989) effectively identify spatial gradients of water motion as the stimulus for the auditory and hydrodynamic senses. While they caution little relevant experimental data has been collected, anecdotal evidence exists. In addition to Haro et al. (1998), Fletcher (1994) found in the testing of large double-entry screen systems that fish tended to respond to the velocity gradients as opposed to responding directly to the stationary obstacles, or solid surfaces, that actually induced the gradients. Faler et al. (1988) found that Northern Pikeminnow seem to concentrate at well-developed shear zones along the turbine outflow and fishway entrances. Crowder and Diplas (2002) indicate that both the works of Fausch and White (1981) and Hayes and Jowett (1994) suggest velocity gradients are important habitat features of salmonids, i.e., brown trout (*Salmo trutta*) and brook trout (*Salvelinus fontinalis*). Lastly, Kanter and Coombs (2003) observed in laboratory rheotactic behavioral studies of mottled sculpin that the fish tended to spend more time near the sides of the flow tank than in the center indicating that they may use the orientation of the tank walls as a stimulus in orienting their body. In general, laboratory and field experiments suggest that stream fishes exploit boundary layers created by objects in the water column (Fausch, 1993; McLaughlin and Noakes, 1998), although, to date, we know of no study that attempts to link sensory system capability, river hydrogeomorphology, and observed migrant movement behavior.

River Hydrogeomorphology

Management of migrant dam passage must work within the constraints of evolved sensory abilities to make managed waterways more compatible with salmonid life histories (Meffe, 1992). Kalmijn (2000) states, "the more salient features of the flow field are the variable explanations behind predation and movement, and that in seeking regularity and focusing on the most salient features in their environment, in order to endure and thrive, animals have empirically discovered the laws of nature". With regard to migrant passage on the Columbia and Snake Rivers, however, relatively few attempts have been made to link evolved fish mechanosensory system capabilities, fluid dynamics, and river hydrogeomorphology. The most fundamental, salient feature of free-flowing natural river reaches is the inherent hydrodynamic pattern resulting from geometry and friction forces that, in turn, result from fluvial geomorphological processes (Leopold et al., 1964).

Without flow resistance, there is no force to alter the pattern of bulk flow once it is set in motion (Ojha and Singh, 2002). Flow resistance imposes pattern on the flow field by creating gradients in velocity and other variables. The predominant flow pattern in deep, free-flowing, natural rivers is wall-bounded flow (Figure 1.3). In general, wall-bounded flow is a pattern in which the direction of maximum decreasing water speed is associated with maximum increasing strain (Figure 1.4). Wall-bounded flow originates from bed friction that causes the speed of water to be zero at all solid-water interfaces (e.g., river bank, river bottom, etc.). The resulting pattern in deep, free-flowing river channels is one in which the speed of water decreases at an increasing rate of change as one nears the river's edge. In contrast, the velocity increases at a diminishing rate of change as one nears the centroid of the river cross-sectional area. In theory, the centroid of the river cross-sectional area is

the location of greatest water speed, although the exact location varies and is dependent on the frictional characteristics of the solid-water (Figure 1.3A) and air-water (Figure 1.3B) interfaces. This rate of change in velocity constitutes hydraulic strain.

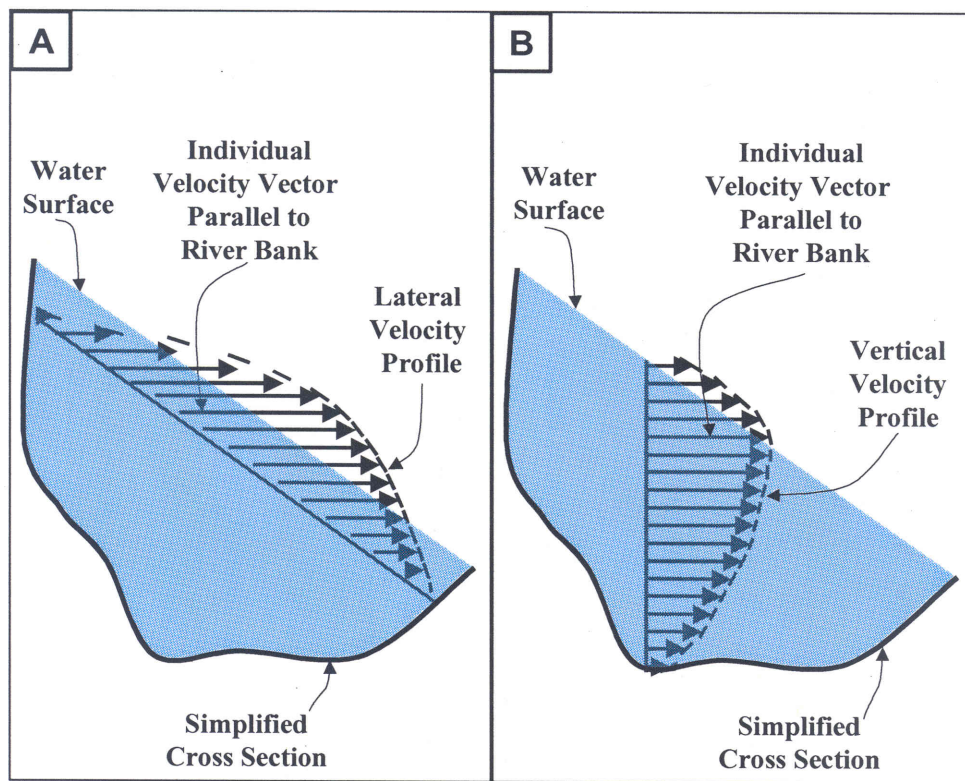


Figure 1.3. The lateral (Plot A) and vertical (Plot B) velocity vector patterns of wall-bounded flow in a simplified river cross-section.

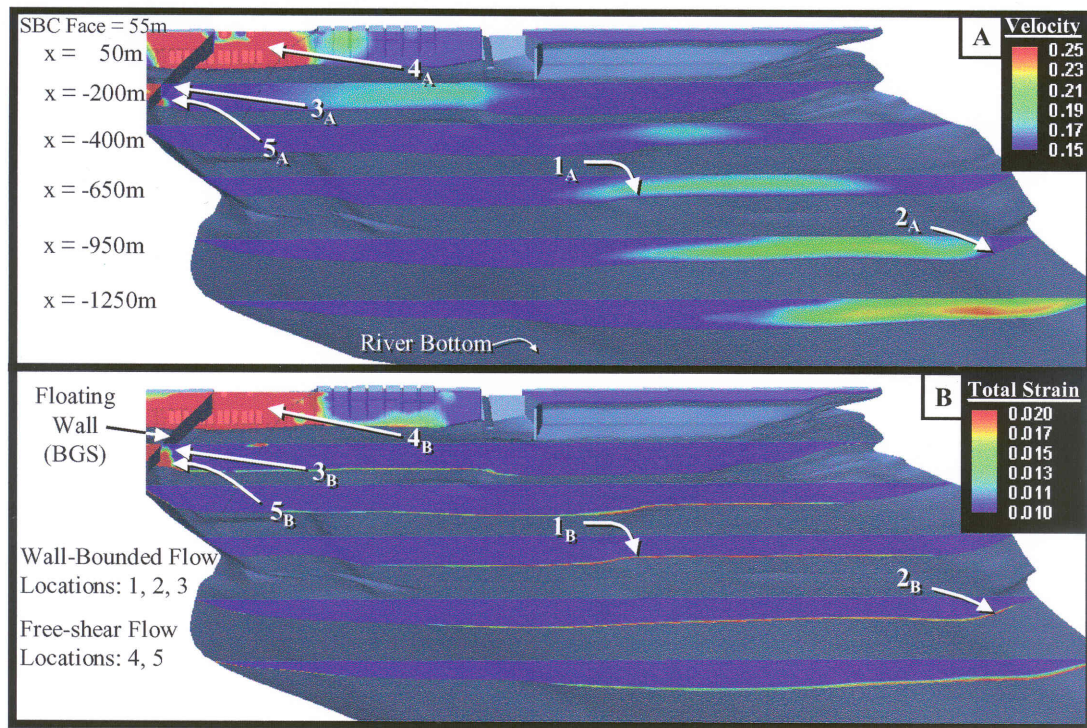


Figure 1.4. Wall-bounded and free-shear flow pattern locations in the forebay of Lower Granite Dam. In general, wall-bounded flow is a pattern in which the direction of maximum decreasing water speed is associated with maximum increasing strain. In contrast, free-shear flow is a pattern in which the direction of maximum increasing strain is associated with maximum increasing water speed. Near the Behavioral Guidance Structure (BGS) floating steel wall, wall-bounded flow is exhibited in the upper portion of the water column where frictional effects of the wall predominate ($3_A, 3_B$). Free-shear flow is exhibited in the lower portion of the water column where flow constriction effects predominate ($5_A, 5_B$). Note: location of maximum water speed in Plot A upstream of the dam does not correspond with the centroid of the river cross-sectional area because of likely hydraulic influences created by the dam.

A second hydrodynamic pattern is relatively rare, if non-existent, in natural deep, free-flowing rivers with a constant cross-sectional area, but is relatively abundant in shallower channels, such as tributaries where wild salmon are reared. Free-shear flow, like wall-bounded flow, is a hydrodynamic pattern imposed on flow

by friction forces. However, unlike wall-bounded flow, free-shear flow emanates predominantly from changes in the channel geometry. In places where the flow cross-sectional area is constricted, i.e., reduced compared to the upstream geometry, the speed of water must increase to maintain a constant flow rate. This increase in velocity is associated with a coincident increase in hydraulic strain. However, unlike the strain-velocity relationship with wall-bounded flow, the strain-velocity relationship with free-shear flow is such that the direction of maximum increasing strain is associated with the direction of maximum increasing water speed (Figure 1.4). These strain-velocity relationships provide the starting point from which to develop a conceptual model, i.e., hypothesis, of how migrants may be responding to stimuli in the forebay of Lower Granite Dam.

Strain-Velocity-Pressure (SVP) Hypothesis

Interpreting the movement behavior of individuals is important because while individual movement can be translated into an understanding of population dynamics, the converse is generally not possible (Turchin, 1997). Juvenile salmon outmigration is known to be a response to currents, with a mix of passive and oriented movements (Arnold, 1974) and not mediated solely by passive mechanisms (Dauble et al., 1989). However, deciphering the proportion of passive and oriented movements and the stimuli eliciting the orientation and speed of ‘oriented’ movements is difficult.

In a dense, fluid environment, such as water, disturbances are generated by anything and everything that moves (Montgomery et al., 1995). Aquatic environments are, thus, often very rich in acoustic and hydrodynamic signals (Schilt and Nestler, 1997; Rogers and Cox, 1988). Additional sensory facilities such as vision, smell, tactile, chemical, electrical, pressure, temperature, and sometimes

magnetic senses (Schilt and Nestler, 1997; Popper and Carlson, 1998) result in a near-limitless number of motivational forces that could potentially influence the movement decisions of an individual fish (Farnsworth and Beecham, 1999). In the full spectrum of prevailing physical, chemical, and biotic conditions, individual behavior is likely mediated by a synergy of diverse sensory inputs with various stimuli evoking conflicts in habitat preference. An individual, therefore, is unlikely to find a location that matches its preference on all environmental gradients, resulting in a potential hierarchy of responses to different cues which take varying precedence during the changing phases of a behavioral sequence (New et al., 2001; Sogard and Olla, 1993).

Therefore, to create a conceptual behavioral program, i.e., a hypothesis of movement behavior, it is necessary to develop a series of behaviors, stimuli, and a process by which behaviors and stimuli interrelate to yield movement. The integration of information from various sensory modalities within a behavioral program is a fundamental issue in attempts to understand sensorimotor integration and the functional relationship between brain and behavior (New et al., 2001). An 'event' is an encounter between an animal and a stimulus in an increment of time (Anderson, 2002), and the interaction between an individual and its environment usually takes place in two stages (Bian, 2003). First, the individual evaluates the stimuli at its location and in the surrounding vicinity. Second, the individual executes a response, i.e., moves (Bian, 2003). We now refine our definition of an 'event' as a change in the attributes of an environmental stimulus (Bian, 2003). The manner in which a stimulus variable is derived from various measured or modeled numerical quantities is not uniform (Anderson, 2002). An appropriate stimulus may be derived from additive, multiplicative, or some other combination (McFarland and Houston, 1981; Anderson, 2002) of biotic and abiotic variables.

To select the proper stimulus variables for migrants, we first begin by assuming that migrants have evolved a downstream navigation strategy in which the predominant hydrodynamic pattern of free-flowing reaches of the Snake and Columbia Rivers, i.e., wall-bounded flow, is a predominant feature in the overall behavioral program of individual migrants. Second, we scale hydraulic strain according to an abbreviated form of the Decibel equation, which is frequently used to characterize stimuli that vary in intensity by orders of magnitude (e.g., sound and light):

$$s = \log_{10} \left(\frac{I}{I_0} \right) \quad [1]$$

where s is strain in scaled form, I is the level of strain at the fish's location, and I_0 is the reference level of strain, i.e., a constant. Equation [1] is applied with the assumption that it results in a value proportionally related to the subjective sensation of 'loudness' as perceived by a fish. This transformation is frequently used to translate the energy output associated with, for instance, sound and light, into a linear scale of perception.

Strain, s , is subsequently translated according to the Weber-Fechner Law (Rapoport, 1983), a well-studied mathematical equation for describing how animals distinguish intensities of stimuli and respond to psychological phenomena. The Weber-Fechner Law relates the physical intensity of a stimulus to its psychologically perceived intensity through calculation of a "just noticeable difference" (JND) in the change of the stimulus with regard to the background, or acclimated, level of the stimulus:

$$\Delta s/s \equiv (s_t - s_{ambient}) / s_{ambient} \quad [2]$$

where s_t is the scaled level of strain at time t from equation [1] and $s_{ambient}$ is the ambient level of strain to which the fish is acclimatized. According to equation [2], a larger change in strain is required at higher ambient strain intensities, to which the fish is already acclimated, in order to elicit the same psychological behavioral response. This treatment of strain is supported by observations of juvenile chum salmon, whose tolerance and resistance to another physiochemical variable, i.e., temperature, is intimately influenced by prior thermal history (Birtwell et al., 2003; Brett, 1952).

The strain stimulus variable value resulting from the Weber-Fechner translation, equation [2], is compared to two thresholds, k_1 and k_2 , used to identify the presence of wall-bounded and free-shear flow, respectively. Environmental thresholds can be thought of as cues that trigger fish movement (Workman et al., 2002). More sophisticated treatments, tests, and threshold criterion may be appropriate for evaluating the presence of wall-bounded and free-shear flow features in the future, but the present focus is limited to the forebay of Lower Granite Dam, and simplicity is a goal of the current treatment. The use of thresholds is supported by prior studies, e.g., Workman et al. (2002) and references therein, evaluating the response of salmonids to other physicochemical stimuli, i.e., temperature, in other aquatic systems. The probability of migrant movement in response to a stimulus increases as the stimulus intensity increasingly exceeds the associated threshold value (Workman et al., 2002).

When the strain stimulus variable value, $\Delta s/s$, exceeds the threshold value used to identify wall-bounded flow, k_1 , (i.e., $\Delta s/s > k_1$), the probability increases that the migrant will move in the direction of increasing flow speed, or flow velocity magnitude. Reasoning for this hypothesis is that in deep, free-flowing river channels exhibiting wall-bounded flow, this response would result in the migrant moving

towards decreasing strain. It is an underlying assumption that migrants prefer to avoid entering high strain areas because of possible impending turbulence, which may result in decreased swimming efficiency and a loss in ability to effectively locate predators and prey. This, however, does not necessarily mean that migrants may not guide along, or trace, contours of strain and, therefore, turbulence (e.g., Coutant 1998, 2001a). Nonetheless, movement mathematically consists of an orientation and a speed and, therefore, a speed response must also be hypothesized. Workman et al. (2002) indicate that behavioral responses usually begin at, or near, the threshold of a stimulus and increase in intensity (i.e., speed) until a maximum rate is reached. Thus, the hypothesis stipulates that migrant speed increases incrementally with time if insufficient progress is made in reducing the level of strain, $\Delta s/s$, below threshold k_1 . Conversely, speed is decremented incrementally if sufficient progress is made. Speed is bounded above by the burst speed of migrants, i.e., approximately 10 body lengths per second (Beamish, 1978), and bounded below by the nominal cruising speed of migrants, i.e., approximately 2 body lengths per second (Beamish, 1978).

When the strain stimulus variable value, $\Delta s/s$, exceeds a second, higher threshold used to identify free-shear flow, k_2 , (i.e., $\Delta s/s > k_2 > k_1$), the probability increases that the migrant will disassociate the direction of increasing flow velocity magnitude with decreasing strain, which would generally hold true in wall-bounded flow areas. More specifically, it is hypothesized that the associated response is generally random in nature, but biased in favor of orienting against the direction of flow. This would endow a migrant with a behavioral program to, generally, maintain its relative position and/or mill in the high-energy areas near the dam without unwanted capture into high-velocity plumes. This behavior is analogous to that observed by Steig and Johnson (1986), who noticed transmitter-equipped migrants

moving laterally back and forth along the dam or just upstream, apparently searching for surface outlets.

The conceptual embodiment of this behavior is that migrants no longer associate the direction of increasing flow velocity with decreasing strain in free-shear flow areas. In a free-flowing stream, this behavior could be expected at locations where, for instance, two boulders bracket and constrict flow in the channel and where juveniles may hesitate, or hold, before acclimating and familiarizing themselves with the elevated strain and velocity signatures before passing. At least with respect to adult upmigration, Standen et al. (2002) suggest that migrating salmonids cross the river and backtrack more frequently at constrictions, possibly, looking for small-scale low velocity fields for continued migration. Acclimatization, familiarization, and seeking a low strain conduit may also be involved behaviors at these constrictions. It is hypothesized that migrant speed increases if the migrant is oriented in the direction opposite the direction of flow, experiences a strain stimulus in excess of k_2 , and is positioned in flow that is greater in speed than the existing migrant speed.

With hypothesized behaviors developed for responses to wall-bounded and free-shear flow hydrodynamic stimuli, a behavior or behaviors must be developed for null event periods, that is, when strain stimuli are absent. Coutant and Whitney (2000) observed that migrants approaching a dam in the forebay, e.g., where strain levels are likely relatively low, tend to follow the flow. Therefore, it is assumed that migrant behavior in relatively low strain environments consists of swimming in the direction of flow, seeking prey, avoiding predators, and other periodic deviations, generally, random in form. Unless a priori information on the 3-D positions of relevant predators and prey can be obtained, however, the evolving hypothesis must limit the 'default' behavior to swimming in the direction of flow with periodic,

random deviations. This treatment is supported by Popper and Carlson (1998), who suggest that the response of fish to hydrodynamics near dams frequently overrides or supercedes the responses to other stimuli. Lastly, speed is hypothesized to be, on average, equal to the cruising speed of migrants.

Above stimuli responses do not provide an explanation for the observed behavior at gatewell slots, that is, in response to changes in hydrostatic pressure. Coutant (2001b) observed that migrants entrained with the flow (into turbine intakes) attempt to resist the change in hydrostatic pressure by swimming up into the gatewell slot. Therefore, an appropriate behavioral response might be the avoidance of large changes in hydrostatic pressure and mitigating changes when they do occur. Since hydrostatic pressure is a 1-D phenomenon, it only requires a 1-D response. Therefore, migrants must employ one of the prior behavioral responses, simultaneously, for horizontal orientation. Hypothesized speed increases in similar form as prior behaviors, that is, incrementally if insufficient progress is made towards mitigating the change in hydrostatic pressure and decremented if sufficient progress is made. Final, resultant speed would then be the largest necessary to respond adequately to horizontal or vertical stimuli.

A vertical response to hydrostatic pressure would be expected when the change in hydrostatic pressure exceeds a threshold value. The variable of hydrostatic pressure, however, can be simplified by substituting the variable depth since depth is directly proportional to hydrostatic pressure. Therefore, the probability of a vertical behavioral response to hydrostatic pressure increases when the hydrostatic pressure stimulus variable value, Δd , exceeds a threshold value, d^* . The hydrostatic pressure stimulus variable value is the change in depth and calculated using the following equation:

$$\Delta d \equiv (\text{depth}_i - \text{depth}_{\text{ambient}}) \quad [3]$$

where $\text{depth}_{\text{ambient}}$ is the ambient depth, i.e., hydrostatic pressure to which the migrant has acclimated.

In summary, the SVP Hypothesis provides a conceptual explanation of observed migrant behavior that links hydraulics, the fish mechanosensory system, river hydrogeomorphology, and mathematical biology (Figure 1.5). The SVP Hypothesis is conducive to analysis with existing 3-D telemetry data and validation using “plug-and-play” simulation.

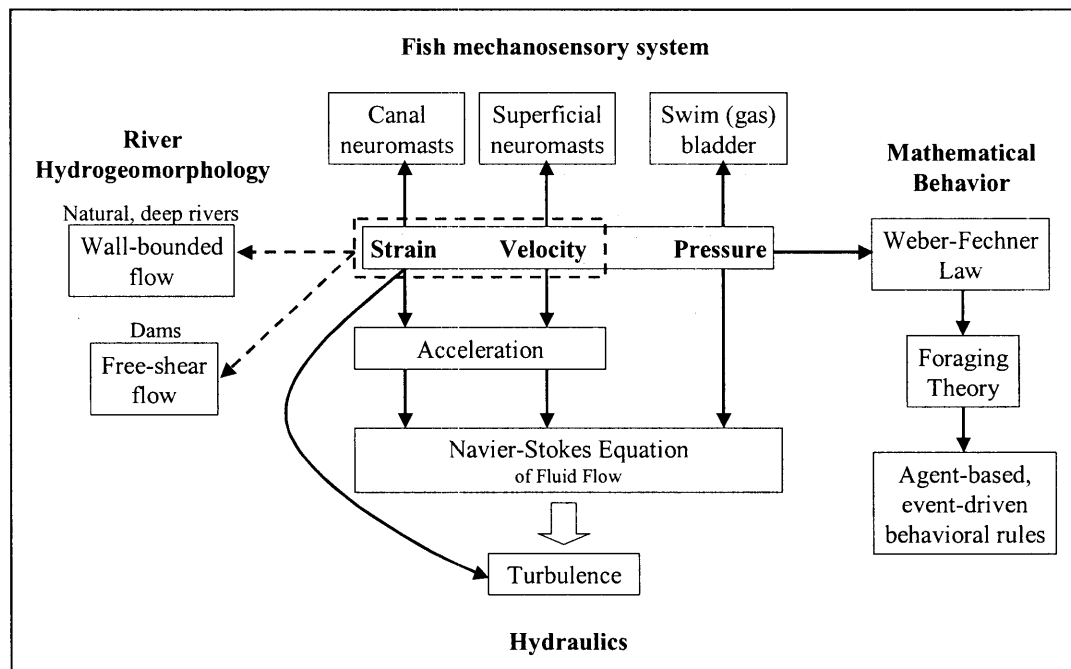


Figure 1.5. Relationship between strain, velocity, and pressure to the fish mechanosensory system of fishes, turbulence and hydraulics, river hydrogeomorphology, and mathematical behavior.

Field Data Analysis

Site Description

Lower Granite Dam (Figure 1.6) is located on the Snake River at river kilometer 173 (mile 107.5). It is a run-of-river project with an effective height of 47 m and a normal operating range of 1.5 m. Moving from south to north, the dam consists of the following structures: a powerhouse, spillway, navigation lock, and an earthen dam located between the lock and northern shore. The 200 m long powerhouse consists of six turbines with a total generating capacity of 810 MW. The total hydraulic capacity of the powerhouse is about $3,680 \text{ m sec}^{-1}$. The forebay is maintained near the minimum operating pool elevation of 223 m (733 ft) above mean sea level during the spring and summer juvenile salmon outmigration. The 156 m long spillway consists of eight spill bays with tainter gates. An angled trashboom deflects debris away from the powerhouse and towards the spillway. The reservoir is about 610 m wide at the dam with maximum forebay depths of about 45 m. The thalweg intersects the dam, approximately, at the intersection of the powerhouse and spillway.

Structural fish bypass features at Lower Granite Dam include a Behavioral Guidance Structure (BGS), a Surface Bypass Collector (SBC) in 2000, and a Removable Spillway Weir (RSW) in 2002. In 2002, the SBC was not used although the dormant SBC structure remained in place, with the exception of the conduit connecting the main SBC gallery to spillbay 1. The BGS consists of two parallel lines of floats suspending a steel curtain originally designed to guide migrants away from the powerhouse and towards the SBC. In 2000 studies, the SBC was configured with two entrances, a BGS entrance located near the intersection of the BGS and SBC and a middle entrance located near the center of the SBC gallery. The SBC was operated in two configurations in 2000. In the single gate configuration,

the BGS entrance was closed and only the middle entrance was open. In the double gate configuration, both entrances were open. Details of project operation during the 2000 evaluation period can be found in Table 1.1 and in HDR Engineering, Inc. and ENSR, Inc (2000). Discharge and velocity measurements for the Surface Bypass Collector (SBC) can be found in Anonymous (2000). Changes from one gate configuration to another in 2000 occurred at 0800 hours on days scheduled for gate changes and generally took about 15 minutes. Detailed information on project operation during the 2002 evaluation period can be found in Anglea et al. (2003), Cash et al. (2003), and Plumb et al. (2003).

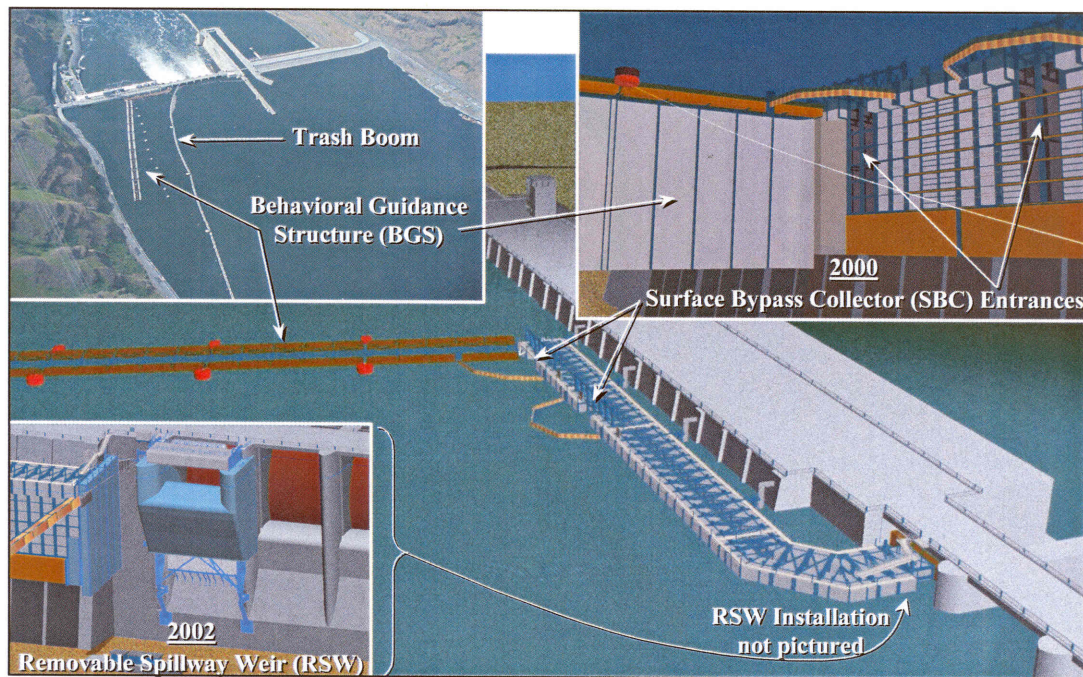


Figure 1.6. Lower Granite Dam structural configurations for 2000 and 2002 analyses. The Behavioral Guidance Structure (BGS) is approximately 24.4m deep at its intersection with the powerhouse and tapers in step-wise manner to a minimum of 16.8m at its upstream end. The trash boom is approximately a constant 1.2m deep. The BGS and trash boom were present for both 2000 and 2002 analyses. Both the SBC (in 2000) and the RSW (in 2002) occupied spillbay 1, i.e., the spillbay nearest the powerhouse.

Table 1.1. General Schedule of Project Operation at Lower Granite Dam during Year 2000 Evaluation.

	Sun.	Mon.	Tues.	Wed.	Thurs.	Fri.	Sat.
April	Day	10	11	12	13	14	15
	Gate	Double	Single	Single	Double	Single	Single
	Load	High	High	Low	Low	High	Low
	16	17	18	19	20	21	22
	Double	Double	Double	Single	Single	Double	Single
	Low	High	Low	High	Low	High	Low
	23	24	25	26	27	28	29
	Single	Double	Double	Single	Double	Single	Double
	High	Low	High	Low	High	High	Low
	30	1	2	3	4	5	6
	Single	Double	Double	Single	Double	Double	Single
	Low	High	Low	High	Low	High	Low
May	7	8	9	10	11	12	13
	Single	Double	Double	Single	Single	Double	Double
	High	Low	High	High	Low	High	Low
	14	15	16	17	18	19	20
	Single	Single	Double	Single	Double	Single	Double
	Low	High	High	Low	Low	High	High
21	22	23	24	25	26	27	
Single	Single	Double	Double	Double	Single	Single	
High	Low	Low	Low	High	Low	High	

In 2000, turbines 1-3 were operated to produce power as specified by the Bonneville Power Administration. Turbine units 1-3 were always operated within but not necessarily near the 1.0-percent limits as prescribed by the Fish Passage Plan. Turbine unit 6 was operated only to meet power and flow demands. Units 4 and 5 were operated during the 2000 evaluation at the power output that approximately corresponds to the lower (100 MW, approximately 13 kcfs) and upper (125 MW, approximately 17 kcfs) percent efficiency settings. A general description of the structural configurations and hydraulic loadings for both 2000 SBC and 2002 Removable Spillway Weir (RSW) evaluations can be found in Table 1.2.

Biological Data

Three-dimensional acoustic-tag (AT) telemetry and multi-beam hydroacoustic (HA) passage data were collected for both 2000 and 2002 studies. Acoustic-tag data collected at Lower Granite Dam (Cash et al., 2002; Cash et al., 2003) describe the 3-D movements of individual hatchery steelhead approaching the powerhouse and spillway. Multi-beam hydroacoustic data collected (Anglea et al., 2001; Anglea et al., 2003) describe the run-at-large passage proportions with which targets (usually fish) used each of the various passage options (i.e., turbines, spillbays, or bypass structure) at Lower Granite Dam. Additional information on acoustic-tag and hydroacoustic technologies may be found in Lucas and Baras (2000), Steig and Timko (2000), Steig (1999), Johnson et al. (1999), and Gerolotto et al. (1999). Acoustic-tag data was categorized by scenario (Table 1.1) and time of day: dawn (0600-0659), day (0700-1659), dusk (1900-1959), and night (2000-0559).

Table 1.2. Hydraulic Scenarios Evaluated at Lower Granite Dam in 2000 and 2002.

Year / Structure	Case ID	# SBC Gates Open	Operating Target / CFD Model Value			Day / Night Evaluation
			<i>Mean HA Instrumentation Value</i>			
			SBC or RSW Loading (m ³ /s)	Powerhouse Loading (m ³ /s)	Spillway Loading (m ³ /s)	
2000 / SBC	DH8	2	99.1 <i>N/A</i>	2055.5 <i>N/A</i>	450.2 <i>N/A</i>	Composite
	DL5	2	99.1 <i>N/A</i>	1497.7 <i>N/A</i>	351.1 <i>N/A</i>	Composite
	SH4	1	96.3 <i>N/A</i>	1755.4 <i>N/A</i>	450.2 <i>N/A</i>	Composite
	SL2	1	96.3 <i>N/A</i>	1860.1 <i>N/A</i>	450.2 <i>N/A</i>	Composite
2002 / RSW	A2	0	198.2 <i>195.3</i>	1698.8 <i>1449.5</i>	240.7 <i>280.3</i>	Composite
	B2	0	198.2 <i>196.5</i>	1274.1 <i>1401.3</i>	438.8 <i>504.3</i>	Composite
	C2	0	0.0 <i>1.9</i>	1812.0 <i>1778.0</i>	0.0 <i>6.3</i>	Day
	D2	0	0.0 <i>0.6</i>	1443.9 <i>646.8</i>	1223.1 <i>1166.5</i>	Night
	E2	0	198.2 <i>193.7</i>	1670.5 <i>1653.5</i>	1427.0 <i>1381.1</i>	Composite
	F2	0	0.0 <i>0.6</i>	1953.6 <i>2039.3</i>	693.7 <i>730.9</i>	Day
	G2	0	0.0 <i>0.2</i>	1528.9 <i>1371.4</i>	1483.6 <i>1530.0</i>	Night

Flow-field Data

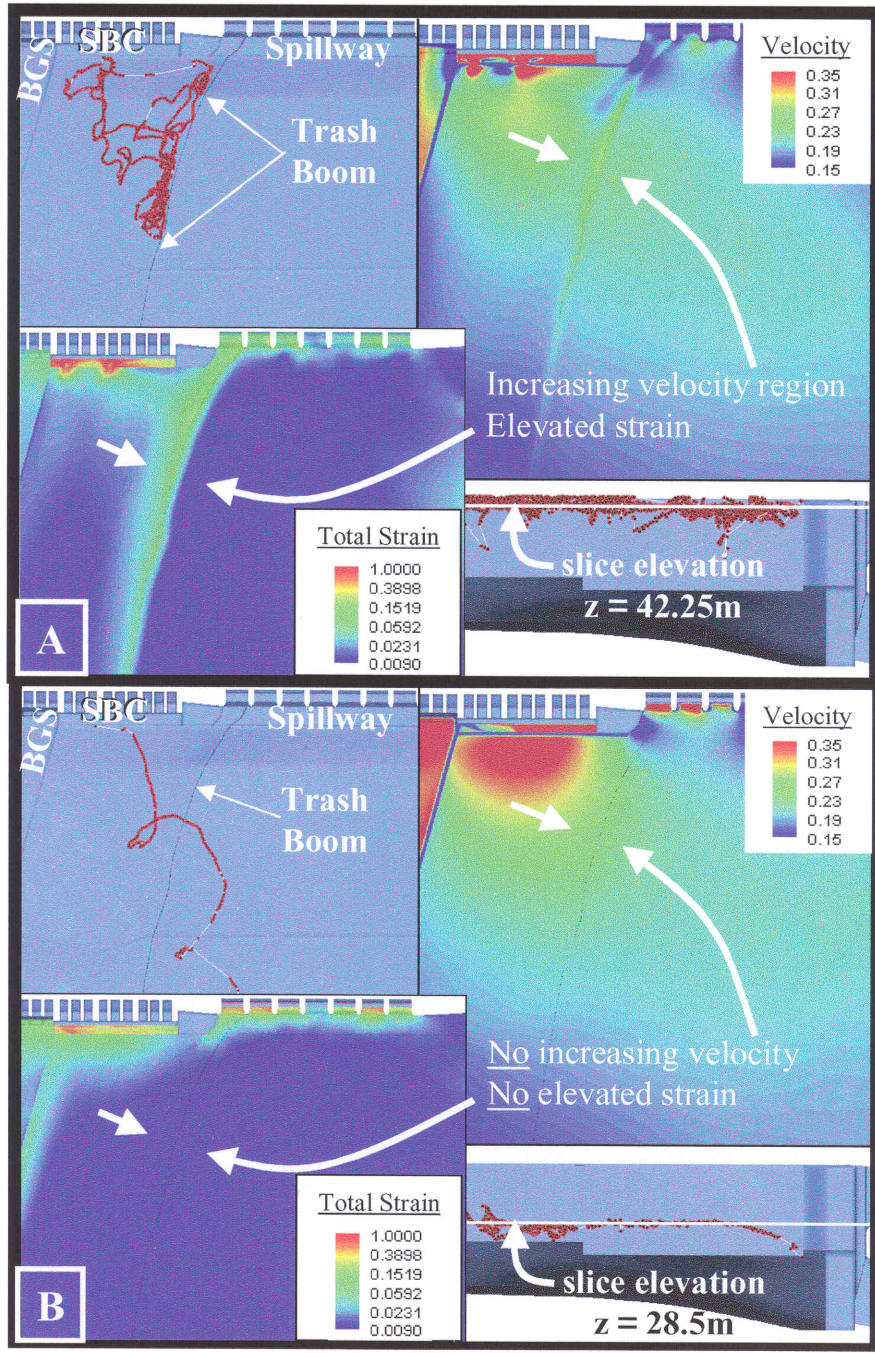
Computational fluid dynamics (CFD) modeling is used to replicate the 3-D steady-state hydraulic patterns and attributes of the Lower Granite Dam forebay associated with 2000 and 2002 studies. When applied appropriately, state-of-the-art CFD models provide accurate depictions of the flow field beyond that available in either physical models or field instrumentation. Forebay hydraulics are simulated using the Unsteady, Unstructured Reynolds-Averaged Navier Stokes (U²RANS) 3-D CFD model developed by the Iowa Institute of Hydraulic Research (IIHR) at the University of Iowa (Lai et al., 2003a; Lai et al., 2003b; Lai, 2000).

Analysis of Integrated 3-D Data

Graphical Analysis

Cash et al. (2002) note that most AT telemetry tracks can be classified according to a simple binary scheme: milling- and direct-path migrants. In general, milling-path migrants (e.g., Figure 1.7A) are observed during the day and direct-path migrants (e.g., Figure 1.7B) at night. Cash et al. (2002) indicate that 83% of milling-path migrants were first detected during the day and 70% of these migrants are located in the upper 4m of the water column. In contrast, Cash et al. (2002) found that 66% of direct-path migrants were first detected at night and 90% of these migrants are located deeper than 4m. Interestingly, nighttime milling-path migrants have a small sample size (Cash et al., 2002). Cash et al. (2002) also note migrants along the trash boom often locate themselves at an elevation just below the structure, Figure 1.7A, which may indicate that migrants are cueing on some hydrodynamic attribute induced by the trash boom rather than the trash boom itself.

Figure 1.7. Representative milling-path (Plot A) and direct-path (Plot B) individual migrant AT telemetry tracks (Cash et al., 2002) for case DH8. Acoustic-tag (AT) telemetry and CFD modeled flow data are integrated using the NFS-VGI module. Total strain (sec^{-1}) and velocity magnitude (i.e., flow speed, m/sec) flow conditions are displayed for the centroid depths of the two tracks. Total strain plotted is the sum of the absolute values of all nine components of strain (Figure 1.1). Plot A illustrates a typical daytime milling-path migrant, i.e., milling and volitional response to the trash boom. Note the elevated strain and velocity signatures near where the migrant mills at the trash boom. Plot B illustrates a typical nighttime direct-path migrant, i.e., no obvious volitional response to the trash boom. In Plot B, note the lack of a strain signature at the depth of the migrant. Water surface elevation is 44.7m. AT data provided by Cash et al. (2002).



To assess this and other plausible hydrodynamic stimuli, acoustic-tag (AT) telemetry data is converted from the original Washington State NAD 1927 grid coordinates to the metric coordinate system of the CFD model. The AT data is then integrated into the CFD modeled data using one of three computer programs that make up the Numerical Fish Surrogate (NFS), discussed in detail later. Integration of AT and CFD modeled data is handled by the NFS Vector Generation & Integration module (NFS-VGI). The NFS-VGI integrates AT-CFD modeled data for both graphical and vector analyses.

Graphical analysis of integrated AT-CFD data for two selected, but representative, AT telemetry tracks are depicted in Figure 1.7. Interesting observations relevant to the wall-bounded flow portion of the SVP Hypothesis can be noted in both the individual milling-path (Figure 1.7A) and direct-path (Figure 1.7B) migrants. First, a high strain and increasing velocity region exists on the powerhouse-side of the trash boom in Figure 1.7A, where the migrant is observed to mill. In contrast, the direct-path migrant in Figure 1.7B appears to be below the hydrodynamic influence of the trash boom. The migrant in Figure 1.7B experiences no apparent strain stimulus associated with the trash boom and, therefore, passes underneath with no apparent response, i.e., a wall-bounded flow response in which the migrant would seek increasing flow speed (as in Figure 1.7A).

Vector Analysis

The NFS-VGI generates vector trajectories for each acoustic-tagged (AT) migrant and interpolates CFD modeled flow information to each observed location (ping) of the migrant. The NFS-VGI dispenses with the arbitrary x-y-z Eulerian grid and orientation of the CFD model and generates a unique ping-to-ping (Lagrangian) reference frame for each migrant (Figure 1.8). The NFS-VGI subtracts the influence

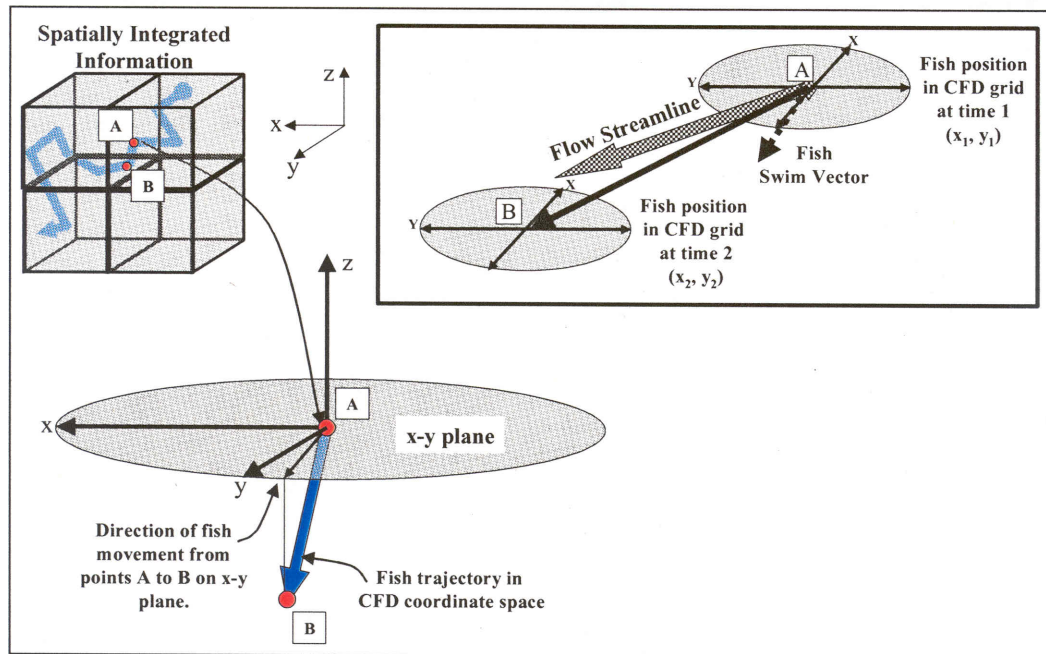


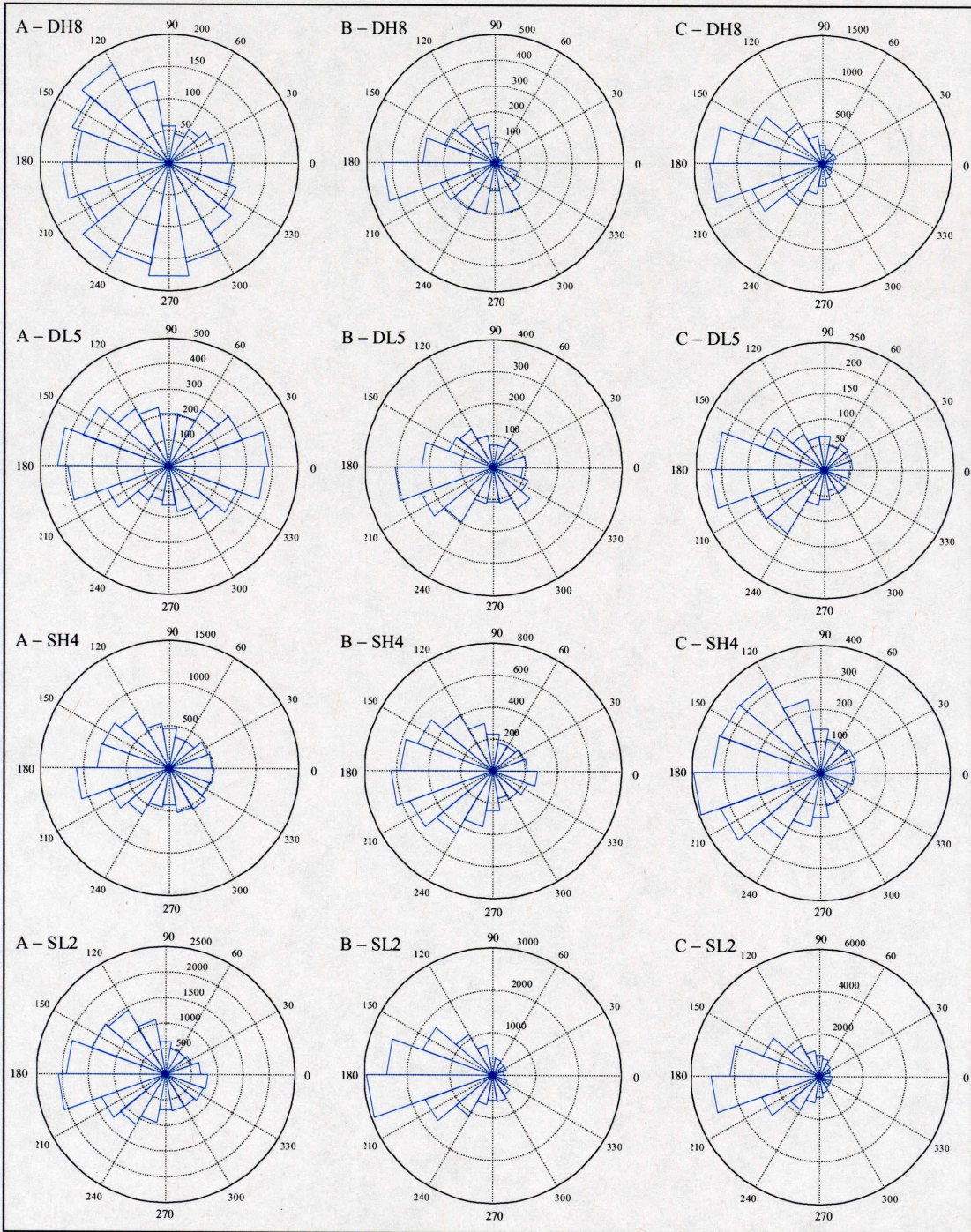
Figure 1.8. Integrating 3-D AT trajectory (Lagrangian) and 3-D CFD modeled (Eulerian grid) data. The NFS-VGI generates ping-to-ping vector trajectories, i.e., from point A to point B, for each individual AT migrant track and interpolates CFD modeled flow information to each location. Passive transport is subtracted from overall movement to yield the volitional swimming component. Movement is then decomposed into xy-plane and vertical components. This treatment is justified since fish have a perception of gravity (Paxton, 2000). Each trajectory is then referenced to four different xy-plane orientations for maximum analytical flexibility. XY-plane trajectory information is referenced to: CFD model grid axes orientation, xy-plane flow vector at the first ping location, prior xy-plane volitional swimming (orientation) vector, and physicochemical gradient directions for all variables available in the CFD model.

of water movement, or passive transport, from each ping-to-ping trajectory to yield the component of volitional movement. The NFS-VGI then decomposes each volitional ping-to-ping trajectory into xy-plane and vertical components. This treatment is justified since fish have a perception of gravity (Paxton, 2000). Analysis then shifts to proper xy-plane trajectory orientation. Considerable ambiguity and

little guidance exists, however, as to the proper reference orientation for migrants. Complicating analysis is the likely fact that perceived xy-plane orientation depends on unique stimulus attributes that vary with each movement (i.e., with time and space). Therefore, the NFS-VGI outputs integrated AT-CFD data in four different xy-oriented reference frames to maximize analytical flexibility. First, each ping-to-ping trajectory is referenced to the CFD model grid axes. While this has little, or no, biological significance in most applications, it may provide a ‘control’, or null hypothesis, for statistical testing. Second, ping-to-ping volitional trajectories are referenced to the direction of flow (i.e., flow vector orientation) at the first ping location in each trajectory. Third, volitional trajectories are referenced to the direction of volitional swimming in the prior movement (i.e., prior volitional vector orientation). Lastly, each ping-to-ping volitional trajectory is referenced to the gradient directions of each physicochemical variable available in the CFD model.

Integrated trajectory data referenced to multiple reference frames provides the means to generate orientation plots (circular histograms) and partition the histograms according to prevailing physicochemical conditions. Figure 1.9 represents a series of circular histograms for 2000 studies (cases DH8, DL5, SH4, and SL2) of nighttime AT migrants. Each ping-to-ping trajectory (xy-plane component) in the data set is referenced to the direction of flow at the first ping in the trajectory. Each trajectory is then grouped into one of three circular histograms, depending on the level of strain at the first ping in the trajectory. An interesting observation relevant to the free-shear flow portion of the SVP Hypothesis can be noted in Figure 1.9. That is, as the level of strain increases (C plots), ping-to-ping trajectories appear to be increasingly oriented in the direction opposite of flow. This trend in Figure 1.9 for all 2000 acoustic-tag (AT) telemetry ping-to-ping trajectories supports the hypothesized response to free-shear flow patterns, i.e., that the

Figure 1.9. Circular histograms for 2000 studies (cases DH8, DL5, SH4, and SL2) of nighttime AT migrant xy-plane swimming orientations (i.e., volitional trajectory directions) with respect to the direction of flow at the first ping in each ping-to-ping trajectory, partitioned by the level of strain. 0° indicates the direction of flow at the first ping location in each ping-to-ping trajectory, and 180° indicates the direction opposite the direction of flow at the first ping in each ping-to-ping trajectory. These trajectories are then grouped statistically as circular histograms and partitioned according to a log transformation of strain, i.e., $\log_{10}(|\text{strain}/1e^{-6}|)$. Individual ping-to-ping trajectories for each AT migrant are grouped into circular histograms according to the following partitions: (A) 0 to 4.0, (B) 4.0 to 4.4771, and (C) 4.4771 to infinity. Note: few AT locations exist in areas where $\Delta s/s < k_I$, thus, the relative absence of significant flow orientation in (A). AT data was sifted to include only those ping-to-ping trajectories with a duration less than 1.5 sec so as to exclude observations where AT migrants most likely exited and then re-entered the hydrophone array. AT data provided by Cash et al. (2002).



associated response is generally random in nature but biased in favor of orienting against the direction of flow.

Shortcomings in Statistical Approaches

While graphical analyses provide support for the wall-bounded and free-shear flow portions of the SVP Hypothesis, statistical analysis of such trajectory data is very difficult and often inconclusive. Methods for analyzing 3-D fish telemetry information are not readily available in the fisheries literature (Steel et al., 2001). This may have to do with several problems associated with traditional statistical approaches. First, traditional statistical methods are burdened by considerable imprecision errors in 3-D locations gathered by field instrumentation. These errors can frequently result in subtle behavioral trends, already often cloaked in the inherent random nature of animal movement, becoming virtually intractable, especially with any level of statistical validity. Second, the biosphere is structured by forces that lead to a lack of independence in the abiotic variables frequently used in statistical analyses (Carroll and Pearson, 2000), e.g., variables interrelated through the Navier-Stokes equation of fluid flow. Similarly, biotic information such as 3-D movement data often exhibits patterns of spatial and temporal dependence. This lack of independence has a variety of damaging effects on statistical analyses (Carroll and Pearson, 2000).

Multivariate techniques are popular because they can incorporate many variables in explaining the variation in data (Wright and Li, 2002). However, for any multivariate analysis there may be numerous possible interpretations and formal testing of a priori hypotheses is difficult (Wright and Li, 2002 and references therein). Associated correlation coefficients do not necessarily imply causation (Harte, 2002). Legendre (1993) and Carroll and Pearson (2000), however, suggest

that analyses continue to frequently rely on statistical methods developed for independent data even though independence is often an unrealistic assumption. Furthermore, interpretation of individual regression coefficients is difficult in multiple regression that includes collinearity of predictors (Smith et al., 2002). This may be one of the primary causes behind the observation by Popper and Carlson (1998) that what may appear to be a positive response by one statistical analysis may appear to be insignificant in another analysis.

Further complicating the task of decoding movement behavior is that observed behavior is likely composed of a series of multiple underlying stimulus responses (Figure 1.10A) organized in hierarchical fashion that dynamically change with time (New et al., 2001; Sogard and Olla, 1993). Outside the laboratory, however, partitioning movement behavior into valid 'treatments' is difficult and, at times, may be impractical or intractable. Statistical and empirical methods, therefore, must be used that are designed to handle such data (e.g., Underwood and Chapman, 1985; Legendre, 1993; Roxburgh and Matsuki, 1999; Epperson, 2000; references in Carroll and Pearson, 2000; Bäckman and Alerstam, 2002; Prior et al., 2002). These and other relevant statistical approaches can provide insight into the building blocks of behavior. However, statistics alone cannot translate observed behavior into a mechanistic, rule-based mathematical description of the underlying mechanisms (Holland, 2003). Identifying patterns and the mechanisms that generate them, however, are needed to improve our ability to predict (Harte, 2002). Therefore, a new paradigm of analysis is needed that incorporates spatial autocorrelation and other dependencies as the common state (Legendre, 1993; Carroll and Pearson, 2000) so that behavioral studies can be evaluated generically enough to transcend site specificity (Popper and Carlson, 1998). Harte (2002) suggests using simple, mechanistic models.

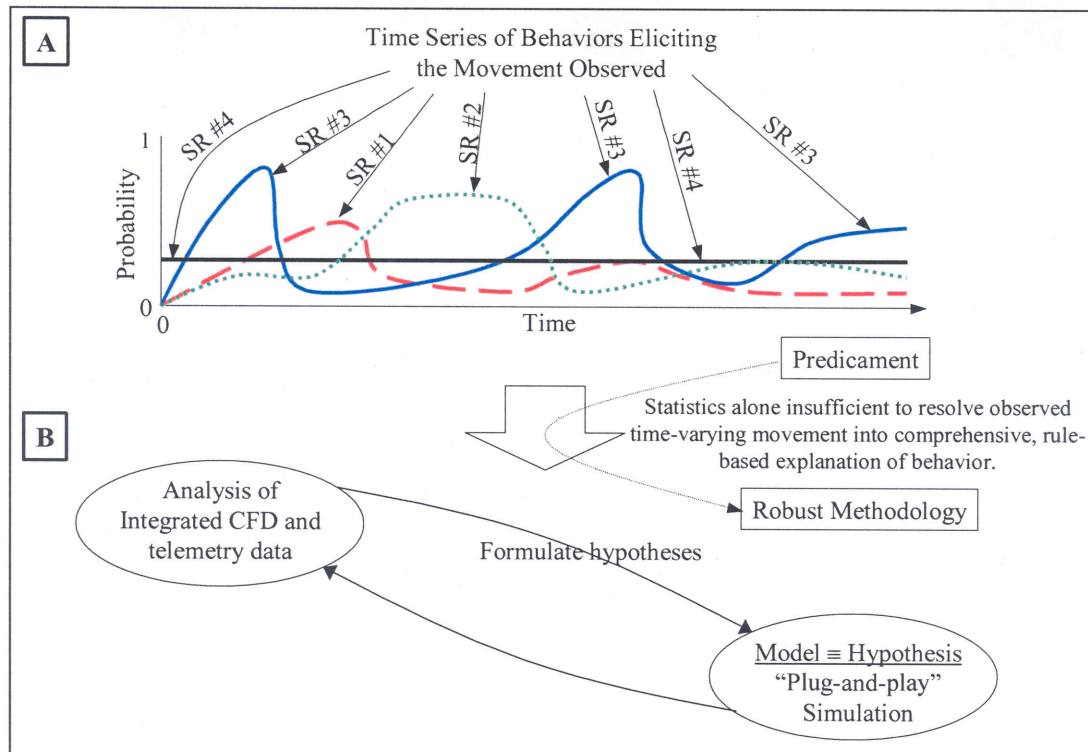


Figure 1.10. Observed movement behavior is likely composed of a series of multiple underlying stimulus responses (SR) organized in hierarchical fashion that dynamically change with time (New et al., 2001; Sogard and Olla, 1993) (Plot A). Partitioning each stimulus response and each behavior transition into a statistically-valid treatment is often impractical, or intractable, in field studies. The utility of rule-based, mechanistic “plug-and-play” simulation is the ability to replicate movement behavior in the same form as field collected data using a numerical embodiment of the proposed hypothesis. This provides a means to evaluate the relative success and failure points of a hypothesis without being burdened with limitations on statistical analyses introduced by autocorrelation.

The development of mechanistic models involves developing and implementing mathematical, rule-based hypotheses of behavior. Since laws in ecology do not have the exactness and universality of physical laws (Harte, 2002), it should be expected that there will be approximations and exceptions in their formulation and application (Harte, 2002). Nonetheless, mathematical, rule-based

hypotheses provide the greatest potential for establishing hypotheses that are portable between operations, structural configurations, meteorological events, and hydropower projects. A rule-based approach involves mathematically defining and delineating key states of hypothesized behavior and transition processes. A hypothesis can then be implemented objectively and numerically using “plug-and-play” simulation and evaluated using data of the same form as that collected in the field (Figure 1.10B). This provides a means to assess the relative success and failure points in a hypothesis in a manner that circumvents autocorrelation problems limiting direct application of traditional statistical approaches.

Plug-and-Play Simulation

Anderson (1988) first proposed integrating system hydraulics with information about the behavior and biology of fish into a mathematical model to better understand the influence of fish diversion and bypass structures. Anderson (1991) subsequently introduced a model for fish diversion and bypass systems based on fish behavior in conjunction with system structural and hydraulic properties. Until recently, however, a robust, integrated modeling scheme did not exist that would permit “plug-and-play” behavior simulation in a theoretically- and computationally-robust manner. Traditionally, the analysis and simulation of biological population dynamics has used one of three major theoretical approaches: Eulerian, Lagrangian, or discrete rules (agent-based) simulation (Parrish and Edelstein-Keshet, 1999). Eulerian approaches use partial differential equations to describe movement in terms of density or mass fluxes of individuals. Lagrangian approaches use equations of motion, detailed forces, and velocities attributed to individuals. Agent-based approaches use discrete individual behavioral rules and dispense with other equations of motion. Robust “plug-and-play” behavior

simulation requires, however, a theoretical approach for handling the interplay between deterministic and stochastic components of movement behavior in 3-D space-time, includes local and long-range effects, and provides the ability to link model output with real-world phenomena and data.

A coupled Eulerian-Lagrangian agent- and individual-based model (CEL Agent IBM) integrates the theoretical and computational advantages of the theoretical approaches described in Parrish and Edelstein-Keshet (1999) into a robust modeling scheme for “plug-and-play” behavior simulation. The “plug-and-play” tool is one of three tools comprising the Numerical Fish Surrogate (NFS) analysis protocol (Figure 1.11). CEL Agent IBMs are described in detail in chapter 2. In short, CEL Agent IBMs consist of a 3-D Lagrangian particle-tracking algorithm that is supplemented with behavioral rules (Schilt and Norris, 1997) from an agent-based, event-driven foraging model (Anderson, 2002). Three-dimensional movement behavior is then implemented within a 3-D CFD model, U²RANS, to take advantage of state-of-the-art numerical modeling of physicochemical fields in aquatic systems (Goodwin et al., 2001; Nestler et al., 2002; Nestler and Goodwin, in review). Theoretically, the movement decisions of aquatic species (i.e., whether an individual, school, or some aggregate of the population) are viewed as a balance of attractions to and repulsions from various sources or foci (Okubo, 1980, Parrish and Turchin, 1997). The calculations of decision probabilities are based on concepts and mathematical techniques derived from game theory, neuroscience, psychology, computer science, and foraging theory (chapter 2; Anderson, 2002).

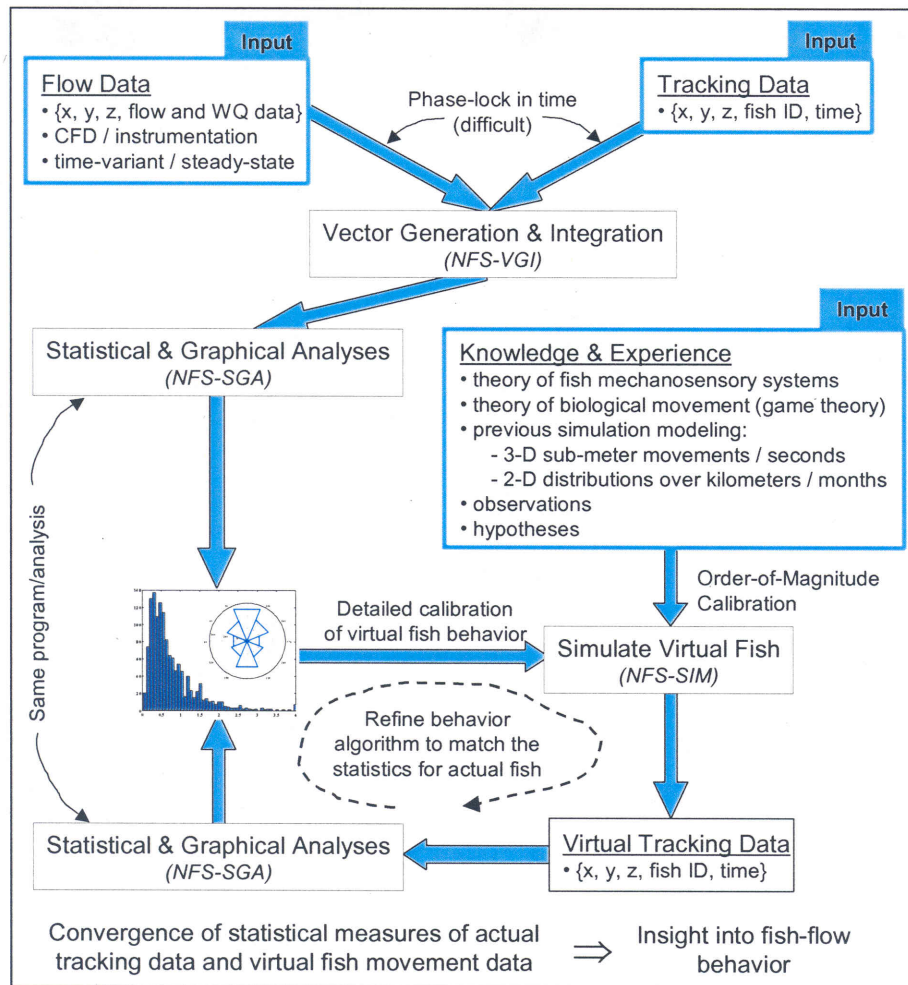


Figure 1.11. Numerical Fish Surrogate (NFS) analysis protocol. NFS-SIM is the CEL Agent IBM (chapter 2) providing “plug-and-play” behavior simulation capability.

Evaluating the SVP Hypothesis

Using “plug-and-play” simulation, the SVP Hypothesis (Figure 1.12) is numerically implemented to objectively evaluate overall effectiveness in capturing observed migrant behavior and passage patterns at Lower Granite Dam. A detailed description of the modeling protocol, theory, and results may be found in chapter 2.

An abbreviated comparison of field collected and virtual fish movement and passage patterns is provided here to substantiate the validity of the SVP Hypothesis.

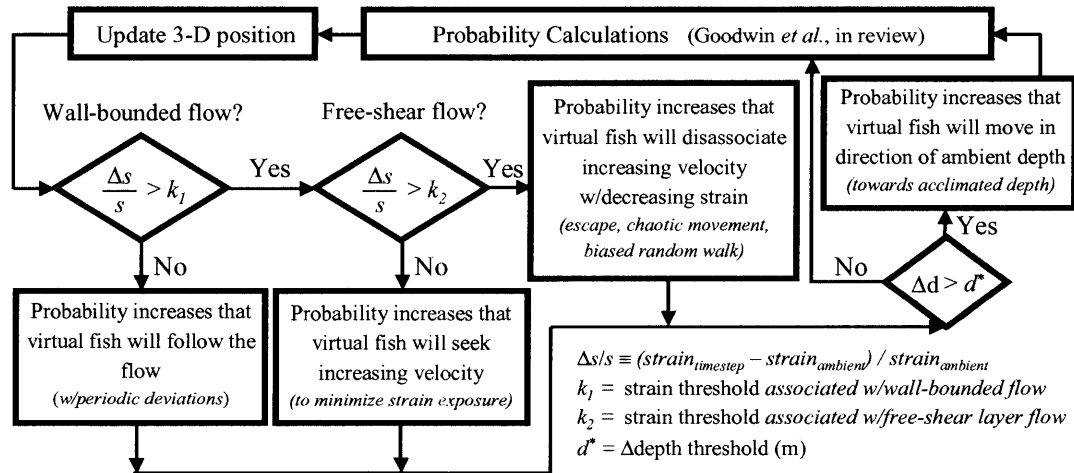


Figure 1.12. Flowchart of Strain-Velocity-Pressure (SVP) Hypothesis.

Movement Patterns

The most intuitive means to compare field collected and simulated fish movement is direct, visual comparison. Figure 1.13 is a multi-angle view of five virtual migrants embodying the SVP Hypothesis, which are released near the dam under case DH8 flow patterns. Figure 1.14A shows the path of five neutrally-buoyant particles (i.e., passive transport) released from the same locations as those in Figure 1.13 under case DH8 flow conditions. The difference, however, is that in Figure 1.14A virtual migrant rules are turned off, i.e., virtual migrants exhibit no volitional swimming. Figures 1.13 and 1.14B indicate that the SVP Hypothesis, when implemented numerically, appears to capture the observed movement pattern of daytime acoustic-tagged (AT) migrants (often milling-path migrants). That is,

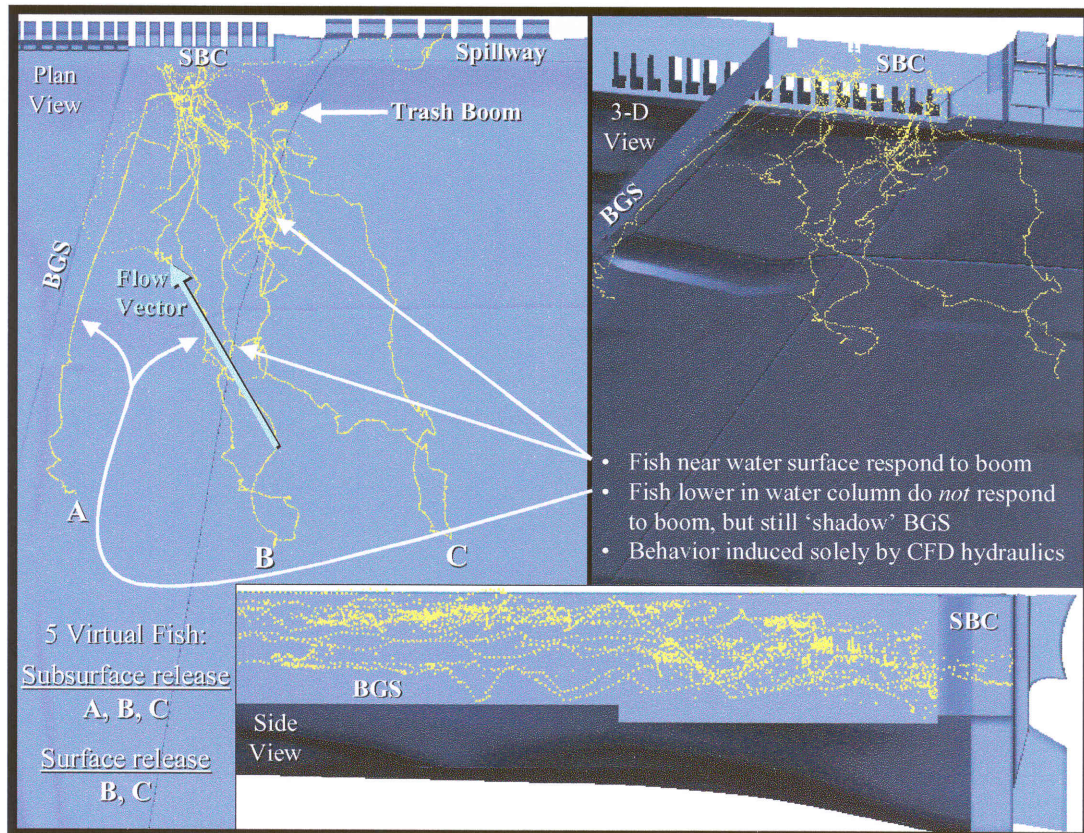


Figure 1.13. Plan, 3-D, and side views of the movement patterns of five virtual fish for case DH8.

both AT (Figure 1.14B) and virtual (Figure 1.13) migrants near the water surface move back and forth between the middle gate opening to the Surface Bypass Collector (SBC) and the powerhouse side of the trash boom. Figures 1.13 and 1.14C indicate that the SVP Hypothesis appears to capture the observed movement pattern of nighttime AT migrants (often direct-path migrants). That is, both AT (Figure 1.14C) and virtual (Figure 1.13) migrants lower in the water column pass underneath the trash boom with little-to-no response and, subsequently, approach the Behavioral

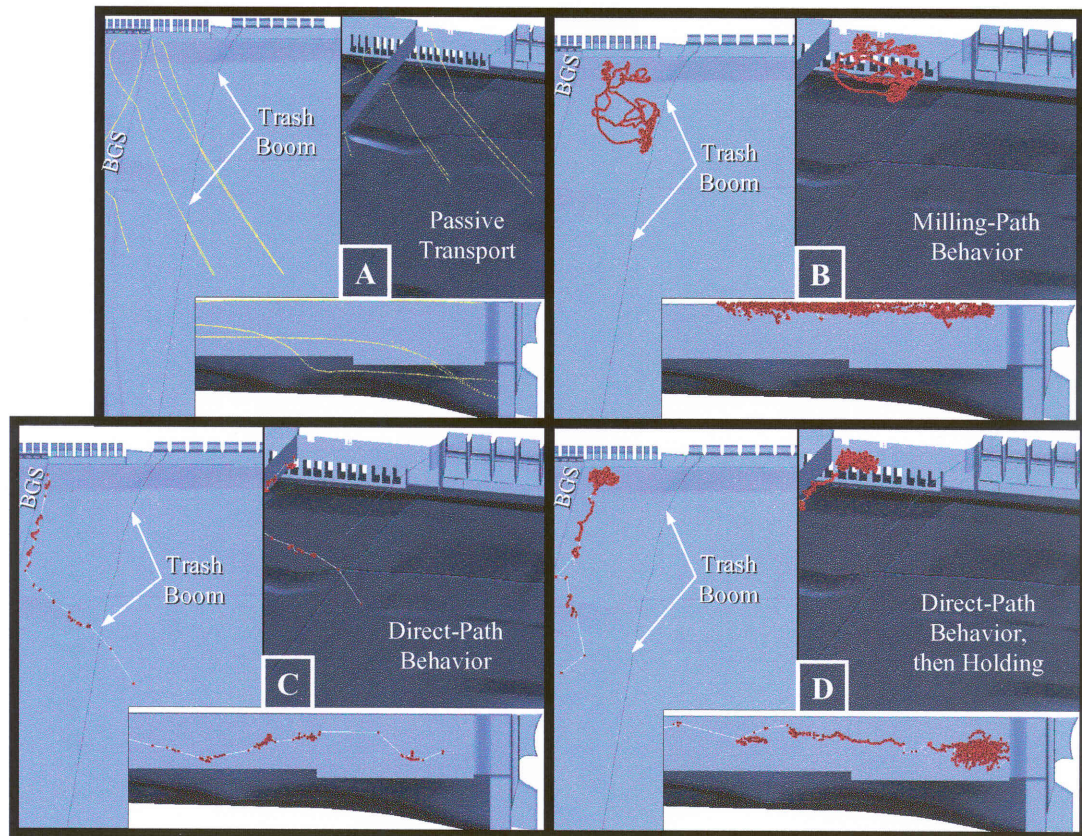


Figure 1.14. Comparison of the movements of five neutrally-buoyant passive particles (Plot A) and the movement patterns of selected, representative AT migrants for case DH8 (Plots B, C, D). Plot B illustrates the typical movement of migrants observed during the day (milling-path) when migrants are nearer the water surface. Plots C and D both illustrate typical movements of migrants observed at night (direct-path) when migrants are distributed deeper in the water column. AT data provided by Cash et al. (2002).

Guidance Structure (BGS) at approximately the same angle as the flow. Upon nearing the BGS, both the AT and virtual migrants shadow the BGS. This behavior is noteworthy as a migrant must exhibit a significant oriented volitional response while near the BGS, otherwise, the migrant will be swept against and then under the BGS. Acoustic-tagged (AT) migrants in Figures 1.14C and 1.14D are unlikely to be

responding to the BGS using visual acuity since these AT tracks were collected at night. Figures 1.13 and 1.14D indicate that the SVP Hypothesis appears to capture the observed milling location of nighttime AT migrants near the dam. Virtual migrants lower in the water column that approach the dam appear to mill, similarly, below the entrance to the middle gate opening to the SBC, yet above the turbine intake. Strain and velocity magnitude (speed) flow conditions may be viewed in Figure 1.15.

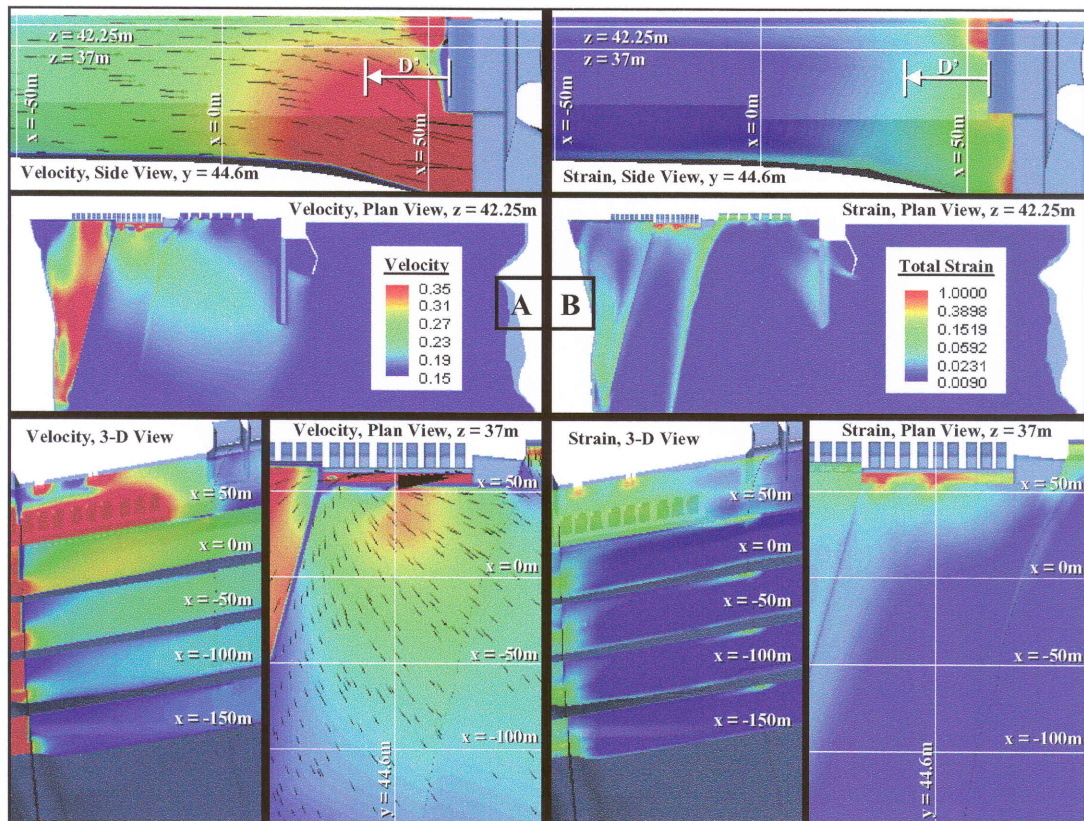


Figure 1.15. Resultant 3-D velocity magnitude (i.e., flow speed, m/sec, A plots on left half) and hydraulic strain (sec^{-1} , B plots on right half) for case DH8 flow conditions. Vertical and horizontal slices taken through the middle gate opening of the SBC. Note the pattern of free-shear flow (i.e., high strain, high velocity) enveloping all passage routes at the dam. The reference distance, D' , is the same distance as D' in Figure 1.17.

Fish Passage

Figure 1.16 indicates that the SVP Hypothesis, when implemented numerically, appears to capture the percentages with which the run-at-large fish population, i.e., all multi-beam hydroacoustic (HA) targets thought to be fish, used the various passage routes available at Lower Granite Dam in both 2000 and 2002 studies. This is noteworthy as only 2000 acoustic-tag (AT) telemetry and HA passage data were used to calibrate the coefficients of the numerically implemented version of the SVP Hypothesis in the “plug-and-play” simulation model. 2002 data were used strictly for blind validation. In other words, the SVP Hypothesis was refined and calibrated, numerically, with 2000 AT and HA data and then implemented for both 2000 and 2002 flow conditions using a priori CFD modeled data, but with no prior knowledge of 2002 AT or multi-beam hydroacoustic (HA) passage data. Initial comparison of 2002 actual and virtual results was performed by an independent entity.

The 45° line in Figure 1.16 indicates where points would reside if the implemented SVP Hypothesis resulted in a perfect match between HA and virtual migrant passage percentages. Bart (1995) indicates that a concurrence between observed and virtual distributions may be regarded as a strong test of the model, i.e., the implemented hypothesis. Statistical evaluation of the variance about the 45° line results in an r^2 equal to 0.80, when all cases are considered. That is, 80% of the variation in HA passage estimates may be explained by the SVP Hypothesis. However, if only composite and nighttime cases are evaluated, r^2 improves to 0.85. During the day, the visual acuity of migrants likely reduces the role hydrodynamics play in eliciting overall movement behavior. Therefore, it is not surprising that by leaving out cases C2 and F2 (i.e., the day-only studies, Table 1.2) results in an

improved r-squared value. Prairie (1996) indicates that a model (i.e., an implemented hypothesis) has rapidly increasing utility as r^2 exceeds 0.65.

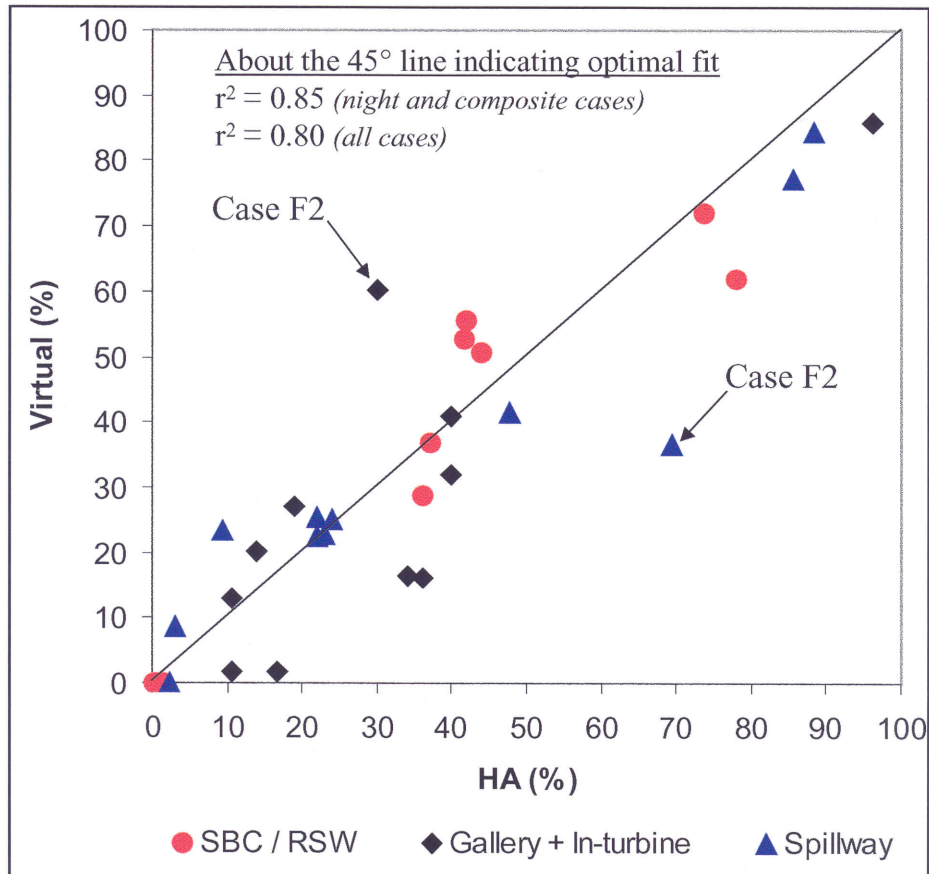


Figure 1.16. Comparison of multi-beam hydroacoustic (i.e., run-at-large) and virtual fish passage estimates at Lower Granite Dam. The three routes of passage available to migrants are: the SBC (in 2000) or RSW (in 2002) surface bypass structure, the spillway, or the turbine (includes both gallery and in-turbine passage). Of eleven total cases, only case C2 and F2 are day-only studies (Table 1.2). The 45° line indicates where all points would lie if “plug-and-play” predictions perfectly matched HA passage estimates. With respect to the 45° line, $r^2 = 0.80$ if all cases are used, and $r^2 = 0.85$ if day-only cases are not considered. Prairie (1996) indicates that predictive models have rapidly increasing utility as r^2 exceeds 0.65. HA passage data provided by Anglea et al. (2001, 2003).

Discussion

Utility of SVP Hypothesis

Complex problems in ecology sometimes have simple explanations (Côté and Reynolds, 2002). Many individuals following a few simple rules can result in complex and powerful behavior (Whitfield, 2001). In other words, complex properties often emerge from simple interactions (Whitfield, 2001). The SVP Hypothesis provides a tractable explanation of migrant movement behavior and passage observed at Lower Granite Dam that incorporates sensory biology, river hydrogeomorphology, turbulence, and other fundamentals of fluid dynamics. Furthermore, by graphically comparing the relative size in strain and velocity magnitude signatures associated with the Surface Bypass Collector (SBC, Figure 1.15) and Removable Spillway Weir (RSW, Figure 1.17), it is apparent why the RSW is associated with greater passage than the SBC. By the time the strain stimulus variable value, $\Delta s/s$, of an individual migrant approaching the RSW exceeds the strain threshold k_2 , the migrant is most likely already located in an area where the flow velocity exceeds its maximum burst speed. While the projection of elevated strain into the forebay is relatively similar for the SBC and RSW, the RSW projects a much larger velocity. In other words, for an equivalent location of k_2 , the speed of flow into the bypass structure is likely much larger at the location of k_2 for the RSW than the SBC. This would result in an increased probability that the migrant will be captured in the velocity plume of the RSW.

The distribution of forebay residence times (Cash et al., 2002; chapter 2) may be explained by considering the unique, individual experiences of each migrant. The ambient condition variables in the SVP Hypothesis, i.e., $s_{ambient}$ and $depth_{ambient}$, directly impact the values of the stimulus variable values, $\Delta s/s$ and Δd . Therefore, a migrant milling in relatively low-energy areas, i.e., low strain, will not acclimate to

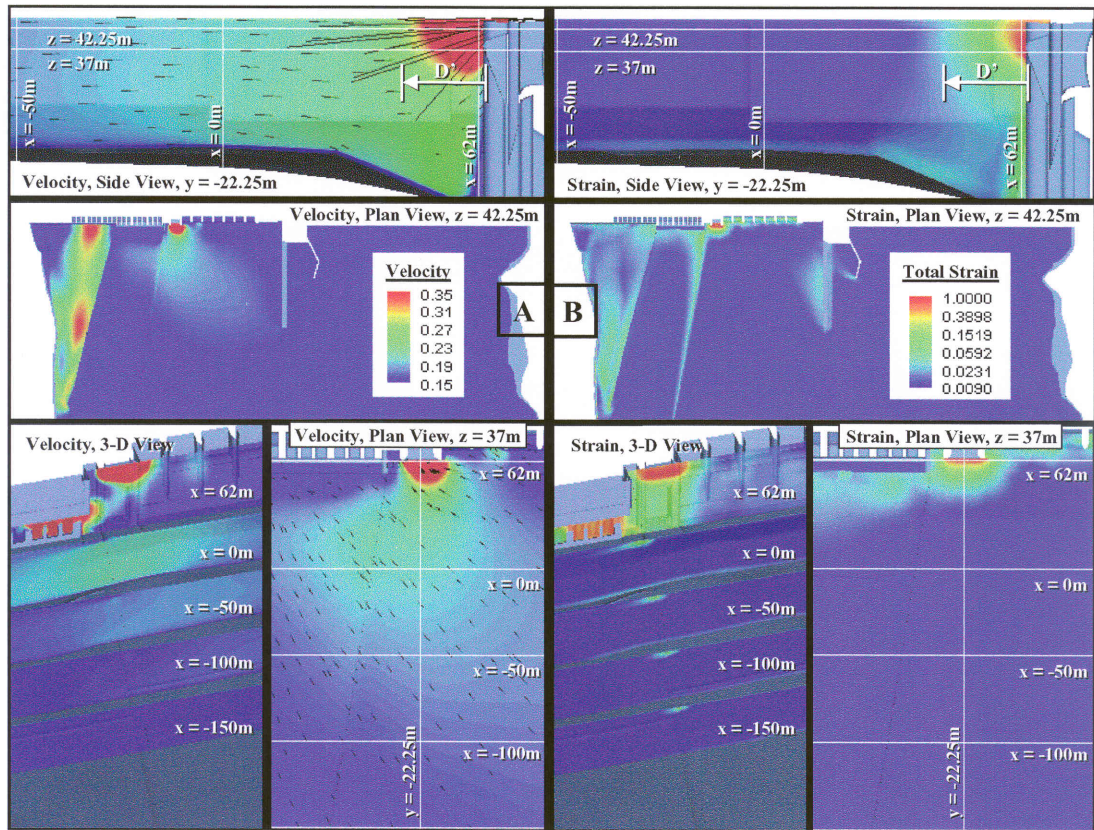


Figure 1.17. Resultant 3-D velocity magnitude (i.e., flow speed, m/sec, A plots on left half) and hydraulic strain (sec^{-1} , B plots on right half) for case A2 flow conditions. Vertical and horizontal slices taken through the middle of the RSW. Note the pattern of free-shear flow (i.e., high strain, high velocity) enveloping all passage routes at the dam. The reference distance, D' , is the same distance as D' in Figure 1.15. While the size of the strain signature associated with the RSW (B plots) and the SBC (Figure 1.15B) are approximately equal, the velocity plume associated with the RSW (A plots) is much larger than for the middle gate opening of the SBC (Figure 1.15A).

strain as quickly as migrants milling in relatively high-energy areas. Migrants milling in high-energy areas are likely to acclimate to higher levels of strain more quickly, thereby, reducing the stimulus variable value, $\Delta s/s$, below thresholds k_1 and k_2 more quickly. This would likely result in migrants milling in high-energy areas passing sooner, on average, than migrants milling in low-energy areas. Also, since

size influences the hydrodynamic picture available to migrants (Denton and Gray, 1983, 1988, 1989; Kalmijn, 1988, 1989; Coombs, 1996, 1999), it is plausible that k_1 and k_2 are slightly different for different sized migrants. This, together with possible species differences in k_1 and k_2 , provide additional explanation for the observed variation in forebay residence times. Size and differences in prior location experience may, possibly, explain the observation in Haro et al. (1998) that when Atlantic salmon smolts reached a point where water velocity was 2.25 m/s, some passed while others bursted upstream in an apparent escape response.

The SVP Hypothesis provides a foundation upon which to begin evaluating observed differences in wild and hatchery migrant behavior. Haro et al. (1998) suggest that bypass efficiencies may have a significant probabilistic component determined, in part, by whether the juvenile is a wild or hatchery fish. It is plausible that migrants raised in hatcheries would respond more adversely to (i.e., either not enter or take longer to enter into) designed surface bypass structures associated with elevated levels of strain that are foreign in hatchery environments. Although the hydrodynamic feature of free-shear flow is relatively rare in hatcheries and in deep free-flowing rivers, free-shear flow is a frequent feature in small streams where wild migrants are reared. Manga and Kirchner (2000), in fact, found in central Oregon streams that large woody debris covering less than 2% of the streambed can produce significant (approximately 50%) of the flow resistance. Since large woody debris reduces conveyance area, this form of flow resistance translates into free-shear flow patterns. In contrast, hatcheries are almost exclusively wall-bounded flow environments. This suggests that wild migrants may inherently develop an improved ability to respond to free-shear flow patterns in a manner conducive to entry into designed bypass structures, i.e., that are enveloped in free-shear flow. Interestingly, Plumb et al. (2002, 2003) found that hatchery migrants exhibit longer residence

times than wild steelhead in 2000 studies and in 2002 cases when the Removable Spillway Weir (RSW) was not operated (Table 1.2). Plumb et al. (2002, 2003) also indicate that hatchery migrants entered the Surface Bypass Collector (SBC, in year 2000) less frequently than wild migrants, although trends in both passage and forebay residence times are not statistically significant because of small sample sizes. In 2002, Plumb et al. (2003) indicate that hatchery and wild migrants passed in approximately the same proportions and with no appreciable difference in forebay residence times. It is plausible, however, that the larger velocity capture zone associated with the RSW (in 2002) results in a reduction of observed differences in wild and hatchery migrant passage since, even if wild and hatchery migrants respond to different threshold levels, both threshold levels may still be associated with velocities greater than maximum burst speed. Nonetheless, evidence exists to suggest that wild and hatchery migrants may respond differently to the same stimulus.

Knudsen et al. (1992) found in lab experiments that wild juvenile Atlantic salmon would respond to noise disturbances by swimming to the deepest part of the pool. In contrast, hatchery fish would simply swim away from the source with no favored, discernable orientation. Knudsen et al. (1992) suggest that the explanation for the discrepancy may be found by considering that hatchery fish are reared in tanks with uniform flow and deprived of the conditioning of seeking deep parts of the river for refuge.

Discrepancies

Although the SVP Hypothesis appears to capture significant portions of observed behavior, discrepancies exist. Nonetheless, many of the discrepancies are associated with reasonable explanations. First, the primary outliers in passage

comparisons (Figure 1.16) are associated with case F2. Interestingly, cases F2 and C2 are the two cases for which the model (i.e., the SVP Hypothesis) performed relatively poorly (chapter 2). Interestingly, they are also the only daytime studies (Table 1.2). This is not altogether surprising. During the day, vision can dominate other sensory modalities relegating the mechanosensory system to a secondary contributor in determining overall movement behavior (New and Kang, 2000; Montgomery et al., 1995). This may explain why Pavlov (1994) found that when light was low, juvenile river fish were more likely to drift with the current rather than maintain position. Haro et al. (1998) found that under very low light and dark conditions Atlantic salmon smolts tended to orient upstream more frequently, and Larinier and Boyer-Bernard (1991) (as summarized in Haro et al., 1998) found that Atlantic salmon smolt passage rates increased when lights at bypass entrances were turned off. Therefore, it is plausible that shadows cast by Lower Granite Dam, the Behavioral Guidance Structure (BGS), and the trash boom as well as other visual stimuli influence migrant behavior during the day in a manner that reduces hydrodynamic stimuli to a secondary contributor in overall movement behavior.

Second, the use of strain thresholds, k_1 and k_2 , to identify wall-bounded and free-shear flow patterns is a simplification of actual phenomenon. More thorough, i.e., mathematically complex, descriptions of these patterns could be used and may, possibly, improve results. Third, the presence of wall-bounded and free-shear flow patterns as perceived by an actual migrant is influenced by several attributes of the river environment nearly impossible to capture in a model. Fourth, factors influencing behavior decisions of an actual migrant likely depend, to some degree, on the species, health, size, anxiety, and exhaustion of the fish as well as background noise. In fact, the influence of these attributes on the preference, tolerance, resistance, and overall response of fish to another physicochemical stimulus has been

observed. Birtwell et al. (2003) found that level of starvation, physiological activities, prior history, age, and infections influence the thermal preferendum of fish.

Improving the SVP Hypothesis

Inevitably, the manner in which a migrant responds to its fluid environment depends inherently on the stability (i.e., transient nature) of associated hydrodynamic features. The ability to capture the transient nature of fluid flow and, therefore, the contribution of the inner ear sensory organ is not possible with steady-state simulations of fluid flow. Steady-state simulations eliminate the temporal components of fluid acceleration to which the inner ear is responsive. Hydraulic strain is equivalent to spatial acceleration. However, canal neuromast responses are, themselves, more nearly proportional to the net acceleration (temporal and spatial components of acceleration) between the fish and the surrounding water (Coombs et al., 2001; Kroese and Schellart, 1992). Thus, it is likely that with time-variant flow simulations, the influence of the inner ear and flow acceleration (both temporal and spatial components) can be more appropriately factored into the SVP Hypothesis.

Conclusion

While more sophisticated treatments of flow are likely to provide additional facility for decoding migrant movement behavior, the existing manifestation of the SVP Hypothesis provides a theoretically robust explanation of behaviors observed at Lower Granite Dam. Together, the SVP Hypothesis and “plug-and-play” simulation provide the means to evaluate plausible responses of migrants to future designs of bypass structures at Lower Granite Dam before they are built. Additional validation

of the SVP Hypothesis at other dams in the region would provide the foundation for region-wide improvements in the bypass methods needed for migrants.

REFERENCES

- Anderson, R. A. and Enger, P. S. (1968). "Microphonic potentials from the sacculus of a teleost fish." *Comparative Biochemistry and Physiology*, **27**, 879-881.
- Anderson, J. J. (2002). "An agent-based event driven foraging model." *Natural Resource Modeling*, **15**(1), Spring 2002.
- Anderson, J. J. (1991). "Fish bypass system mathematical models." *Proceedings from ASCE Waterpower '91*, Denver, CO, July 24-26, 1991.
- Anderson, J. J. (1988). "Diverting migrating fish past turbines." *The Northwest Environmental Journal*, **4**, 109-128.
- Anglea, S. M., Ham, K. D., Johnson, G. E., Simmons, M. A., Simmons, C. S., Kudera, E. and Skalski, J. R. (2003). "Hydroacoustic evaluation of the removable spillway weir at Lower Granite Dam in 2002." Final report prepared by Battelle Pacific Northwest Division for U.S. Army Corps of Engineers, Walla Walla District, PNWD-3219, Walla Walla, WA.
- Anglea, S. M., Johnson, R. L., Simmons, M. A., Thorsten, S. L., Duncan, J. P., Chamness, M. A., McKinstry, C. A., Kudera, E. A., and Skalski, J. R. (2001). "Fixed-location hydroacoustic evaluation of the prototype surface bypass and collector at Lower Granite Dam in 2000." Final report prepared by Battelle Pacific Northwest Division for U.S. Army Corps of Engineers, Walla Walla District, under Contract No. DACW68-96-D-002, Walla Walla, WA.
- Anonymous. (2000). Lower Granite Lock and Dam. Discharge and Velocity Measurements in Surface Bypass and Collector. US Army Corps of Engineers, Walla Walla District, September 2000.
- Arnold, G. P. (1974). "Rheotropism in fishes." *Biological Review*, **49**, 515-576.

- Bart, J. (1995). "Acceptance criteria for using individual-based models to make management decisions." *Ecological Applications*, **5**(2), 411-420.
- Bäckman, J. and Alerstam, T. (2002). "Harmonic oscillatory orientation relative to the wind in nocturnal roosting flights of the swift *Apus apus*." *Journal of Experimental Biology*, **205**, 905-910.
- Beamish, F. W. H. (1978). Fish physiology volume VII "Locomotion". W. S. Hoar and D. J. Randall (eds.), Academic Press, New York, NY, p. 101-183.
- Bian, L. (2003). "The representation of the environment in the context of individual-based modeling." *Ecological Modelling*, **159**, 279-296.
- Bickford, S. A. and Skalski, J. R. (2000). "Reanalysis, and interpretation of 25 years of Snake-Columbia River juvenile salmonid survival studies." *North American Journal of Fisheries Management*, **20**, 53-68.
- Birtwell, I. K., Korstrom, J. S., and Brotherston, A. E. (2003). "Laboratory studies on the effects of thermal change on the behaviour and distribution of juvenile chum salmon in sea water." *Journal of Fish Biology*, **62**, 85-96.
- Braun, C. B. and Coombs, S. (2000). "The overlapping roles of the inner ear and lateral line: the active space of dipole source detection." *Philosophical Transactions of The Royal Society of London series B*, **355**(1401), 1115-1119.
- Brett, J. R. (1952). "Temperature tolerance in young Pacific salmon, genus *Oncorhynchus*." *Journal of the Fisheries Research Board of Canada*, **9**, 265-323.
- Brett, J. R. and Alderdice, D. F. (1958). "Research on guiding young salmon at two British Columbia field stations." *Fisheries Research Board of Canada Bulletin*, **117**.

- Budy, P., Thiede, G. P., Bouwes, N., Petrosky, C. E., and Schaller, H. (2002). "Evidence linking delayed mortality of Snake River salmon to their earlier hydrosystem experience." *North American Journal of Fisheries Management*, **22**, 35-51.
- Carroll, S. S. and Pearson, D. L. (2000). "Detecting and modeling spatial and temporal dependence in conservation biology." *Conservation Biology*, **14**(6), 1893-1897.
- Cash, K. M., Hatton, T. W., Jones, E. C., Magie, R. J., Mayer, K. C., Swyers, N. M., Adams, N. S., and Rondorf, D. W. (2003). "Three-dimensional fish tracking to evaluate the removable spillway weir at Lower Granite Dam during 2002." Draft report prepared by U.S. Geological Survey Columbia River Research Laboratory for the U.S. Army Corps of Engineers, Walla Walla District, Walla Walla, WA.
- Cash, K. M., Adams, N. S., Hatton, T. W., Jones, E. C., and Rondorf, D. W. (2002). "Three-dimensional fish tracking to evaluate the operation of the Lower Granite surface bypass collector and behavioral guidance structure during 2000." Final report prepared by U.S. Geological Survey Columbia River Research Laboratory for the U.S. Army Corps of Engineers, Walla Walla District, Walla Walla, WA.
- Coombs, S. (1999). "Signal detection theory, lateral-line excitation patterns and prey capture behaviour of mottled sculpin." *Animal Behaviour*, **58**, 421-430.
- Coombs, S. (1996). "Interpore spacings on canals may determine distance range of lateral line system." *Society of Neuroscience Abstracts*, **22**, 1819.
- Coombs, S., Braun, C. B., and Donovan, B. (2001). "The orienting response of Lake Michigan mottled sculpin is mediated by canal neuromasts." *Journal of Experimental Biology*, **204**, 337-348.

- Coombs, S., Finneran, J. J., and Conley, R. A. (2000). "Hydrodynamic image formation by the peripheral lateral line system of the Lake Michigan mottled sculpin, *Cottus bairdi*." *Philosophical Transactions of The Royal Society of London series B*, **355**(1401), 1111-1114.
- Coombs, S. and Montgomery, J. C. (1999). The enigmatic lateral line system. In: *Comparative Hearing: Fishes and Amphibians*, A. N. Popper and R. R. Fay (eds.), Springer-Verlag, New York, NY, 319-363.
- Côté, I. M. and Reynolds, J. D. (2002). "Predictive ecology to the rescue?" *Science*, **298**, 1181-1182.
- Coutant, C. C. (2001a). "Turbulent attraction flows for guiding juvenile salmonids at dams." *Behavioral Technologies for Fish Guidance*, C. C. Coutant, ed., pp 57-77, American Fisheries Society, Symposium, **26**, Bethesda, MD.
- Coutant, C. C. (2001b). "Integrated, multi-sensory, behavioral guidance systems for fish diversions." *Behavioral Technologies for Fish Guidance*, C. C. Coutant, ed., pp 105-113, American Fisheries Society, Symposium, **26**, Bethesda, MD.
- Coutant, C. C. (1998). "Turbulent attraction flows for juvenile salmonid passage at dams." Report ORNL/TM-13608, Oak Ridge National Laboratory, Oak Ridge, TN.
- Coutant, C. C. and Whitney, R. R. (2000). "Fish behavior in relation to passage through hydropower turbines: a review." *Transactions of the American Fisheries Society*, **129**, 351-380.
- Crowder, D. W. and Diplas, P. (2002). "Vorticity and circulation: spatial metrics for evaluating flow complexity in stream habitats." *Canadian Journal of Fisheries and Aquatic Sciences*, **59**, 633-645.

- Dauble, D. D., Page, T. L., and Hanf, Jr., R. W. (1989). "Spatial distribution of juvenile salmonids in the Hanford Reach, Columbia River." *Fishery Bulletin*, **87**(4), 775-790.
- Denton, E. J. and Gray, J. A. (1983). "Mechanical factors in the excitation of clupeid lateral lines." *Proceedings of the Royal Society of London, series B*, **218**, 1-26.
- Denton, E. J. and Gray, J. A. (1988). "Mechanical factors in the excitation of the lateral line of fishes." *Sensory Biology of Aquatic Animals*, J. Atema, R. R. Fay, A. N. Popper, and W. N. Tavolga, eds., Springer, New York, NY, 595-617.
- Denton, E. J. and Gray, J. A. (1989). "Some observations on the forces acting on neuromasts in fish lateral line canals." *The Mechanosensory Lateral Line: Neurobiology and Evolution*, S. Coombs, P. Görner, and H. Münz, eds., Springer-Verlag, New York, NY, 229-246.
- Dijkgraaf, S. (1963). "The functioning and significance of the lateral line organs." *Biol. Rev.*, **38**, 51-105.
- Epperson, B. K. (2000). "Spatial and space-time correlations in ecological models." *Ecological Modelling*, **132**, 63-76.
- Faler, M. P., Miller, L. M., and Welke, K. I. (1988). "Effects of variation in flow on distributions of Northern Squawfish in the Columbia River below McNary Dam." *North American Journal of Fisheries Management*, **8**, 30-35.
- Farnsworth, K. D. and Beecham, J. A. (1999). "How do grazers achieve their distribution? A continuum of models from random diffusion to the ideal free distribution using biased random walks." *The American Naturalist*, **153**(5), 509-526.

- Fausch, K. D. (1993). "Experimental analysis of microhabitat selection by juvenile steelhead (*Oncorhynchus mykiss*) and coho salmon (*O. kisutch*) in a British Columbia stream." *Canadian Journal of Fisheries and Aquatic Sciences*, **50**, 1198-1207.
- Fausch, K. D. and White, R. J. (1981). "Competition between brook trout (*Salvelinus fontinalis*) and brown trout (*Salmo trutta*) for position in a Michigan stream." *Canadian Journal of Fisheries and Aquatic Sciences*, **38**, 1220-1227.
- Fay, R. R. and Edds-Walton, P. L. (2000). "Directional encoding by fish auditory systems." *Philosophical Transactions of The Royal Society of London, series B*, **355**(1401), 1281-1284.
- Fletcher, R. I. (1994). "Flows and fish behavior: large double-entry screening systems." *Transactions of the American Fisheries Society*, **123**, 866-885.
- Gerolotto, F., Soria, M., and Fréon, P. (1999). "From two dimensions to three: The use of multi-beam sonar for a new approach to fisheries acoustics." *Canadian Journal of Fisheries and Aquatic Sciences*, **56**(1), 6-12.
- Goodwin, R. A., Nestler, J. M., Loucks, D. P., and Chapman, R. S. (2001). "Simulating mobile populations in aquatic ecosystems." *Journal of Water Resources Planning and Management*, **127**(6), 386-393.
- Haro, A., Odeh, M., Noreika, J., and Castro-Santos, T. (1998). "Effect of water acceleration on downstream migratory behavior and passage of Atlantic salmon smolts and juvenile American shad at surface bypasses." *Transactions of the American Fisheries Society*, **127**, 118-127.
- Harte, J. (2002). "Toward a synthesis of the Newtonian and Darwinian worldviews." *Physics Today*, **55**(10), p 29.

- Hayes, J. W. and Jowett, I. G. (1994). "Microhabitat models of large drift-feeding brown trout in three New Zealand rivers." *North American Journal of Fisheries Management*, **14**, 710-725.
- HDR Engineering, Inc. and ENSR, Inc. (2000). Lower Granite Surface Bypass and Collector 2000 Prototype Tests: Documentation of Hydraulic Conditions and Project Operation. Final Report prepared for Walla Walla District, USACE, under Delivery Order Number 3, Contract Number DAXW68-00-D-0001, August 2000.
- Holland, J. H. (2003). Keynote Address. Seventh Annual Swarm Users/Researchers Conference, SwarmFest 2003, McKenna Hall, Notre Dame, Indiana, USA, April 13-15, 2003.
- Hotchkiss, R. H. (2002). "Turbulence investigation and reproduction for assisting downstream migrating juvenile salmonids." Final report prepared by Albrook Hydraulics Laboratory, Department of Civil and Environmental Engineering, Washington State University for Bonneville Power Administration, Portland, OR.
- Hudspeth, A. J. (1989). "How the ear's works work." *Nature*, **341**, 397-404.
- Johnson, W. R., Johnson, L., and Weitkamp, D. E., (1987). "Hydroacoustic evaluation of the spill program for fish passage at The Dalles Dam in 1986" Final Report, U.S. Army Corps of Engineers, Portland District, Portland, OR. March 1987.
- Johnson, G. E., (1996). "Fisheries research on phenomena in the forebay of Wells Dam in spring 1995 related to the surface flow smolt bypass" Final Report, U.S. Army Corps of Engineers, Walla Walla District, Walla Walla, WA. March 1996.

- Johnson, R. L., Anglea, S. M., Blanton, S. L., Simmons, M. A., Moursund, R. A., Johnson, G. E., Kudrea, E. A., Thomas, J., and Skalski, J. R. (1999). Hydroacoustic Evaluation of Fish Passage and Behavior at Lower Granite Dam in Spring 1998. Final Report prepared for U.S. Army Engineer District, Walla Walla by Battelle Pacific Northwest National Laboratories, Richland, WA.
- Johnson, G., Hedgepeth, J., Giorgi, A., and Skalski, J. (2000a). "Evaluation of smolt movements using an active fish tracking sonar at the sluiceway surface bypass, The Dalles Dam, 2000" Draft Final Report, U.S. Army Corps of Engineers, Portland District, Portland, OR. October 31, 2000.
- Johnson, G. E., Adams, N. S., Johnson, R. L., Rondorf, D. W., Dauble, D. D., and Barila, T. Y. (2000b). "Evaluation of the prototype surface bypass for salmonid smolts in spring 1996 and 1997 at Lower Granite Dam on the Snake River, Washington." *Transactions of the American Fisheries Society*, **129**, 381-397.
- Kalmijn, A. J. (2000). "Detection and processing of electromagnetic and near-field acoustic signals in elasmobranch fishes." *Philosophical Transactions of The Royal Society of London series B*, **355**(1401), 1135-1141.
- Kalmijn, A. J. (1989). "Functional evolution of lateral line and inner-ear sensory systems." *The Mechanosensory Lateral Line: Neurobiology and Evolution*, S. Coombs, P. Görner, and H. Münz, eds., Springer-Verlag, New York, NY, 187-215.
- Kalmijn, A. J. (1988). "Hydrodynamic and acoustic field detection." *Sensory Biology of Aquatic Animals*, J. Atema, R. R. Fay, A. N. Popper, and W. N. Tavolga, eds., Springer, New York, NY, 83-130.

- Kanter, M. J. and Coombs, S. (2003). "Rheotaxis and prey detection in uniform currents by Lake Michigan mottled sculpin (*Cottus bairdi*).” *Journal of Experimental Biology*, **206**, 59-70.
- Knudsen, F. R., Enger, P. S., and Sand, O. (1992). "Awareness reactions and avoidance responses to sound in juvenile Atlantic salmon, *Salmo salar L.*” *Journal of Fish Biology*, **40**, 523-534.
- Kroese, A. B. A. and Schellart, N. A. M. (1992). "Velocity- and acceleration-sensitive units in the trunk lateral line of the trout.” *Journal of Neurophysiology*, **68**(6), 2212-2221.
- Lai, Y. G., Weber, L. J., and Patel, V. C. (2003a). "Nonhydrostatic three-dimensional model for hydraulic flow simulation. I: Formulation and Verification.” *ASCE Journal of Hydraulic Engineering*, **129**(3), 196-205.
- Lai, Y. G., Weber, L. J., and Patel, V. C. (2003b). "Nonhydrostatic three-dimensional model for hydraulic flow simulation. II: Validation and Application.” *ASCE Journal of Hydraulic Engineering*, **129**(3), 206-214.
- Lai, Y. G. (2000). "Unstructured grid arbitrarily shaped element method for fluid flow simulation.” *AIAA Journal*, **38**(12), 2246-2252.
- Larinier, M. and Boyer-Bernard, S. (1991). "Dévalaison des smolts et efficacité d'un exutoire de dévalaison à l'usine hydroélectrique d'Halsou sur la Nive.” *Bulletin Français de la Pêche et de la Pisciculture*, **321**, 72-92.
- Legendre, P. (1993). "Spatial autocorrelation: trouble or new paradigm?” *Ecology*, **74**(6), 1659-1673.
- Leopold, L. B., Wolman, M. G., and Miller, J. P. (1964). *Fluvial processes in geomorphology*. W. H. Freeman and Company, San Francisco, CA, 522 pp.
- Lucas, M. C. and Baras, E. (2000). "Methods for studying spatial behaviour of freshwater fishes in the natural environment.” *Fish and Fisheries*, **1**, 283-316.

- Manga, M. and Kirchner, J. W. (2000). "Stress partitioning in streams by large woody debris." *Water Resources Research*, **36**(8), 2373-2379.
- McFarland, D. and Houston, A. (1981). *Quantitative Ethology: The State Space Approach*, Pitman Advanced Publ. Program, Boston, MA.
- McLaughlin, R. L. and Noakes, D. L. (1998). "Going against the flow: an examination of the propulsive movements made by young brook trout in streams." *Canadian Journal of Fisheries and Aquatic Sciences*, **55**, 853-860.
- Meffe, G. K. (1992). "Techno-arrogance and halfway technologies: salmon hatcheries on the Pacific coast of North America." *Conservation Biology*, **6**(3), 350-354.
- Montgomery, J. C., Baker, C. F., and Carton, A. G. (1997). "The lateral line can mediate rheotaxis in fish." *Nature*, **389**, 960-963.
- Montgomery, J. C., Carton, A. G., Voigt, R., Baker, C. F., and Diebel, C. (2000). "Sensory processing of water currents by fishes." *Philosophical Transactions of The Royal Society of London series B*, **355**(1401), 1325-1327.
- Montgomery, J. C., Coombs, S., and Halstead, M. (1995). "Biology of the mechanosensory lateral line in fishes." *Reviews in Fish Biology and Fisheries*, **5**, 399-416.
- Nestler, J. M. and Goodwin, R. A. (in review). "Eulerian-Lagrangian coupling of engineering and biological models." Accepted for publication by *Journal of Water Resources Planning and Management*.
- Nestler, J. M., Goodwin, R. A., Cole, T., Degan, D. and Dennerline, D. (2002). "Simulating movement patterns of blueback herring in a stratified southern impoundment." *Transactions of the American Fisheries Society*, **131**, 55-69.

- New, J. G., Fewkes, L. A., and Khan, A. N. (2001). "Strike feeding behavior in the muskellunge, *Esox masquinongy*: contributions of the lateral line and visual sensory systems." *Journal of Experimental Biology*, **204**, 1207-1221.
- New, J. G. and Kang, P. Y. (2000). "Multimodal sensory integration in the strike-feeding behaviour of predatory fishes." *Philosophical Transactions of The Royal Society of London series B*, **355**(1401), 1321-1324.
- Ojha, C. S. P. and Singh, R. P. (2002). "Flow distribution parameters in relation to flow resistance in an upflow anaerobic sludge blanket reactor system." *Journal of Environmental Engineering*, **128**(2), 196-200.
- Okubo, A. (1980). Diffusion and Ecological Problems: Mathematical Models, Lecture Notes in Biomathematics, Vol. 10, Springer-Verlag, New York, NY, p.254.
- Parrish, J. K. and Edelstein-Keshet, L. (1999). "Complexity, pattern, and evolutionary trade-offs in animal aggregation." *Science*, **284**, 99-101.
- Parrish, J. K. and Turchin, P. (1997). "Individual decisions, traffic rules, and emergent pattern in schooling fish." *Animal Groups in Three Dimensions*, J. K. Parrish and W. M. Hamner, eds., Cambridge University Press, New York, NY, 126-142.
- Pavlov, D. S. (1994). "The downstream migration of young fishes in rivers: mechanisms and distribution." *Folia Zoologica*, **43**, 193-208.
- Paxton, J. R. (2000). "Fish otoliths: do sizes correlate with taxonomic group, habitat and/or luminescence?" *Philosophical Transactions of The Royal Society of London series B*, **355**(1401), 1299-1303.
- Plumb, J. M., Braatz, A. C., Lucchesi, J. N., Fielding, S. D., Sprando, J. M., George, G. T., Adams, N. S., and Rondorf, D. W. (2003). "Behavior of radio-tagged juvenile Chinook salmon and steelhead and performance of a removable

- spillway weir at Lower Granite Dam, Washington, 2002.” Draft report prepared by U.S. Geological Survey Columbia River Research Laboratory for U.S. Army Corps of Engineers, Walla Walla District, Walla Walla, WA.
- Plumb, J. M., Novick, M. S., Adams, N. S., and Rondorf, D. W. (2002). “Behavior of radio-tagged juvenile Chinook salmon and steelhead in the forebay of Lower Granite Dam relative to the 2000 surface bypass and behavioral guidance structure tests.” Final report prepared by U.S. Geological Survey Columbia River Research Laboratory for U.S. Army Corps of Engineers, Walla Walla District, Walla Walla, WA.
- Popper, A. N. and Carlson, T. J. (1998). “Application of sound and other stimuli to control fish behavior.” *Transactions of the American Fisheries Society*, **127**, 673-707.
- Prairie, Y. T. (1996). “Evaluating the predictive power of regression models.” *Canadian Journal of Fisheries and Aquatic Sciences*, **53**, 490-492.
- Prior, H., Lingenauber, F., Nitschke, J., and Güntürkün, O. (2002). “Orientation and lateralized cue use in pigeons navigating a large indoor environment.” *Journal of Experimental Biology*, **205**, 1795-1805.
- Railsback, S. F., Lamberson, R. H., Harvey, B. C., and Duffy, W. E. (1999). “Movement rules for individual-based models of stream fish.” *Ecological Modelling*, **123**, 73-89.
- Rapoport, A. (1983). *Mathematical models in social and behavioral sciences*. John Wiley & Sons, Inc., New York, NY, 507 pp.
- Rogers, P. H. and Cox, M. (1988). “Underwater sound as a biological stimulus” *Sensory Biology of Aquatic Animals*, J. Atema, R. R. Fay, A. N. Popper, and W. N. Tavolga, eds., Springer, New York, NY, 131-149.

- Roxburgh, S. H. and Matsuki, M. (1999). "The statistical validation of null models used in spatial association analyses." *Oikos*, **85**, 68-78.
- Ruggles, C. P. and Ryan, P. (1964). "An investigation of louvers as a method of guiding juvenile Pacific salmon." *Canadian Fish Culturist*, **33**, 3-67.
- Schilt, C. R. and Nestler, J. M. (1997). "Fish bioacoustics: considerations for hydropower industry workers." *Proceedings of the International Conference on Hydropower*, August 5-8, Atlanta, GA.
- Schilt, C. R. and Norris, K. S. (1997). "Perspectives on sensory integration systems: Problems, opportunities, and predictions." *Animal Groups in Three Dimensions*, J. K. Parrish and W. M. Hamner, eds., Cambridge University Press, New York, NY, 225-244.
- Schwartz, E. (1974). "Lateral-line mechano-receptors in fishes and amphibians." In: *Handbook of sensory physiology III/3*, A. Fessard (ed.), Springer-Verlag, New York, NY, pages 257-270.
- Smith, D. L. (2003). The shear flow environment of juvenile salmonids. Ph.D. dissertation. Department of Natural Resources, University of Idaho, Moscow, Idaho.
- Smith, S. G., Muir, W. D., Williams, J. G., and Skalski, J. R. (2002). "Factors associated with travel time and survival of migrant yearling Chinook salmon and Steelhead in the lower Snake River." *North American Journal of Fisheries Management*, **22**, 385-405.
- Skorogobogatov, M. A., Mosiyevskiy, A. A., Korolyov, V. G., and Tyuryukov, S. N. (1993). "Hydraulic and biological research of fish bypasses for high-head hydropower systems." *Energeticheskoye stroitelstvo*, December 1993, 67-71 (in Russian; translation available from C. C. Coutant).

- Sogard, S. M. and Olla, B. L. (1993). "Effects of light, thermoclines and predator presence on vertical distribution and behavioral interactions of juvenile walleye pollock, *Theragra chalcogramma* Pallas." *Journal of Exp. Mar. Biol. Ecol.*, **167**, 179-195.
- Standen, E. M., Hinch, S. G., Healey, M. C., and Farrell, A. P. (2002). "Energetic costs of migration through the Fraser River Canyon, British Columbia, in adult pink (*Oncorhynchus gorbuscha*) and sockeye (*Oncorhynchus nerka*) salmon as assessed by EMG telemetry." *Canadian Journal of Fisheries and Aquatic Sciences*, **59**, 1809-1818.
- Steel, E. A., Guttorp, P., Anderson, J. J., and Caccia, D. C. (2001). "Modeling juvenile migration using a simple Markov chain." *Journal of Agricultural, Biological, and Environmental Statistics*, **6**(1), 80-88.
- Steig, T. W. and Timko, M. A. (2000). "Using acoustic tags for monitoring juvenile Chinook and steelhead migration routes in the forebay of Rocky Reach Dam during the spring and summer of 1999." Report to Chelan County PUD No. 1, Wenatchee, WA, by Hydroacoustic Technology, Inc., Seattle, WA.
- Steig, T. W. (1999). "The use of acoustic tags to monitor the movement of juvenile salmonids approaching a dam on the Columbia River." Proceedings of the 15th International Symposium on Biotelemetry, Juneau, Alaska, 9-14, May, 1999.
- Steig, T. W. and Johnson, W. R. (1986). "Hydroacoustic assessment of downstream migrating salmonids at The Dalles Dam in spring and summer 1985" Final Report DOE/BP-23174-2, U.S. Department of Energy, Bonneville Power Administration, Portland, OR.
- Suckling, E. E. and Suckling, J. A. (1964). "Lateral line as a vibration receptor." *Journal of the Acoustical Society of America*, **36**, 2214-2216.

- Tennekes, H. and Lumley, J. L. (1972). A first course in turbulence. The MIT Press, Cambridge, MA, 300 pp.
- Travade, F. and Larinier, M. (1992). "La migration de dévalaison: problèmes et dispositifs." *Bulletin Français de la Pêche et de la Pisciculture*, **326-327**, 165-176.
- Turchin, P. (1997). "Quantitative analysis of animal movements in congregations." *Animal Groups in Three Dimensions*, J. K. Parrish and W. M. Hamner, eds., Cambridge University Press, New York, NY, 107-112.
- Underwood, A. J. and Chapman, M. G. (1985). "Multifactorial analyses of directions of movement of animals." *Journal of Experimental Marine Biology and Ecology*, **91**, 17-43.
- Voigt, R., Carton, A. G., and Montgomery, J. C. (2000). "Responses of anterior lateral line afferent neurones to water flow." *Journal of Experimental Biology*, **203**, 2495-2502.
- Webb, J. F. and Smith, W. L. (2000). "The laterophysic connection in chaetodontid butterflyfish: morphological variation and speculations on sensory function." *Philosophical Transactions of The Royal Society of London series B*, **355**(1401), 1125-1129.
- Whitfield, J. (2001). "Ant group dynamics." *Nature, Science Update*, July 19, 2001.
- Workman, R. D., Hayes, D. B., and Coon, T. G. (2002). "A model of steelhead movement in relation to water temperature in two Lake Michigan tributaries." *Transactions of the American Fisheries Society*, **131**, 463-475.
- Wright, K. K. and Li, J. L. (2002). "From continua to patches: examining stream community structure over large environmental gradients." *Canadian Journal of Fisheries and Aquatic Sciences*, **59**, 1404-1417.

Decoding Movement Patterns of Fish for Forecast Simulation Using CEL Agent Individual-based Modeling

Abstract

A theoretically- and computationally-robust mathematical approach for decoding the movement patterns of individual fish in 3-D space-time with respect to prevailing 3-D biotic and abiotic (physicochemical) stimuli is described. The modeling scheme, coupled Eulerian-Lagrangian agent- and individual-based modeling (CEL Agent IBM) unifies the three primary theoretical frameworks for mathematically describing the movement behavior of aquatic species in 3-D space-time. The CEL Agent IBM method is intuitive and based on well-established principles in computer science, fluid and water quality dynamics, computational fluid dynamics (CFD) modeling, and foraging theory. In short, the CEL Agent IBM method couples a 3-D Lagrangian particle-tracker supplemented with behavioral rules into a 3-D Eulerian CFD model. The mathematical structure of the behavioral rules is derived from an agent-based, event-driven foraging model. Stimuli are queried from the physicochemical information provided by the CFD model and other a priori field data. CEL Agent IBM coefficients are biologically tractable and may be evaluated in a laboratory, at proper scales, for further validation. Back-casting simulation analysis results in mathematical behavior formulations amendable to forecast simulation. In this paper, we demonstrate how a CEL Agent IBM was used to mathematically and theoretically decode the mechanics eliciting 3-D movement patterns of downstream migrating juvenile salmon observed approaching and passing Lower Granite Dam on the Snake River, Washington, USA. The CEL Agent IBM calibrated and, subsequently, validated on multiple independent data sets collected in two different years and at two different hydraulically-based fish bypass structures.

The CEL Agent IBM discussed herein, the Numerical Fish Surrogate, is presently being used by the US Army Corps of Engineers to quantitatively evaluate virtual designs of future fish bypass systems at federal hydropower dams before they are built and installed. CEL Agent IBMs are applicable to many aquatic systems and provide the theoretical and computational facility for improving the simulation of population dynamics. The methodology is collapsible to 2-D and 1-D, if necessary.

Introduction

The movement dynamics of mobile populations is central to many studies of aquatic ecosystem health. Therefore, understanding the spatial dynamics of aquatic populations and identifying factors contributing to movement behavior dynamics is critical to assessing and managing fisheries (Schmalz et al., 2002; Pelletier and Parma, 1994) and for improving water resource management strategies (Van Winkle et al., 1993), e.g., for hydropower generation, sport fisheries, and even landscape development. In many systems, the distribution of organisms is driven by environmental factors (Pientka and Parrish, 2002). Consequently, the influence of the physicochemical regime on movement patterns should be evaluated prior to the evaluation of hypothetical biological interactions (Hussko et al., 1996; Pientka and Parrish, 2002). Identifying patterns and the underlying mechanisms that generate them improve the ability of decision-makers to forecast (Harte, 2002) potential impacts of alternative management strategies.

Understanding the movement of individuals is important because while individual movement can be translated into an understanding of population dynamics, the converse is generally not possible (Turchin, 1997). Advances in telemetry technologies (e.g., Steig, 1999; Gerolotto et al., 1999; Johnson et al., 1999) have led to a proliferation of high-resolution 3-D tracking data and laboratory

research is rapidly expanding our understanding of fish sensory capabilities (e.g., Coombs et al., 2001; Kröther et al., 2002). However, methods for analyzing, decoding, and interpreting integrated tracking and physicochemical information are not readily available (Steel et al., 2001), particularly with regard to the purview of forecasting.

We introduce a mathematical method for decoding the movement patterns of individuals in 3-D space-time with respect to prevailing biotic and abiotic (physicochemical) stimuli. The method is intuitive and based on well-established principles in computer science, fluid dynamics, computational fluid dynamics (CFD) modeling, and foraging theory. Mathematical formulations resulting from back-casting simulation analysis are theoretically-robust and, therefore, amendable to forecast simulation. The method uses coefficients that are biologically tractable and may be evaluated in a laboratory, at the appropriate scales, for additional validation and analysis. In this paper, we briefly discuss several modeling approaches used to capture fish movement, introduce an intuitive integrated, or intermediate, modeling approach, and demonstrate how the methodology was successfully applied to mathematically and theoretically decode the mechanics eliciting 3-D movement patterns of downstream outmigrating juvenile salmon (migrants) observed approaching and passing Lower Granite Dam on the Snake River, Washington, USA. The model was calibrated and, subsequently, validated on multiple independent data sets collected in two different years and for two different hydraulically-based fish bypass structures. The modeling approach is generally applicable to many aquatic systems and is collapsible to 2-D and 1-D, if necessary.

Modeling Approaches

Deciphering and interpreting the hierarchical organization of responses to various stimulus cues and the integration of information from various sensory modalities within a behavioral program are fundamental issues in attempts to understand sensorimotor integration and the functional relationship between brain and behavior (New et al., 2001). Kalmijn (2000) suggests that at the most fundamental, scientific level, "the more salient features of the flow field are the variable explanations behind predation and movement, and that in seeking regularity and focusing on the most salient features in their environment, in order to endure and thrive, animals have empirically discovered the laws of nature". Methods for decoding, interpreting, and forecasting the relationship between individual and the physicochemical regime may be generally classified according to the scale at which processes are evaluated: physical, empirical, and intermediate.

Physical Approaches

Physical approaches may be generally described as attempts to capture indisputable physical relationships and, thus, rely to a minimum degree on an accumulating chain of assumptions. With respect to fluid dynamics, the behavior of water in nature obeys known laws of fluid mechanics and thermodynamics, but its movement cannot be described either simply or completely as one cannot possibly account for the effects of each small perturbation on the flow or phase changes in the hydrodynamic environment (Brutsaert, 1986). State-of-the-art methods continue to improve the spatiotemporal scale at which fluid dynamics can be resolved (e.g., Sotiropoulos, in press). However, the physical approach is likely to remain intangible with respect to fluid dynamics because properties of fluid systems can never be measured accurately enough and solutions based on internal physical

relationships can only be obtained for grossly idealized conditions that are coarse approximations of any real situation (Brutsaert, 1986).

With respect to functional relationships between sensory acuity, brain, and behavior, biologists can now selectively deactivate certain specific sensory modalities of the fish mechanosensory system, which permits in-depth analysis of the function and interrelationships between modalities. While some models of the fish sensory system exist (e.g., Coombs et al., 2000), functional subdivision of the lateral line periphery and other modalities continue to be refined (Kröther et al., 2002). Haefner and Bowen (2002) indicate that Terzopoulos et al. (1995) and Ijspeert and Kodjabachian (1999) developed models of fish swimming from the perspective of muscle and neuron interactions and produced a repertoire of behaviors including schooling, feeding, courtship, and predator avoidance. While not attempting to simulate volitional behavior, Jones et al. (2002) describe preliminary attempts at capturing and simulating unsteady fluid dynamics and forces at the surface of a flexible fish body in turbine environments using large-eddy simulation (LES). In short, physical approaches provide valuable insight into the small-scale phenomenon fundamental to observed behavior, although in the near future they are likely to remain the purview of relatively focused, small-scale analyses and impractical for larger-scale, in-situ analysis.

Empirical Approaches

Empirical, or “black box”, methods may be generally described as focusing on the discovery of mathematical relationships between external input and external output without respect to the underlying physical relationships (Brutsaert, 1986). As Harte (2002) points out, however, correlation does not necessarily imply causation. Presently, methods are being developed to better interpret the relative influence of

input variables in artificial neural networks (e.g., Olden and Jackson, 2002; Gevrey et al., 2003), and some neural nets with feedback loops have demonstrated the capacity for learning intricate concepts (Holland, 2003). To date, however, neural networks cannot translate observed behavior into a mechanistic, rule-based mathematical description of the underlying mechanisms eliciting behavior (Holland, 2003). In the future this may change, but identifying patterns and the underlying mechanisms that generate them are necessary to improve the ability to predict (Harte, 2002).

Expanding existing models, which often involves adding complexity, requires the facility to assess the present model structure to determine if additional complexity is really necessary (Ginot et al., 2002). Ginot et al. (2002) extend one of Grimm's (1999) primary criticisms of the use of IBMs to suggest that black box approaches do not provide the facility needed in biological simulations to sufficiently explore model structure and its relationship with the output. Harte (2002) suggests that what is needed are simple, mechanistic models (the intermediate approach).

Intermediate Approach

An intermediate approach may be generally described as structuring input-output response functions using tractable and suitably simplified equations of the physical processes perceived to be relevant (Brutsaert, 1986). In essence, while physical and empirical approaches appear incompatible in their detail, they can still be used to deal with different aspects of the same phenomenon. The problem is not deciding on which modeling approach is most appropriate, but rather one of proper parameterization. That is, replacing complicated interactions at smaller scales than those handled explicitly in the model and describing the subresolution or microscale processes of the phenomenon in terms of resolvable scale variables, which can be

treated explicitly in the analysis and/or model (Brutsaert, 1986). Laws in ecology do not have the exactness and universality of physical laws and, therefore, there will be approximations and exceptions in their formulation and application (Harte, 2002). Even if all the laws of nature were known, it is still likely the utility of computer models would be limited, without simplification of the equations, because of the computational time and parameterization required (Alewell and Manderscheid, 1998).

Complex simulation models are not new in ecology and have been criticized for three primary reasons: complex models are hard to develop, hard to communicate, and hard to understand (Grimm et al., 1999). Critical to the development of simple, mechanistic models (the intermediate approach) is the identification of appropriately lumped system variables that can substitute for subsets of the detailed variables in traditional complex models (Grimm, 1999; Harte, 2002). This, in turn, depends on the spatiotemporal scale, or scales, of the analysis. To find the appropriate scale, Grimm (1999) suggests the 'scaling-down' approach, which entails starting with a very coarse resolution model and increasing resolution until some general pattern of interest is reproduced. The best model, then, is the one that best captures features of interest with the fewest details (Haw, 2001). This maximizes dexterity and the interpretative value of the model. Furthermore, the model is easier to use, modify, and transport to other applications. Presently, however, this process is confounded by different theoretical approaches used in the analysis of animal movement and aggregation. In general, theoretical approaches may be classified as: Eulerian, Lagrangian, or discrete rules (agent-based) simulation (Parrish and Edelstein-Keshet, 1999).

Eulerian approaches use partial differential equations to describe movement in terms of density or mass fluxes of individuals. Individuals, however, are not

handled as discrete singular entities. The Lagrangian approach avoids this liability by using equations of motion, detailed forces, and velocities attributed to individuals. The Lagrangian approach, however, is computationally impractical for solving mass- and energy-fluxes critical to simulating 3-D fluid environments using establish, fundamental equations of physiochemical dynamics. Discrete-rules (agent-based) simulation dispenses with equations of motion in Newtonian space and focuses solely on behavioral rules for discrete entities. An example of this third approach is the multi-agent simulation system SWARM (e.g., Minar et al., 1996; Luna and Perrone, 2001). None of the three predominant theoretical frameworks, however, provides robust facility for handling the interplay between deterministic and stochastic components of discrete individual movement behavior in a 3-D space-time physicochemical environment. Furthermore, none of the frameworks provide the computational means for linking local and long-range model output in a manner compatible with field collected data of the real-world phenomena.

Progress in understanding biological problems depends on mathematical advances in spatial dynamics and finding ways to compare model output to field collected data (Hastings and Palmer, 2003). At the same time, simplicity is a criterion of good models because all-inclusive models can be too complicated to be understood, reducing their use by managers (Fagerström, 1987; Hanna et al., 1999) and researchers alike. Hanna et al. (1999) and DeAngelis and Cushman (1990) advocate using combined, or coupled, models to examine causal linkages between system processes. An appealing aspect of linking models is that it simplifies the modeling of aquatic processes (Hanna et al., 1999). Model power and simplicity are achieved, simultaneously, by coupling the models in a manner that maximizes the utility and minimizes the liability of each (Nestler and Goodwin, in review). In this paper, we describe, demonstrate, and evaluate the utility of a linked, or coupled,

modeling approach. Coupled Eulerian-Lagrangian agent- and individual-based modeling (CEL Agent IBM) provides a conceptually simple integrated modeling approach that unites the theoretical frameworks in Parrish and Edelstein-Keshet (1999). In a CEL Agent IBM, a 3-D Lagrangian particle-tracking algorithm is supplemented with behavioral rules (Schilt and Norris, 1997) from an agent-based, event-driven foraging model (Anderson, 2002). Theoretically, the movement decisions of aquatic species (i.e., whether an individual, school, or some aggregate of the population) are viewed as a balance of attractions to and repulsions from various sources or foci (Okubo, 1980; Parrish and Turchin, 1997) using concepts and mathematics derived from game theory, neuroscience, psychology, computer science, and foraging theory (Anderson, 2002). Three-dimensional movement behavior is then implemented within a 3-D CFD model, U²RANS (Lai et al., 2003a; Lai et al., 2003b; Lai, 2000), to take advantage of state-of-the-art numerical modeling of physicochemical fields in aquatic systems (Goodwin et al., 2001; Nestler et al., 2002; Nestler and Goodwin, in review).

Three-dimensional CEL Agent individual-based modeling is derived, primarily, from two works: Goodwin et al. (2001) and Anderson (2002). However, 3-D CEL Agent modeling is, more broadly, developed from and embodies a synthesis of attributes from many prior works. These include: Eulerian-Lagrangian methods used in the study and simulation of hydrodynamics (e.g., Costa and Ferreira, 2000), CEL hybrid modeling theory (Nestler and Goodwin, in review), foraging theory, grid-, agent-, and object-oriented concepts for describing the environment (e.g., Lai et al., 2003a; Bian, 2003), event-based concepts (e.g., Ewing et al., 2002), existing spatially-explicit IBMs (e.g., Dunning et al., 1995; Romey, 1996; Clark and Rose, 1997; Van Winkle et al., 1998; Railsback et al., 1999a; Dagorn et al., 2000; Gaff et al., 2000; Petersen and DeAngelis, 2000; Xiao, 2000),

linked models of physicochemical dynamics and individual fish behavior (e.g., Hinckley et al., 1996; Bourque et al., 1999; Railsback et al., 1999b; Anderson, 2000a; Haefner and Bowen, 2002; Hinrichsen et al., 2002; Nestler et al., 2002; Karim et al., 2003), and other particle-based applications (e.g., Haefner and Bowen, 2002; Scheibe and Richmond, 2002). The resulting CEL Agent individual-based modeling construct provides the theoretical and computational basis to elicit vector-based virtual movement in response to both physicochemical stimuli from CFD models (Tischendorf, 1997) as well as other abiotic and biotic sources for which data exists. This enhances the compatibility with tracking data and analytical treatments of movement processes (Tischendorf, 1997).

Virtual Sampling

A primary benefit of CEL Agent individual-based modeling is that it facilitates the use of virtual sampling (Goodwin et al., 2001; Nestler and Goodwin, in review). Virtual sampling is an intuitive description of the sampling protocol introduced by Halle and Halle (1999). Halle and Halle (1999) discuss the use of a virtual observer who samples data from the model population in accordance with the same protocol applied in the field experiment. The virtue of this approach is that it takes into account the possible limitations and biases of the sampling protocol applied (Grimm et al., 1999). Virtual sampling is an extremely powerful tool with high potential for critically assessing model results when used in combination with statistics (Grimm et al., 1999).

Formulating a CEL Agent IBM

With the theoretical and computational framework established for mechanically describing movement, the focal point of analysis then shifts to the

individual where one can explore hypothetical swim path selection behaviors using the virtual organism as a surrogate for the real organism. The specific goal is to uncover the behavior rules that embody the primary components of the strategy an individual of a target species, size, age, and life-stage uses to make movement decisions. To be consistent with the philosophy of the intermediate approach, behavior rules must be structured consistent with existing knowledge of the movement behavior of the organism, but must also lend themselves to parameterization with resolvable variables. The CEL Agent IBM application discussed herein, i.e., the Numerical Fish Surrogate (NFS), pertains to the movement dynamics of downstream outmigrating juvenile salmon (migrants) observed approaching and passing Lower Granite Dam on the Snake River in Washington, USA. The protocol for structuring and calibrating the model is generally applicable, however, to other species that actively move in 3-D space (e.g., other species of fish, geese migration, etc.).

Integrating system hydraulics and information about the behavior and biology of fishes in a mathematical model to better understand and forecast the influence of fish diversion and bypass structures on the Snake and Columbia Rivers was first proposed by Anderson (1988). Anderson (1991) subsequently introduced the first such mathematical model for decision-support. However, model success and applicability was limited due to the inadequacy of 3-D biological and fluid dynamics information available at the time. To date, the relationship between migrant and hydrodynamics remains a mystery, in large part, at hydropower dams on the Snake and Columbia Rivers and, more importantly, near the fish bypass structures designed to entice migrants into the collector and then pass them around the dam.

Potential Stimuli

In a dense, fluid environment, such as water, disturbances are generated by anything and everything that moves (Montgomery et al., 1995). Aquatic environments are, thus, often very rich in acoustic and hydrodynamic signals (Schilt and Nestler, 1997; Rogers and Cox, 1988). Many species of fish have excellent vision, taste, smell, tactile, chemical, electrical, pressure, temperature, and sometimes magnetic senses (Schilt and Nestler, 1997; Popper and Carlson, 1998). These and other, e.g., biotic, stimuli result in a near-limitless number of motivational forces that could potentially be influencing the movement decisions of individual fish (Farnsworth and Beecham, 1999).

In the full spectrum of prevailing physical, chemical, and biotic conditions, individual behavior is likely mediated by a synergy of diverse sensory inputs with various stimuli evoking conflicts in habitat preference. An individual, therefore, is unlikely to find a location that matches its preference on all environmental gradients, resulting in a potential hierarchy of responses to different cues which take varying precedence during the changing phases of a behavioral sequence (New et al., 2001; Sogard and Olla, 1993). The organization of such hierarchies and the integration of information from various sensory modalities within a behavioral program are, therefore, critical to robust simulations of individual movement behaviors. Game theory has been used extensively to describe behavior mathematically and foraging theory has been used to decipher the relationships between biotic stimuli (i.e., predators and prey) and emergent behavior. Not surprisingly, Hirvonen et al. (1999) suggest that combining individual-based modeling and foraging theory would be productive, although research in this area has been, to date, relatively scant.

Development and application of the Numerical Fish Surrogate (NFS) at Lower Granite Dam is described in the following manner. First, general concepts

relating to agent-based modeling are reviewed in the context of structuring the agents and other necessary metrics. Second, the computational issues regarding movement behavior implementation in a coupled Eulerian-Lagrangian construct are described. Lastly, calibration and verification results are evaluated.

Behavioral Rules

Behavioral rules governing the orientation and speed of individual movement are typically based on some measure of how an individual's fitness is expected to vary among alternative locations, under the assumption that animals make movement decisions at least in part to increase their fitness (Railsback et al., 1999a). The formulation and measure of fitness are critical components in the development of movement rules (Railsback et al., 1999a). Furthermore, the advantages of the IBM approach can best be realized using simple, direct measures of an animal's fitness as the basis for movement (Railsback et al., 1999a) given that many individuals following a few simple rules can result in complex and robust behavior (Whitfield, 2001). In other words, complex properties often emerge from simple interactions (Whitfield, 2001). However, formulations and measures of fitness at relevant spatial and temporal scales are a critical research need (Railsback et al., 1999a).

Optimal foraging theory states that animals forage in ways that maximize energy input and minimize energy loss, which in turn influences movement patterns (Nowak and Quinn, 2002). Efficient foraging in a spatially and temporally heterogeneous environment requires that individuals be capable of acquiring and integrating different sources of information from within their environment (Hirvonen et al., 1999). However, incompatibility issues associated with information sources that differ in their metrics and dimensionality require a novel scheme so information can be handled in common form. The field of computer science developed such a

novel scheme called object-orientation. Object-orientation provides a means of representation and formalism (Bian, 2003) for explicitly representing individuals and the interactions between individuals in a manner that is both conceptually and technically advantageous (Bian, 2003 and references therein). The main representational strength of object-orientation is that the world is represented in a manner that closely corresponds to animal perceptions (Bian, 2003 and references therein). More specifically, a phenomenon can be perceived as either an object or a field depending on several considerations such as the purpose of the study, scale of observation, and the convention employed to perceive a phenomenon (Bian, 2003).

The notion of an “object” can often be described interchangeably with the computer term “agent”. Multi-agent systems (MAS) are powerful and flexible because the computer script is no longer centralized, but distributed in a multitude of autonomous agents (Ginot et al., 2002). One can, therefore, add, eliminate or modify agents without affecting the rest of the model (Ginot et al., 2002). This results in a computer programming scheme that is both theoretically advantageous and one that is more efficient to create, evaluate, and modify compared to conventional techniques (Ginot et al., 2002).

The utility of agent concepts lays the foundation for behavioral rules. Rules are derived from the agent-based, event-driven foraging model developed by Anderson (2002). Anderson’s (2002) foraging model melds classical approaches of game theory with precepts from neurobiology and bioenergetics. The model assumes that animals are rational operators that assess the opportunities and conditions of the environment and select behaviors that optimize their fitness. The animal’s environment is described in terms of agents representing prey, predators, and features of the physicochemical regime. Two modes of behavior are associated with each agent. Tactical behaviors alter the outcomes of events (i.e., encounters

with an agent) and strategic behaviors alter the probability of future events. Depending on the agent, one or both of these behaviors may be relevant. The possibilities of event outcomes are represented as utilities that have both benefit and cost components. Switches in behavior occur when the expected utility of one behavior, i.e., associated with a unique agent, exceeds that of the others. For instance, a fish initially following temperature gradients to find cooler water may switch behaviors and, instead, follow gradients of increasing dissolved oxygen if dissolved oxygen levels drop below some threshold value. At the switch point, the expected utilities of the various behaviors are equivalent, which provides the means for evaluating model coefficients in a laboratory. The Numerical Fish Surrogate (NFS), however, was successfully calibrated outside the laboratory using straightforward trial-and-error.

Selection of Agents

Building behavioral rules begins with the identification of physical, chemical, and biological entities believed to contribute to observed movement behavior. The entities are defined as ‘agents’ and make-up the stimulus field that will be queried to evaluate spatial alternatives in fitness level. Agents may include various hydrodynamic, water quality, and biotic attributes (Figure 2.1). Agents in the NFS (Figure 2.2) were identified by synthesizing information from peer-reviewed fisheries literature (chapter 1), preliminary analyses of integrated CFD-telemetry data, and trial-and-error calibration. Agents identified for the NFS are: (1) food and predators, (2) wall-bounded flow hydraulic patterns, (3) free-shear flow hydraulic patterns, and (4) hydrostatic pressure (Figure 2.2).

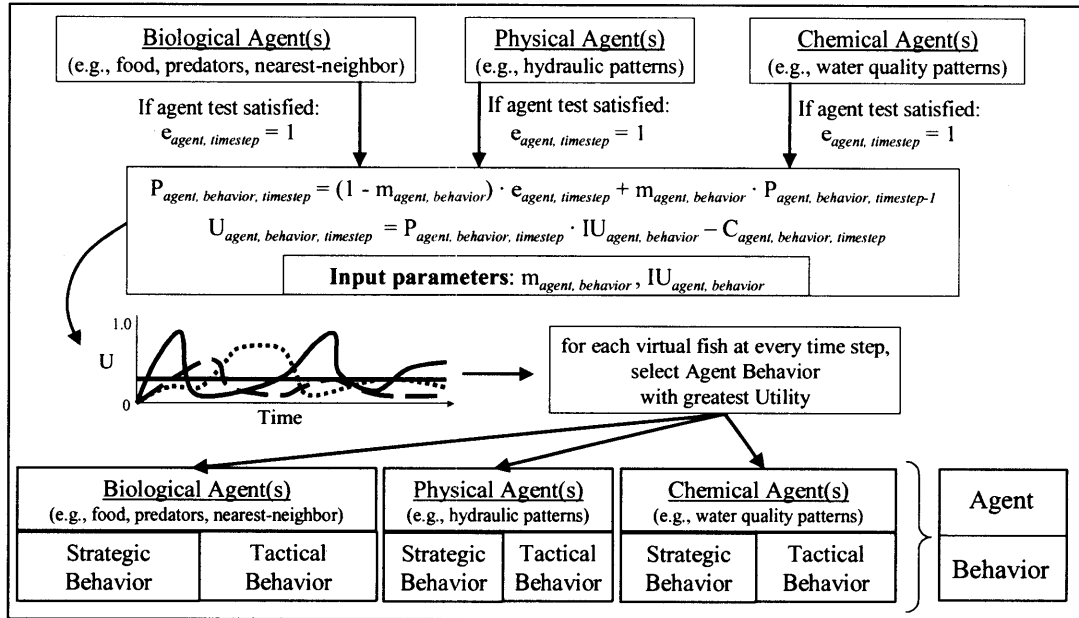


Figure 2.1. Relationship between agents, events, and behaviors in a CEL Agent IBM. To facilitate trial-and-error calibration, use as few agents, events, and behaviors as possible.

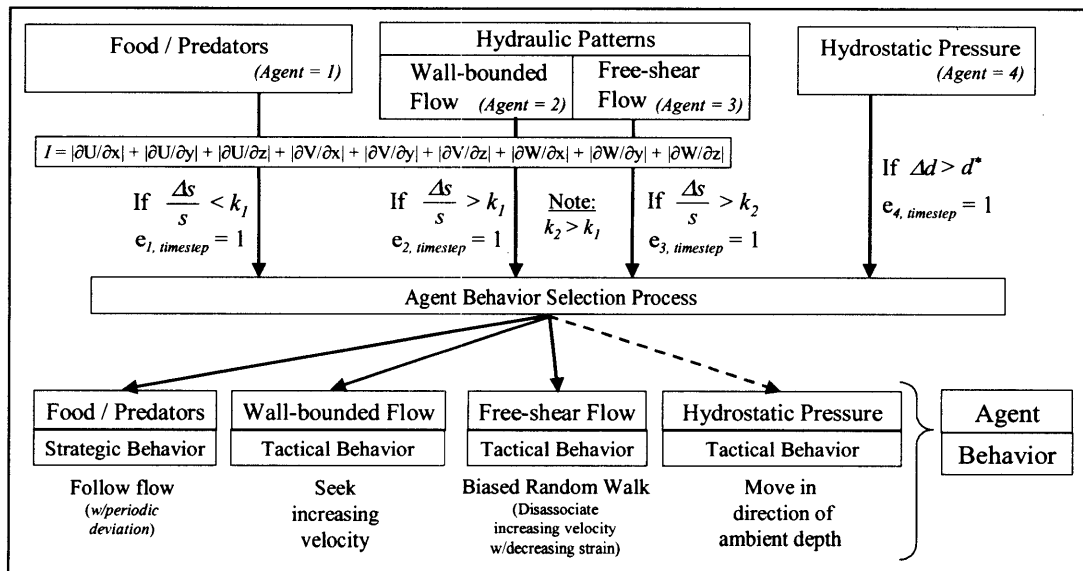


Figure 2.2. Agents, events, and behaviors used in the Numerical Fish Surrogate (NFS) application at Lower Granite Dam. $k_1 = 0.12$, $k_2 = 0.30$, $d^* = 2.0$.

Events

An event is an encounter between the animal and an agent in an increment of time (Anderson, 2002). This interaction between individual and its environment usually occurs in a small area and is implemented in two stages (Bian, 2003). First, the individual evaluates the attribute values at its location and in the surrounding vicinity. Second, the individual then executes a response to the interaction, i.e., moving, (Bian, 2003). An event usually refers to a change in the attributes of an agent (Bian, 2003) and, therefore, the nebulous concept of an agent must be translated into a numerical product, i.e., agent variable or variables, for evaluation. How biotic and abiotic variables are combined to constitute an agent variable is not uniform (Anderson, 2002). Agent variables may be derived from an additive, multiplicative, or some other combination (McFarland and Houston, 1981; Anderson, 2002) of biotic and abiotic variables. Agent variables then provide the numerical means to quantitatively evaluate the relative presence, absence, or change in an agent.

Agent variables used in the Numerical Fish Surrogate (NFS) were identified using a variety of different means, including the review of pertinent literature on hydrodynamics, turbulence, river hydrogeomorphology, fisheries, mathematical biology, and fish mechanosensory system biology (chapter 1). Initial review of the literature highlighted many potential agent variables available from the CFD model including hydraulic strain, velocity, acceleration, vorticity, turbulent kinetic energy, turbulent length scales, and hydrostatic pressure. Using trial-and-error calibration, the many potential agent variables and numerous event formulations were reduced to two agent variables and four events (Figure 2.2). In the future, optimization techniques such as genetic algorithms (e.g., D'heygere et al., 2003) may facilitate the selection of agent variables.

The agent variables in the Numerical Fish Surrogate (NFS) are hydraulic strain and depth (chapter 1). Strain relates to agents (2) wall-bounded and (3) free-shear flow patterns. Depth is directly proportional to agent (4) hydrostatic pressure. Agent (1) was selected as the default agent, that is, the stimulus of interest in the absence of all other agents. The treatment of agent (1) is discussed later. Structuring event evaluations begins with the notion that environmental thresholds exist that may be thought of as cues that trigger fish movement (Workman et al., 2002). In the NFS, event evaluations formulated for agents (2) and (3) were structured such that a wall-bounded flow event (agent 2) occurs when the change in strain exceeds a threshold, k_1 (Figure 2.3). A free-shear flow event occurs when the change in strain exceeds a second, higher threshold, k_2 . The probability of movement in response to the agent increases as the agent variable increasingly exceeds the threshold value (Workman et al., 2002). Event thresholds are not necessarily fixed, however. In some cases, event thresholds could be modified by experience (Anderson, 2002). Also, with respect to the NFS event formulations, more sophisticated treatments may be appropriate for evaluating the presence of wall-bounded and free-shear flow features in future studies, but the interest in simplicity and the apparent success of the existing formulation encouraged the present treatment. Nonetheless, the use of thresholds is consistent with the approach used in other studies evaluating the response of salmonids to physicochemical stimuli, e.g., temperature, in other systems (Workman et al., 2002 and references therein).

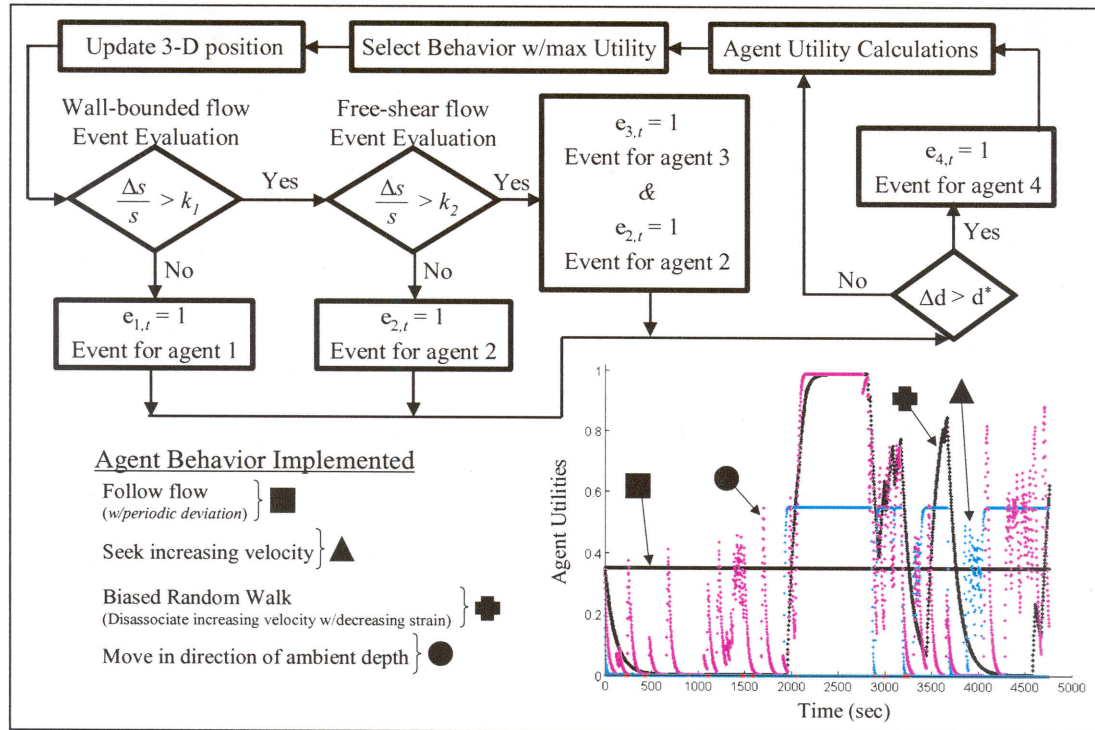


Figure 2.3. Flowchart of event evaluations, order of primary computations, and a time-series output of resultant agent utility values for a simulated virtual fish (case DH8).

Before wall-bounded and free-shear flow event evaluations, strain is scaled according to an abbreviated form of the Decibel equation frequently used to assess stimuli that vary in intensity by orders of magnitude (e.g., sound and light):

$$s = \log_{10} \left(\frac{I}{I_0} \right) \quad [1]$$

where s is strain in scaled form, I is the level of strain interpolated to the centroid of the fish's exact 3-D position, and I_0 is the reference level of strain, i.e., an input value arbitrarily set to $1e^{-6}$ ($I_0 = 1e^{-6}$). The level of strain, I , is calculated by summing the

absolute values of all nine components of strain (Figure 2.2). Equation [1] is applied with the assumption that it results in a value proportionally related to the subjective sensation of ‘loudness’ as perceived by fish. This transformation is frequently used to translate the energy output associated with, for instance, sound and light, into a linear scale of perception.

Strain, s , is subsequently translated according to the Weber-Fechner Law (Rapoport, 1983), a well-studied mathematical equation for describing how animals distinguish intensities of stimuli and respond to psychological phenomena. The Weber-Fechner Law relates the physical intensity of a stimulus to its psychologically perceived intensity through calculation of a “just noticeable difference” (JND) in the change of the stimulus with regard to the background, or acclimated, level of the stimulus (Rapoport, 1983):

$$\Delta s/s \equiv (s_t - s_{ambient}) / s_{ambient} \quad [2]$$

where s_t is the scaled level of strain at time step t from equation [1] and $s_{ambient}$ is the ambient level of strain to which the fish is acclimatized. The strain value resulting from the Weber-Fechner translation, equation [2], is the agent variable value used in comparison with thresholds k_1 and k_2 (Figure 2.3). In the NFS, therefore, a larger change in strain is required at higher ambient strain intensities, to which the fish is already acclimated, in order to elicit the same psychological behavioral response. The ambient level of strain, $s_{ambient}$, to which the fish is acclimated is updated according to the following equation:

$$s_{ambient} = (1 - m_{strain}) \cdot s_t + m_{strain} \cdot s_{ambient} \quad [3]$$

The memory coefficient, m_{strain} , relates to a fundamental question in the behavioral ecology of foraging, that is, how much information from the immediate past is combined with information from the more distant past (Hirvonen et al., 1999). Hirvonen et al. (1999) advocate the use of memory properties as critical in the examinations of prey choice and suggest using a form of exponentially devaluating weights for past events to emulate individual memory behavior. m_{strain} in equation [3] ranges from zero to one and updates the ambient level of strain, to which the virtual fish is acclimated, in a manner that embodies attributes of the approach suggested by Hirvonen et al. (1999). Values near one weight past conditions more than current conditions and values near zero weight the current conditions more highly (Anderson, 2002). The memory coefficient, however, is inherently linked to the time step of the model. The calibrated NFS value for m_{strain} is 0.99981 with a 2-second time step. Hirvonen et al. (1999) indicate that both Kacelnik et al. (1987) and Devenport and Devenport (1994) also use the approach of devaluating outdated information with a relative weighting of past and present experience. These concepts are simply extended to physicochemical stimulus conditions. This treatment of physicochemical stimuli is supported by observations of juvenile chum salmon, whose thermal tolerance and resistance is intimately influenced by prior thermal history (Birtwell et al., 2003; Brett, 1952).

The use of memory coefficients is extended to hydrostatic pressure, or depth, event evaluations. An event occurs for the hydrostatic pressure agent when the change in depth, which is directly proportional to hydrostatic pressure, exceeds a threshold, d^* (Figure 2.3). The change in depth is calculated using the following equation:

$$\Delta d \equiv (depth_t - depth_{ambient}) \quad [4]$$

where $depth_{ambient}$ is the ambient depth and updated similarly to ambient strain using the following equation:

$$depth_{ambient} = (1 - m_{depth}) \cdot depth_t + m_{depth} \cdot depth_{ambient} \quad [5]$$

m_{depth} is the memory coefficient specifying the rate at which virtual fish will acclimate and deacclimate to new depths, i.e., hydrostatic pressure, and is analogous to the coefficient used to update ambient strain. The calibrated NFS value for m_{depth} is 0.9970.

Numerically Defining Behavior

Explicit behaviors consisting of an orientation and speed response must be defined for all event outcomes for all agents. At a minimum, each agent must be associated with either a tactical or a strategic behavior. Some agents may lend themselves to both tactical and strategic behaviors, and in some cases even more complex arrangements may be pertinent (described in detail in Anderson, 2002). While agents may be associated with multiple behaviors, for simplicity, it is advocated that a minimum number be used.

In the Numerical Fish Surrogate (NFS), the behavioral response to agent (2) is tactical in nature and relates to the avoidance of undesired hydrodynamic features associated with wall-bounded flow (chapter 1). The response to agent (2) involves orienting in the direction of increasing water velocity magnitude. In a deep, free-flowing river such as free-flowing sections of the Snake River, this has the implied effect of moving the virtual fish from near the river's edge (i.e., where wall-bounded flow is most prevalent) towards the center of the channel and, subsequently, in the direction of decreasing strain (chapter 1).

Typically, movements begin at the threshold and increase until a maximum movement rate is reached (Workman et al., 2002). The speed response for all agents was calibrated using trail-and-error and resulted in a formulation by which virtual migrants increase their speed incrementally, by a user-defined amount, each time step insufficient progress is made in decreasing the strain stimulus variable value, $\Delta s/s$, at the fish's centroid position. Conversely, speed is decreased incrementally each time step as long as $\Delta s/s$ continues to decrease in subsequent time steps. Speed is bounded above by the burst speed of migrants, i.e., approximately 10 body lengths per second (Beamish, 1978), and below by the nominal cruising speed of migrants, i.e., approximately 2 body lengths per second (Beamish, 1978).

The behavioral response to agent (3) is tactical in nature and relates to the avoidance of undesired hydrodynamic features associated with free-shear flow (chapter 1). The response to agent (3) involves random, but persistent oriented movements in which the probability of a new orientation increases as the time spent at the present orientation continues. Orientations, while random, are biased in favor of orienting against the direction of flow. The resultant behavior is one in which virtual fish maintain their relative position and/or mill in the high-energy areas near the dam superstructure without unwanted capture in high-velocity plumes. The resultant behavior is analogous to that observed by Steig and Johnson (1986), who noticed transmitter-equipped migrants moving laterally back and forth along the dam or just upstream, apparently searching for surface outlets. Conceptually, this numerical embodiment of behavior equates to the notion that the fish no longer associates the direction of increasing flow velocity with decreasing strain. In a free-flowing stream, this behavior could be expected at locations where, for instance, two boulders bracket and constrict flow in the channel and where wild-reared juvenile migrants may hesitate, or hold, until they have acclimated to the elevated strain

associated with the flow constriction before passing. Additional evidence may be found by consulting literature on adult upmigration. Standen et al. (2002) suggest that upmigrating adult salmonids cross the river and backtrack more frequently at constrictions possibly looking for small-scale low velocity fields for continued upmigration. These low velocity fields may also be associated with decreased strain levels. Lastly, virtual fish speed increases incrementally each subsequent time step the fish is oriented in the direction opposite the direction of flow and experiences a free-shear flow event and water speed is greater than the existing fish speed. Speed is bounded above and below in the same manner as for agent (2).

The behavioral response to agent (1), food and predators, is strategic in nature and the default behavioral response. As the default, the behavioral response to agent (1) is related to null event periods, that is, when events for other agents are absent for significant periods of time. For purposes of this study, it was assumed the downstream migratory movement behavior of migrants, in free-flowing sections of the Snake River, consist of the following behaviors: swimming in the direction of flow, seeking prey, avoiding predators, and other periodic deviations that may be described as inherently random in form. The lack of a priori 3-D position data for both relevant predators and prey limited the response behaviors associated with agent (1) to swimming in the direction of flow and periodic, random deviations. However, this treatment of migrant behavior is consistent with the observation of Coutant and Whitney (2000), who indicate that migrants tend to follow the flow as they approach dams in the forebay. Also, Popper and Carlson (1998) suggest the response of fish to hydrodynamics near dams frequently overrides, or supercedes, the responses to many, other stimuli. Virtual fish speed is set, on average, to the cruising speed of migrants.

The behavioral response to agent (4) is tactical in nature and relates to the avoidance of undesired changes in hydrostatic pressure (chapter 1). The response to agent (4) involves moving in the vertical direction necessary to mediate the change in pressure (depth) just experienced, i.e., swim towards ambient depth. This behavior is consistent with the observation of Coutant (2001) that migrants entrained with the flow (into turbine intakes) attempt to resist the change in pressure by swimming up into the gatewell slot. Hydrostatic pressure is a 1-D phenomenon and, therefore, only requires a 1-D response. By definition, then, fish must employ another behavioral response for horizontal orientation. Therefore, when a behavioral response to agent (4) is elicited another behavioral response associated with one of the prior agents, (1) - (3), will be elicited for horizontal orientation. Virtual fish speed, with respect to agent (4), increases incrementally each time step insufficient progress is made towards mitigating the pressure change. Speed is reduced if sufficient progress is made. The speed elicited is, then, the largest one of the following: response to agent (4) and response to the agent selected for horizontal movement. Similarly, speed is bounded above and below by burst and cruising speeds, respectively.

Selecting Behavior

The behavioral response implemented is the one associated with maximum utility. Utility is a measure of the nebulous concept of fitness. That is, utility is a measure of the relative benefit in fitness an individual could expect from executing a specific behavior. A utility value is associated with each behavioral response at each time step. Utility has both benefit and cost components and is related to event outcomes through the following equations:

$$P_{agent, behavior, timestep} = (1 - m_{agent, behavior}) \cdot e_{agent, timestep} + m_{agent, behavior} \cdot P_{agent, behavior, timestep-1}$$

[6]

$$U_{agent, behavior, timestep} = P_{agent, behavior, timestep} \cdot IU_{agent, behavior} - C_{agent, behavior, timestep}$$

[7]

$U_{agent, behavior, timestep}$ is the utility associated with a specific agent behavior for a given fish at a given time step and ranges from zero to one. $IU_{agent, behavior}$ is the intrinsic utility, or value, associated with a particular agent behavior. Intrinsic utility is a calibrated coefficient that can range from zero to one and may be viewed, conceptually, as the relative worth of a specific agent behavior if, theoretically, all agent stimuli could be set equal. In other words, intrinsic utility is a numerical value that could be used to rank the various agent behaviors according to the inherent preferences of the animal, if all stimuli could be set equal. The NFS intrinsic utility values are tabulated in Table 2.1. $C_{agent, behavior, timestep}$ is the bioenergetic cost associated with a specific agent behavior for a given fish at a given time step and is a scaled value that also ranges from zero to one. The NFS does not, presently, require a bioenergetics model at Lower Granite Dam, but uses the Wisconsin Fish Bioenergetic model (Hanson et al., 1997), as detailed in Anderson (2002), when needed. $P_{agent, behavior, timestep}$ is the perceived probability of obtaining a unit of utility as a result of executing the associated agent behavior and ranges in value from zero to one. $m_{agent, behavior}$ is the memory coefficient specifying the degree to which the current event, or lack of an event, impacts the evaluation of anticipated utility relative to past events. This memory coefficient is similar in concept, form, and function to the memory coefficients used to update ambient strain and depth conditions. The NFS memory coefficients are tabulated in Table 2.1. Finally, $e_{agent,$

$timestep$ is the binary result, 0 or 1, of the agent event evaluation, i.e., $e_{agent, timestep} = 1$ if the agent is present and $e_{agent, timestep} = 0$ if the agent is absent.

Table 2.1. Intrinsic Utility and Memory Coefficient Values in Numerical Fish Surrogate.

Agent	Tactical or Strategic	Agent Behavior	Intrinsic Utility	Memory Coefficient
Food / Predators	Tactical	<i>Not Needed</i>	--	--
	Strategic	Follow Flow (<i>default</i>)	0.35	1.00
Wall-Bounded Flow	Tactical	Seek Increasing Velocity	0.55	0.80
	Strategic	<i>Not needed</i>	--	--
Free-Shear Flow	Tactical	Biased Random Walk	0.99	0.982
	Strategic	<i>Not needed</i>	--	--
Hydrostatic Pressure	Tactical	Swim toward Ambient Depth	0.99	0.935
	Strategic	<i>Not needed</i>	--	--

The resultant structure of the utility formulation has several emergent properties of significant value, two of which are discussed here. First, behavior implementation is related to fitness, or utility, which in turn is dynamically organized in hierarchical fashion with time (Figure 2.4). When the utility associated with one agent behavior exceeds that of another, the behavior changes. This embodies the attribute of behavior described in both Sogard and Olla (1993) and New et al. (2001). That is, an individual is unlikely to find a location that matches its preference on all stimulus gradients, resulting in a hierarchy of responses to different cues that take varying precedence during the changing phases of a behavioral sequence. The

probability of movement in response to an agent, therefore, increases as the associated agent variable increasingly exceeds the physicochemical threshold value (Workman et al., 2002).

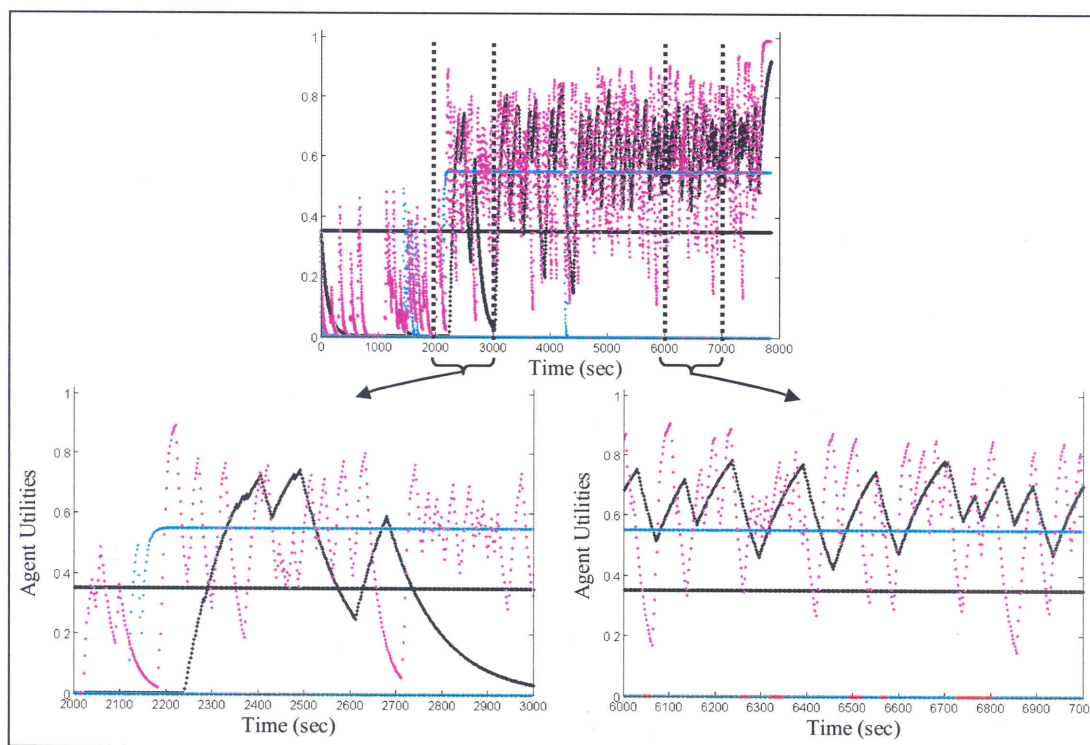


Figure 2.4. Agent utility values for a simulated virtual fish (case DH8). Virtual fish behavior implementation is related to fitness, or utility, which in turn is dynamically organized in hierarchical fashion with time. When the utility associated with one agent behavior exceeds that of another, the behavior changes. This scheme is consistent with the hierarchical attribute of behavior described in Sogard and Olla (1993) and New et al. (2001). Also, the exponential decay property of utilities is consistent with the suggestion in Hirvonen et al. (1999) that past events should be devaluated exponentially in emulating individual memory behavior.

Second, implicit in the utility formulation are components of the event space concept. In the current utility formulation, events drive probability, which then drives utility calculations and finally the selection of behavior. In event-structured

simulations, however, the concept of time is driven by the occurrence of events (Ewing et al., 2002). There is some evidence to suggest that animals are unable to measure temporal events objectively and that time perception is influenced by factors external to the animal (Hills and Adler, 2002 and references therein). In other words, animals may view time according to the rate of events and not according to the fixed time increment convention most frequently used in computer programming. This paradox may be at least partially resolved in the following manner. For fixed time increments, i.e., length of time between t and $t+1$, in which no events occur for a particular agent, $e_{agent, timestep}$ is simply set to zero for that agent. For fixed time increments in which one or more events occur for a particular agent, e.g., $\Delta s/s > 2 \cdot k_1$, the probability equation, equation [6], is applied (calculated) recursively multiple times within the fixed time step for that particular agent. In other words, if $2 \cdot k_1 < \Delta s/s < 3 \cdot k_1$, then equation [6] would be applied two times, recursively, for the wall-bounded flow agent. When equation [6] is applied recursively, $e_{agent, timestep}$ is set to 1 for all calculations. The result is that probabilities are linked to event-structured time and, therefore, virtual individuals experience time in pseudo event-structured time. This treatment subsequently embodies some of the attributes of the event-structured method in Ewing et al. (2002).

Behavior Implementation

The interaction between an individual and its environment usually occurs in a small area and is implemented in two stages (Bian, 2003). First, the individual evaluates the attribute values at its location and in the surrounding vicinity. Second, the individual then executes a decision, i.e., moves (Bian, 2003).

Computational Sensory Environment

Evidence from many stream fishes indicates they are familiar with their surroundings over substantial distances and are able to find good habitat quickly (Railsback et al., 1999a). IBMs should assume fish are familiar with their surroundings over an area greater than their current location (Railsback et al., 1999a). To provide virtual fish with a 'sense' of their local environment, a computational sensory ovoid is created that is consistent with the dimensional scale of the CFD model used. For instance, a 2-D sensory ovoid is used in 2-D laterally- or depth-averaged CFD models and a 3-D sensory ovoid is used in 3-D CFD models. In some cases, it may be appropriate to use asymmetrical, or distorted, sensory ovoids, i.e., ovoids with aspect ratios other than 1:1:1 (Figure 2.5). For instance, Goodwin et al. (2001) use asymmetrical sensory ovoids in the simulation of pelagic blueback herring movement. In such circumstances, the minimum query distance (MQD = the minimum distance between the centroid of the virtual fish and any of the cardinal positions, or sensory points, along the sensory ovoid) and 'size' of the sensory ovoid represent different quantities. However, many modeling applications will likely use symmetrical sensory ovoids, i.e., where the distance between the centroid of the virtual fish and all locations along the periphery of the sensory ovoid are equal. In such circumstances, MQD and 'size' of the sensory ovoid may be used interchangeably.

Generally, the sensory ovoid may be partitioned into horizontal and vertical components for easier analysis and construction. All fishes possess an inner ear consisting of acceleration-sensitive otolithic organs (Braun and Coombs, 2000). These otolithic endorgans are greater in density than the fish itself and, therefore, lag behind the motions of the fish providing it with three-dimensional information on the motions of its body (Braun and Coombs, 2000) and a perception of gravity (Paxton,

2000). The operating range of the lateral-line mechanosensory system is considered to be a function of fish length (Coombs, 1999). The longer the fish, the further away a given hydrodynamic stimulus source can be detected (Denton and Gray, 1983, 1988, 1989; Kalmijn, 1988, 1989; Coombs, 1996, 1999). With respect to prey items, the operating range of the lateral line system falls within one to two body lengths (Coombs, 1999). However, the distance range or ‘active space’ of the lateral line system is likely dependent on a number of factors including the size of the disturbance source (Coombs, 1999).

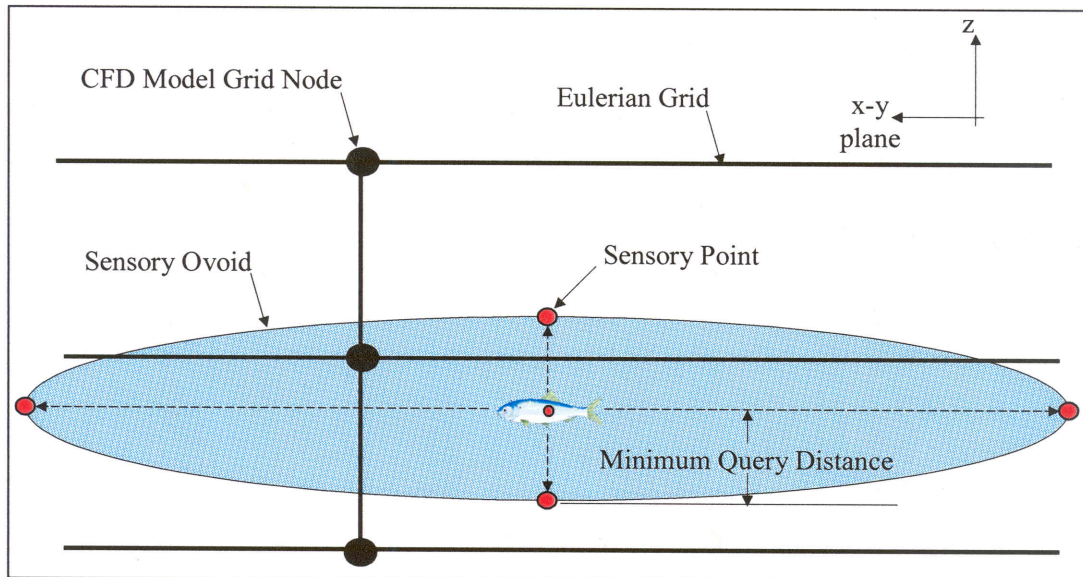


Figure 2.5. Two-dimensional view (longitudinal and vertical) of a virtual fish computational sensory ovoid. Note the sensory ovoid is not affected or dependent on the gridding of the CFD model, i.e., the Eulerian grid. Sensory points that initially exceed the system boundary, i.e., when the fish is near the system boundary, are placed at the boundary.

Each virtual fish is endowed with a computational sensory ovoid of given scale (MQD) so as to equal the sensory acquisition capabilities of the associated, real

target species (MQD_b) or meet the minimum query distance required to extract accurate gradient information from the CFD model (MQD_{CFD}), whichever is greater. The minimum query distance using biological means (MQD_b) is calculated as follows:

$$MQD_b = TS_{NFS} \cdot FS \cdot DFSA \quad [8]$$

MQD_b = minimum query distance (meters) using biological means, TS_{NFS} = time step (seconds) of the fish simulation module, FS = fish size (meters), $DFSA$ = distance (body lengths) of the fish's sensory acuity to the physicochemical stimuli of interest. MQD_b represents, from a biological perspective, the volume that would likely be sampled by an individual of the target fish species in a given time step.

Modelers must be keenly aware of accuracy resolution afforded by the CFD model, however. Often the numerical resolution of the CFD model will dictate the value of MQD required such that the value used is greater than that suggested by peer-reviewed literature on the sensory acuity of the target species of interest (i.e., MQD_b). MQD is selected using the following logic:

$$MQD = \text{maximum} \{MQD_b, MQD_{CFD}\} \quad [9]$$

MQD_{CFD} = minimum query distance (meters) due to numerical resolution afforded by gradient calculations. Gradient values are calculated by computing the difference between CFD modeled values at the centroid of the fish location and at the sensory points located at cardinal positions on the periphery of the sensory ovoid, oriented with the fish (Figure 2.5). Using a MQD that is too small results in behavior computations ultimately based on gradient values with no significant digits. Conceptually, this means the virtual fish is unable to distinguish between legitimate

trends in environmental gradients. The number of significant digits left after gradient value calculations is impacted by the resolution of the CFD model, order of the interpolation scheme used, and variable precision used, or afforded, by the programming language and computing platform. In most cases, a single set of sensory points at the periphery (e.g., Figure 2.5) is sufficient. However, there may exist cases where CFD model data is of such high resolution that nested sensory points may allow even higher-order gradient values in local physicochemical stimuli to be computed.

Third, MQD may be modified in simulation according to factors such as physiological condition of the individual fish, time of day, water quality conditions, and whether the individual fish is swimming alone or as part of a school. Nonetheless, MQD is adjusted upward, e.g., increased, randomly at each time step as suggested by Railsback et al. (1999) and Goodwin et al. (2001). The use of random query distances equal to or greater than that of MQD from equation [9] enhances the ability to capture environmental gradients of multiple spatial scales.

In short, the use of sensory ovoids inherently translates the quantities of the CFD model to the virtual fish reference frame uniquely oriented in time, thereby allowing the modeler to conceptually dispense with the arbitrary axes orientation of the Eulerian grid. This allows virtual fish to make movement decisions based on various physical, chemical, and/or biological stimuli queried from the CFD model (Tischendorf, 1997) or Lagrangian-based quantities (e.g., nearest-neighbor distance) that have been scaled and oriented appropriately for each individual virtual fish at every time step.

The Numerical Fish Surrogate (NFS) uses a symmetrical 3-D sensory ovoid. Size of the sensory ovoid was based on several factors. First, the NFS uses a 2.0-second time step and virtual juvenile salmon are sized at 0.2 meters. The inner ear

detects accelerations due to unsteady flow features (Montgomery et al., 2000) and is capable of picking up flow attributes beyond the reach of the lateral line (Kalmijn, 1989) where the higher-order moments detected by the lateral line are negligibly weak (Kalmijn, 1989). However, the NFS at Lower Granite Dam is confined to steady-state hydraulics where unsteady flows do not exist and, therefore, the sensory acuity afforded by a virtual inner ear otolith is compromised. For this reason, the sensory acuity biologically appropriate for NFS virtual fish, or MQD_b , focused on the sensory acuity afforded by the lateral line. A juvenile salmon sampling the flow along its and one additional body length (two body lengths total) during a 2.0-second time step could be expected to sample a volume with a maximum radius of approximately 0.8 meters ($MQD_b = 0.8$ meters). However, gradient values calculated with a MQD of 0.8 meters had insufficient significant digits. Using trial-and-error, MQD_{CFD} and, thus, MQD was set to 1.25 meters. The query distance, or sensory ovoid size, at any given time step was selected from a uniform distribution of random numbers that varied between a MQD of 1.25 meters and 150% of MQD , or $1.5MQD$. The value of $1.5MQD$ was also selected using trial-and-error.

Movement in Computational Space

CEL Agent IBMs implement 3-D movement embodying attributes discussed in Wu et al. (2000). That is, movements exhibit persistence, i.e., the direction of travel during time step t is dependent on the direction traveled in time step $t-1$. This attribute inherently derives from the hierarchical structure of agent utilities and associated agent behaviors. Wu et al. (2000) indicate that Marsh and Jones (1988) classify simulated movement depending on whether step length (speed) and direction are interdependent or independent. Individual movement parameters in the Numerical Fish Surrogate (NFS) are interdependent. Marsh and Jones (1988) further

subdivide each class into subclasses: ‘oriented models’ chose direction relative to a fixed compass direction (e.g., Eulerian CFD model grid axis orientation) and ‘unoriented models’ where direction at each time step is relative to the preceding step. In the NFS, a time-varying Lagrangian reference frame is developed for each virtual fish at every time step and oriented in the direction the fish is pointed (Figure 2.6). This results in ‘unoriented’ movement, i.e., elicited movement orientation depends on the direction the fish is pointed in the preceding step.

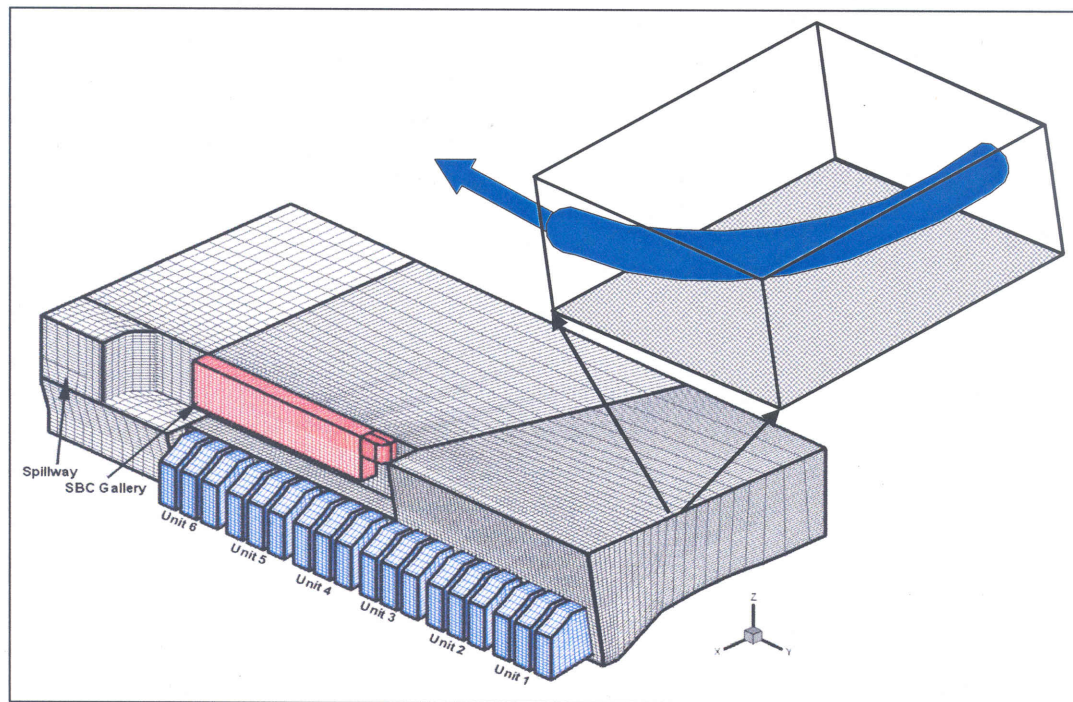


Figure 2.6. Eulerian discretization of the Lower Granite Dam forebay near the powerhouse structure, and conceptually dispensing with the arbitrary Eulerian grid orientation by defining a supplemental Lagrangian reference frame (for the virtual fish) that is uniquely oriented in time and space.

Once the resultant 3-D fish movement vector (i.e., movement orientation and speed) is computed for each virtual fish for the time step, movement is decomposed

into Cartesian vector form and then further into contravariant vector form for final implementation. Cartesian-based volitional swimming vectors, U_{fish} , V_{fish} , and W_{fish} , are the end-product of the NFS behavioral rules. These vectors are then added to Cartesian flow vectors, U , V , and W , using the following equations:

$$X_t = X_{t-1} + (U + U_{fish}) \cdot \Delta t \quad [10]$$

$$Y_t = Y_{t-1} + (V + V_{fish}) \cdot \Delta t \quad [11]$$

$$Z_t = Z_{t-1} + (W + W_{fish}) \cdot \Delta t \quad [12]$$

where X_t is the Cartesian x-position (meters) of the centroid of the virtual fish at time t , X_{t-1} is the x-position at time $t-1$, U is the Cartesian flow velocity vector (meters per second) in the x-direction at time $t-1$ at the centroid of the virtual fish, and Δt is the time step of the NFS, which can be different from the time step of the CFD model in a transient (time-varying) application. Y_t , Y_{t-1} , and V are defined similarly for the Cartesian y-direction and Z_t , Z_{t-1} , and W for the Cartesian z-, or vertical, direction.

Simulation of movement is difficult in computational constructs where individuals are represented as point data and space is represented as a series of arbitrarily shaped cells (Bian, 2003). This difficulty has significantly limited the use of integrated Eulerian-Lagrangian approaches in individual-based modeling and the modeling of individual movements in general (Bian, 2003). Computationally, the most difficult task in implementing virtual fish behavior is adding volitional swimming vectors to a particle-tracking algorithm capable of providing the interpolation and particle bookkeeping schemes necessary to implement equations [10] thru [12], rigorously, for the grid structure used in the CFD model. In general, most existing finite-difference and finite-volume 3-D models use structured grids with hexahedral cells, while finite-element models use unstructured grids with fixed

mesh shapes (Lai et al., 2003a). State-of-the-art 3-D CFD models can now provide equally accurate hydraulic simulations using either multi-block, near-orthogonal structured grids or other grid topologies using arbitrarily shaped cells (e.g., Lai et al., 2003a; Lai et al., 2003b; Lai, 2000). While the relative advantages and disadvantages of different grid topologies continue to be a subject of debate (Lai et al., 2003a), the later are easier to generate for complex natural geometries. However, advances in CFD modeling have outpaced advances in 3-D particle-tracking algorithms. Three-dimensional particle-tracking algorithms exist for multi-block, near-orthogonal structured grids (Figure 2.6) and require significantly less computational resources (i.e., memory and processor time). In contrast, unstructured particle-tracking algorithms provide the means to work with grids that are easier to generate for highly complex natural geometries, but often require significant computational resources compared to that of structured grid particle-tracking algorithms. Presently, structured particle-tracking algorithms may be efficiently run on state-of-the-art PowerPCs, while unstructured particle-tracking algorithms often require the use of supercomputers and parallel processing when simulating many thousands of virtual fish, which inherently limits the practical utility of the tool. However, as PowerPCs improve, it is expected these practical limitations will be resolved in the near future.

The particle-tracking algorithm in the NFS works within multi-block, near-orthogonal structured grids by converting 3-D space from Cartesian to contravariant space (Figure 2.7) in which all 3-D cells are translated to unit size, i.e., $1 \times 1 \times 1$. Vector quantities are appropriately scaled. Once 3-D space and vector quantities have been converted to contravariant space, 2nd order interpolation schemes are relatively straightforward and bookkeeping schemes are intuitive. Bookkeeping the position of a virtual fish in contravariant space requires tracking the virtual fish's

displacement within the cell (i.e., the unit cube) and the Cartesian position of the reference node for the cell in which the fish resides (Figure 2.8). Position of the virtual fish in contravariant space guides the nodes used in the interpolation of CFD modeled values to the fish position and its associated sensory points.

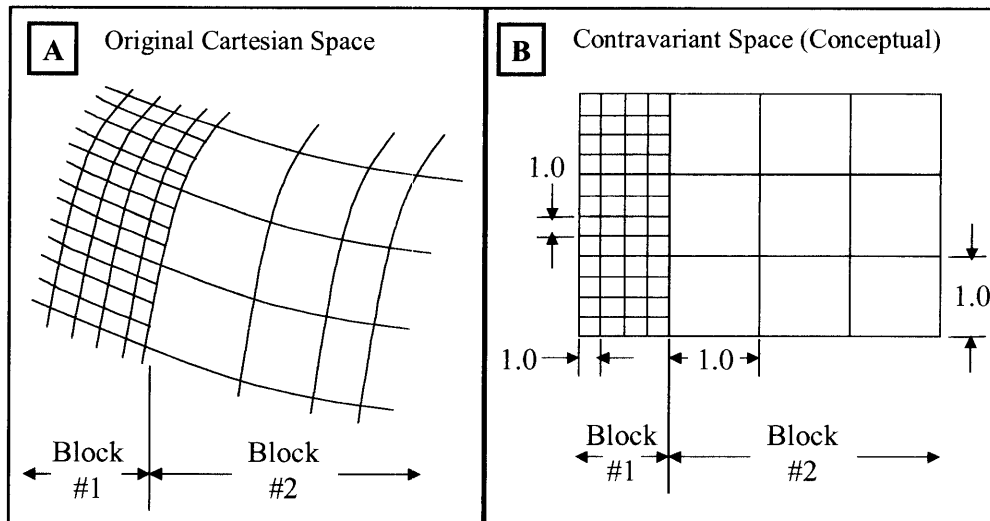


Figure 2.7. Comparison of a multi-block, near-orthogonal structured grid (2-D) in original Cartesian space (Plot A) and then in (conceptual) contravariant space (Plot B). All vector quantities are appropriately scaled in contravariant space to maintain conservation principles.

Results from movement calculations, equations [10] through [12], are converted into contravariant space displacements and used to update the position of the virtual fish within the modeled system. As the virtual fish moves across various cell faces in a given time step to its new position, the inherent bookkeeping afforded by contravariant space facilitates computationally efficient boundary checks. A virtual fish only crosses a cell face if the displacement (in contravariant space) in a given direction either exceeds unity or falls below zero. This provides an intuitive opportunity to ensure the virtual fish does not pass through an impermeable

boundary, for instance, a wall modeled as a series of adjoining, impermeable, and infinitely thin cell faces. This bookkeeping scheme highlights the primary difference with, and difficulty in, particle-tracking in unstructured grids. Unstructured grids cannot use the contravariant space transformation technique and, therefore, must depend on 3-D equations to mathematically define the face of each cell for every element in the grid in order to conduct the necessary boundary checks.

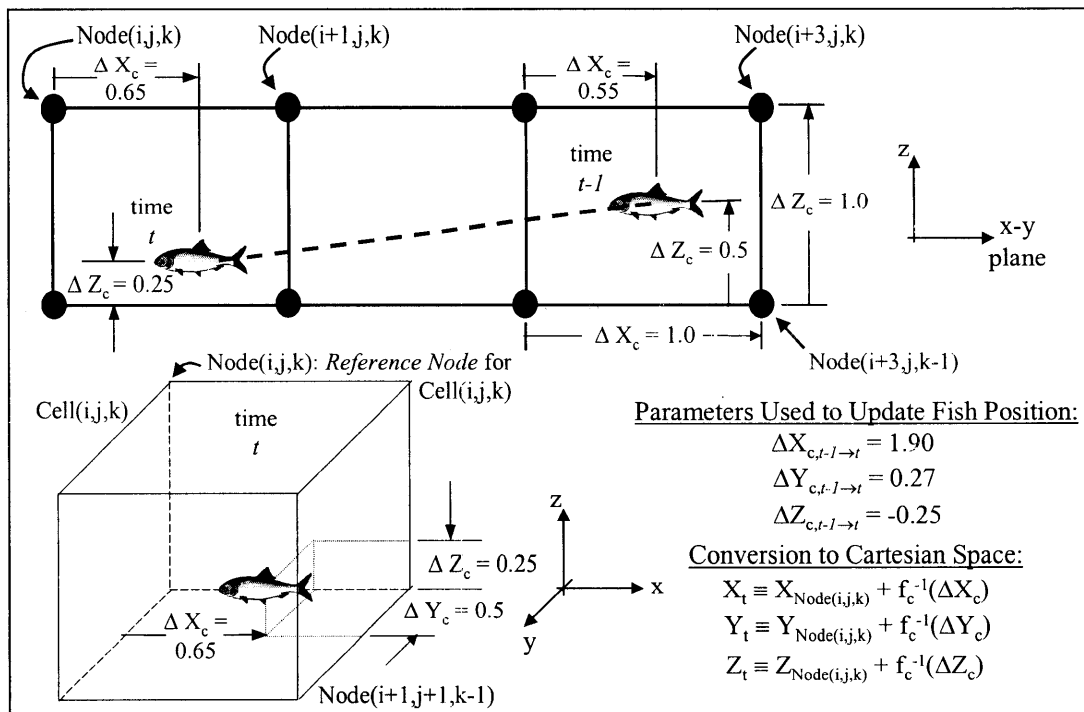


Figure 2.8. Bookkeeping virtual fish movement in contravariant space. f_c^{-1} is the inverse function for converting contravariant displacements within a unit cube into Cartesian space displacements for graphical output and analysis.

Behavior Calibration

Once computational facility exists for implementing behavior in robust fashion, the decoding process moves to the behavior calibration phase. Primarily, calibration of virtual behavior involves appropriate selection of agents, behaviors,

and event evaluations, which requires knowledge of the associated biology. However, the intuitive nature of the game-theoretic and agent-based rule construct facilitates the process by which a trial-and-error process may be used to evaluate uncertain hypotheses. This is a primary benefit of CEL Agent IBMs. This facility is frequently needed, as comprehensive hypotheses rarely exist. Once a hypothesized set of agents, behaviors, and event evaluations have been identified, the process of trial-and-error calibration then proceeds to the selection of event thresholds (e.g., k_1 , k_2 , and d^*), intrinsic utility values ($IU_{agent, behavior}$), and memory coefficients ($m_{agent, behavior}$). Coefficients are biologically tractable and, therefore, lend themselves to evaluation, or further validation, in laboratory experiments. Alternatively, the coefficients can be calibrated using trial-and-error using resultant agent utilities, e.g., Figure 2.4, as a guide to evaluate success and failure points in the implemented hypothesis.

Lower Granite Dam Application

The CEL Agent IBM developed for decoding the observed movement of migrants at Lower Granite Dam in 2000 and 2002, i.e., the NFS, actually consists of several integrated modules (Figure 2.9). The Numerical Fish Surrogate simulation module (NFS-SIM) consists of, approximately, 20,000 lines of original FORTRAN90 source code. This code handles conversion to and from contravariant space, 2nd order interpolation of CFD modeled values, and harbors the behavioral rules and the associated input deck. The low computational overhead afforded by dynamic memory allocation in FORTRAN90 allows the simulation of 1000 virtual fish per 35 minutes in a 1.5 million-node CFD model grid using a dual 3.2 GHz Pentium 4 Xeon processor PC with 4Gb of RAM. NFS-SIM outputs 3-D virtual fish trajectories and interpolated flow information to each fish position in the same

format as that provided for actual 3-D telemetry data integrated into the CFD grid using the Vector Generation and Integration module (NFS-VGI). Tecplot is used to graphically display and animate virtual fish behavior from multiple, simultaneous angles so the implemented hypothesis and associated behaviors can be evaluated in a dynamic context.

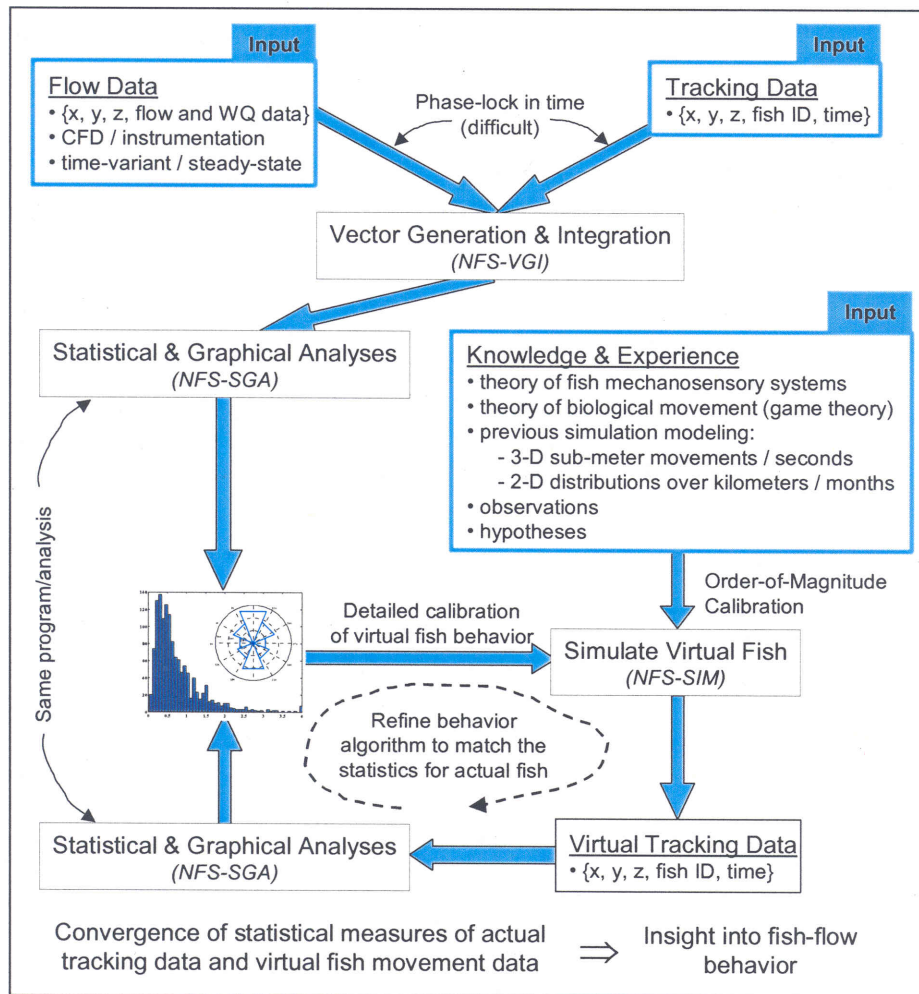


Figure 2.9. Integrated modules of the Numerical Fish Surrogate, the CEL Agent IBM developed and applied for decoding the movement of outmigrating juvenile salmon observed approaching and passing Lower Granite Dam in 2000 and 2002.

Objective

The primary objective of the Numerical Fish Surrogate (NFS) is to decode and replicate, in a simulative context, the 3-D movement patterns of migrants at Lower Granite Dam and the percentages with which run-at-large fish were observed to use each of the available passage routes at the dam. Three-dimensional information on the movement of individual fish (hatchery steelhead) was obtained through the use of acoustic-tags (Cash et al., 2002; Cash et al., 2003; Lucas and Baras, 2000). Run-at-large (i.e., non-species-specific) fish passage data was collected through the use of multi-beam hydroacoustics placed at each passage route (Anglea et al., 2001; Anglea et al., 2003), i.e., each turbine intake, spillbay, and the surface bypass structure. Acoustic-tag (AT) telemetry and hydroacoustic (HA) passage data collected during 2000 studies were available and used to calibrate the 3-D movement and passage of virtual fish for the NFS.

Acoustic-tag (AT) telemetry and HA passage data were collected during 2002 studies at Lower Granite Dam as well. However, processing of AT and HA data was not completed until after calibration of the NFS (to 2000 data) was complete in mid-February 2003. CFD model data for 2002 flow conditions were provided in early April 2003 using the target operating conditions (Appendix A). CFD model runs were completed before actual flow rates were available from the deployed multi-beam hydroacoustic (HA) instrumentation. CFD modeled 2002 flow data and the Numerical Fish Surrogate (NFS) were then used to ‘blindly’ predict 2002 fish passage results, i.e., prior to 2002 HA fish passage results being available. Lastly, HA and NFS fish passage estimates were then compared by an independent entity in late April 2003.

Acoustic-tag (AT) telemetry, multi-beam hydroacoustic (HA) passage, and CFD modeled flow data for 2000 and 2002 studies were divided into independent

data sets for simulation analyses (Table 2.2). Data in 2000 were collected to evaluate and decode behavior with respect to a Surface Bypass Collector (SBC, Figure 2.10), installed in the spillbay nearest the Lower Granite Dam powerhouse, to collect surface-oriented migrants in front of the powerhouse. Data in 2002 were collected to evaluate the behavior of surface-oriented migrants with respect to a Removable Spillway Weir (RSW, Figure 2.10) and to validate the hypothesis developed using the NFS and 2000 data. During 2002 RSW data collection, the SBC was not active, although the dormant SBC structure remained in place, with the exception of the conduit connecting the main SBC gallery to spillbay 1.

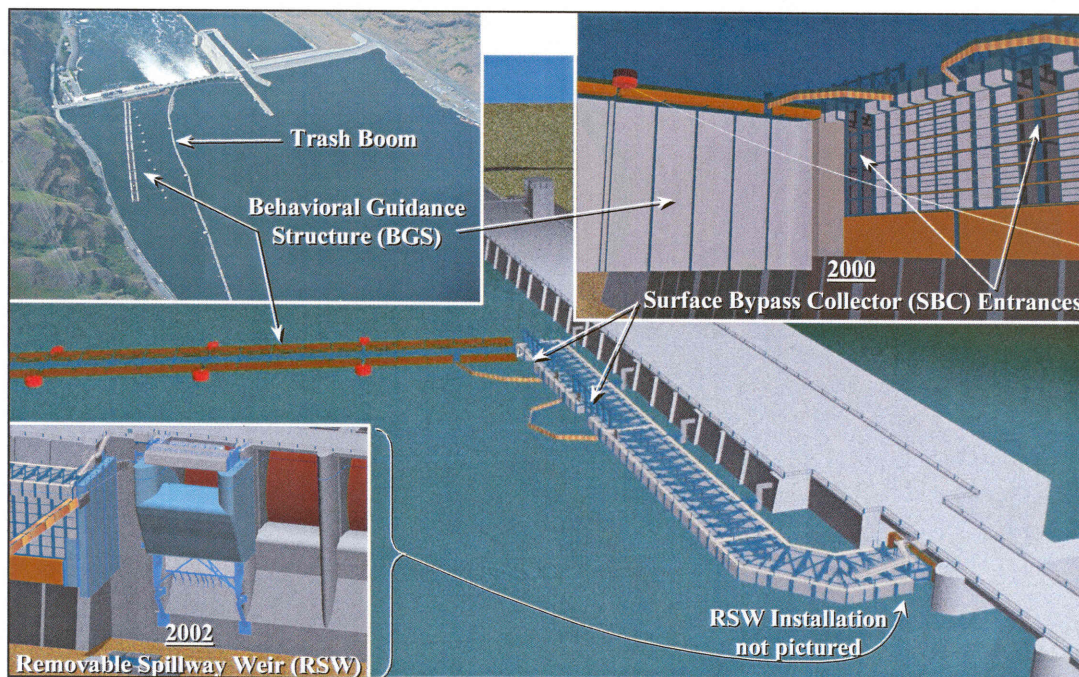


Figure 2.10. Lower Granite Dam structural configurations for 2000 and 2002 analyses. The Behavioral Guidance Structure (BGS) is approximately 24.4m (80') deep at its intersection with the powerhouse and tapers in step-wise manner to a minimum of 16.8m (55') at its upstream end. The trash boom is approximately a constant 1.2m (4') deep. The BGS and trash boom were present for both 2000 and 2002 analyses. Both the SBC (in 2000) and the RSW (in 2002) occupied spillbay 1, i.e., the spillbay nearest the powerhouse.

Table 2.2. Hydraulic Scenarios Evaluated at Lower Granite Dam in 2000 and 2002.

Year / Structure	Case ID	# SBC Gates Open	Operating Target / CFD Model Value			Day / Night Evaluation
			<i>Mean HA Instrumentation Value</i>			
			SBC or RSW Loading (m ³ /s)	Powerhouse Loading (m ³ /s)	Spillway Loading (m ³ /s)	
2000 / SBC	DH8	2	99.1 <i>N/A</i>	2055.5 <i>N/A</i>	450.2 <i>N/A</i>	Composite
	DL5	2	99.1 <i>N/A</i>	1497.7 <i>N/A</i>	351.1 <i>N/A</i>	Composite
	SH4	1	96.3 <i>N/A</i>	1755.4 <i>N/A</i>	450.2 <i>N/A</i>	Composite
	SL2	1	96.3 <i>N/A</i>	1860.1 <i>N/A</i>	450.2 <i>N/A</i>	Composite
2002 / RSW	A2	0	198.2 <i>195.3</i>	1698.8 <i>1449.5</i>	240.7 <i>280.3</i>	Composite
	B2	0	198.2 <i>196.5</i>	1274.1 <i>1401.3</i>	438.8 <i>504.3</i>	Composite
	C2	0	0.0 <i>1.9</i>	1812.0 <i>1778.0</i>	0.0 <i>6.3</i>	Day
	D2	0	0.0 <i>0.6</i>	1443.9 <i>646.8</i>	1223.1 <i>1166.5</i>	Night
	E2	0	198.2 <i>193.7</i>	1670.5 <i>1653.5</i>	1427.0 <i>1381.1</i>	Composite
	F2	0	0.0 <i>0.6</i>	1953.6 <i>2039.3</i>	693.7 <i>730.9</i>	Day
	G2	0	0.0 <i>0.2</i>	1528.9 <i>1371.4</i>	1483.6 <i>1530.0</i>	Night

Virtual Fish Release Locations

Diel period appears to be the most influential variable governing how migrants approach Lower Granite Dam (Cash et al., 2002). Coutant and Whitney (2000) found that 92% of migrants were in the upper 11 meters of the 30m water column. These observations are consistent with the observation of Steig and Johnson (1986), who observed migrants at the powerhouse of The Dalles Dam, downstream of Lower Granite Dam. Steig and Johnson (1986) found that 90% of tracked migrants were within 7.5 m of the water surface during the day and 70% at night. Acoustic-tag (AT) telemetry data collected at Lower Granite Dam in 2000 (i.e., Cash et al., 2001) suggests that migrants approaching the dam during daylight hours are, on average, relatively close (i.e., within 4 meters) to the water surface while nighttime migrants, on average, were below 4 meters and located over a wider range of depths. However, the acoustic-tag (AT) telemetry hydrophone array did not extend far enough upstream to determine the lateral distribution of migrants entering the Lower Granite Dam forebay. Other data are inconclusive. Therefore, 1000 virtual fish were released approximately 800 meters upstream of the dam for each hydraulic scenario (Table 2.2) according to a relatively uniform lateral distribution in the middle 80% of the river (Figure 2.11). Virtual fish were released higher or lower in the water column depending on whether the hydraulic scenario evaluated is associated with a daytime, nighttime, or composite (night and day) data set. Upstream release locations, i.e., approximately 1500 meters upstream of the dam, were evaluated as part of a sensitivity analysis of the NFS.

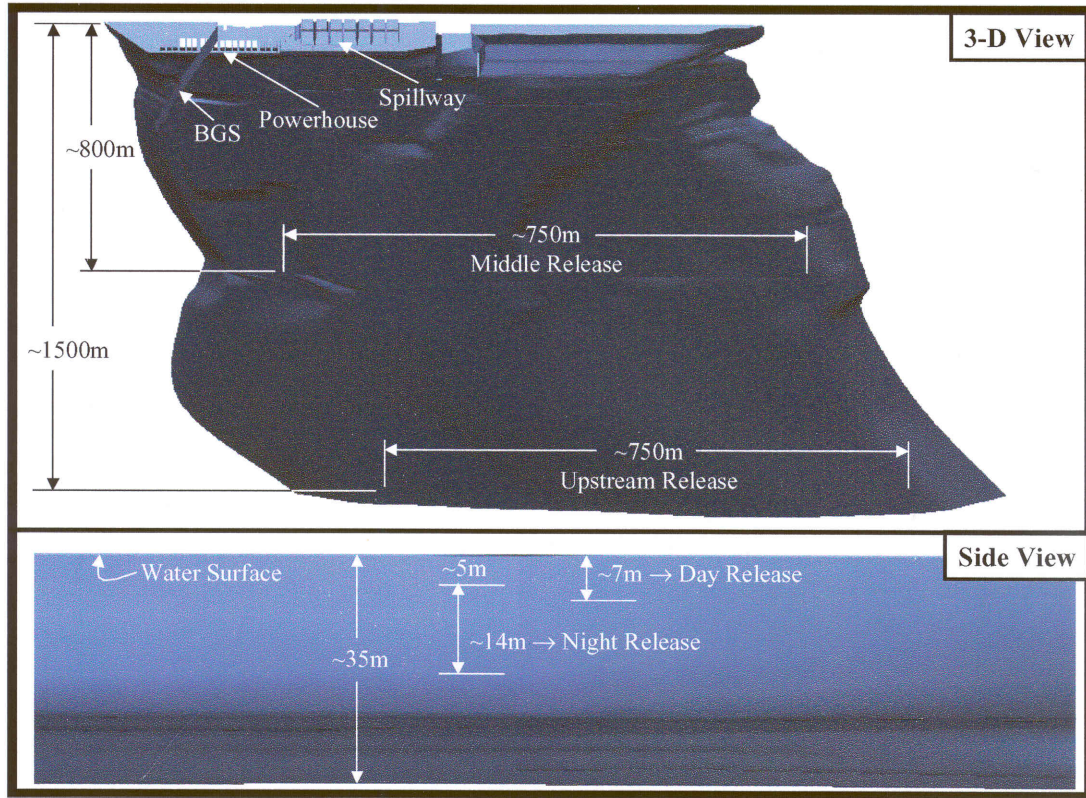


Figure 2.11. Approximate virtual fish release locations for both 2000 and 2002 analyses.

Results

Movement Patterns

The most intuitive means to compare simulated and field observed fish movement is direct visual comparison. Figure 2.12 illustrates the movement patterns of five virtual fish released near the dam under case DH8 flow conditions. Figure 2.13 illustrates the trajectories of neutrally-buoyant particles (i.e., virtual fish with behavioral rules turned off) and three different acoustic-tagged migrants observed under case DH8 flow conditions. Figures 2.12 and 2.13B indicate both virtual and acoustic-tag daytime fish (i.e., usually relatively close to the water surface) appear to

move back and forth between the middle gate opening to the Surface Bypass Collector (SBC) and the trash boom slightly upstream from where the trash boom connects to the spillway. The similarity is noteworthy because both virtual and actual migrants must exhibit oriented volitional swimming to approach and maintain position near the trash boom since the direction of flow (Figure 2.13A) leads away from the trash boom at approximately 45° toward the powerhouse.

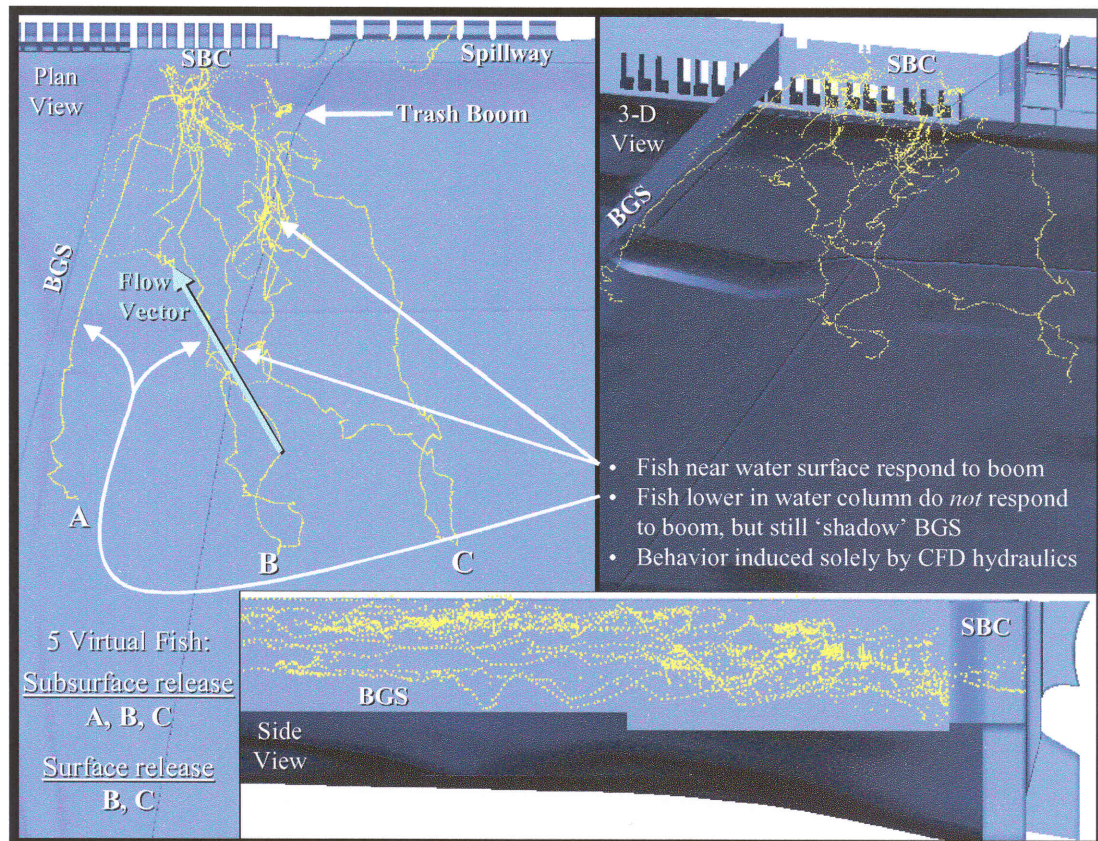


Figure 2.12. Plan, 3-D, and side views of the movement patterns of five virtual fish for case DH8.

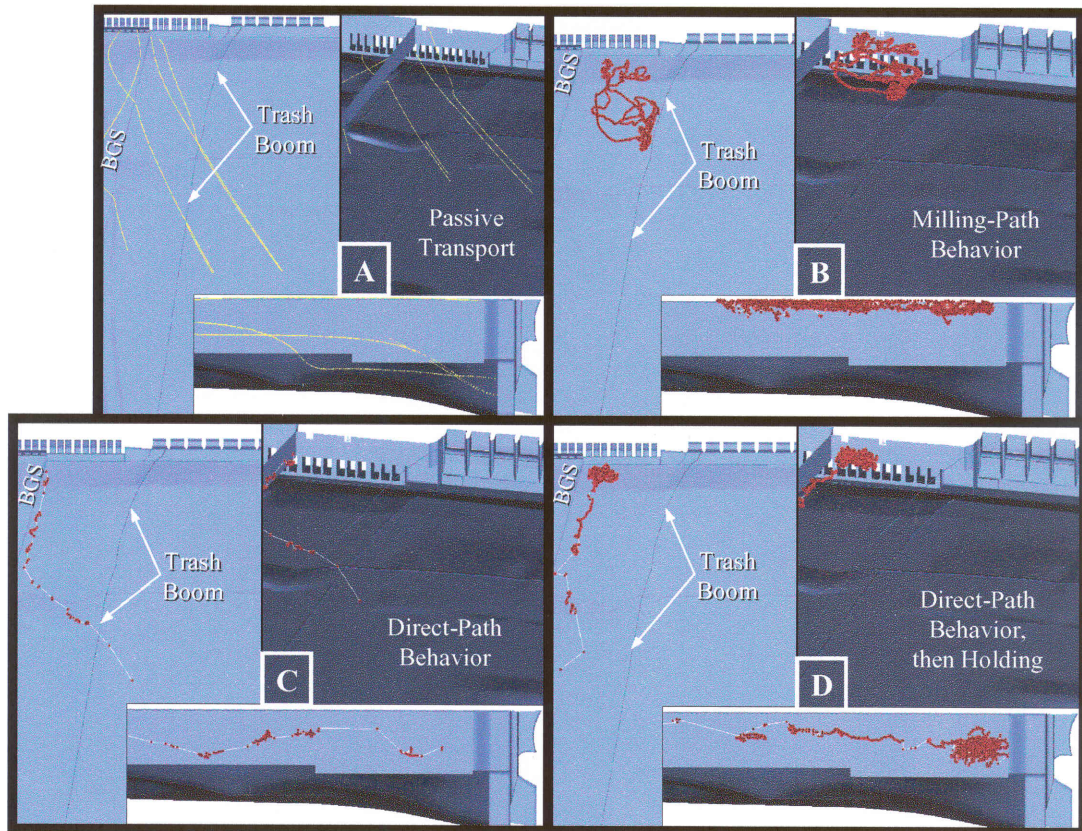


Figure 2.13. Comparison of the movements of five neutrally-buoyant passive particles (Plot A) and the movement patterns of selected, representative AT migrants for case DH8 (Plots B, C, D). Plot B illustrates the typical movement of migrants observed during the day (milling-path) when migrants are nearer the water surface. Plots C and D both illustrate typical movements of migrants observed at night (direct-path) when migrants are distributed deeper in the water column. AT data provided by Cash et al. (2002).

Figures 2.12 and 2.13C indicate both virtual and acoustic-tag nighttime fish (i.e., usually relatively low in the water column) approach the Behavioral Guidance Structure (BGS, Figure 2.10) at approximately the same angle as the direction of flow, but then swim parallel to the BGS once in the local vicinity of the structure. The similarity is noteworthy because both virtual and actual migrants must exhibit

oriented volitional swimming to maintain a position so close to the BGS since the flow intersects and dives under the BGS at approximately 45° . The same pattern is observed in Figure 2.13D. Transmitter-equipped migrants in both Figures 2.13C and 2.13D were observed at night where visual acuity is impaired and movement is, therefore, likely stimulated primarily by hydrodynamics.

Figures 2.12 and 2.13D indicate that both virtual and acoustic-tag nighttime fish mill below the entrance to the middle gate opening to the SBC, but above the turbine intakes. The similarity is noteworthy because both virtual and actual migrants must exhibit oriented volitional swimming to maintain such a milling location in the relatively high-energy environment where the resultant direction of velocity exceeds 45° in the downward direction. Also, it is unlikely observed migrants are seeking a low-energy refugia as the milling location in Figure 2.13D is neither a low-velocity nor a low-strain environment compared to just several meters upstream of the observed milling location.

Fish Passage

Figure 2.14 plots multi-beam hydroacoustic (HA) versus virtual fish passage estimates. Passage estimates are grouped according to the type of passage route used, i.e., the SBC (in 2000) or RSW (in 2002), gallery or in-turbine, and the spillway. The predictive capability of the Numerical Fish Surrogate (NFS) is readily apparent both graphically and statistically. In Figure 2.14, the solid line at 45° indicates where points would reside if the NFS passage results perfectly matched HA estimates. Bart (1995) indicates that concurrence between observed and virtual distributions may be regarded as a strong test of the model. A statistical evaluation of the variance about the 45° line results in an r^2 equal to 0.80, when all cases are considered. In brief, r^2 indicates the proportion of variation in HA fish passage

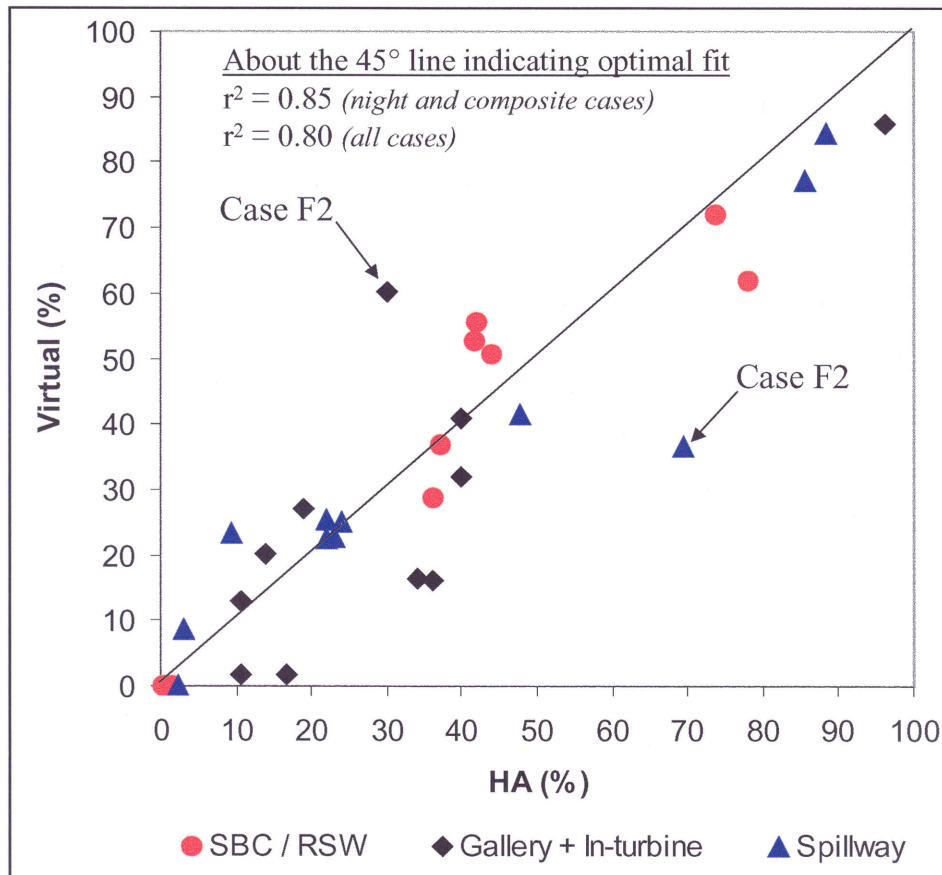


Figure 2.14. Comparison of multi-beam hydroacoustic (i.e., run-at-large) and virtual fish passage estimates at Lower Granite Dam. The three routes of passage available to migrants are: the SBC (in 2000) or RSW (in 2002) surface bypass structure, the spillway, or the turbine (includes both gallery and in-turbine passage). Of eleven total cases, only case C2 and F2 are day-only studies (Table 2.2). The 45° line indicates where all points would lie if NFS predictions perfectly matched HA passage estimates. With respect to the 45° line, $r^2 = 0.80$ if all cases are used, and $r^2 = 0.85$ if day-only cases are not considered. Prairie (1996) indicates that predictive models have rapidly increasing utility as r^2 exceeds 0.65. HA passage data provided by Anglea et al. (2001, 2003).

estimates that can be explained by the NFS. During the day, the visual acuity of migrants likely reduces the role hydrodynamics play in eliciting overall movement behavior. Therefore, it is not surprising that leaving out cases C2 and F2 (i.e., the

day-only studies, Table 2.2) results in an improved r^2 of 0.85. Since both multi-beam hydroacoustic (HA) and NFS fish passage estimates have error (i.e., process error for NFS estimates and experimental error for HA estimates), the variance about the 45° line is actually a maximum error estimate of the entire modeling process. Nonetheless, Prairie (1996) indicates that predictive models have rapidly increasing utility as r^2 exceeds 0.65.

The primary outliers in Figure 2.14 are both associated with case F2. Case F2 and C2 are the only daytime studies. Interestingly, virtual fish passage estimates for cases F2 and C2 were relatively poor compared to other cases, although much of the discrepancy in case C2 (Appendix A, Figure A.20A) may be attributed to discrepancies in CFD modeled flow conditions and actual dam operations (Appendix A, Figure A.20B). Regardless, shortcomings in the ability to accurately simulate daytime passage are expected. During the day, when vision can dominate other sensory modalities, the mechanosensory system may be a secondary contributor to overall movement behavior (New and Kang, 2000; Montgomery et al., 1995).

Differences in day and night behavior have been observed in many fish species, including salmonids. Haro et al. (1998) found that under very low light and dark conditions Atlantic salmon smolts tended to orient upstream more frequently. Nowak and Quinn (2002) found that salmonids in Lake Washington, in the Pacific Northwest, demonstrated a decrease in activity in the middle of the night. Furthermore, Pavlov (1994) found that when light was low, juvenile river fish were more likely to drift with the current rather than maintain position. This, in turn, may partly explain the observation by Larinier and Boyer-Bernard (1991) (summarized in Haro et al., 1998) that Atlantic salmon smolt passage rates increased when lights at bypass entrances were turned off. Furthermore, Nowak and Quinn (2002) found that trout are likely to be closer to the surface during the day to maximize the ambient

light levels that facilitate visual feeding of insects and larval fishes. Although a lake setting, Nowak and Quinn (2002) found that trout in Lake Washington foraged in littoral areas exclusively during daylight hours. Ample evidence exists to suggest that migrants at Lower Granite Dam may be responding to visual cues not available at night, e.g., shadows cast by the dam, Behavioral Guidance Structure (BGS), and trash boom, and, thus, possibly explains the relatively poor performance of the NFS to capture daytime HA passage estimates.

Residence Times

Figure 2.15 shows the forebay detection residence times of milling- and direct-path acoustic-tagged (AT) migrants for 2000 studies. Figure 2.16 shows the forebay residence times of 400 virtual fish, i.e., 100 fish for each 2000 case, released 800 meters upstream at a composite depth. The milling- and direct-path classification (Cash et al., 2002) is a binary scheme based on the predominate movement pattern detected in the forebay (e.g., Figure 2.13B, C, and D). Milling-path fish are, generally, observed during the day and direct-path fish are, generally, observed at night. AT migrants are only observed in the vicinity of the deployed hydrophone array (Cash et al., 2002), but could be sampled for long periods of time. In contrast, virtual fish are tracked from their release location far upstream of the hydrophone array, but are simulated for only five hours due to computational resources. Nonetheless, a fundamental attribute exists in both real and virtual data sets. Both real and virtual residence times exhibit a bimodal distribution in which many fish appear to pass with relatively little time spent at the dam followed by a later, more distributed, wave of fish that are, presumably, delayed due to milling near and around structures such as the trash boom. Longer simulations are needed to determine whether the tail of the distribution of virtual milling fish residence times is

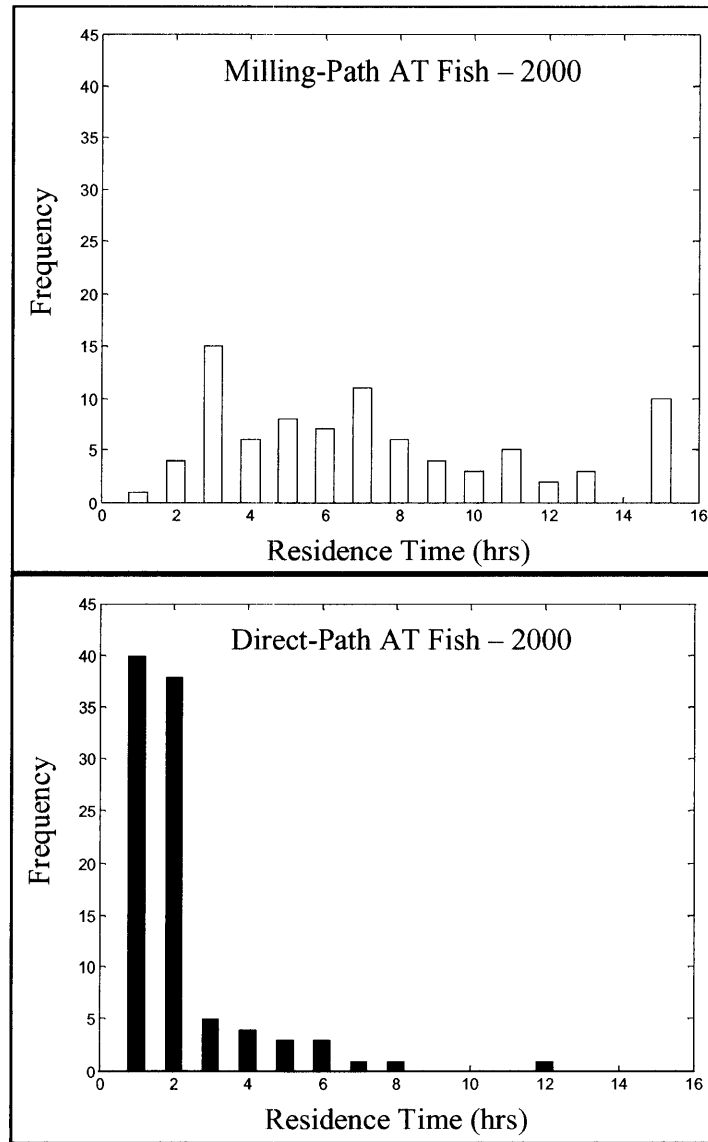


Figure 2.15. Detected forebay residence times of acoustic-tagged migrants, divided into milling- and direct-path classifications (Cash et al., 2002). Residence time is the sum of detection hours inside the hydrophone array. Cash et al. (2002) indicate that 83% of milling-path migrants were first detected during the day and 70% of these migrants are located in the upper 4m of the water column. In contrast, 66% of direct-path migrants were first detected at night and 90% of these migrants are located deeper than 4m. Milling-path fish at night had a small sample size. Most migrants passed within 16 hours of first detection; migrants with residence times in excess of 16 hours are not displayed.

of similar form to the distribution of AT milling-path fish residence times. However, even very long simulations, e.g., greater than 48 hours, are unlikely to capture all the nuances observed with regard to residence times. For instance, Beeman and Maule (2001) indicate that Venditti et al. (2000) found migrants milling in the forebay for days and some even traveling back upstream for as much as 14 km before returning to the dam.

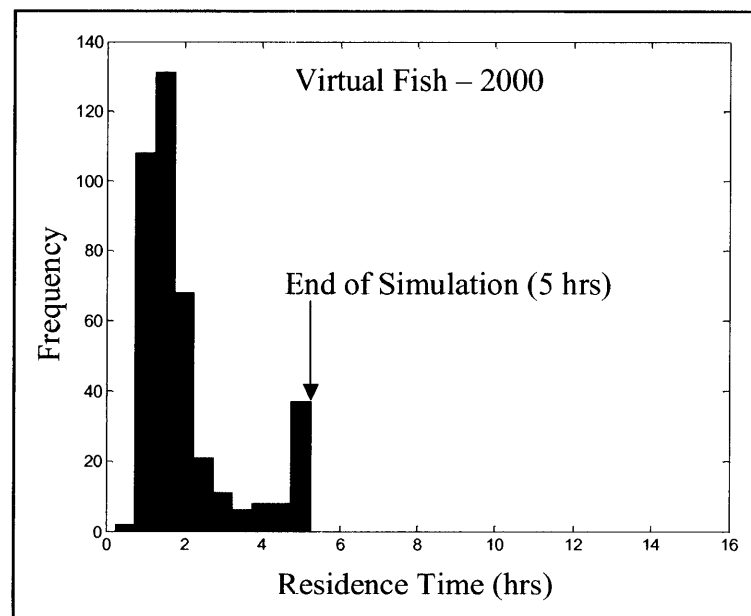


Figure 2.16. Forebay residence times of 400 virtual fish, i.e., 100 virtual fish for each 2000 case (released at a composite depth 800m upstream of the dam). In contrast to Figure 2.15, virtual fish are tracked from their release location several hundred meters upstream of the extent of the AT hydrophone. However, unlike the AT hydrophone array that can track AT migrants for long periods of time, virtual fish simulations are presently limited to 5 hours due to computational resources.

Speed Distributions

Figure 2.17 shows the distribution of volitional swimming speeds for nighttime AT migrants and 100 virtual fish for case DH8. The central tendencies

(modes) of both distributions are approximately equal although discrepancies exist in the tails.

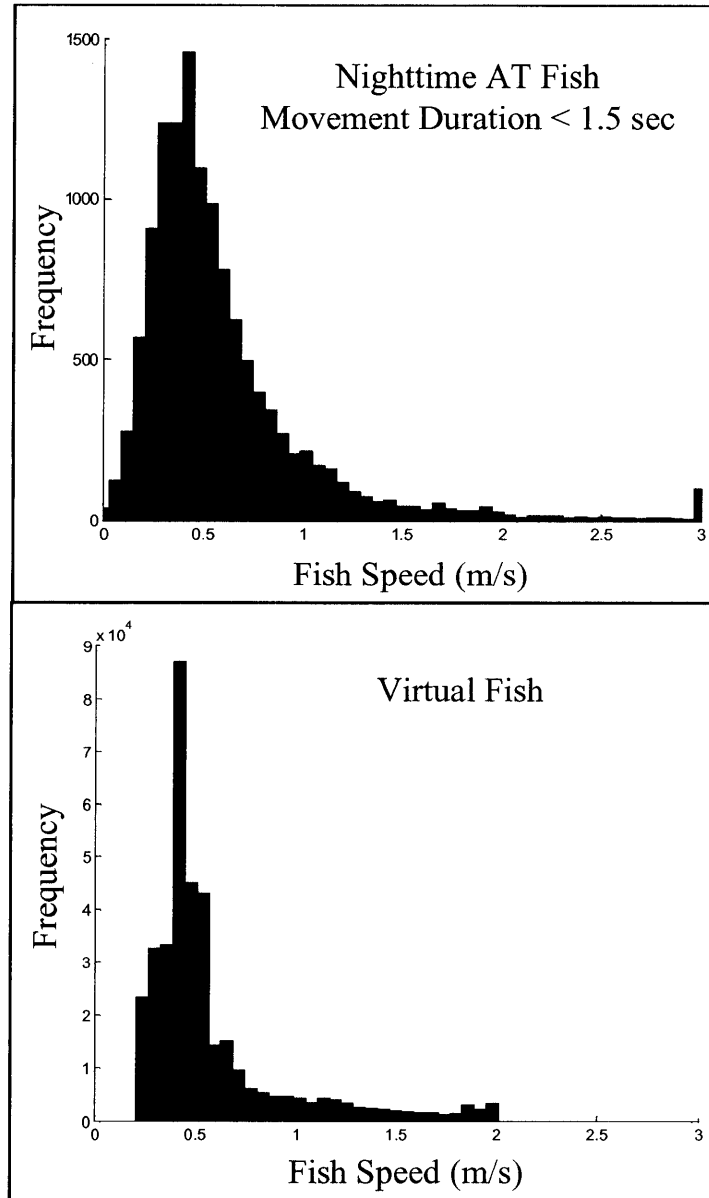


Figure 2.17. Volitional swimming speed distributions of nighttime AT migrant and 100 virtual fish for case DH8 (i.e., composite 800m upstream release). AT data was sifted to include only those AT migrant movements with a duration less than 1.5 sec so as to exclude observations where AT migrants most likely exited and then re-entered the hydrophone array. AT data provided by Cash et al. (2002).

Sensitivity Analysis

A sensitivity analysis of virtual fish release locations on NFS passage estimates was performed to evaluate the influence of this initial condition. Sensitivity analysis is important because the spatial distribution of real fish entering the forebay of Lower Granite Dam is largely unknown. Several patterns emerge from the sensitivity analyses of release locations (Appendix A, Figures A.3-A.13 and A25-A35). First, daytime releases for 2000 cases result in increased Surface Bypass Collector (SBC) passage compared to nighttime releases, which is expected since a greater proportion of fish are surface-oriented during the day. Anglea et al. (2001) point out that the rate of passage of daytime fish (i.e., the number of fish observed compared to the number of fish that actually entered) into the SBC was significantly lower ($p < 0.1$) than for nighttime fish. This conundrum may be explained by considering the influence of vision and the observation of Pavlov (1994), who found that juvenile river fish were more likely to drift with the current when light was low. Interestingly, Larinier and Boyer-Bernard (1991) found that Atlantic salmon smolt passage rates also increased when lights at bypass entrances were turned off. Second, NFS spillway passage for both 2000 and 2002 cases was generally higher for daytime releases.

Sensitivity analyses highlight interesting patterns. First, upstream releases (1500m, Figure 2.11) are, predictably, associated with greater proportions of virtual fish remaining in the forebay prior to termination of the simulation. Second, in general, the percent of fish observed by HA instrumentation using each of the available passage routes appears to be more pronounced in 2002 studies. Interestingly, sensitivity analyses of these cases also exhibit more pronounced patterning than in 2000 cases, the notable exception being case A2. While the underlying cause may be related to improved study design or a greater influence of

the Removable Spillway Weir (RSW) on fish passage, regardless, the Numerical Fish Surrogate (NFS) appears to be more reliable (stable) when multi-beam hydroacoustic (HA) passage estimates, themselves, are more pronounced, i.e., exhibit strong patterning. Year 2000 cases and case A2 raise the interesting prospect that some configurations may inherently be associated with better conditioned (stable) flow patterns that are more amendable to steady-state CFD modeling and, therefore, HA passage estimates that are more conducive to existing NFS prediction.

With the exception of daytime studies (i.e., cases C2 and F2), case SH4, SL2, and A2 are associated with NFS predictions of greatest discrepancy. Interestingly, however, HA and NFS fish passage estimates are nearly identical in cases SH4 and SL2 if a nighttime release is used instead of a composite release at 800m upstream (Figure 2.18). Similarly, HA and NFS fish passage estimates are nearly identical in case A2 if a daytime release is used instead of a composite release at 800m upstream.

Lastly, all random computations in the NFS are based on a user-defined random number seed. A sensitivity analysis was, therefore, performed to assess the impact of seed choice on NFS fish passage estimates. Results tabulated in Table 2.3 clearly indicate that NFS passage estimates are not heavily influenced by the choice of the random number seed, a desired quality in a model.

Discussion

Other syntheses and techniques for simulating individual-based movement in spatially-explicit fashion have been discussed, e.g., Berec (2002). However, the CEL Agent IBM framework clearly demonstrates the ability to provide robust mathematical decoding of observed movement patterns at appropriate spatiotemporal scales that is amendable to forecast simulation using only trial-and-error calibration. Also, the Numerical Fish Surrogate (NFS) clearly substantiates the observation by

Figure 2.18. Sensitivity analyses of different virtual fish release locations on passage estimates for cases SH4, SL2, and A2. Note that a nighttime release of virtual fish from the same location upstream used to generate Figure 2.14 results (i.e., ~800m upstream of the dam) results in HA and NFS fish passage estimates that are nearly identical for cases SH4 and SL2. A daytime release of virtual fish from the same location results in nearly identical HA and NFS fish passage estimates for case A2. HA passage data provided by Anglea et al. (2001, 2003).

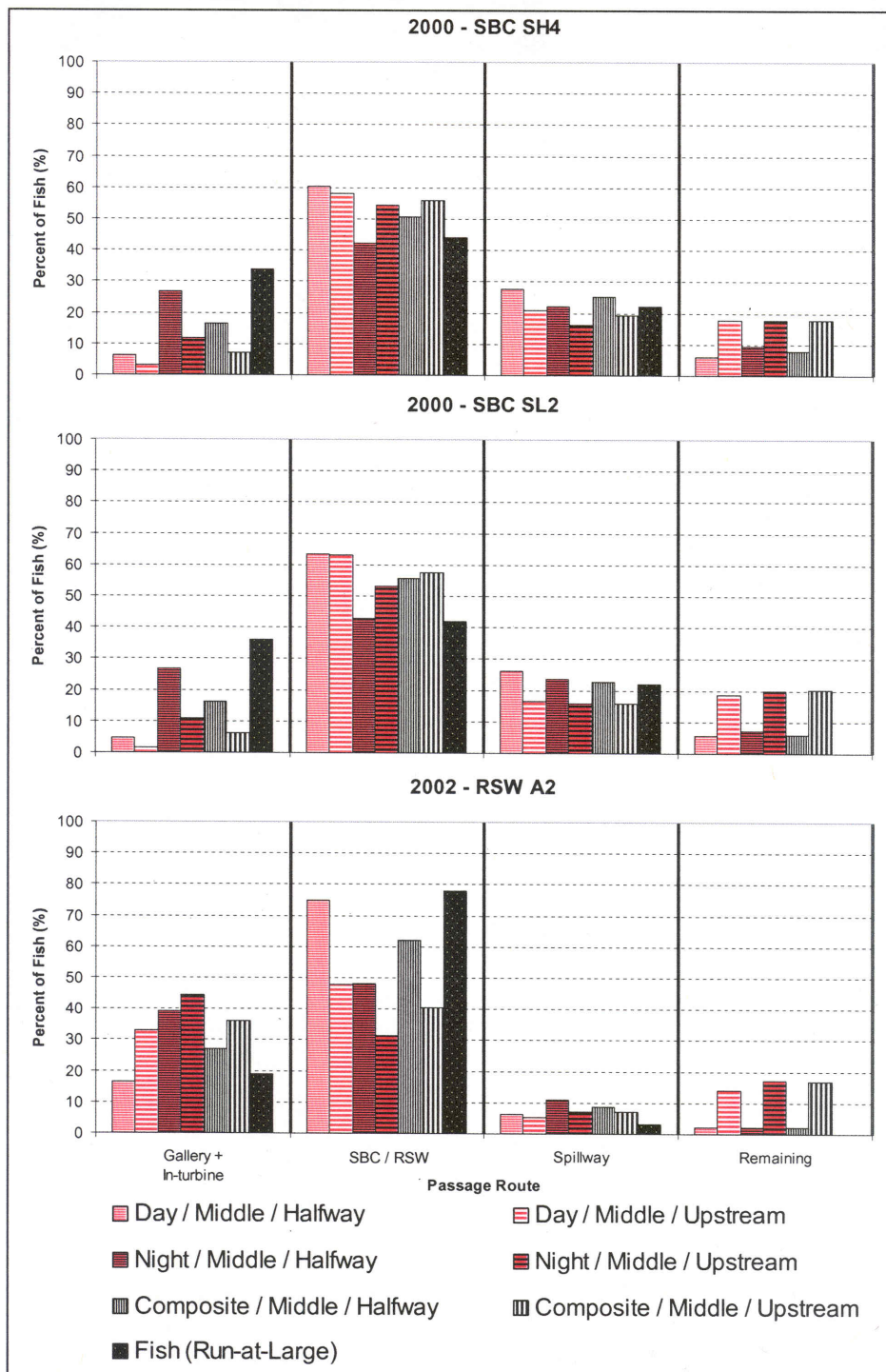


Table 2.3. Random Number Seed Sensitivity Analysis for Case DH8.

Virtual Fish Passage			
Passage Route	Seed ¹	Mean ²	95% CI ²
Turbine 1	0.0	0.0	0.0
Turbine 2	0.3	0.5	0.0
Turbine 3	7.5	7.8	0.1
Turbine 4	16.4	17.6	0.5
Turbine 5	16.6	15.5	0.4
Turbine 6	0.0	0.0	0.0
SBC	28.8	28.8	0.4
Spillbay 2	2.8	2.6	0.1
Spillbay 3	12.3	14.9	0.6
Spillbay 4	0.8	0.6	0.0
Spillbay 5	0.0	0.0	0.0
Spillbay 6	0.0	0.3	0.0
Spillbay 7	9.2	6.4	0.3
Spillbay 8	0.1	0.1	0.0

¹ Random number seed used in NFS simulations for generating fish passage estimates.

² Results based on 30 runs with different random number seeds.

Whitfield (2001) that many individuals following a few simple rules can result in complex and powerful behavior. A complex set of rules is not necessary for patterns to emerge as ecosystems show complex 'emergent' properties from simple

interactions (Whitfield, 2001). CEL Agent IBMs facilitate implementation of this modeling philosophy using theoretically- and computationally-robust means.

Reasons for Discrepancies

Although actual and virtual fish movements are similar in many regards, discrepancies exist. Several factors may be contributing to this phenomenon. First, the spatial extent of the lateral line depends on the size of the fish and, therefore, hydrodynamic sources can be detected further away by larger fish (Denton and Gray, 1983, 1988, 1989; Kalmijn, 1988, 1989; Coombs, 1996, 1999). While fish passing Lower Granite Dam are composed of many sizes and species, virtual fish are presently simulated as a single virtual size. Second, the position of the trash boom in the CFD model for 2002 flow simulations is a gross approximation, as CFD model results were completed prior to acoustic-tag (AT) telemetry data being available, which shows the exact position of the trash boom during data collection efforts.

Third, by purposeful design, strain thresholds, k_1 and k_2 , are a simplified mathematical description of wall-bounded and free-shear flow patterns. These thresholds, for a given individual fish, are likely dependent on a number of factors including the species, health, and size of the fish as well as the stability (i.e., transient nature) of the hydrodynamic features, background noise and turbulence, and the fish's level of anxiety and exhaustion. In fact, the preference, tolerance, resistance, and overall response to strain are likely influenced by the same factors known to influence thermal preferendum, e.g., level of starvation, physiological activities, prior history, age, and infections (Birtwell et al., 2003).

Model Utility

The purpose of a model is not just to evaluate alternative projects, but to also provide understanding of the dynamics of systems and the opportunities for cost-effective intervention that will improve the system operation (Stedinger, 2000). Researchers have often failed to take behavior into consideration when developing bypass systems (Popper and Carlson, 1998). If behavioral stimuli are ever to be widely used for fish protection, they must eventually be integrated into common engineering practice (Popper and Carlson, 1998). Despite inevitable model discrepancies, the Numerical Fish Surrogate (NFS) and other CEL Agent IBMs provide the means necessary to translate field data into an understanding of behavior and, further, an understanding of behavior into engineering decision-support. Presently, the mathematical hypothesis developed from the NFS, i.e., the Strain-Velocity-Pressure (SVP) Hypothesis, as well as the NFS, itself, are being used to redesign fish bypass structures at three federal hydropower dams on the Snake and Columbia Rivers in the Pacific Northwest.

Virtual System Concept

CEL Agent IBMs provide the facility for improving the evaluation of developed hypotheses beyond the means described in this paper. Hypotheses on the interaction between individual phenotypic differences and spatiotemporal differences in environmental factors can be more rigorously evaluated with a thorough implementation of the virtual system concept (Figure 2.19). In the virtual system concept, outputted 3-D information from the NFS is compared in statistically rigorous fashion with 3-D information on actual fish movement, of similar form, provided by the NFS-VGI (Figure 2.9). This form of analysis circumvents many of

the inherent statistical limitations that inhibit direct application of popular statistical methods to inherently auto- and serially-autocorrelated 3-D data (chapter 1).

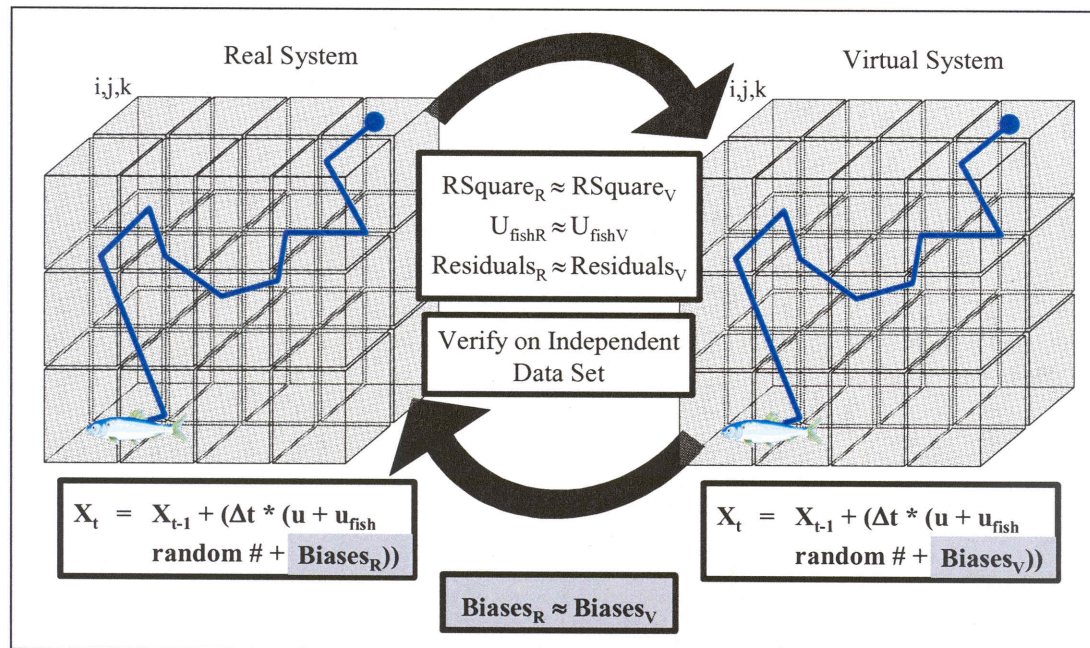


Figure 2.19. The virtual system concept involves generating numerical ‘hypothesized’ movement behavior of similar form as the data collected by field instrumentation for ‘real’ animals. Comparing virtual and actual animal movement of similar form circumvents the inherent statistical limitations (e.g., autocorrelation) impeding a direct application of traditional, solo statistical approaches.

Scale Issues

Managing aquatic biological populations requires increasingly robust tools to handle the inherent complexity of interrelated scale-oriented ecological processes. One of the most pressing needs is the ability to link, through mechanistic means, pertinent fluid and water quality dynamics and observed movement behaviors. Results of the Numerical Fish Surrogate (NFS) indicate that CEL Agent IBMs provide the facility needed. The behavior of water in nature is difficult to simulate

and cannot be described either simply or completely. Although the effects of each small perturbation on the flow in large-scale natural settings are presently impossible to capture, a description of the inner mechanisms leading to observed movement can be achieved at the level for which resolvable variables (e.g., accurate physicochemical and biological data) exist.

The scale level at which resolvable movement patterns exist, coincident patterns in associated stimuli likely also exist at the same scale. In other words, fish are simultaneously responding to instantaneous and unpredictable stimuli in their small-scale movements and to inherent biases and trends in the stimuli over larger scales. If an animal is responding to physicochemical and biological stimuli over very small scales, but these same stimuli are associated with large-scale biases and trends, one could expect distinguishable movement patterns at the scale of the biases and trends, i.e., at the scale at or above those available to resolvable variables. Consequently, the spatiotemporal scale for which decoding and associated forecast simulation can be expected to succeed is inherently linked to the scale for which discernable, robust, and accurate patterns in relevant stimuli can be captured by resolvable variables. This partly addresses the concerns raised in Kondolf et al. (2000), Bult et al. (1999), and Railsback (1999) regarding the discontinuity in, and mismatch between, the spatial scale at which hydraulics are often modeled and the spatial scales at which fish respond to hydraulics.

Archiving Knowledge

The agent- and event-based construct of the behavioral rules provides the means to enumerate hypotheses of movement behavior of a target species for optimal contribution to a regional knowledge base. Agents, behaviors, and event thresholds may be categorized and compared for a variety of target species and life-stages to

expand the discovery of plausible rules based on the relative success and/or shortcoming of various rule structures evaluated. Historically, system-wide hydraulic designs for fish passage structures have been based on the ‘build-and-test’ paradigm. That is, designs are not clearly based on fish behavior, so a prolonged period of testing and adjustment is typically necessary to refine operation to acceptable limits. Agents, variables, and event thresholds can now be evaluated at multiple dams on a given river system to determine if fish behavior changes spatially or seasonally (e.g., as fish smolt) and assimilated into the system-wide knowledge base to improve future designs.

Future Improvements

CFD Modeling

The spatiotemporal scale at which CEL Agent IBMs are applied is inherently linked to the scale at which CFD models can provide robust, accurate resolvable variables for associated fluid and water quality dynamics. Large-scale movement (meters-to-kilometers) patterns in relatively low energy intransient environments are likely influenced by stimuli at the spatial scale currently afforded by existing steady-state CFD models. However, small-scale movement (sub-meter) patterns in relatively high energy transient environments are likely influenced by stimuli at spatial and temporal scales not afforded by steady-state CFD models. New, innovative CFD models such as large-eddy simulation (LES) provide sufficient resolution to address increasingly small-scale movement issues.

CEL Agent IBM Improvements

Numerous opportunities exist for expanding the current utility and capability of CEL Agent IBMs. First, optimization methods suitable for refining the

coefficients may facilitate efficient and robust calibration, if proper optimization metrics can be developed. Second, if an explanation of the observed spatiotemporal pattern is not necessarily the modeling objective, a CEL Agent IBM can still serve as both a screening guide for finding the appropriate level of resolution (Grimm, 1999), and a robust computational framework, for assessing other biological dynamics, e.g., bioenergetics and foraging (Stockwell and Johnson, 1997), growth, recruitment, mortality, nutrient cycling (Schindler and Eby, 1997), schooling and/or predator-prey interactions (Huth and Wissel, 1992, 1994; Niwa, 1994; Nonacs et al., 1994; Reuter and Breckling, 1994).

Third, CEL Agent IBMs provide the computational and theoretical means to couple particle-based IBMs to existing, calibrated 3-D eutrophication models. This provides the computational doorway to evaluate land-use changes on fish and individuals of other aquatic species. Karim et al. (2003) demonstrate such models are valuable. To date, however, particle-based IBMs linked to eutrophication models have generally been considered beyond the present state-of-the-art (Cercio and Meyers, 2000). CEL Agent IBMs provide the facility to more accurately assess the exposures of individuals to environmental conditions that may be related to survival estimates of certain species (Smith et al., 2002), the overlap with other species (Pientka and Parrish, 2002), and the outcome of associated interspecific competition and predation (Reese and Harvey, 2002).

With regard to dams on the Columbia and Snake Rivers, the existing CEL Agent IBM can provide an improved means to assess the impact of various operating scenarios on the volitional egress movements, predator locations and predator-prey interactions (Petersen and DeAngelis, 2000), and temperature and dissolved gas exposure histories (Anderson, 2000b; Backman et al., 2002; Nestler et al., 2002; Scheibe and Richmond, 2002) of fish in tailraces, which can result in fish injury and

mortality (Coutant, 1987; Christie and Regier, 1988). Lastly, CEL Agent IBMs provide an innovative means for evaluating the inverse problem. Few models exist for evaluating the contamination dynamics of aquatic systems driven, in part, by the movement of highly mobile populations, although Monte (2002) describes a general methodology for linking biological uptake models and the movement of biota.

The implicit result of adding utility to the model is increasing the model's complexity. A decentralized, modular format, however, together with methods for calibrating complex models with emergent synergies, e.g., van Nes et al. (2002), can mitigate the inherent problems associated with using a model of increasing complexity, if and when increasing complexity is needed. By appropriately managing the level of model complexity needed, CEL Agent IBMs provide a robust computational backbone from which to employ optimization methods frequently used in water resource systems engineering (e.g., Loucks et al., 1981) to develop improved management strategies (e.g., Jager and Rose, 2003) using transparent and intuitive means that are also easy to visualize, communicate, and evaluate.

Conclusion

Coupled Eulerian-Lagrangian agent- and individual-based modeling (CEL Agent IBMs) provide a theoretically-sound and computationally-robust framework from which to mathematically and mechanistically decode the movement patterns of mobile aquatic species in a manner that provides utility for forecast simulation. CEL Agent IBMs provide a scaleable framework from which to archive results of movement pattern analysis at varying scales and for specific species and life-stages of individuals. The modeling scheme is designed to accommodate increasingly robust algorithms from the field of individual-based models to formulate a modeling framework with an expanded ecosystem perspective for system-wide analyses.

REFERENCES

- Alewell, C. and Manderscheid, B. (1998). "Use of objective criteria for the assessment of biogeochemical ecosystem models." *Ecological Modelling*, **107**, 213-224.
- Anderson, J. J. (2002). "An agent-based event driven foraging model." *Natural Resource Modeling*, **15**(1), Spring 2002.
- Anderson, J. D. (2000a). Modeling impacts of multiple stresses on aquatic ecosystems: case study of juvenile Chinook salmon in the Sacramento River system. Ph.D. dissertation. Department of Civil and Environmental Engineering, University of California at Davis, Davis, California.
- Anderson, J. J. (2000b). "A vitality-based model relating stressors and environmental properties to organism survival." *Ecological Monographs*, **70**(3), 445-470.
- Anderson, J. J. (1991). "Fish bypass system mathematical models." *Proceedings from ASCE Waterpower '91*, Denver, CO, July 24-26, 1991.
- Anderson, J. J. (1988). "Diverting migrating fish past turbines." *The Northwest Environmental Journal*, **4**, 109-128.
- Anglea, S. M., Ham, K. D., Johnson, G. E., Simmons, M. A., Simmons, C. S., Kudera, E. and Skalski, J. R. (2003). "Hydroacoustic evaluation of the removable spillway weir at Lower Granite Dam in 2002." Final report prepared by Battelle Pacific Northwest Division for U.S. Army Corps of Engineers, Walla Walla District, PNWD-3219, Walla Walla, WA.
- Anglea, S. M., Johnson, R. L., Simmons, M. A., Thorsten, S. L., Duncan, J. P., Chamness, M. A., McKinstry, C. A., Kudera, E. A., and Skalski, J. R. (2001). "Fixed-location hydroacoustic evaluation of the prototype surface bypass and collector at Lower Granite Dam in 2000." Final report prepared

by Battelle Pacific Northwest Division for U.S. Army Corps of Engineers, Walla Walla District, under Contract No. DACW68-96-D-002, Walla Walla, WA.

- Backman, T. W. H., Evans, A. F., and Robertson, M. S. (2002). "Gas bubble trauma incidence in juvenile salmonids in the lower Columbia and Snake Rivers." *North American Journal of Fisheries Management*, **22**, 965-972.
- Bart, J. (1995). "Acceptance criteria for using individual-based models to make management decisions." *Ecological Applications*, **5**(2), 411-420.
- Beamish, F. W. H. (1978). Fish physiology volume VII "Locomotion". W. S. Hoar and D. J. Randall (eds.), Academic Press, New York, NY, p. 101-183.
- Beeman, J. W. and Maule, A. G. (2001). "Residence times and diel passage distributions of radio-tagged juvenile spring chinook salmon and steelhead in a gatewell and fish collection channel of a Columbia River dam." *North American Journal of Fisheries Management*, **21**, 455-463.
- Berec, L. (2002). "Techniques of spatially explicit individual-based models: construction, simulation, and mean-field analysis." *Ecological Modelling*, **150**, 55-81.
- Bian, L. (2003). "The representation of the environment in the context of individual-based modeling." *Ecological Modelling*, **159**, 279-296.
- Birtwell, I. K., Korstrom, J. S., and Brotherston, A. E. (2003). "Laboratory studies on the effects of thermal change on the behaviour and distribution of juvenile chum salmon in sea water." *Journal of Fish Biology*, **62**, 85-96.
- Bourque, M.-C., LeBlond, P. H., and Cummins, P. F. (1999). "Effects of tidal currents on Pacific salmon migration: results from a fine-resolution coastal model." *Canadian Journal of Fisheries and Aquatic Sciences*, **56**, 839-846.

- Braun, C. B. and Coombs, S. (2000). "The overlapping roles of the inner ear and lateral line: the active space of dipole source detection." *Philosophical Transactions of The Royal Society of London series B*, **355**(1401), 1115-1119.
- Brett, J. R. (1952). "Temperature tolerance in young Pacific salmon, genus *Oncorhynchus*." *Journal of the Fisheries Research Board of Canada*, **9**, 265-323.
- Brutsaert, W. (1986). "Catchment-scale evaporation and the atmospheric boundary layer." *Water Resources Research*, **22**(9), 39S-45S.
- Bult, T. P., Riley, S. C., Haedrich, R. L., Gibson, R. J., and Heggenes, J. (1999). "Density-dependent habitat selection by juvenile Atlantic salmon (*Salmo salar*) in experimental riverine habitats." *Canadian Journal of Fisheries and Aquatic Sciences*, **56**, 1298-1306.
- Cash, K. M., Hatton, T. W., Jones, E. C., Magie, R. J., Mayer, K. C., Swyers, N. M., Adams, N. S., and Rondorf, D. W. (2003). "Three-dimensional fish tracking to evaluate the removable spillway weir at Lower Granite Dam during 2002." Draft report prepared by U.S. Geological Survey Columbia River Research Laboratory for the U.S. Army Corps of Engineers, Walla Walla District, Walla Walla, WA.
- Cash, K. M., Adams, N. S., Hatton, T. W., Jones, E. C., and Rondorf, D. W. (2002). "Three-dimensional fish tracking to evaluate the operation of the Lower Granite surface bypass collector and behavioral guidance structure during 2000." Final report prepared by U.S. Geological Survey Columbia River Research Laboratory for the U.S. Army Corps of Engineers, Walla Walla District, Walla Walla, WA.

- Cerco, C. F. and Meyers, M. (2000). "Tributary refinements to Chesapeake Bay model." *ASCE Journal of Environmental Engineering*, **126**(2), 164-174.
- Christie, C. G. and Regier, H. A. (1988). "Measurements of optimal habitat and their relationship to yields for four commercial fish species." *Canadian Journal of Fisheries and Aquatic Sciences*, **45**, 301-314.
- Clark, M. E. and Rose, K. A. (1997). "Individual-based model of stream-resident rainbow trout and brook char: model description, corroboration, and effects of sympatry and spawning season duration." *Ecological Modelling*, **94**, 157-175.
- Coombs, S. (1999). "Signal detection theory, lateral-line excitation patterns and prey capture behaviour of mottled sculpin." *Animal Behaviour*, **58**, 421-430.
- Coombs, S. (1996). "Interpore spacings on canals may determine distance range of lateral line system." *Society of Neuroscience Abstracts*, **22**, 1819.
- Coombs, S., Braun, C. B., and Donovan, B. (2001). "The orienting response of Lake Michigan mottled sculpin is mediated by canal neuromasts." *Journal of Experimental Biology*, **204**, 337-348.
- Coombs, S., Finneran, J. J., and Conley, R. A. (2000). "Hydrodynamic image formation by the peripheral lateral line system of the Lake Michigan mottled sculpin, *Cottus bairdi*." *Philosophical Transactions of The Royal Society of London series B*, **355**(1401), 1111-1114.
- Costa, M. and Ferreira, J. S. (2000). "Discrete particle distribution model for advection-diffusion transport." *ASCE Journal of Hydraulic Engineering*, **126**(7), 525-532.
- Coutant, C. C. (2001). "Integrated, multi-sensory, behavioral guidance systems for fish diversions." *Behavioral Technologies for Fish Guidance*, C. C. Coutant, ed., pp 105-113, American Fisheries Society, Symposium, **26**, Bethesda, MD.

- Coutant, C. C. (1987). "Thermal preference: when does an asset become a liability?" *Environ. Biol. Fish.*, **18**, 161-172.
- Coutant, C. C. and Whitney, R. R. (2000). "Fish behavior in relation to passage through hydropower turbines: a review." *Transactions of the American Fisheries Society*, **129**, 351-380.
- D'heygere, T., Goethals, P. L. M., and De Pauw, N. (2003). "Use of genetic algorithms to select input variables in decision tree models for the prediction of benthic macroinvertebrates." *Ecological Modelling*, **160**, 291-300.
- Dagorn, L., Menczer, F., Bach, P., and Olson, R. J. (2000). "Co-evolution of movement behaviours by tropical pelagic predatory fishes in response to prey environment: a simulation model." *Ecological Modelling*, **134**, 325-341.
- DeAngelis, D. L. and Cushman, R. M. (1990). "Potential applications of models in forecasting the effects of climate change on fisheries." *Transactions of the American Fisheries Society*, **119**, 224-239.
- Denton, E. J. and Gray, J. A. (1983). "Mechanical factors in the excitation of clupeid lateral lines." *Proceedings of the Royal Society of London, series B*, **218**, 1-26.
- Denton, E. J. and Gray, J. A. (1988). "Mechanical factors in the excitation of the lateral line of fishes." *Sensory Biology of Aquatic Animals*, J. Atema, R. R. Fay, A. N. Popper, and W. N. Tavolga, eds., Springer, New York, NY, 595-617.
- Denton, E. J. and Gray, J. A. (1989). "Some observations on the forces acting on neuromasts in fish lateral line canals." *The Mechanosensory Lateral Line: Neurobiology and Evolution*, S. Coombs, P. Görner, and H. Münz, eds., Springer-Verlag, New York, NY, 229-246.

- Devenport, L. D. and Devenport, J. A. (1994). "Time-dependent averaging of foraging information in least chipmunks and golden-mantled ground squirrels." *Anim. Behav.*, **47**, 787-802.
- Dunning, J. B., Stewart, D. J., Danielson, B. J. N. R., Noon, B. R., Root, T. R., Lamberson, R. H., and Stevens, E. E. (1995). "Spatially explicit population models: current forms and future uses." *Ecological Applications*, **5**, 3-11.
- Ewing, B., Yandell, B. S., Barbieri, J. F., Luck, R. F., and Forster, L. D. (2002). "Event-driven competing risks." *Ecological Modelling*, **158**, 35-50.
- Fagerström, T. (1987). "On theory, data and mathematics in ecology." *Oikos*, **50**(2), 258-261.
- Farnsworth, K. D. and Beecham, J. A. (1999). "How do grazers achieve their distribution? A continuum of models from random diffusion to the ideal free distribution using biased random walks." *The American Naturalist*, **153**(5), 509-526.
- Gaff, H., DeAngelis, D. L., Gross, L. J., Salinas, R., and Shorrosh, M. (2000). "A dynamic landscape model for fish in the Everglades and its application to restoration." *Ecological Modelling*, **127**, 33-52.
- Gerolotto, F., Soria, M., and Frøen, P. (1999). "From two dimensions to three: The use of multi-beam sonar for a new approach to fisheries acoustics." *Canadian Journal of Fisheries and Aquatic Sciences*, **56**(1), 6-12.
- Gevrey, M., Dimopoulos, I., and Lek, S. (2003). "Review and comparison of methods to study the contribution of variables in artificial neural network models." *Ecological Modelling*, **160**, 249-264.
- Ginot, V., Le Page, C., and Souissi, S. (2002). "A multi-agents architecture to enhance end-user individual-based modelling." *Ecological Modelling*, **157**, 23-41.

- Goodwin, R. A., Nestler, J. M., Loucks, D. P., and Chapman, R. S. (2001). "Simulating mobile populations in aquatic ecosystems." *Journal of Water Resources Planning and Management*, **127**(6), 386-393.
- Grimm, V. (1999). "Ten years of individual-based modelling in ecology: what have we learned and what could we learn in the future?" *Ecological Modelling*, **115**, 129-148.
- Grimm, V., Wyszomirski, T., Aikman, D., and Uchmański, J. (1999). "Individual-based modeling and ecological theory: synthesis of a workshop." *Ecological Modelling*, **115**, 275-282.
- Haefner, J. W. and Bowen, M. D. (2002). "Physical-based model of fish movement in fish extraction facilities." *Ecological Modelling*, **152**, 227-245.
- Halle, S. and Halle, B. (1999). "Modelling activity synchronization in free-ranging microtine rodents." *Ecological Modelling*, **115**, 165-176.
- Hanna, R. B., Saito, L., Bartholow, J. M., and Sandelin, J. (1999). "Results of simulated temperature control device operations on in-reservoir and discharge water temperatures using CE-QUAL-W2." *Journal of Lake and Reservoir Management*, **15**(2), 87-102.
- Hanson, P. C., Johnson, T. B., Schindler, D. E., and Kitchell, J. E. (1997). Fish Bioenergetics 3.0, Board of Regents, University of Wisconsin System Sea Grant Institute, Center for Limnology.
- Haro, A., Odeh, M., Noreika, J., and Castro-Santos, T. (1998). "Effect of water acceleration on downstream migratory behavior and passage of Atlantic salmon smolts and juvenile American shad at surface bypasses." *Transactions of the American Fisheries Society*, **127**, 118-127.
- Harte, J. (2002). "Toward a synthesis of the Newtonian and Darwinian worldviews." *Physics Today*, **55**(10), p 29.

- Hastings, A. and Palmer, M. A. (2003). "A bright future for biologists and mathematicians?" *Science*, **299**, 2003-2004.
- Haw, M. (2001). "Stockbrokers may act like sheep." *Nature, Science Update*, January 3, 2001.
- Hills, T. T. and Adler, F. R. (2002). "Time's crooked arrow: optimal foraging and rate-biased time perception." *Animal Behaviour*, **64**, 589-597.
- Hinckley, S., Hermann, A. J., and Megrey, B. A. (1996). "Development of a spatially explicit, individual-based model of marine fish early life history." *Marine Ecology Progress Series*, **139**, 47-68.
- Hinrichsen, H.-H., Möllmann, C., Voss, R., Köster, F. W., and Kornilovs, G. (2002). "Biophysical modeling of larval Baltic cod (*Gadus morhua*) growth and survival." *Canadian Journal of Fisheries and Aquatic Sciences*, **59**, 1858-1873.
- Hirvonen, H., Ranta, E., Rita, H., and Peuhkuri, N. (1999). "Significance of memory properties in prey choice decisions." *Ecological Modelling*, **115**, 177-189.
- Holland, J. H. (2003). Keynote Address. Seventh Annual Swarm Users/Researchers Conference, SwarmFest 2003, McKenna Hall, Notre Dame, Indiana, USA, April 13-15, 2003.
- Husko, A., Vuorimies, O., and Sutela, T. (1996). "Temperature- and light-mediated predation by perch on vendace larvae." *Journal of Fish Biology*, **49**, 441-457.
- Huth, A. and Wissel, C. (1994). "The simulation of fish schools in comparison with experimental data." *Ecological Modelling*, **75/76**, 135-145.
- Huth, A. and Wissel, C. (1992). "The simulation of the movement of fish shoals." *Journal of Theoretical Biology*, **156**, 365-385.

- Ijspeert, A. J. and Kodjabachian, J. (1999). "Evolution and development of a central pattern generator for the swimming of a lamprey." *Artificial Life*, **5**, 247-269.
- Jager, H. I. and Rose, K. A. (2003). "Designing optimal flow patterns for fall Chinook salmon in a Central Valley, California, river." *North American Journal of Fisheries Management*, **23**, 1-21.
- Johnson, R. L., Anglea, S. M., Blanton, S. L., Simmons, M. A., Moursund, R. A., Johnson, G. E., Kudrea, E. A., Thomas, J., and Skalsik, J. R. (1999). Hydro-acoustic Evaluation of Fish Passage and Behavior at Lower Granite Dam in Spring 1998. Final Report prepared for U.S. Army Engineer District, Walla Walla by Battelle Pacific Northwest National Laboratories, Richland, WA.
- Jones, S. C., Gilmanov, A. N., Paik, J., Sotiropoulos, F., and Sale, M. J. (2002). "Modeling the passage of fish through hydropower facilities." *Proceedings of the Bioengineering Symposium, American Fisheries Society Annual Conference*, Baltimore, Maryland, August 21, 2002.
- Kacelnik, A., Krebs, J. R., and Ens, B. (1987). Foraging in a changing environment: an experiment with starlings (*Sturnus vulgaris*). In: Commons, M. L., Shettleworth, S. J., and Kacelnik, A. (eds.), Quantitative analyses of behaviour, vol. 6, Foraging, Lawrence Erlbaum Associates, Publishers, Hillsdale, pp. 63-87.
- Kalmijn, A. J. (2000). "Detection and processing of electromagnetic and near-field acoustic signals in elasmobranch fishes." *Philosophical Transactions of The Royal Society of London series B*, **355**(1401), 1135-1141.
- Kalmijn, A. J. (1989). "Functional evolution of lateral line and inner-ear sensory systems." *The Mechanosensory Lateral Line: Neurobiology and Evolution*, S. Coombs, P. Görner, and H. Münz, eds., Springer-Verlag, New York, NY, 187-215.

- Kalmijn, A. J. (1988). "Hydrodynamic and acoustic field detection." *Sensory Biology of Aquatic Animals*, J. Atema, R. R. Fay, A. N. Popper, and W. N. Tavolga, eds., Springer, New York, NY, 83-130.
- Karim, M. R., Sekine, M., Higuchi, T., Imai, T., and Ukita, M. (2003). "Simulation of fish behavior and mortality in hypoxic water in an enclosed bay." *Ecological Modelling*, **159**, 27-42.
- Kondolf, G. M., Larsen, E. W., and Williams, J. G. (2000). "Measuring and modeling the hydraulic environment for assessing instream flows." *North American Journal of Fisheries Management*, **20**, 1016-1028.
- Kröther, S., Mogdans, J., and Bleckmann, H. (2002). "Brainstem lateral line responses to sinusoidal wave stimuli in still and running water." *Journal of Experimental Biology*, **205**, 1471-1484.
- Lai, Y. G., Weber, L. J., and Patel, V. C. (2003a). "Nonhydrostatic three-dimensional model for hydraulic flow simulation. I: Formulation and Verification." *ASCE Journal of Hydraulic Engineering*, **129**(3), 196-205.
- Lai, Y. G., Weber, L. J., and Patel, V. C. (2003b). "Nonhydrostatic three-dimensional model for hydraulic flow simulation. II: Validation and Application." *ASCE Journal of Hydraulic Engineering*, **129**(3), 206-214.
- Lai, Y. G. (2000). "Unstructured grid arbitrarily shaped element method for fluid flow simulation." *AIAA Journal*, **38**(12), 2246-2252.
- Larinier, M. and Boyer-Bernard, S. (1991). "Dévalaison des smolts et efficacité d'un exutoire de dévalaison à l'usine hydroélectrique d'Halsou sur la Nive." *Bulletin Français de la Pêche et de la Pisciculture*, **321**, 72-92.
- Loucks, D. P., Stedinger, J. R., and Haith, D. A. (1981). *Water Resource Systems Planning and Analysis*, Prentice-Hall, Englewood Cliffs, NJ.

- Lucas, M. C. and Baras, E. (2000). "Methods for studying spatial behaviour of freshwater fishes in the natural environment." *Fish and Fisheries*, **1**, 283-316.
- Luna, F. and Perrone, A., eds. (2001). Agent-Based Methods in Economics and Finance: Simulations in Swarm. Book Series: ADVANCES IN COMPUTATIONAL ECONOMICS, Volume 17, Hans Amman and Anna Nagurney, Kluwer Academic Publishers.
- Marsh, L. M. and Jones, R. E. (1988). "The form and consequences of random walk movement models." *Journal of Theoretical Biology*, **133**, 113-131.
- McFarland, D. and Houston, A. (1981). Quantitative Ethology: The State Space Approach, Pitman Advanced Publ. Program, Boston, MA.
- Minar, H., Burkhart, R., Langton, C., and Askenazi, M. (1996). The SWARM simulation system: a toolkit for building multiagent simulations. Santa Fe Institute Working Paper 96-06-042.
- Monte, L. (2002). "A methodology for modelling the contamination of moving organisms in water bodies with spatial and time dependent pollution levels." *Ecological Modelling*, **158**, 21-33.
- Montgomery, J. C., Carton, A. G., Voigt, R., Baker, C. F., and Diebel, C. (2000). "Sensory processing of water currents by fishes." *Philosophical Transactions of The Royal Society of London series B*, **355**(1401), 1325-1327.
- Montgomery, J. C., Coombs, S., and Halstead, M. (1995). "Biology of the mechanosensory lateral line in fishes." *Reviews in Fish Biology and Fisheries*, **5**, 399-416.
- Nestler, J. M. and Goodwin, R. A. (in review). "Eulerian-Lagrangian coupling of engineering and biological models." Accepted for publication by *Journal of Water Resources Planning and Management*.

- Nestler, J. M., Goodwin, R. A., Cole, T., Degan, D. and Dennerline, D. (2002).
“Simulating movement patterns of blueback herring in a stratified southern
impoundment.” *Transactions of the American Fisheries Society*, **131**, 55-69.
- New, J. G., Fewkes, L. A., and Khan, A. N. (2001). “Strike feeding behavior in the
muskellunge, *Esox masquinongy*: contributions of the lateral line and visual
sensory systems.” *Journal of Experimental Biology*, **204**, 1207-1221.
- New, J. G. and Kang, P. Y. (2000). “Multimodal sensory integration in the strike-
feeding behaviour of predatory fishes.” *Philosophical Transactions of The
Royal Society of London series B*, **355**(1401), 1321-1324.
- Niwa, H. S. (1994). “Self-organizing dynamic model of fish schooling.” *Journal of
Theoretical Biology*, **171**, 123-136.
- Nonacs, P., Smith, P. E., Bouskila, A., and Luttbeg, B. (1994). “Modeling the
behavior of the northern anchovy, *Engraulis mordax*, as a schooling predator
exploiting patchy prey.” *Deep-Sea Research II*, **41**(1), Elsevier Science Ltd,
Great Britain, 147-169.
- Nowak, G. M. and Quinn, T. P. (2002). “Diel and seasonal patterns of horizontal
and vertical movements of telemetered cutthroat trout in Lake Washington,
Washington.” *Transactions of the American Fisheries Society*, **131**, 452-462.
- Okubo, A. (1980). *Diffusion and Ecological Problems: Mathematical Models*,
Lecture Notes in Biomathematics, Vol. 10, Springer-Verlag, New York, NY,
p.254.
- Olden, J. D. and Jackson, D. A. (2002). “Illuminating the ‘black box’: a
randomization approach for understanding variable contributions in artificial
neural networks.” *Ecological Modelling*, **154**, 135-150.
- Parrish, J. K. and Edelstein-Keshet, L. (1999). “Complexity, pattern, and
evolutionary trade-offs in animal aggregation.” *Science*, **284**, 99-101.

- Parrish, J. K. and Turchin, P. (1997). "Individual decisions, traffic rules, and emergent pattern in schooling fish." *Animal Groups in Three Dimensions*, J. K. Parrish and W. M. Hamner, eds., Cambridge University Press, New York, NY, 126-142.
- Pavlov, D. S. (1994). "The downstream migration of young fishes in rivers: mechanisms and distribution." *Folia Zoologica*, **43**, 193-208.
- Paxton, J. R. (2000). "Fish otoliths: do sizes correlate with taxonomic group, habitat and/or luminescence?" *Philosophical Transactions of The Royal Society of London series B*, **355**(1401), 1299-1303.
- Pelletier, D. and Parma, A. M. (1994). "Spatial distribution of Pacific halibut (*Hippoglossus stenolepis*): an application of geostatistics to longline survey data." *Canadian Journal of Fisheries and Aquatic Sciences*, **51**, 1506-1518.
- Petersen, J. H. and DeAngelis, D. L. (2000). "Dynamics of prey moving through a predator field: a model of migrating juvenile salmon." *Mathematical Biosciences*, **165**, 97-114.
- Pientka, B. and Parrish, D. L. (2002). "Habitat selection of predator and prey: Atlantic salmon and rainbow smelt overlap, based on temperature and dissolved oxygen." *Transactions of the American Fisheries Society*, **131**, 1180-1193.
- Popper, A. N. and Carlson, T. J. (1998). "Application of sound and other stimuli to control fish behavior." *Transactions of the American Fisheries Society*, **127**, 673-707.
- Prairie, Y. T. (1996). "Evaluating the predictive power of regression models." *Canadian Journal of Fisheries and Aquatic Sciences*, **53**, 490-492.
- Railsback, S. (1999). "Reducing uncertainties in instream flow studies." *Fisheries*, **24**(4), 24-26.

- Railsback, S. F., Lamberson, R. H., Harvey, B. C., and Duffy, W. E. (1999a). "Movement rules for individual-based models of stream fish." *Ecological Modelling*, **123**, 73-89.
- Railsback, S. F., Lamberson, R. H., and Jackson, S. (1999b). "Individual-based Models: Progress Toward Viability for Fisheries Management." Presentation at Spatial Processes and Management of Fish Populations, 17th Lowell Wakefield Symposium, Anchorage, Alaska.
- Rapoport, A. (1983). *Mathematical models in social and behavioral sciences*. John Wiley & Sons, Inc., New York, NY, 507 pp.
- Reese, C. D. and Harvey, B. C. (2002). "Temperature-dependent interactions between juvenile steelhead and Sacramento pikeminnow in laboratory streams." *Transactions of the American Fisheries Society*, **131**, 599-606.
- Reuter, H. and Breckling, B. (1994). "Selforganization of fish schools: an object-oriented model." *Ecological Modelling*, **75/76**, 147-159.
- Romey, W. L. (1996). "Individual differences make a difference in the trajectories of simulated schools of fish." *Ecological Modelling*, **92**, 65-77.
- Rogers, P. H. and Cox, M. (1988). "Underwater sound as a biological stimulus" *Sensory Biology of Aquatic Animals*, J. Atema, R. R. Fay, A. N. Popper, and W. N. Tavolga, eds., Springer, New York, NY, 131-149.
- Scheibe, T. D. and Richmond, M. C. (2002). "Fish individual-based numerical simulator (FINS): a particle-based model of juvenile salmonid movement and dissolved gas exposure history in the Columbia River basin." *Ecological Modelling*, **147**, 233-252.
- Schilt, C. R. and Nestler, J. M. (1997). "Fish bioacoustics: considerations for hydropower industry workers." *Proceedings of the International Conference on Hydropower*, August 5-8, Atlanta, GA.

- Schilt, C. R. and Norris, K. S. (1997). "Perspectives on sensory integration systems: Problems, opportunities, and predictions." *Animal Groups in Three Dimensions*, J. K. Parrish and W. M. Hamner, eds., Cambridge University Press, New York, NY, 225-244.
- Schindler, D. E. and Eby, L. A. (1997). "Stoichiometry of fishes and their prey: implications for nutrient recycling." *Ecology*, **78**(6), 1816-1831.
- Schmalz, P. J., Hansen, M. J., Holey, M. E., McKee, P. C., and Toney, M. L. (2002). "Lake Trout movements in northwestern Lake Michigan." *North American Journal of Fisheries Management*, **22**, 737-749.
- Smith, S. G., Muir, W. D., Williams, J. G., and Skalski, J. R. (2002). "Factors associated with travel time and survival of migrant yearling Chinook salmon and Steelhead in the lower Snake River." *North American Journal of Fisheries Management*, **22**, 385-405.
- Sogard, S. M. and Olla, B. L. (1993). "Effects of light, thermoclines and predator presence on vertical distribution and behavioral interactions of juvenile walleye pollock, *Theragra chalcogramma* Pallas." *Journal of Exp. Mar. Biol. Ecol.*, **167**, 179-195.
- Sotiropoulos, F. (in press). Progress in modeling 3D shear flows using RANS equations and advanced turbulence models. In: *Calculation of Complex Turbulent Flows*. WIT Press, Southampton, United Kingdom.
- Standen, E. M., Hinch, S. G., Healey, M. C., and Farrell, A. P. (2002). "Energetic costs of migration through the Fraser River Canyon, British Columbia, in adult pink (*Oncorhynchus gorbuscha*) and sockeye (*Oncorhynchus nerka*) salmon as assessed by EMG telemetry." *Canadian Journal of Fisheries and Aquatic Sciences*, **59**, 1809-1818.

- Stedinger, J. R. (2000). The use of risk and uncertainty analyses within the US Army Corps of Engineers Civil Works Programs. Prepared for USACE Institute for Water Resources by Cornell University, Ithaca, NY.
- Steel, E. A., Guttorp, P., Anderson, J. J., and Caccia, D. C. (2001). "Modeling juvenile migration using a simple Markov chain." *Journal of Agricultural, Biological, and Environmental Statistics*, **6**(1), 80-88.
- Steig, T. W. (1999). "The use of acoustic tags to monitor the movement of juvenile salmonids approaching a dam on the Columbia River." Proceedings of the 15th International Symposium on Biotelemetry, Juneau, Alaska, 9-14, May, 1999.
- Steig, T. W. and Johnson, W. R. (1986). "Hydroacoustic assessment of downstream migrating salmonids at The Dalles Dam in spring and summer 1985" Final Report DOE/BP-23174-2, U.S. Department of Energy, Bonneville Power Administration, Portland, OR.
- Stockwell, J. D. and Johnson, B. M. (1997). "Refinement and calibration of a bioenergetics-based foraging model for kokanee (*Oncorhynchus nerka*)." *Canadian Journal of Fisheries and Aquatic Sciences*, **54**(11), 2659-2676.
- Terzopoulos, D., Tu, X., and Grezeszczuk, R. (1995). "Artificial fishes: autonomous locomotion, perception, behavior, and learning in a simulated physical world." *Artificial Life*, **1**, 327-351.
- Tischendorf, L. (1997). "Modelling individual movements in heterogeneous landscapes: potentials of a new approach." *Ecological Modelling*, **103**, 33-42.
- Turchin, P. (1997). "Quantitative analysis of animal movements in congregations." *Animal Groups in Three Dimensions*, J. K. Parrish and W. M. Hamner, eds., Cambridge University Press, New York, NY, 107-112.

- van Nes, E. H., Lammens, E. H. R. R., and Scheffer, M. (2002). "PISCATOR, an individual-based model to analyze the dynamics of lake fish communities." *Ecological Modelling*, **152**, 261-278.
- Van Winkle, W., Rose, K. A., and Chambers, R. C. (1993). "Individual-based approach to fish population dynamics: An overview." *Transactions of the American Fisheries Society*, **122**, 397-403.
- Van Winkle, W., Jager, H. I., Railsback, S. F., Holcomb, B. D., Studley, T. K., and Baldrige, J. E. (1998). "Individual-based model for sympatric populations of brown and rainbow trout for instream flow assessment: model description and calibration." *Ecological Modelling*, **110**, 175-207.
- Venditti, D. A., Rondorf, D. W., and Kraut, J. M. (2000). "Migratory behavior, and forebay delay of radio-tagged juvenile fall chinook salmon in a lower Snake River impoundment." *North American Journal of Fisheries Management*, **20**, 41-52.
- Whitfield, J. (2001). "Ant group dynamics." *Nature, Science Update*, July 19, 2001.
- Workman, R. D., Hayes, D. B., and Coon, T. G. (2002). "A model of steelhead movement in relation to water temperature in two Lake Michigan tributaries." *Transactions of the American Fisheries Society*, **131**, 463-475.
- Wu, H., Li, B.-L., Springer, T. A., and Neill, W. H. (2000). "Modelling animal movement as a persistent random walk in two dimensions: expected magnitude of net displacement." *Ecological Modelling*, **132**, 115-124.
- Xiao, Y. (2000). "An individual-based approach to evaluating experimental designs for estimating rates of fish movement from tag recoveries." *Ecological Modelling*, **128**, 149-163.

APPENDIX A

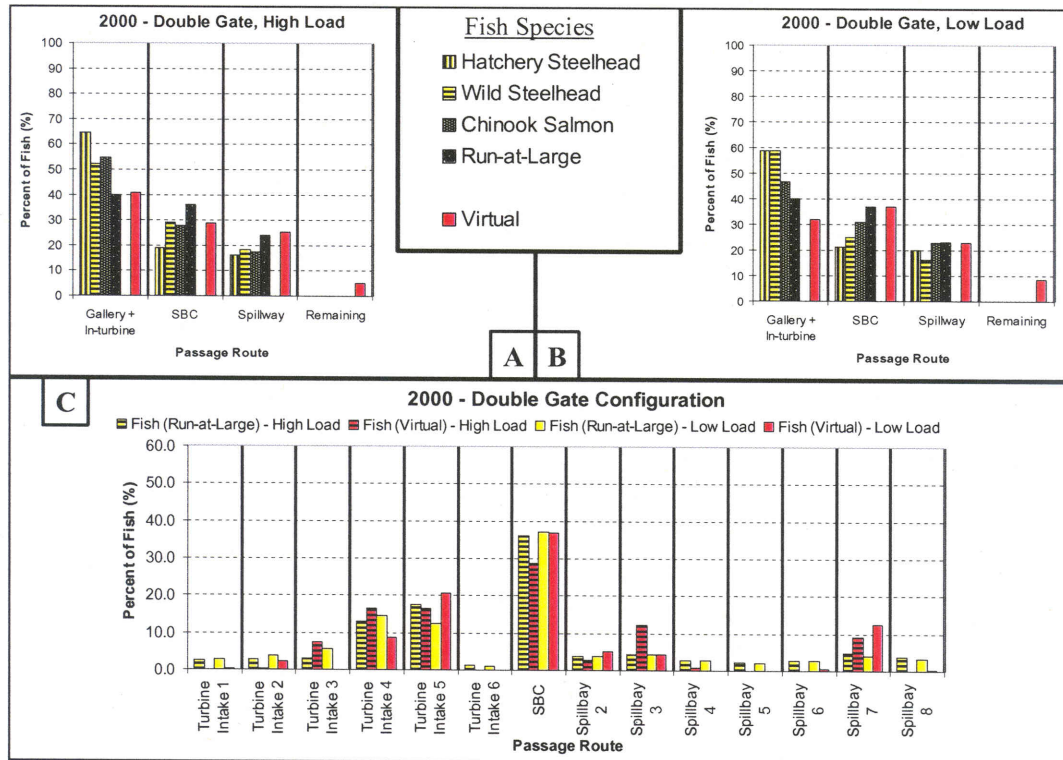


Figure A.1. Fish passage estimates for double gate SBC configuration at Lower Granite Dam in 2000. Species-specific passage estimates for high and low powerhouse loads in Plots A and B, respectively, provided by radio-tag instrumentation (Plumb et al., 2002). Multi-beam hydroacoustic (HA), or run-at-large, passage data provided by Anglea et al. (2001). HA and virtual fish passage estimates for both double gate SBC flow scenarios in Plot C.

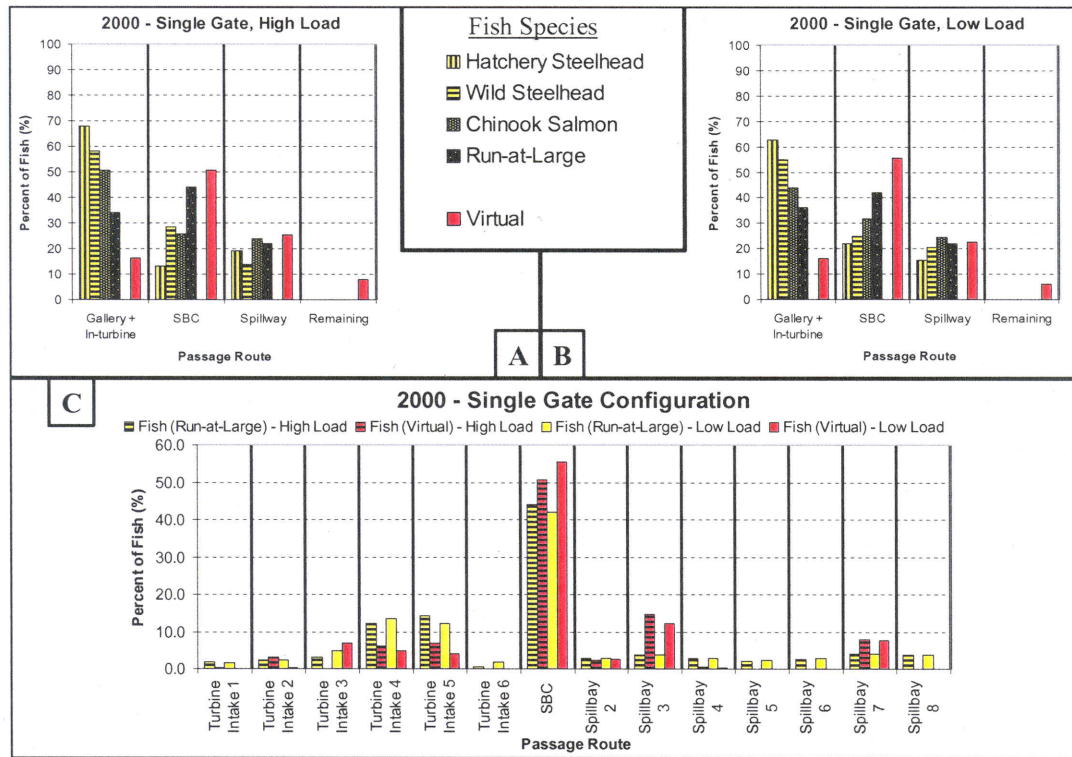


Figure A.2. Fish passage estimates for single gate SBC configuration at Lower Granite Dam in 2000. Species-specific passage estimates for high and low powerhouse loads in Plots A and B, respectively, provided by radio-tag instrumentation (Plumb et al., 2002). Multi-beam hydroacoustic (HA), or run-at-large, passage data provided by Anglea et al. (2001). HA and virtual fish passage estimates for both single gate SBC flow scenarios in Plot C.

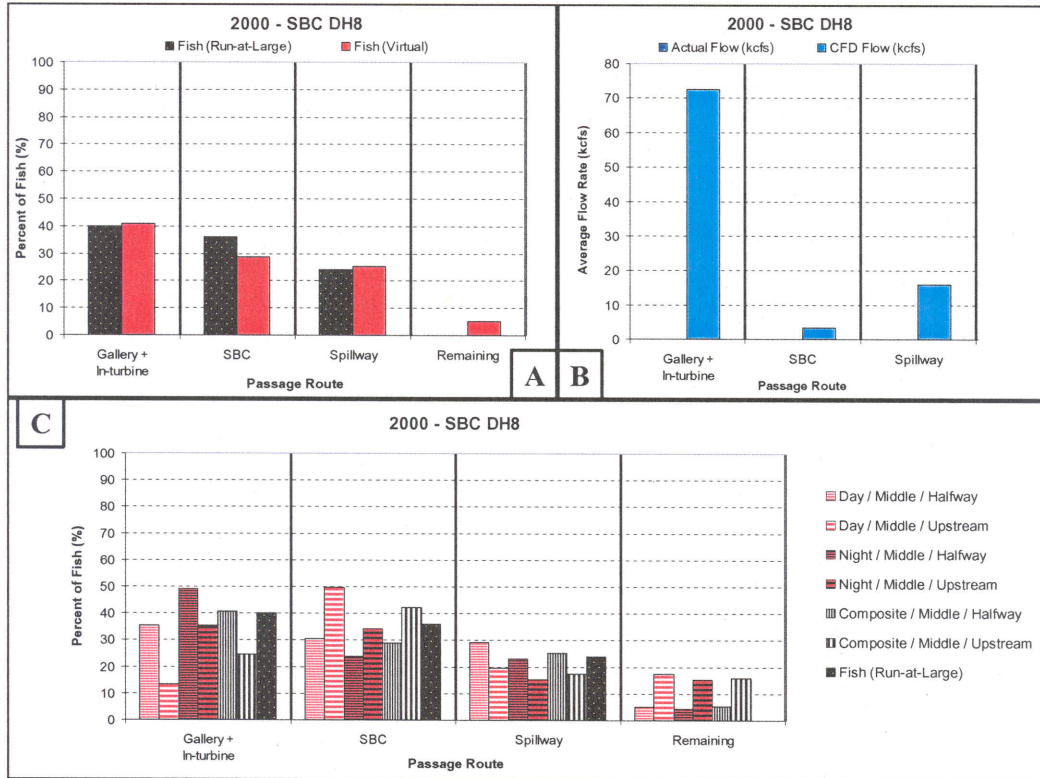


Figure A.3. Hydroacoustic (HA), or run-at-large, and virtual fish passage estimates (Plot A), CFD modeled flow rates through the powerhouse, the two SBC orifices, and the spillway (Plot B), and sensitivity analyses of release locations (Plot C) for case DH8 in 2000. Multi-beam hydroacoustic (HA), or run-at-large, passage data provided by Anglea et al. (2001). DH8 was the only case data set used to calibrate the CEL Agent IBM coefficients. Data on actual flow rates through various passage routes are not available for 2000 studies. CFD modeled flow rates reflect the target flow operating conditions. In 2000, it was generally observed, however, that actual flow rates were in relatively close agreement with target flow operating conditions, more so than for 2002 studies.

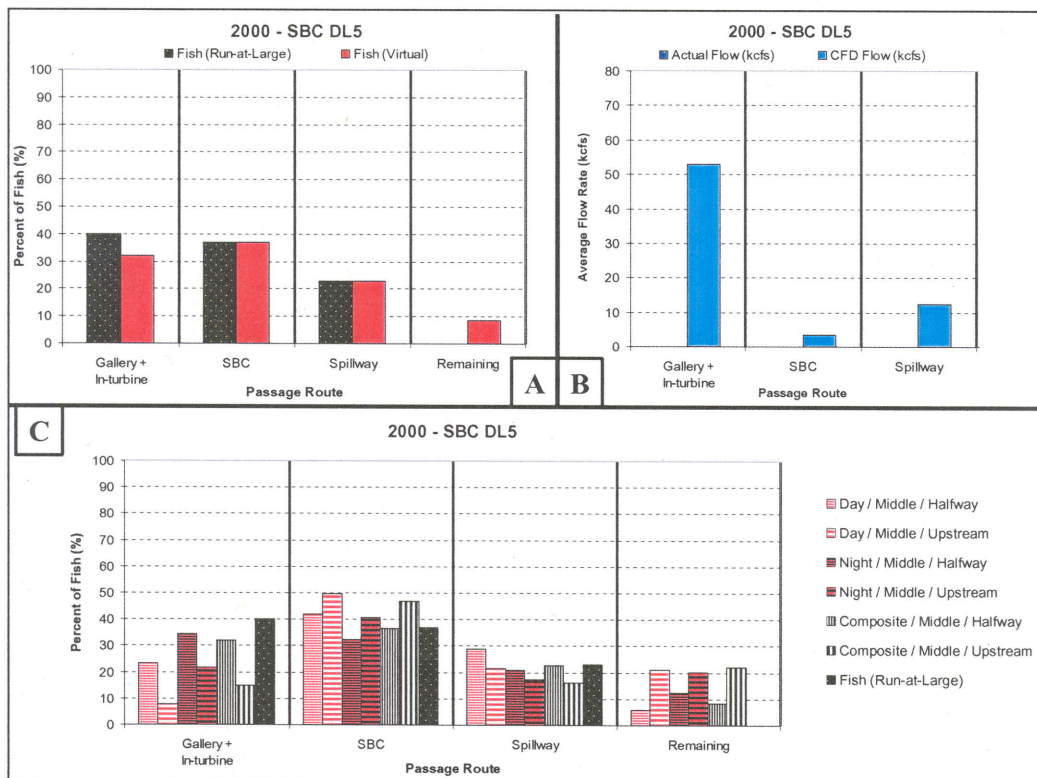


Figure A.4. Hydroacoustic (HA), or run-at-large, and virtual fish passage estimates (Plot A), CFD modeled flow rates through the powerhouse, the two SBC orifices, and the spillway (Plot B), and sensitivity analyses of release locations (Plot C) for case DL5 in 2000. Multi-beam hydroacoustic (HA), or run-at-large, passage data provided by Anglea et al. (2001). Data on actual flow rates through various passage routes are not available for 2000 studies. CFD modeled flow rates reflect the target flow operating conditions. In 2000, it was generally observed, however, that actual flow rates were in relatively close agreement with target flow operating conditions, more so than for 2002 studies.

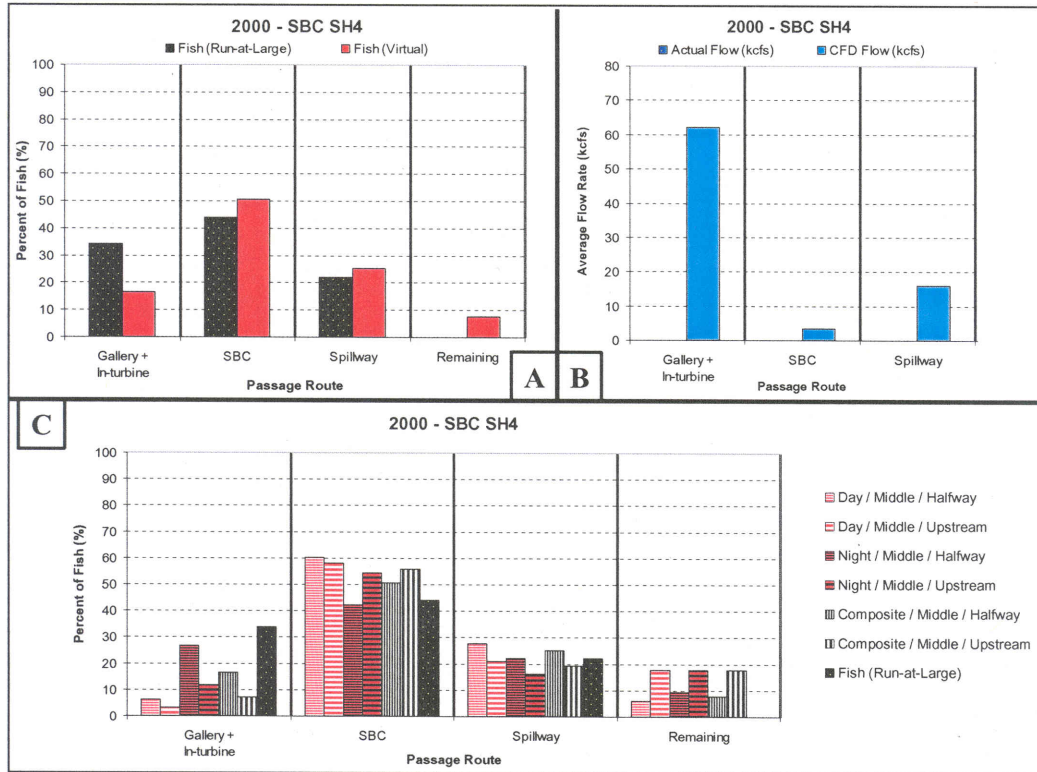


Figure A.5. Hydroacoustic (HA), or run-at-large, and virtual fish passage estimates (Plot A), CFD modeled flow rates through the powerhouse, the single SBC orifice, and the spillway (Plot B), and sensitivity analyses of release locations (Plot C) for case SH4 in 2000. Multi-beam hydroacoustic (HA), or run-at-large, passage data provided by Anglea et al. (2001). Data on actual flow rates through various passage routes are not available for 2000 studies. CFD modeled flow rates reflect the target flow operating conditions. In 2000, it was generally observed, however, that actual flow rates were in relatively close agreement with target flow operating conditions, more so than for 2002 studies. Note that a night release of virtual fish from the same location upstream (~800m) as the virtual fish released for the composite run in Plot A results in virtual fish passage estimates even closer to the HA, or run-at-large, estimate.

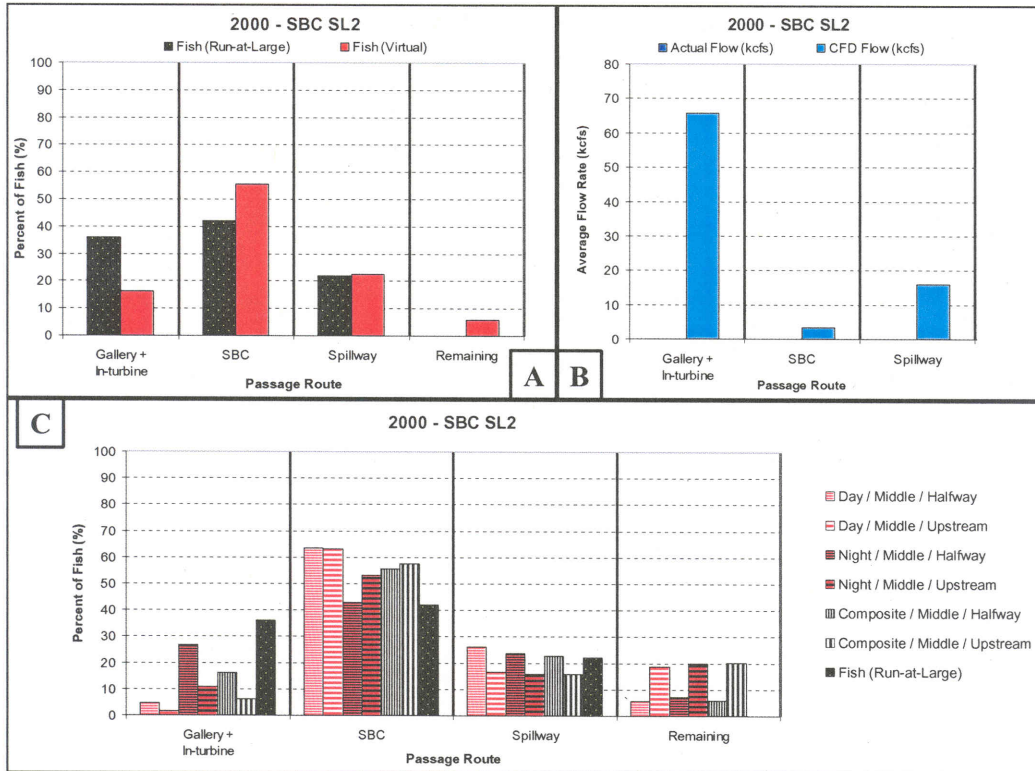


Figure A.6. Hydroacoustic (HA), or run-at-large, and virtual fish passage estimates (Plot A), CFD modeled flow rates through the powerhouse, the single SBC orifice, and the spillway (Plot B), and sensitivity analyses of release locations (Plot C) for case SL2 in 2000. Multi-beam hydroacoustic (HA), or run-at-large, passage data provided by Anglea et al. (2001). Data on actual flow rates through various passage routes are not available for 2000 studies. CFD modeled flow rates reflect the target flow operating conditions. In 2000, it was generally observed, however, that actual flow rates were in relatively close agreement with target flow operating conditions, more so than for 2002 studies. Note that a night release of virtual fish from the same location upstream (~800m) as the virtual fish released for the composite run in Plot A results in virtual fish passage estimates even closer to the HA, or run-at-large, estimate.

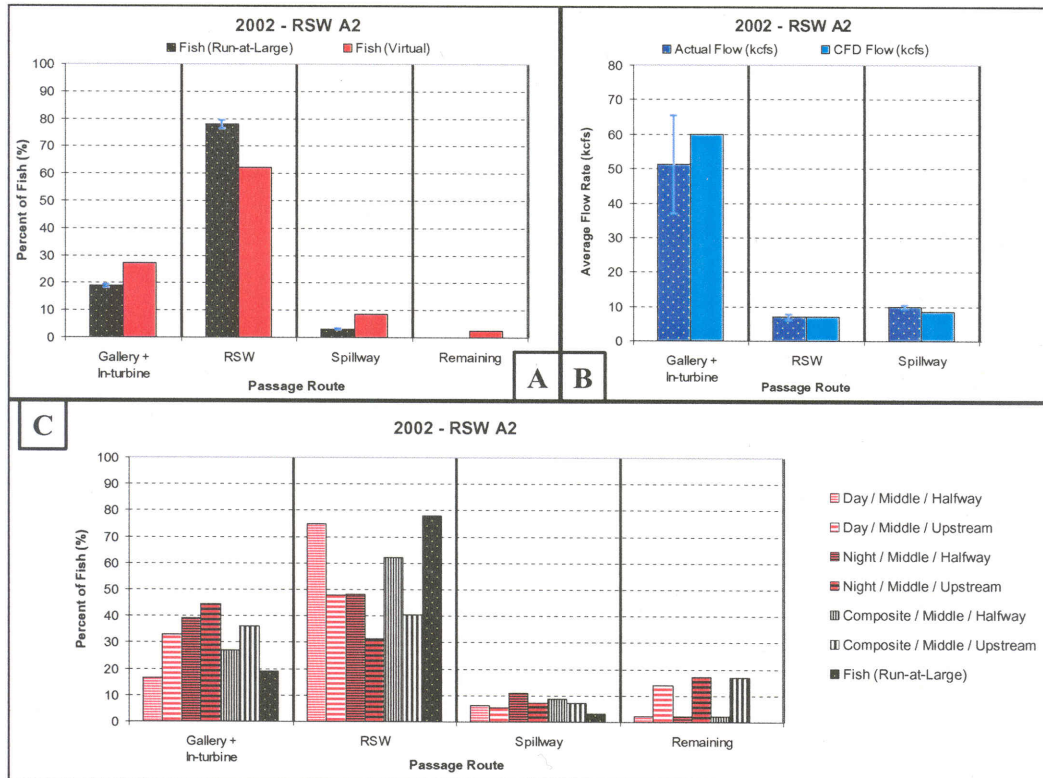


Figure A.7. Hydroacoustic (HA), or run-at-large, and virtual fish passage estimates (Plot A), flow rates through the powerhouse, RSW, and spillway (Plot B), and sensitivity analyses of release locations (Plot C) for case A2 in 2002. HA passage estimates and actual flow rates (mean and standard deviation, Plot B) provided by Anglea *et al.* (2003). CFD modeled flow rates reflect the target flow operating condition and were simulated before HA data on actual flow rates was available. Error bars in Plot A represent the 95% confidence interval (CI) of the HA, or run-at-large, fish passage estimates and in Plot B represent one standard deviation of the time-varying (actual) flow rate. Note that a day release of virtual fish from the same location upstream (~800m) as the virtual fish released for the composite run in Plot A results in virtual fish passage estimates even closer to the HA, or run-at-large, estimate.

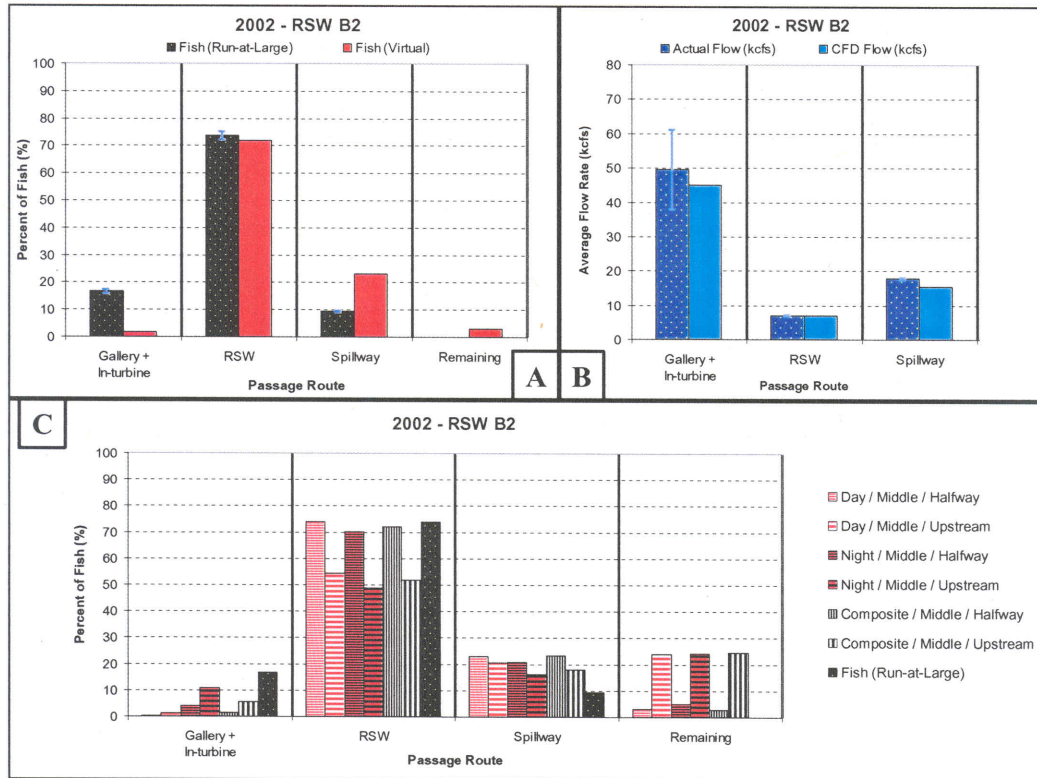


Figure A.8. Hydroacoustic (HA), or run-at-large, and virtual fish passage estimates (Plot A), flow rates through the powerhouse, RSW, and spillway (Plot B), and sensitivity analyses of release locations (Plot C) for case B2 in 2002. HA passage estimates and actual flow rates (mean and standard deviation, Plot B) provided by Anglea *et al.* (2003). CFD modeled flow rates reflect the target flow operating condition and were simulated before HA data on actual flow rates was available. Error bars in Plot A represent the 95% confidence interval (CI) of the HA, or run-at-large, fish passage estimates and in Plot B represent one standard deviation of the time-varying (actual) flow rate.

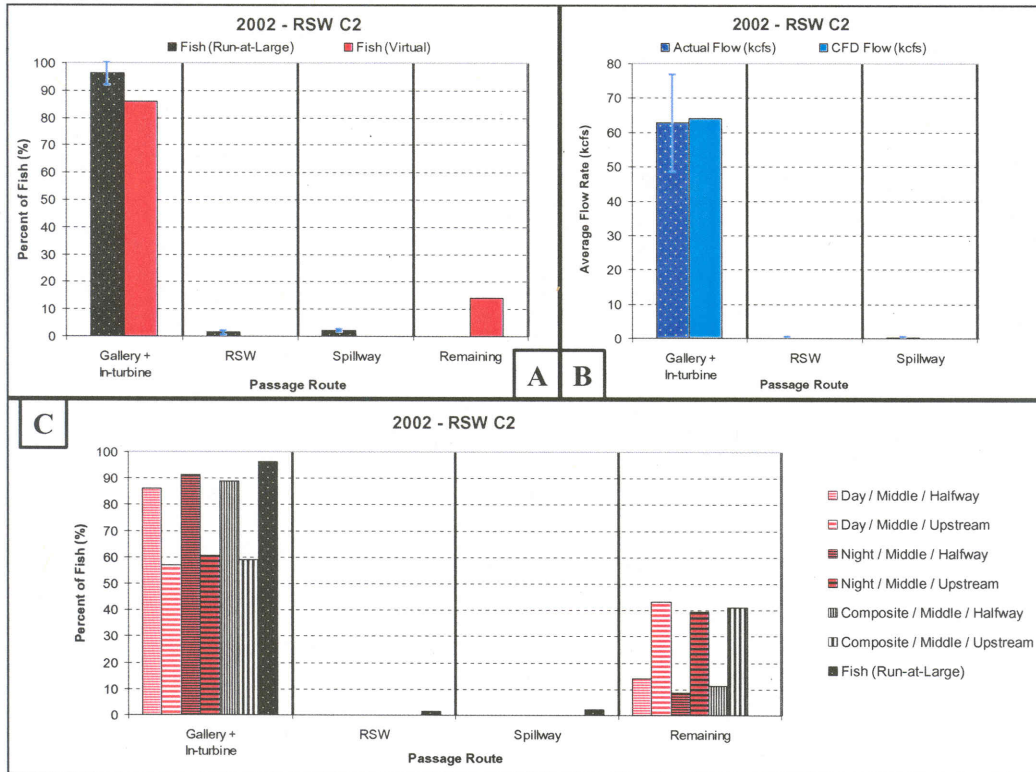


Figure A.9. Hydroacoustic (HA), or run-at-large, and virtual fish passage estimates (Plot A), flow rates through the powerhouse, RSW, and spillway (Plot B), and sensitivity analyses of release locations (Plot C) for case C2 in 2002. HA passage estimates and actual flow rates (mean and standard deviation, Plot B) provided by Anglea *et al.* (2003). CFD modeled flow rates reflect the target flow operating condition and were simulated before HA data on actual flow rates was available. Error bars in Plot A represent the 95% confidence interval (CI) of the HA, or run-at-large, fish passage estimates and in Plot B represent one standard deviation of the time-varying (actual) flow rate.

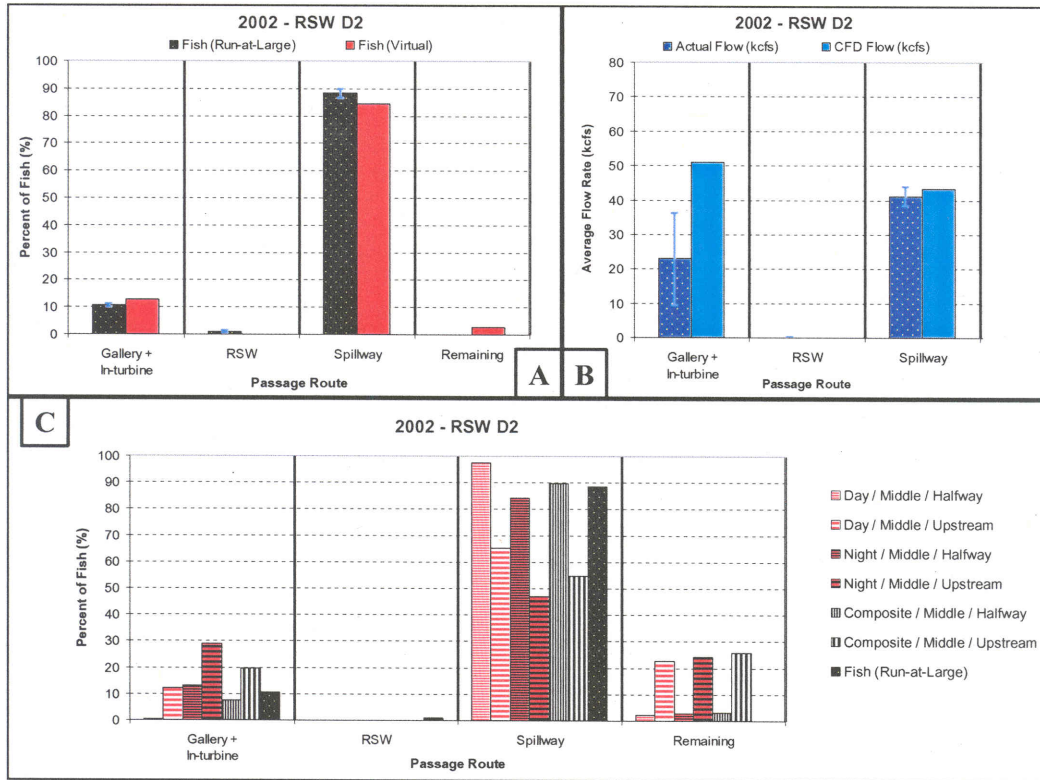


Figure A.10. Hydroacoustic (HA), or run-at-large, and virtual fish passage estimates (Plot A), flow rates through the powerhouse, RSW, and spillway (Plot B), and sensitivity analyses of release locations (Plot C) for case D2 in 2002. HA passage estimates and actual flow rates (mean and standard deviation, Plot B) provided by Anglea *et al.* (2003). CFD modeled flow rates reflect the target flow operating condition and were simulated before HA data on actual flow rates was available. Error bars in Plot A represent the 95% confidence interval (CI) of the HA, or run-at-large, fish passage estimates and in Plot B represent one standard deviation of the time-varying (actual) flow rate.

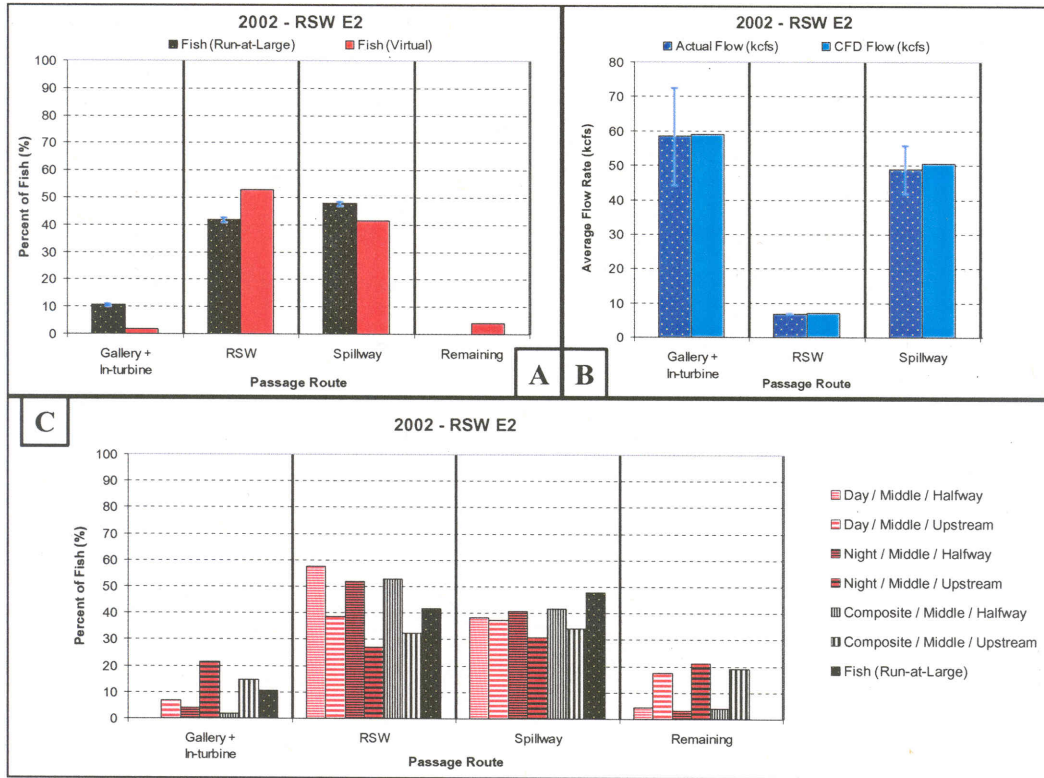


Figure A.11. Hydroacoustic (HA), or run-at-large, and virtual fish passage estimates (Plot A), flow rates through the powerhouse, RSW, and spillway (Plot B), and sensitivity analyses of release locations (Plot C) for case E2 in 2002. HA passage estimates and actual flow rates (mean and standard deviation, Plot B) provided by Anglea *et al.* (2003). CFD modeled flow rates reflect the target flow operating condition and were simulated before HA data on actual flow rates was available. Error bars in Plot A represent the 95% confidence interval (CI) of the HA, or run-at-large, fish passage estimates and in Plot B represent one standard deviation of the time-varying (actual) flow rate.

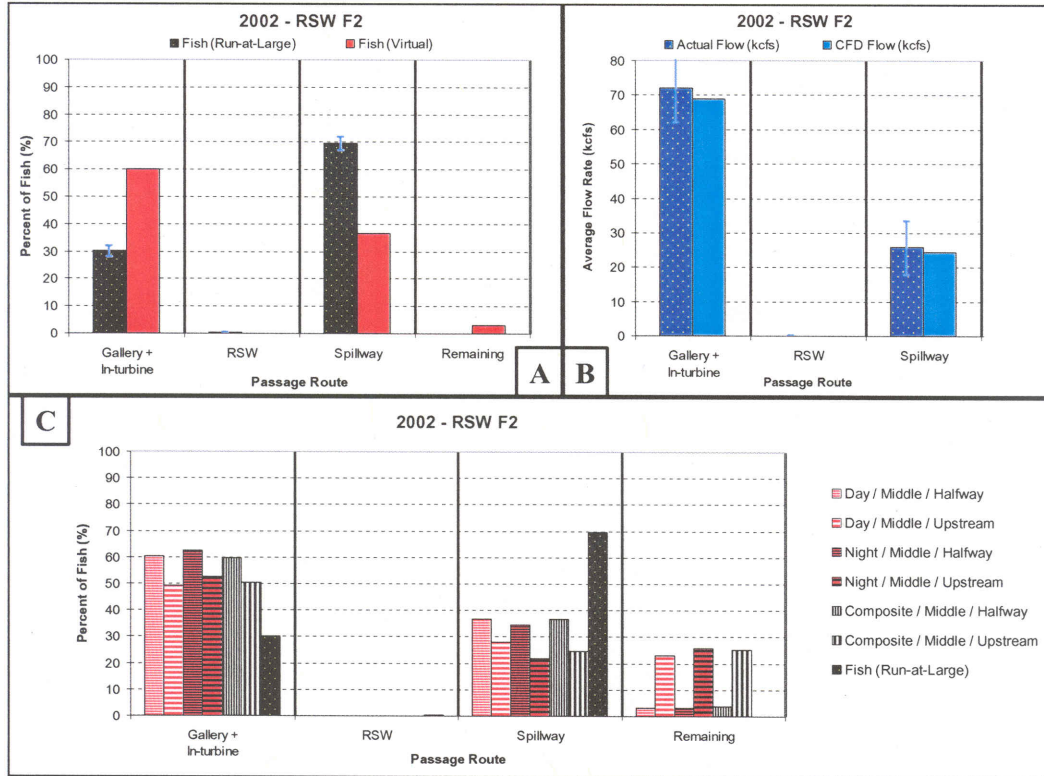


Figure A.12. Hydroacoustic (HA), or run-at-large, and virtual fish passage estimates (Plot A), flow rates through the powerhouse, RSW, and spillway (Plot B), and sensitivity analyses of release locations (Plot C) for case F2 in 2002. HA passage estimates and actual flow rates (mean and standard deviation, Plot B) provided by Anglea *et al.* (2003). CFD modeled flow rates reflect the target flow operating condition and were simulated before HA data on actual flow rates was available. Error bars in Plot A represent the 95% confidence interval (CI) of the HA, or run-at-large, fish passage estimates and in Plot B represent one standard deviation of the time-varying (actual) flow rate.

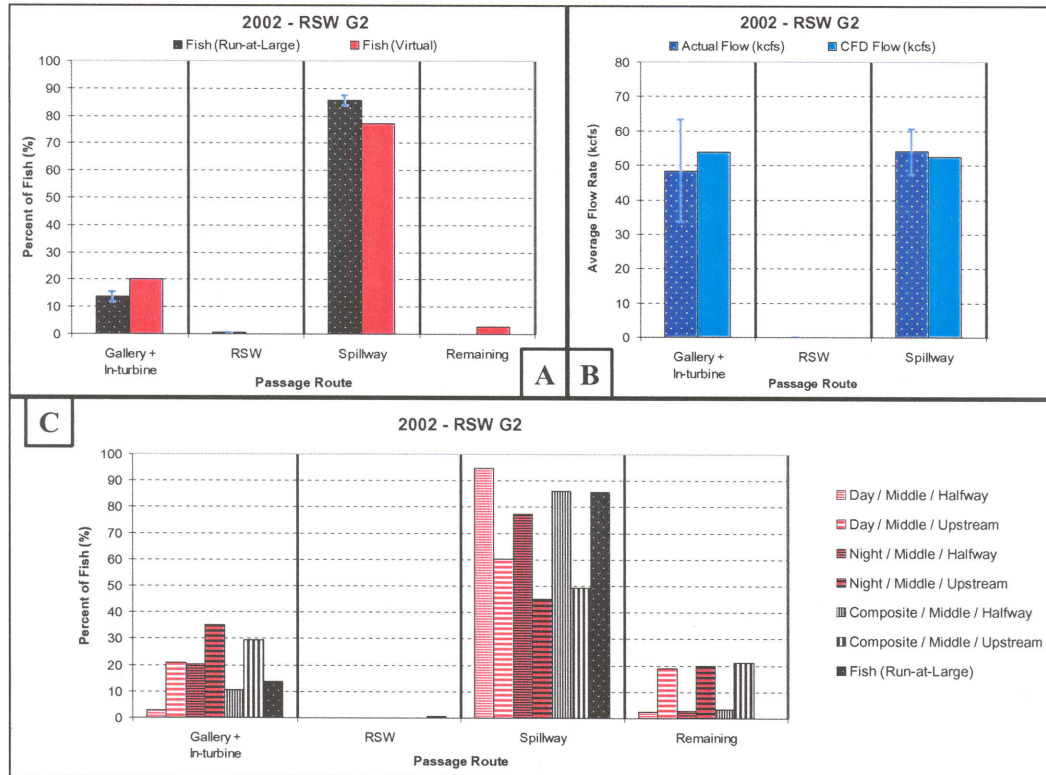


Figure A.13. Hydroacoustic (HA), or run-at-large, and virtual fish passage estimates (Plot A), flow rates through the powerhouse, RSW, and spillway (Plot B), and sensitivity analyses of release locations (Plot C) for case G2 in 2002. HA passage estimates and actual flow rates (mean and standard deviation, Plot B) provided by Anglea *et al.* (2003). CFD modeled flow rates reflect the target flow operating condition and were simulated before HA data on actual flow rates was available. Error bars in Plot A represent the 95% confidence interval (CI) of the HA, or run-at-large, fish passage estimates and in Plot B represent one standard deviation of the time-varying (actual) flow rate.

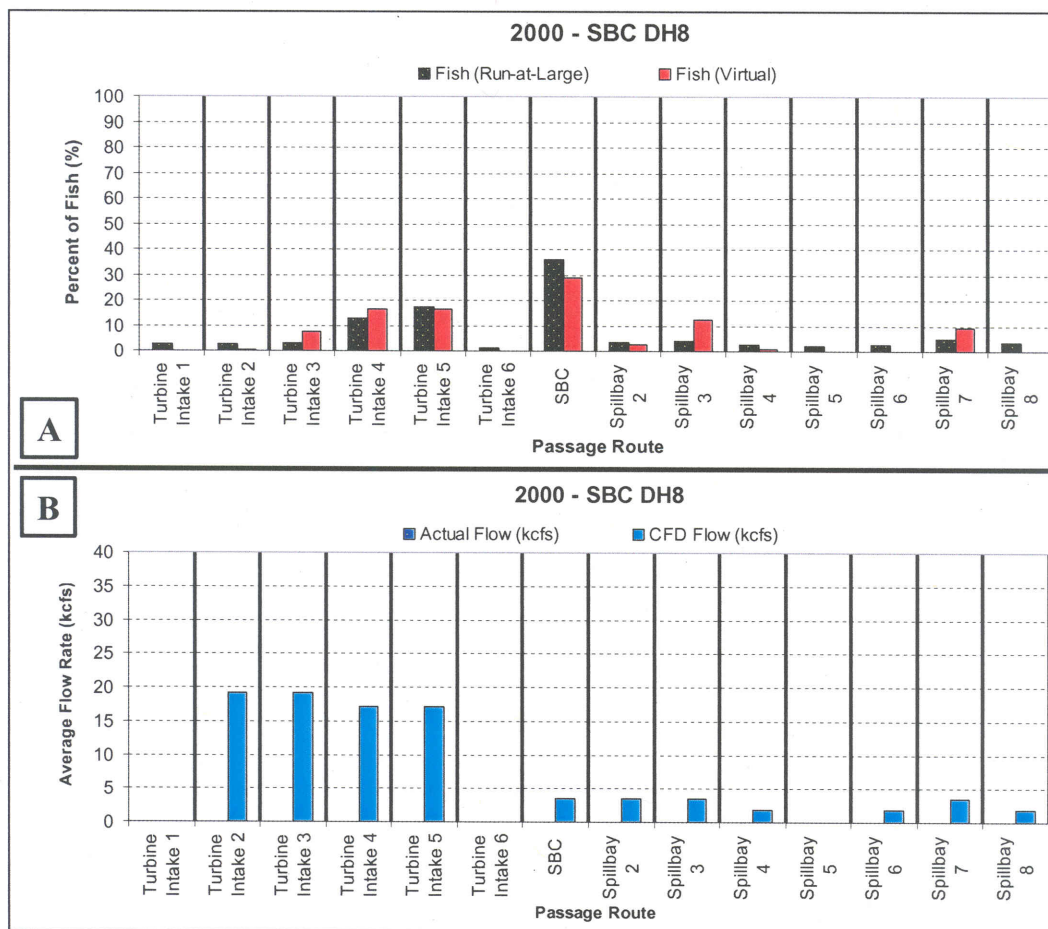


Figure A.14. Hydroacoustic (HA), or run-at-large, and virtual fish passage estimates (Plot A) and CFD modeled flow rates through each powerhouse turbine unit, the two SBC orifices, and each spillbay (Plot B) for case DH8 in 2000. Multi-beam hydroacoustic (HA), or run-at-large, passage data provided by Anglea et al. (2001). DH8 was the only case data set used to calibrate the CEL Agent IBM coefficients. Data on actual flow rates through various passage routes are not available for 2000 studies. CFD modeled flow rates reflect the target flow operating conditions. In 2000, it was generally observed, however, that actual flow rates were in relatively close agreement with target flow operating conditions, more so than for 2002 studies.

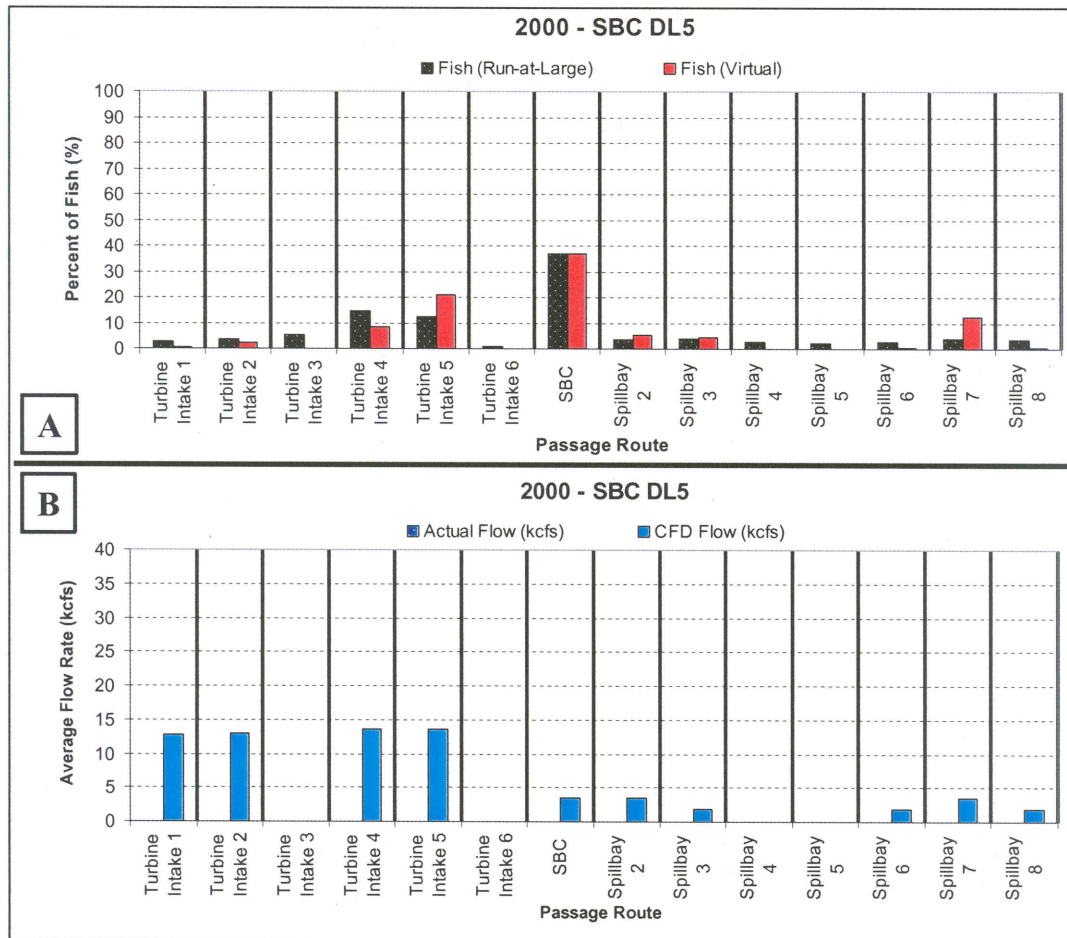


Figure A.15. Hydroacoustic (HA), or run-at-large, and virtual fish passage estimates (Plot A) and CFD modeled flow rates through each powerhouse turbine unit, the two SBC orifices, and each spillbay (Plot B) for case DL5 in 2000. Multi-beam hydroacoustic (HA), or run-at-large, passage data provided by Anglea et al. (2001). Data on actual flow rates through various passage routes are not available for 2000 studies. CFD modeled flow rates reflect the target flow operating conditions. In 2000, it was generally observed, however, that actual flow rates were in relatively close agreement with target flow operating conditions, more so than for 2002 studies.

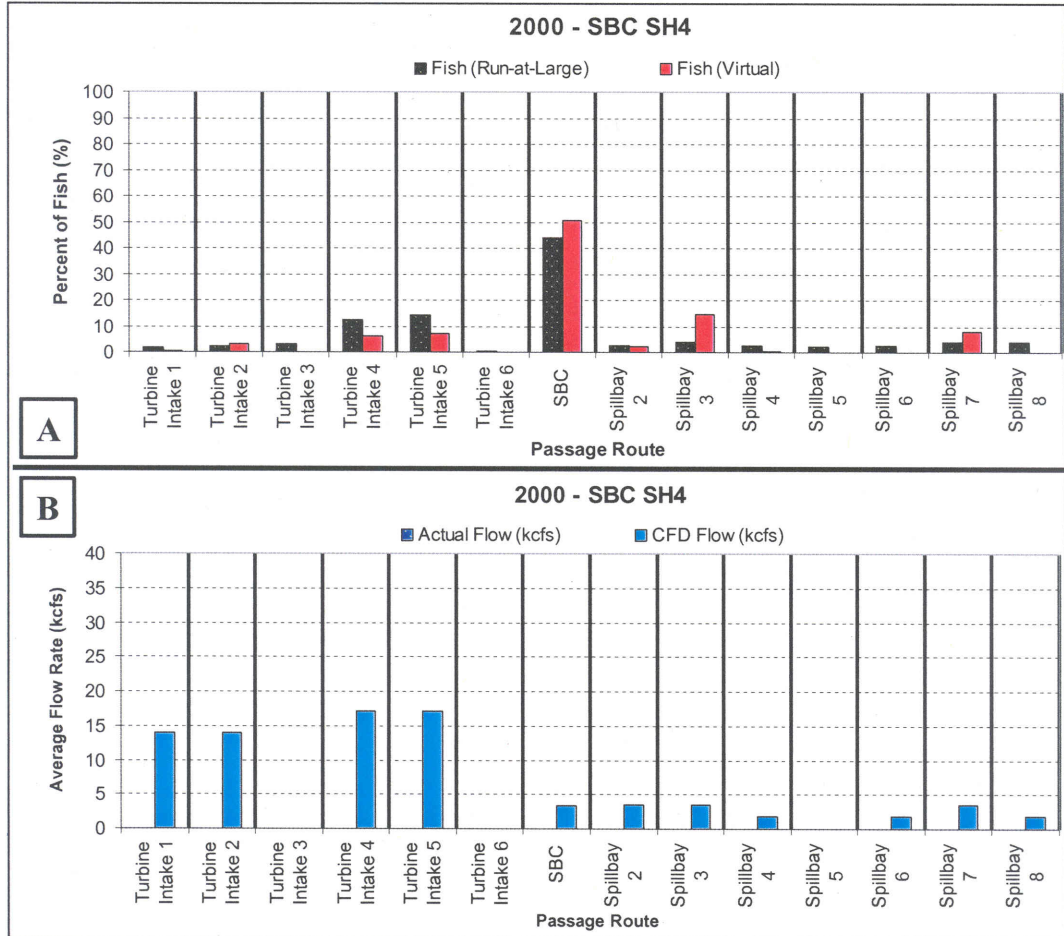


Figure A.16. Hydroacoustic (HA), or run-at-large, and virtual fish passage estimates (Plot A) and CFD modeled flow rates through each powerhouse turbine unit, the single SBC orifice, and each spillbay (Plot B) for case SH4 in 2000. Multi-beam hydroacoustic (HA), or run-at-large, passage data provided by Anglea et al. (2001). Data on actual flow rates through various passage routes are not available for 2000 studies. CFD modeled flow rates reflect the target flow operating conditions. In 2000, it was generally observed, however, that actual flow rates were in relatively close agreement with target flow operating conditions, more so than for 2002 studies.

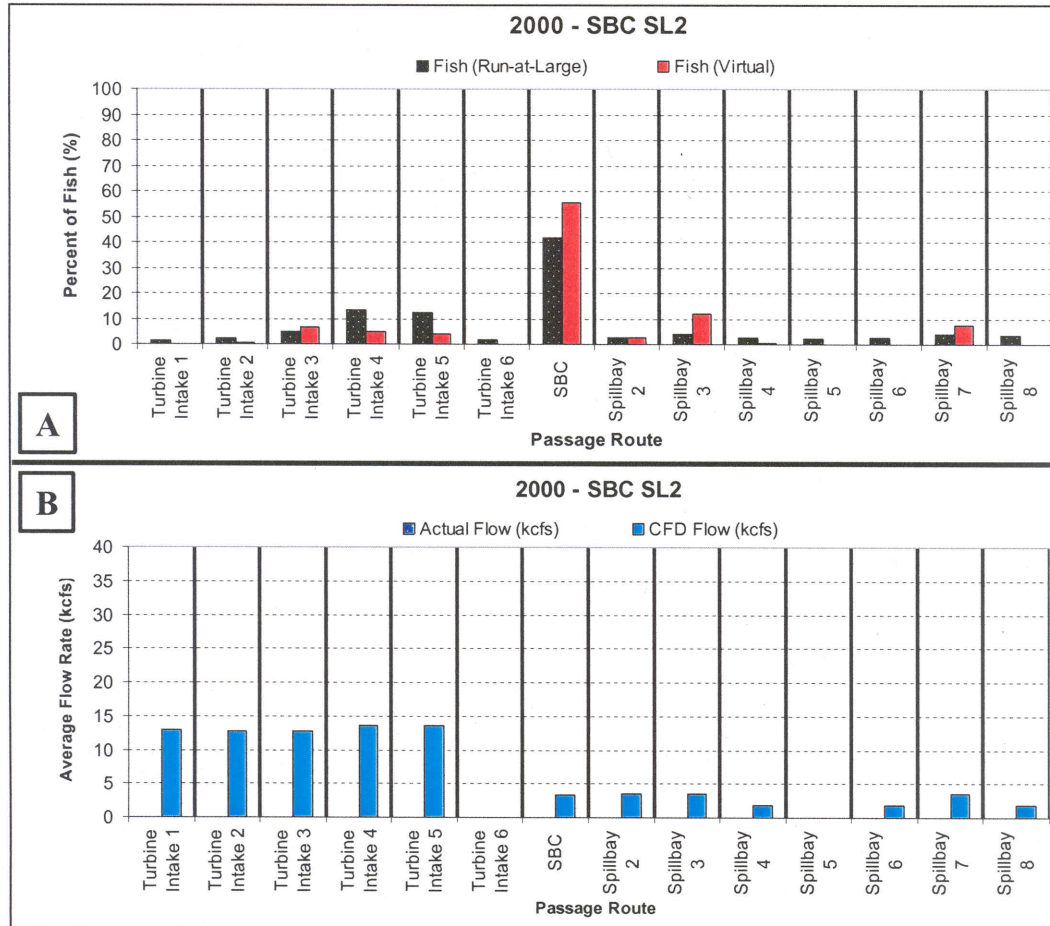


Figure A.17. Hydroacoustic (HA), or run-at-large, and virtual fish passage estimates (Plot A) and CFD modeled flow rates through each powerhouse turbine unit, the single SBC orifice, and each spillbay (Plot B) for case SL2 in 2000. Multi-beam hydroacoustic (HA), or run-at-large, passage data provided by Anglea et al. (2001). Data on actual flow rates through various passage routes are not available for 2000 studies. CFD modeled flow rates reflect the target flow operating conditions. In 2000, it was generally observed, however, that actual flow rates were in relatively close agreement with target flow operating conditions, more so than for 2002 studies.

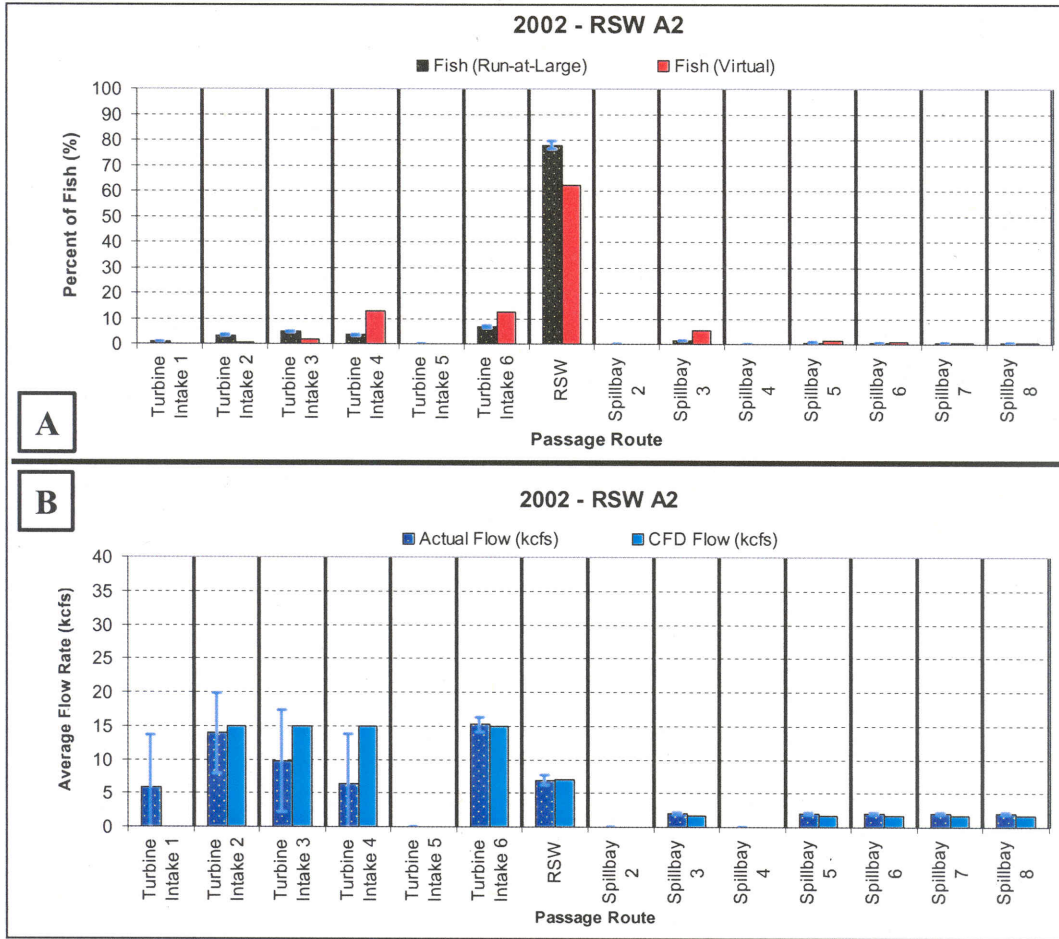


Figure A.18. Hydroacoustic (HA), or run-at-large, and virtual fish passage estimates (Plot A) and flow rates through each powerhouse turbine unit, the RSW, and each spillbay (Plot B) for case A2 in 2002. HA passage estimates and actual flow rates (mean and standard deviation, Plot B) provided by Anglea *et al.* (2003). CFD modeled flow rates reflect the target flow operating condition and were simulated before HA data on actual flow rates was available. Error bars in Plot A represent the 95% confidence interval (CI) of the HA, or run-at-large, fish passage estimates and in Plot B represent one standard deviation of the time-varying (actual) flow rate.

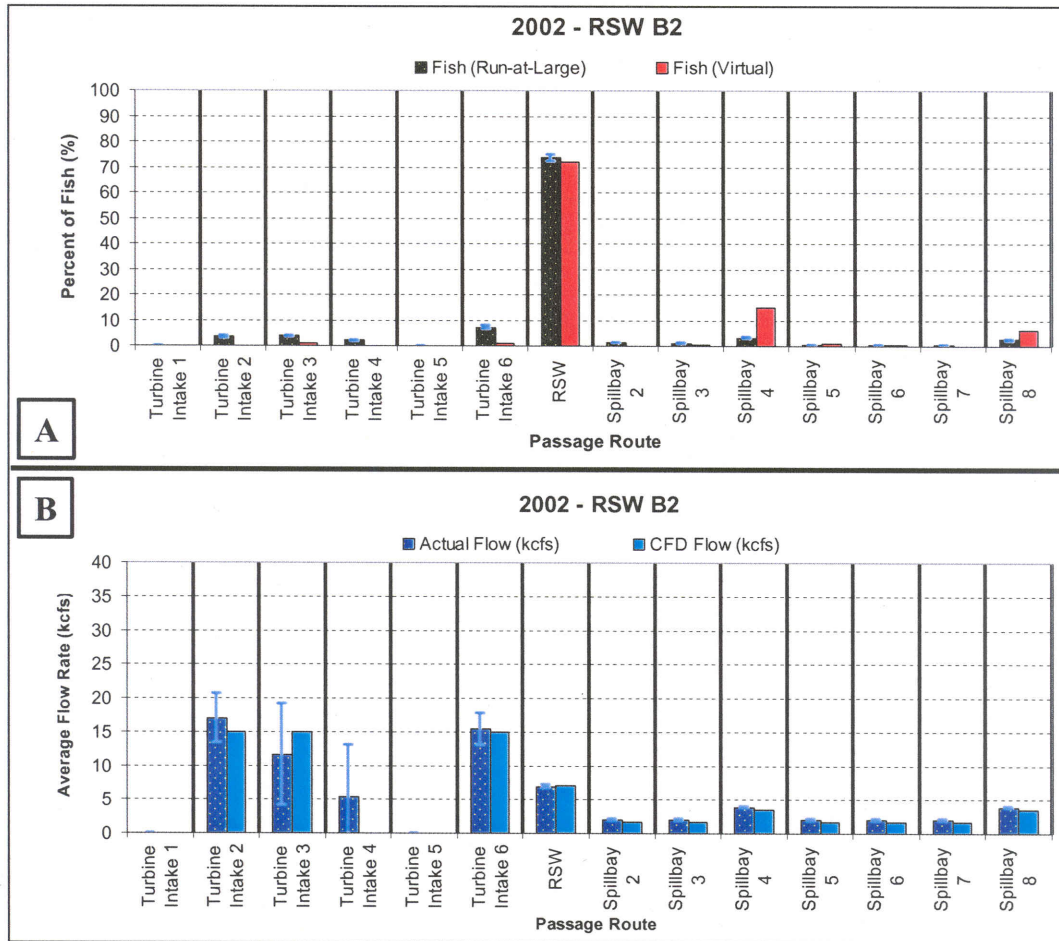


Figure A.19. Hydroacoustic (HA), or run-at-large, and virtual fish passage estimates (Plot A) and flow rates through each powerhouse turbine unit, the RSW, and each spillbay (Plot B) for case B2 in 2002. HA passage estimates and actual flow rates (mean and standard deviation, Plot B) provided by Anglea *et al.* (2003). CFD modeled flow rates reflect the target flow operating condition and were simulated before HA data on actual flow rates was available. Error bars in Plot A represent the 95% confidence interval (CI) of the HA, or run-at-large, fish passage estimates and in Plot B represent one standard deviation of the time-varying (actual) flow rate.

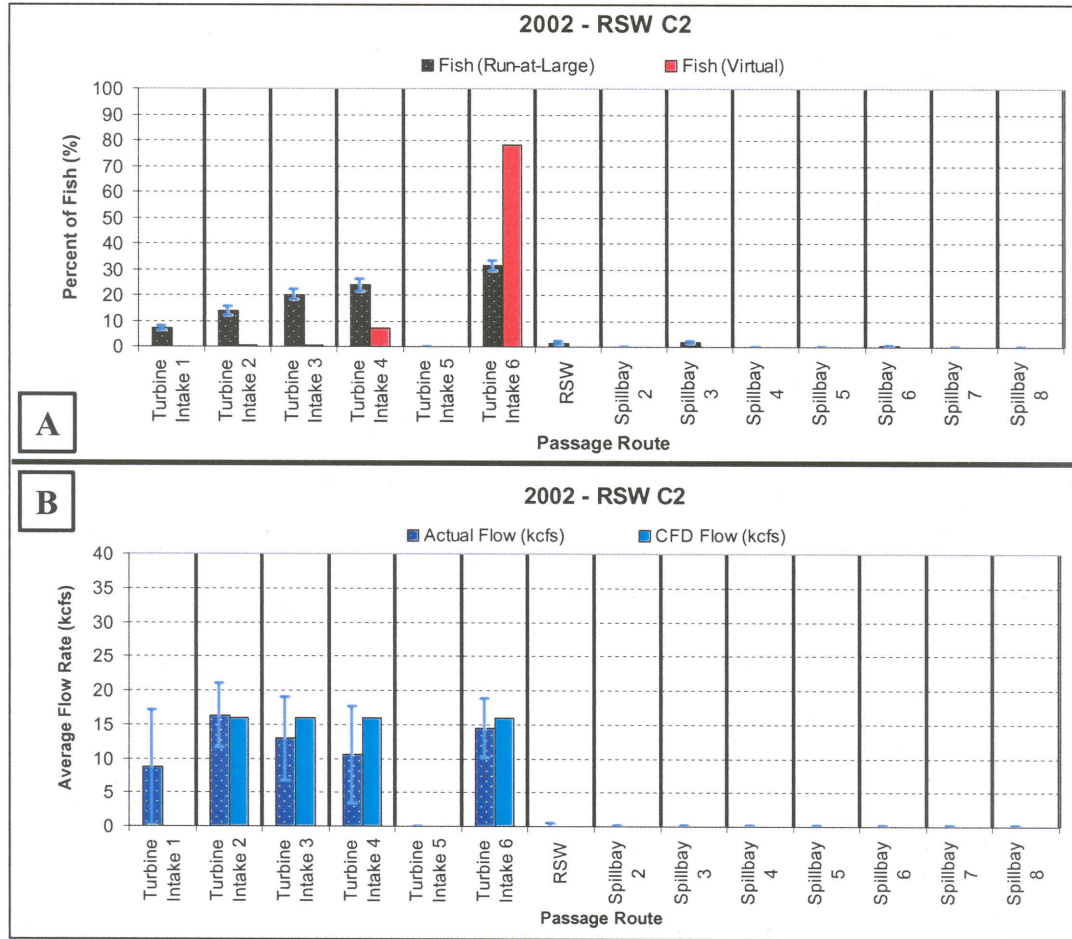


Figure A.20. Hydroacoustic (HA), or run-at-large, and virtual fish passage estimates (Plot A) and flow rates through each powerhouse turbine unit, the RSW, and each spillbay (Plot B) for case C2 in 2002. HA passage estimates and actual flow rates (mean and standard deviation, Plot B) provided by Anglea *et al.* (2003). CFD modeled flow rates reflect the target flow operating condition and were simulated before HA data on actual flow rates was available. Error bars in Plot A represent the 95% confidence interval (CI) of the HA, or run-at-large, fish passage estimates and in Plot B represent one standard deviation of the time-varying (actual) flow rate.

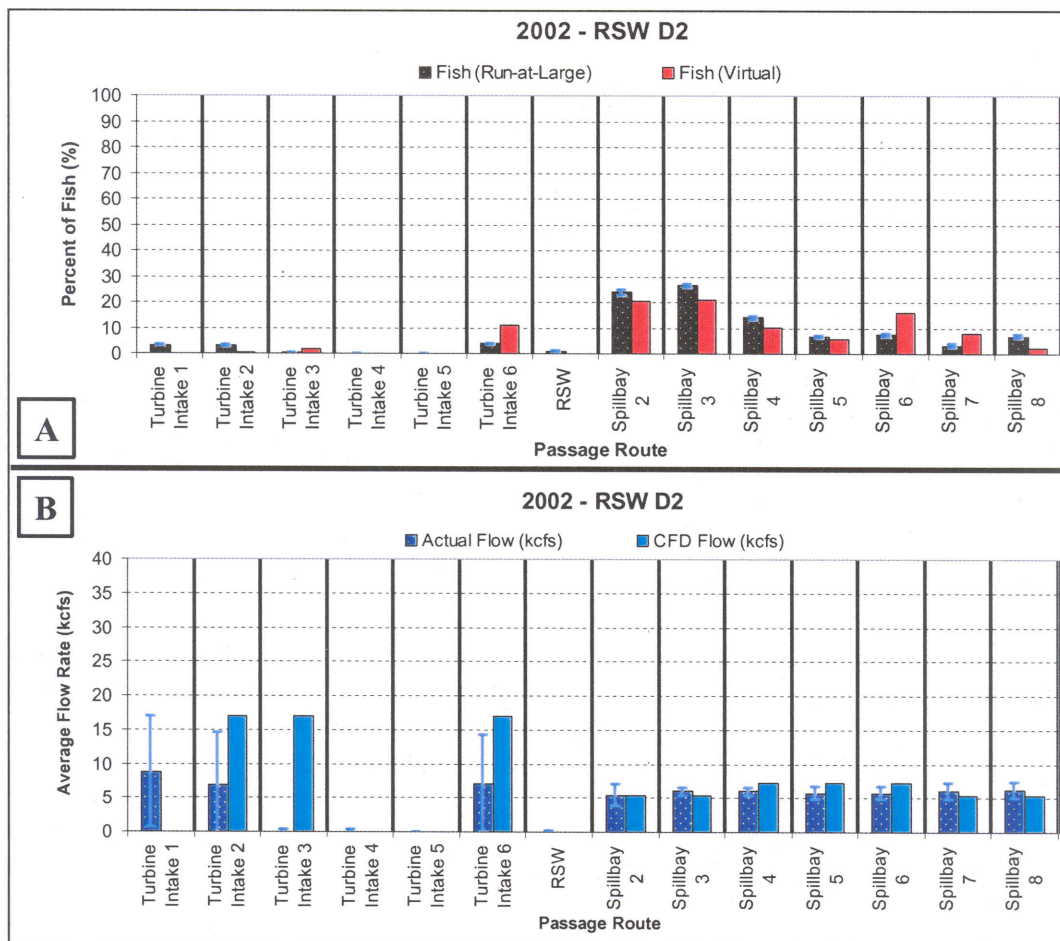


Figure A.21. Hydroacoustic (HA), or run-at-large, and virtual fish passage estimates (Plot A) and flow rates through each powerhouse turbine unit, the RSW, and each spillbay (Plot B) for case D2 in 2002. HA passage estimates and actual flow rates (mean and standard deviation, Plot B) provided by Anglea *et al.* (2003). CFD modeled flow rates reflect the target flow operating condition and were simulated before HA data on actual flow rates was available. Error bars in Plot A represent the 95% confidence interval (CI) of the HA, or run-at-large, fish passage estimates and in Plot B represent one standard deviation of the time-varying (actual) flow rate.

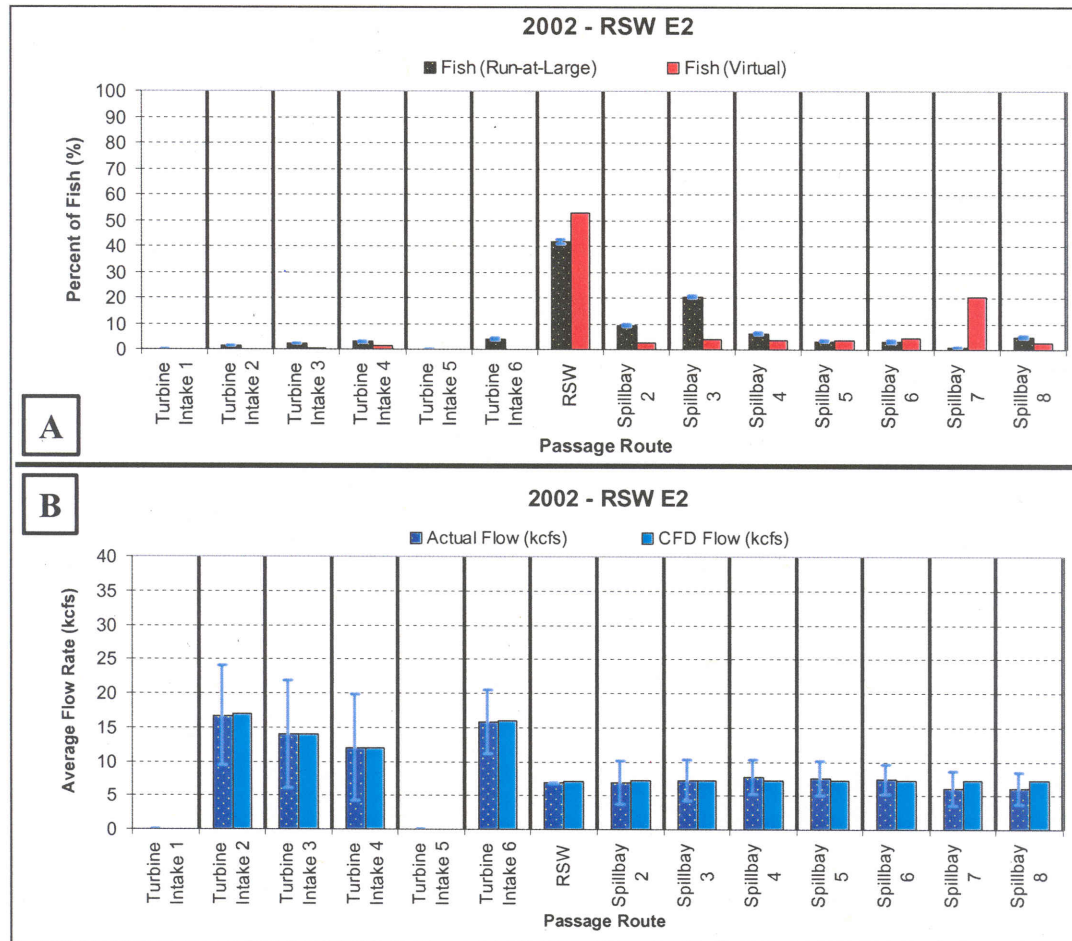


Figure A.22. Hydroacoustic (HA), or run-at-large, and virtual fish passage estimates (Plot A) and flow rates through each powerhouse turbine unit, the RSW, and each spillbay (Plot B) for case E2 in 2002. HA passage estimates and actual flow rates (mean and standard deviation, Plot B) provided by Anglea *et al.* (2003). CFD modeled flow rates reflect the target flow operating condition and were simulated before HA data on actual flow rates was available. Error bars in Plot A represent the 95% confidence interval (CI) of the HA, or run-at-large, fish passage estimates and in Plot B represent one standard deviation of the time-varying (actual) flow rate.

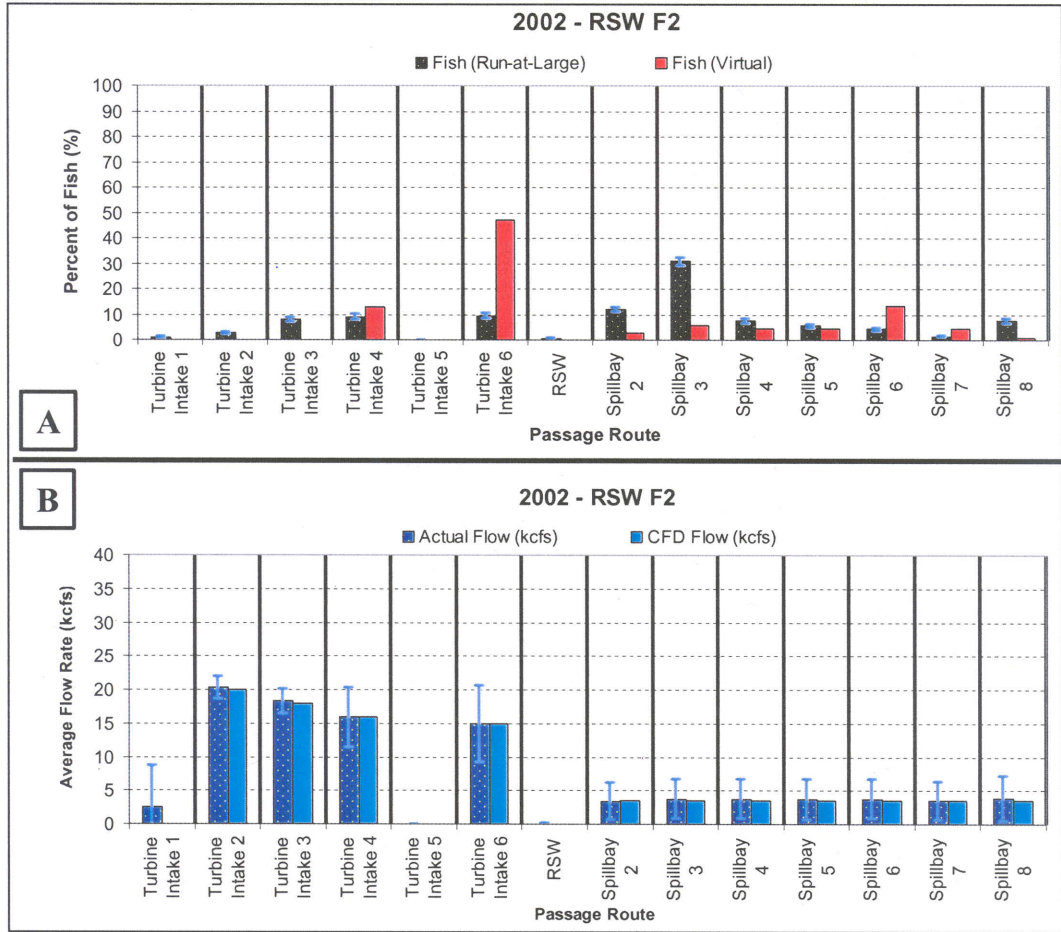


Figure A.23. Hydroacoustic (HA), or run-at-large, and virtual fish passage estimates (Plot A) and flow rates through each powerhouse turbine unit, the RSW, and each spillbay (Plot B) for case F2 in 2002. HA passage estimates and actual flow rates (mean and standard deviation, Plot B) provided by Anglea *et al.* (2003). CFD modeled flow rates reflect the target flow operating condition and were simulated before HA data on actual flow rates was available. Error bars in Plot A represent the 95% confidence interval (CI) of the HA, or run-at-large, fish passage estimates and in Plot B represent one standard deviation of the time-varying (actual) flow rate.

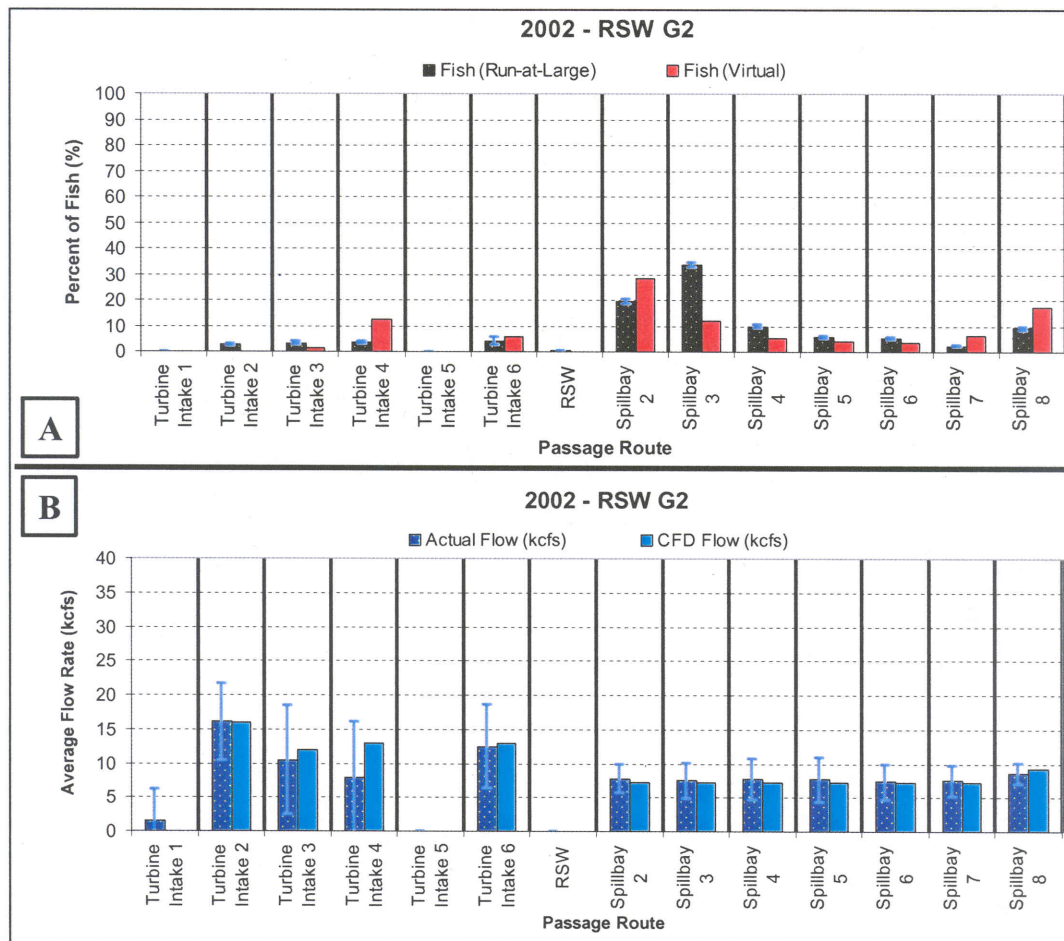


Figure A.24. Hydroacoustic (HA), or run-at-large, and virtual fish passage estimates (Plot A) and flow rates through each powerhouse turbine unit, the RSW, and each spillbay (Plot B) for case G2 in 2002. HA passage estimates and actual flow rates (mean and standard deviation, Plot B) provided by Anglea *et al.* (2003). CFD modeled flow rates reflect the target flow operating condition and were simulated before HA data on actual flow rates was available. Error bars in Plot A represent the 95% confidence interval (CI) of the HA, or run-at-large, fish passage estimates and in Plot B represent one standard deviation of the time-varying (actual) flow rate.

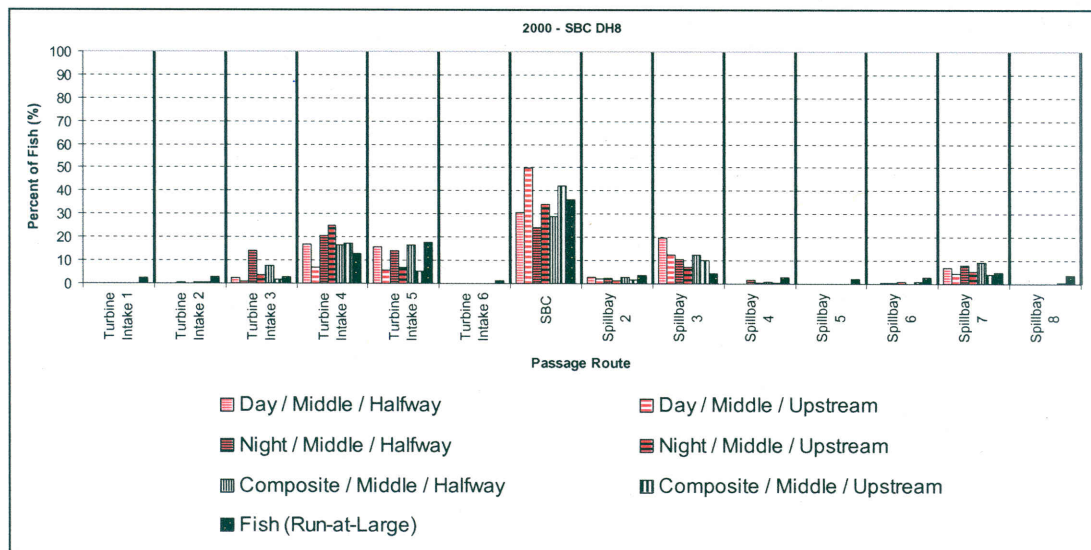


Figure A.25. Sensitivity analyses of fish passage through each powerhouse turbine unit, the two SBC orifices, and each spillbay for different release locations of virtual fish for case DH8 in 2000. Multi-beam hydroacoustic (HA), or run-at-large, passage data provided by Anglea et al. (2001).

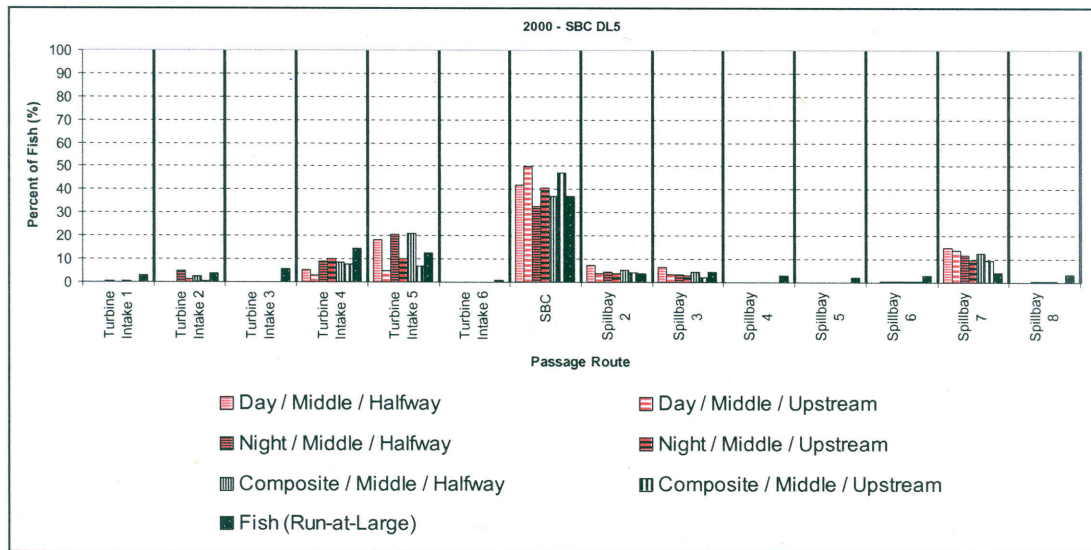


Figure A.26. Sensitivity analyses of fish passage through each powerhouse turbine unit, the two SBC orifices, and each spillbay for different release locations of virtual fish for case DL5 in 2000. Multi-beam hydroacoustic (HA), or run-at-large, passage data provided by Anglea et al. (2001).

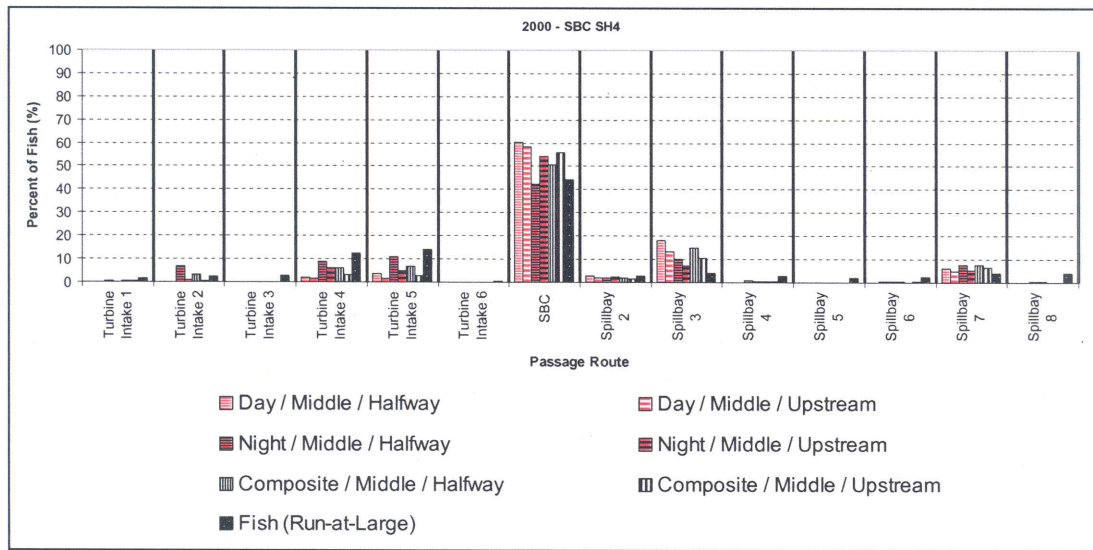


Figure A.27. Sensitivity analyses of fish passage through each powerhouse turbine unit, the single SBC orifice, and each spillbay for different release locations of virtual fish for case SH4 in 2000. Multi-beam hydroacoustic (HA), or run-at-large, passage data provided by Anglea et al. (2001).

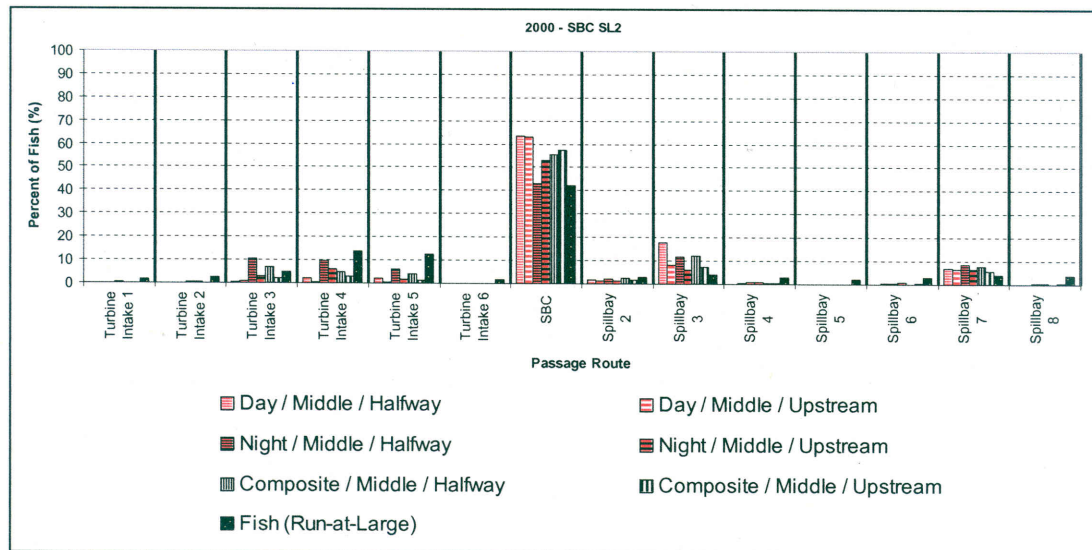


Figure A.28. Sensitivity analyses of fish passage through each powerhouse turbine unit, the single SBC orifice, and each spillbay for different release locations of virtual fish for case SL2 in 2000. Multi-beam hydroacoustic (HA), or run-at-large, passage data provided by Anglea et al. (2001).

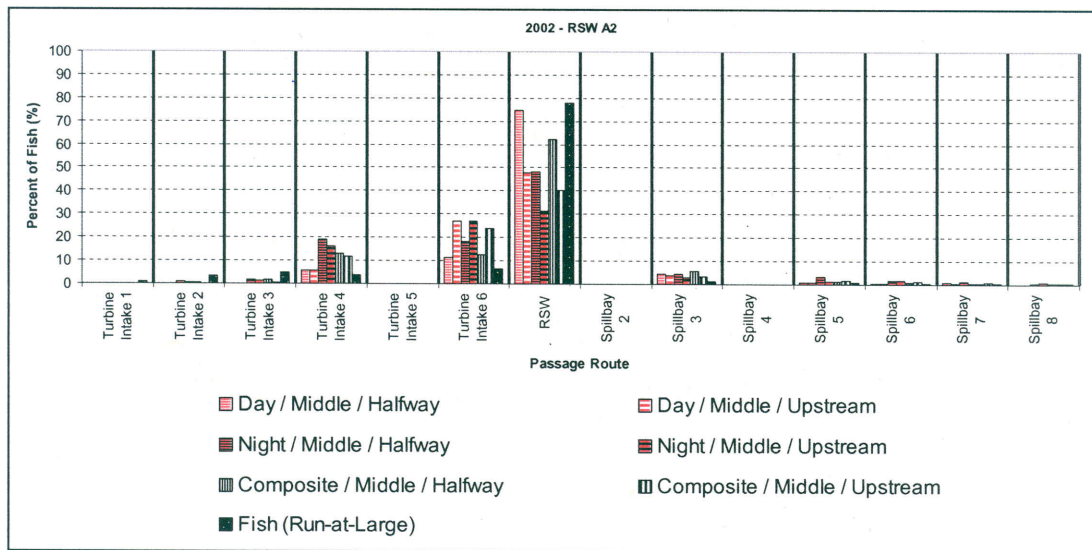


Figure A.29. Sensitivity analyses of fish passage through each powerhouse turbine unit, the RSW, and each spillbay for different release locations of virtual fish for case A2 in 2002. Multi-beam hydroacoustic (HA), or run-at-large, passage data provided by Anglea et al. (2003).

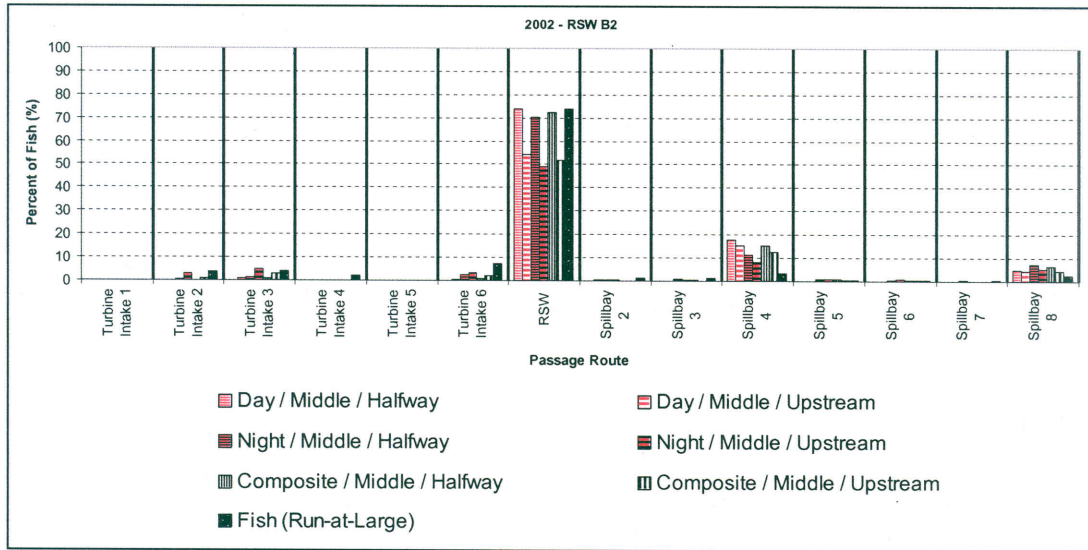


Figure A.30. Sensitivity analyses of fish passage through each powerhouse turbine unit, the RSW, and each spillbay for different release locations of virtual fish for case B2 in 2002. Multi-beam hydroacoustic (HA), or run-at-large, passage data provided by Anglea et al. (2003).

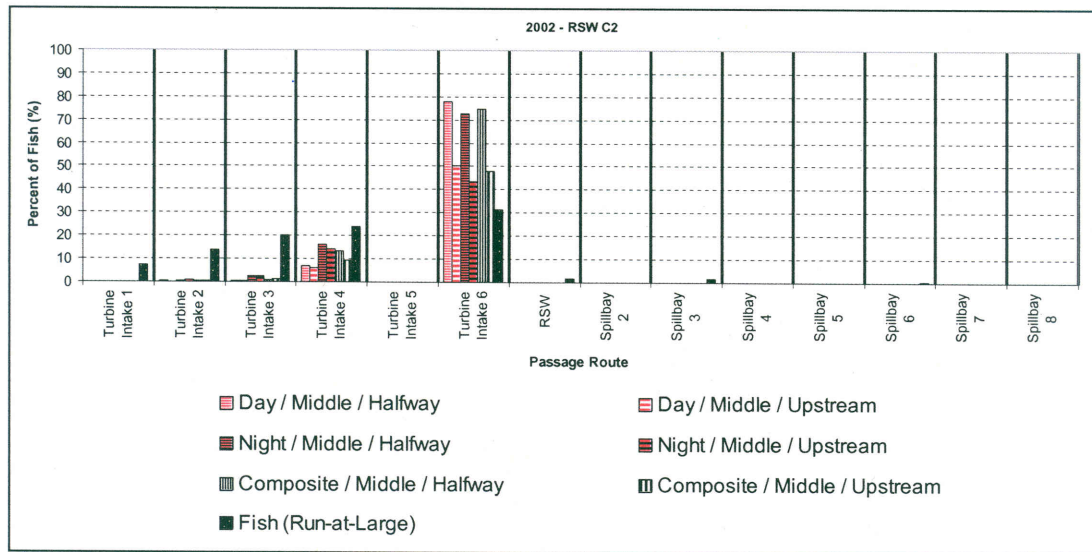


Figure A.31. Sensitivity analyses of fish passage through each powerhouse turbine unit, the RSW, and each spillbay for different release locations of virtual fish for case C2 in 2002. Multi-beam hydroacoustic (HA), or run-at-large, passage data provided by Anglea et al. (2003).

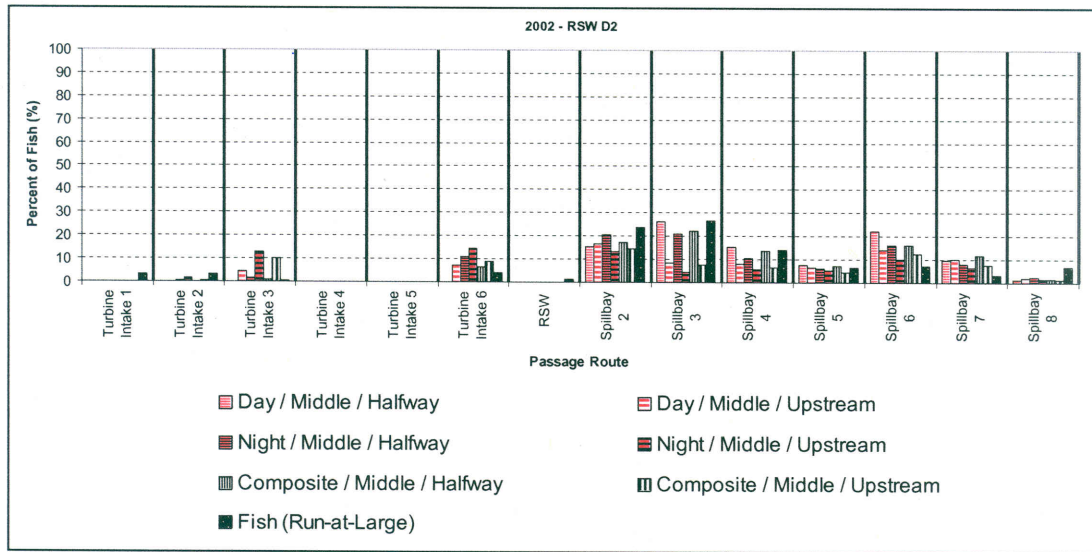


Figure A.32. Sensitivity analyses of fish passage through each powerhouse turbine unit, the RSW, and each spillbay for different release locations of virtual fish for case D2 in 2002. Multi-beam hydroacoustic (HA), or run-at-large, passage data provided by Anglea et al. (2003).

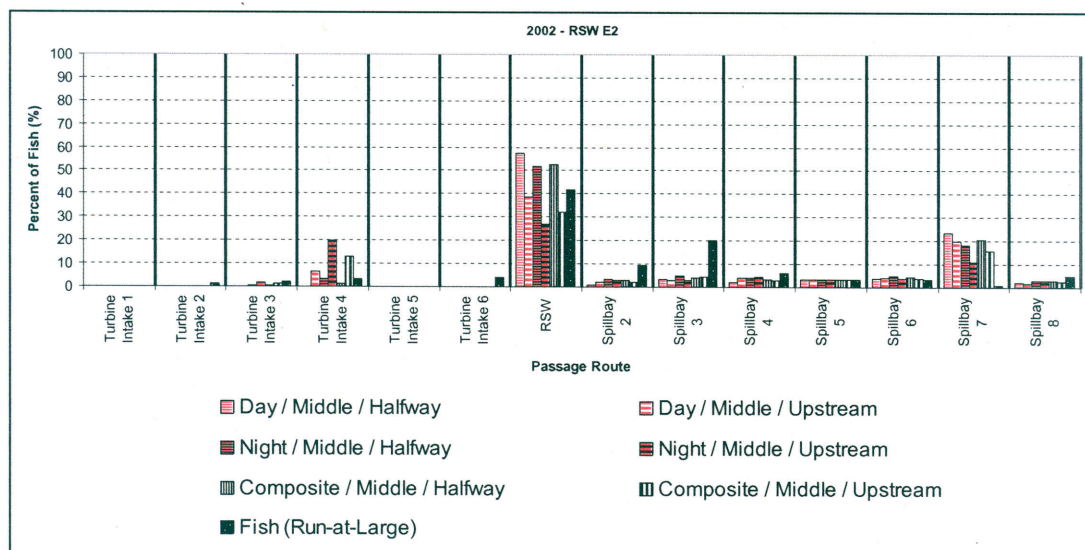


Figure A.33. Sensitivity analyses of fish passage through each powerhouse turbine unit, the RSW, and each spillbay for different release locations of virtual fish for case E2 in 2002. Multi-beam hydroacoustic (HA), or run-at-large, passage data provided by Anglea et al. (2003).

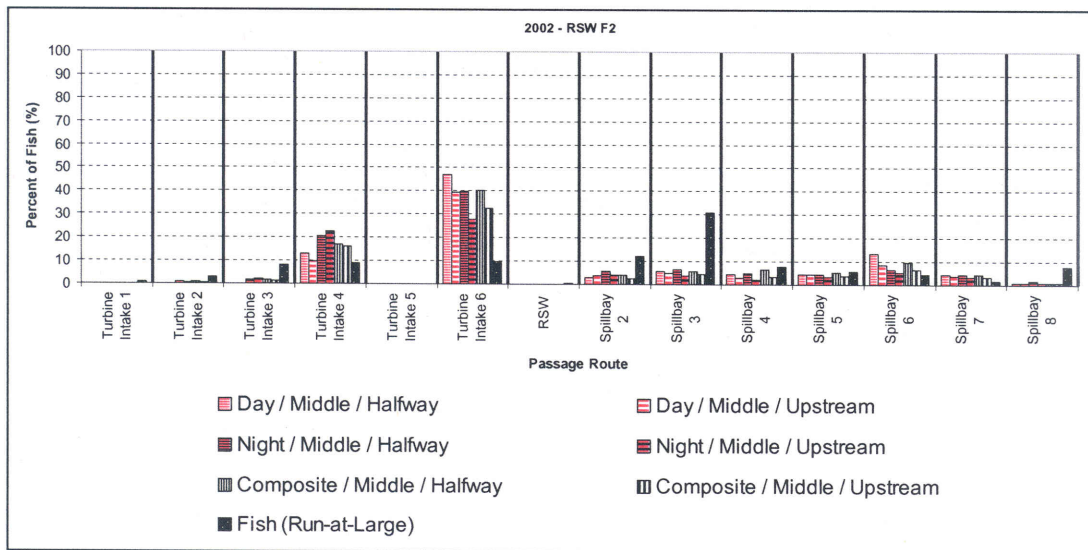


Figure A.34. Sensitivity analyses of fish passage through each powerhouse turbine unit, the RSW, and each spillbay for different release locations of virtual fish for case F2 in 2002. Multi-beam hydroacoustic (HA), or run-at-large, passage data provided by Anglea et al. (2003).

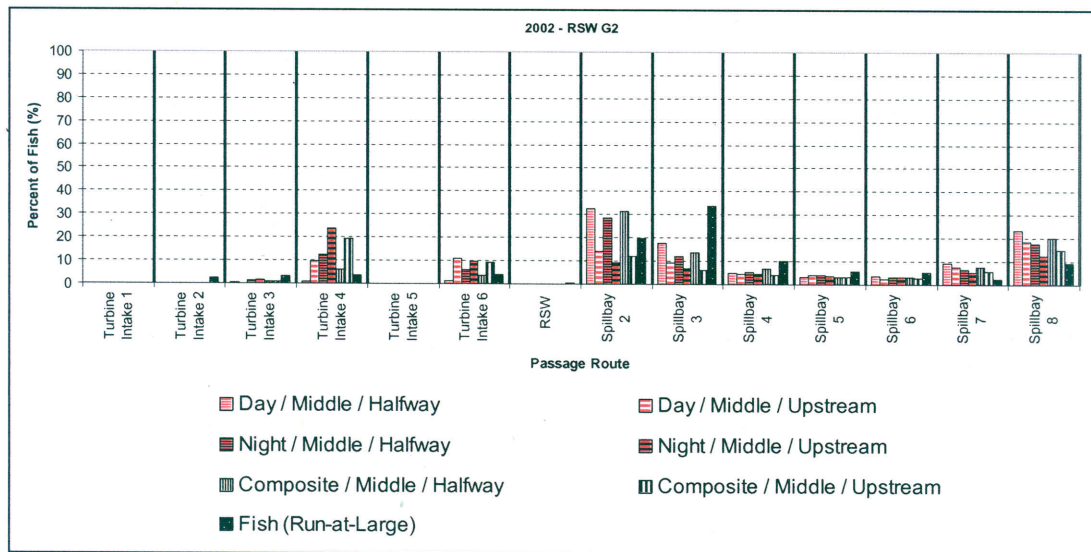


Figure A.35. Sensitivity analyses of fish passage through each powerhouse turbine unit, the RSW, and each spillbay for different release locations of virtual fish for case G2 in 2002. Multi-beam hydroacoustic (HA), or run-at-large, passage data provided by Anglea et al. (2003).

REFERENCES

- Anglea, S. M., Ham, K. D., Johnson, G. E., Simmons, M. A., Simmons, C. S., Kudera, E. and Skalski, J. R. (2003). "Hydroacoustic evaluation of the removable spillway weir at Lower Granite Dam in 2002." Final report prepared by Battelle Pacific Northwest Division for U.S. Army Corps of Engineers, Walla Walla District, PNWD-3219, Walla Walla, WA.
- Anglea, S. M., Johnson, R. L., Simmons, M. A., Thorsten, S. L., Duncan, J. P., Chamness, M. A., McKinstry, C. A., Kudera, E. A., and Skalski, J. R. (2001). "Fixed-location hydroacoustic evaluation of the prototype surface bypass and collector at Lower Granite Dam in 2000." Final report prepared by Battelle Pacific Northwest Division for U.S. Army Corps of Engineers, Walla Walla District, under Contract No. DACW68-96-D-002, Walla Walla, WA.
- Plumb, J. M., Novick, M. S., Adams, N. S., and Rondorf, D. W. (2002). "Behavior of radio-tagged juvenile Chinook salmon and steelhead in the forebay of Lower Granite Dam relative to the 2000 surface bypass and behavioral guidance structure tests." Final report prepared by U.S. Geological Survey Columbia River Research Laboratory for U.S. Army Corps of Engineers, Walla Walla District, Walla Walla, WA.

APPENDIX B

Hydrodynamics and CFD Modeling – The Basics

The field of computational hydrodynamics as well as other fields such as pollutant transport, groundwater, hydrologic, and non-point source pollution process modeling are built on two fundamental equations: the Law of Continuity (or Conservation of Mass) and the Law of Conservation of Linear Momentum. The equation for continuity is derived by equating the net rate of mass accumulation in an elemental fluid volume to the net flux of mass through the volume, i.e., mass out minus mass in, as described using a Taylor series expansion. The continuity equation for laminar flow in Cartesian coordinates and its simplified form if the flow may be assumed incompressible is shown in Figure B.1. The law of continuity indicates that no mass can be generated or lost, and that the difference in mass flux must be equal to the accumulation within the volume.

Equations of Fluid Motion
laminar flow

Continuity Equation (Conservation of Mass) (assuming flow is incompressible)

$$\frac{\partial \rho}{\partial t} + \frac{\partial(\rho u)}{\partial x} + \frac{\partial(\rho v)}{\partial y} + \frac{\partial(\rho w)}{\partial z} = 0 \quad \Rightarrow \quad \frac{\partial u}{\partial x} + \frac{\partial v}{\partial y} + \frac{\partial w}{\partial z} = 0$$

Navier-Stokes Equations (Conservation of Linear Momentum)
x-direction, assuming flow is incompressible and viscosity, μ , is constant

$$\rho \left(\frac{\partial u}{\partial t} + u \frac{\partial u}{\partial x} + v \frac{\partial u}{\partial y} + w \frac{\partial u}{\partial z} \right) = -\frac{\partial p}{\partial x} + \rho g_x + \mu \left(\frac{\partial^2 u}{\partial x^2} + \frac{\partial^2 u}{\partial y^2} + \frac{\partial^2 u}{\partial z^2} \right)$$

acceleration terms = force terms

Figure B.1. Equations of fluid motion for laminar flow. ρ is the density of water, t is time, u , v , and w are the coordinate Cartesian velocities, p is pressure, and g_x is the body force of gravity in the x-direction.

The equation for linear momentum conservation is derived by equating total acceleration (time and convective, or spatial, acceleration terms) to the two primary forces on an elemental volume of water, that is, surface forces due to normal and shear stresses and body forces, in open waters usually considered just the weight of the fluid element. Substituting in the equalities relating normal stresses to pressure, viscosity (a measure of the fluid's resistance to shear, or deform, when the fluid is in motion), and the rates of strain (or rates of elongation/compression deformation) and those equalities relating shear stresses to viscosity and the rates of shearing strain (or rates of angular deformation) yield the Navier-Stokes equations of fluid motion. The Navier-Stokes equation for incompressible laminar flow with constant viscosity, μ , (x-coordinate direction only) is shown in Figure B.1. Each Navier-Stokes equation is simply the acceleration terms (left hand side) set equal to the force terms (right hand side) for that coordinate direction. The Navier-Stokes equations of motion, when combined with the conservation of mass equation, provide a complete mathematical description of the flow of incompressible Newtonian fluids (Munson *et al.*, 1998).

With the Navier-Stokes equations and the equation for continuity (or conservation of mass), there are four equations and four unknowns (the three coordinate Cartesian velocities and pressure). The problem is "well-posed" in mathematical terms because the number of equations and unknowns are equal. However, the nonlinear, second-order partial differential Navier-Stokes equations are not amenable to analytical solutions except in a few well-defined cases. A principal difficulty in solving the Navier-Stokes equations is their nonlinearity arising from the convective acceleration terms. There are no general analytical schemes for solving nonlinear partial differential equations and each problem must be considered individually. Exact analytical solutions have been made where the geometry of the

flow system is such that the convective acceleration terms vanish. The problem becomes intractable, however, with the addition of more terms (more unknowns) when the flow is turbulent. This is the “closure” problem referred to in turbulence modeling.

Turbulence

Turbulent flow is a flow state characterized by random fluctuations in velocity and is a result of laminar flow instability at high Reynolds numbers. Conceptually, it can be visualized as instantaneous random velocity fluctuations about some mean (time-averaged) velocity (Figure B.2). Average of the instantaneous random velocity fluctuations should be zero; otherwise, the average velocity must be modified. Turbulent flow also consists of random pressure fluctuations similar in concept to those described for velocities. Substituting new relationships for pressure and coordinate velocities in turbulent flow (that is, a time-averaged value and a value representing the instantaneous deviation from the mean value) into the Navier-Stokes equations for laminar flow results in the addition of more terms (Figure B.3), which account for the additional momentum transfer due to turbulence. These new terms are often referred to as Reynolds or turbulent stresses, although they actually represent inertia or momentum fluxes/exchange, and are often grouped with the viscosity term used for laminar flow. The viscosity term is then renamed turbulent, or eddy, viscosity. Correct modeling of turbulent flow is strongly dependent on an accurate knowledge of the turbulent stresses, which in turn requires an accurate knowledge of the randomly fluctuating instantaneous velocities.

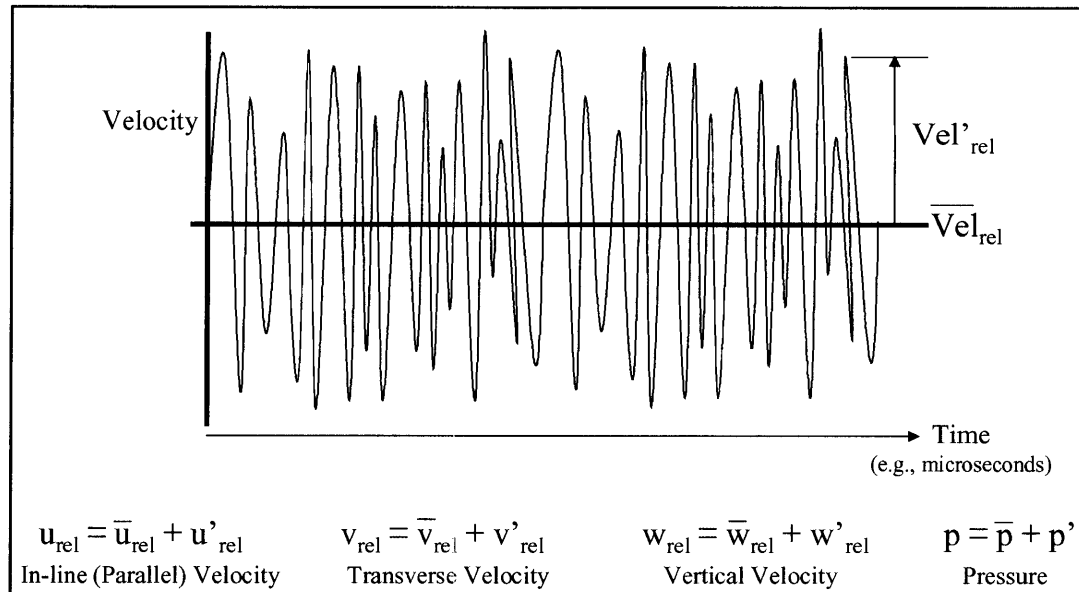


Figure B.2. Turbulent flow can be conceptually visualized as instantaneous random velocity fluctuations about some mean velocity. Vel_{rel} is the velocity relative to the fish at an instant in time and may be mathematically decomposed into a time-averaged component, \overline{Vel}_{rel} , and a randomly varying instantaneous component, Vel'_{rel} . Decomposition of each coordinate velocity (u_{rel} , v_{rel} , and w_{rel}) and pressure (p) is a theoretically valid treatment of these quantities for turbulent flow.

Inability to accurately determine the Reynolds stresses is equivalent to not knowing the eddy viscosity, which if known could provide a route to the solution of the equation for turbulent flow. Determining the eddy viscosity proves quite challenging, however, since the eddy viscosity is a property of the flow, not a property of the fluid itself. Therefore, the eddy viscosity is often different for each flow condition and is not spatially constant even for a given flow. With little hope of finding a direct solution for the Reynolds stresses, or the eddy viscosity, attention shifted to development of empirical theories and relationships that could relate the eddy viscosity to mean velocity. One empirical approach that's proved useful over the years is K- ϵ turbulence modeling (Figure B.4). This modeling scheme relates

Reynolds stresses to the mean rate of strain through the eddy viscosity, which is, in turn, related to the density of water and two turbulence terms: turbulent kinetic energy and turbulence dissipation. Turbulent kinetic energy and turbulence dissipation are variables themselves and numerically resolvable.

Equations of Fluid Motion
turbulent flow

$$u = \bar{u} + u' \quad v = \bar{v} + v' \quad w = \bar{w} + w' \quad p = \bar{p} + p'$$

← Coordinate Velocities → Pressure

substitute

Continuity Equation (Conservation of Mass) (assuming flow is incompressible)

$$\frac{\partial \bar{\rho}}{\partial t} + \frac{\partial(\bar{\rho}u)}{\partial x} + \frac{\partial(\bar{\rho}v)}{\partial y} + \frac{\partial(\bar{\rho}w)}{\partial z} + \frac{\partial(\bar{\rho}'u')}{\partial x} + \frac{\partial(\bar{\rho}'v')}{\partial y} + \frac{\partial(\bar{\rho}'w')}{\partial z} = 0 \quad \Rightarrow \quad \frac{\partial \bar{u}}{\partial x} + \frac{\partial \bar{v}}{\partial y} + \frac{\partial \bar{w}}{\partial z} = 0$$

Navier-Stokes Equations (Conservation of Linear Momentum)
x-direction, assuming flow is incompressible and viscosity, μ , is constant

$$\rho \left(\frac{\partial \bar{u}}{\partial t} + \bar{u} \frac{\partial \bar{u}}{\partial x} + \bar{v} \frac{\partial \bar{u}}{\partial y} + \bar{w} \frac{\partial \bar{u}}{\partial z} \right) = -\frac{\partial \bar{p}}{\partial x} + \rho g_x + \mu \left(\frac{\partial^2 \bar{u}}{\partial x^2} + \frac{\partial^2 \bar{u}}{\partial y^2} + \frac{\partial^2 \bar{u}}{\partial z^2} \right) - \rho \left(\frac{\partial(\bar{u}'u')}{\partial x} + \frac{\partial(\bar{u}'v')}{\partial y} + \frac{\partial(\bar{u}'w')}{\partial z} \right)$$

Factor added due to turbulence

- rearranging the RHS of the Navier-Stokes Eqn, and putting it in more general (tensor) form:

$$\rho \left(\frac{\partial \bar{u}_i}{\partial t} + \bar{u}_j \frac{\partial \bar{u}_i}{\partial x_j} \right) = -\frac{\partial \bar{p}}{\partial x_i} + \rho g_i + \frac{\partial}{\partial x_j} \left(\mu \frac{\partial \bar{u}_i}{\partial x_j} - \rho \bar{u}'_i u'_j \right) \quad \dots \text{in this form, the added terms are often called turbulent or Reynolds stresses}$$

Figure B.3. Equations of fluid motion for turbulent flow.

Navier-Stokes Equation

$$\rho \left(\frac{\partial \bar{u}_i}{\partial t} + \bar{u}_j \frac{\partial \bar{u}_i}{\partial x_j} \right) = -\frac{\partial \bar{p}}{\partial x_i} + \rho g_i + \frac{\partial}{\partial x_j} \left(\mu \frac{\partial \bar{u}_i}{\partial x_j} - \overline{\rho u'_i u'_j} \right)$$

Shear Stress Tensor

$$\tau_{ij} = \mu \left(\frac{\partial \bar{u}_i}{\partial x_j} + \frac{\partial \bar{u}_j}{\partial x_i} \right) - \overline{\rho u'_i u'_j} \text{ for } i \neq j$$

= laminar terms + turbulent terms

↓ another variable to be solved for

K-ε Turbulence Modeling

Turbulent stresses related to the mean rate of strain through an eddy viscosity

$$-\overline{\rho u'_i u'_j} = \mu_t \left(\frac{\partial \bar{u}_i}{\partial x_j} + \frac{\partial \bar{u}_j}{\partial x_i} \right) - \frac{2}{3} \rho K \delta_{ij}$$

where: $\delta_{ij} = 0$ when $i \neq j$
 $\delta_{ij} = 1$ when $i = j$
 $\mu_t = 0.09 \rho \frac{K^2}{\epsilon}$

K-ε Transport Equations:

$$1) \frac{\partial \overline{\rho u'_j K}}{\partial x_j} = \frac{\partial}{\partial x_j} \left[\left(\mu + \frac{\mu_t}{1.0} \right) \frac{\partial K}{\partial x_j} \right] + G - \rho \epsilon$$

$$2) \frac{\partial \overline{\rho u'_j \epsilon}}{\partial x_j} = \frac{\partial}{\partial x_j} \left[\left(\mu + \frac{\mu_t}{1.3} \right) \frac{\partial \epsilon}{\partial x_j} \right] + 1.44 \frac{\epsilon}{K} G - 1.92 \rho \frac{\epsilon^2}{K}$$

where: $G = -\overline{\rho u'_i u'_j} \frac{\partial \bar{u}_i}{\partial x_j}$

... little hope in finding a solution for the turbulent stresses, so must find some way to relate the stresses to other (more resolvable) flow parameters.

Figure B.4. Mathematical treatment for resolving the turbulence “closure” problem using K-ε turbulence modeling. G is the generation of K , turbulent kinetic energy. Once the “closure” problem is fixed, i.e., there are an equal number of equations and unknowns, the governing equations can be solved. Steady-state computational fluid dynamics (CFD) models then solve the relevant equations numerically, primarily using one of three methods: finite difference, finite element, or finite volume.

REFERENCES

Munson, B. R., Young, D. F., and Okiishi, T. H. (1998). Fundamentals of Fluid Mechanics. John Wiley & Sons, Inc., New York, NY, 877 pp.